Understanding the intracellular mechanisms leading to motoneuron degeneration in spinal muscular atrophy disease

Alba Sansa Zaragoza

Universitat de Lleida

TESI DOCTORAL

UNDERSTANDING THE INTRACELLULAR MECHANISMS LEADING TO MOTONEURON DEGENERATION IN SPINAL MUSCULAR ATROPHY DISEASE

ALBA SANSA ZARAGOZA

2023

Memòria per optar al Grau de Doctor per la Universitat de Lleida

Programa de Doctorat en Salut

Directora i tutora

Rosa Mª Soler Tatché

Directora

Ana Garcerá Teruel

This thesis has been funded by:

- Ajuts per a personal predoctoral de la Universitat de Lleida en formació i ajuts Jade Plus per a l'any 2018.
- Ajuts 2021 de Promoció de la Recerca en Salut – 9a Edició.
- Ministerio de Economía y competitividad (Gobierno de España)-Instituto de Salud Carlos III, Fondo de Investigaciones Sanitarias, Unión Europea, Fondo Europeo de Desarrollo Regional (FEDER), "Una manera de hacer Europa". Convocatoria 2017 (PI17/00231).
- Ministerio de Economía y competitividad (Gobierno de España)-Instituto de Salud Carlos III, Fondo de Investigaciones Sanitarias, Unión Europea, Fondo Europeo de Desarrollo Regional (FEDER), "Una manera de hacer Europa". Convocatoria 2020 (PI20/00098).
- Fundació La Marató TV3 (202005-30).

RESUM·RESUMEN·ABSTRACT

RESUM

L'Atròfia Muscular Espinal (AME) és una malaltia neuromuscular degenerativa greu i la primera causa genètica de mort infantil. L'AME s'origina per la pèrdua o mutació del gen *Survival Motor Neuron 1* (*SMN1*) i la disminució de la proteïna Survival Motor Neuron (SMN). Els nivells de SMN contribueixen en la determinació del fenotip i la gravetat de la malaltia. Una duplicació centromèrica d'aquest gen, *SMN2*, és la responsable de la producció de proteïna SMN en la condició d'AME. La disminució sistèmica de SMN resulta en l'afectació de diversos teixits i cèl·lules. Les motoneurones (MNs) de la medul·la espinal son el tipus cel·lular amb majors alteracions. Per desenvolupar noves estratègies terapèutiques que evitin la degeneració de les MNs i la progressió de la malaltia, és necessari conèixer en profunditat els mecanismes cel·lulars que s'hi troben implicats. L'objectiu del present treball ha estat analitzar les alteracions de les vies de senyalització de supervivència neuronal PI3K/Akt i ERK MAPK, així com l'estudi de marcadors d'apoptosi i d'autofàgia en diferents models d'AME, centrant la investigació en la implicació d'aquestes modificacions en les MNs.

Els resultats van mostrar que les MNs dels models d'AME presentaven un increment en la degeneració neurítica, la disminució de la supervivència cel·lular, un augment del tall de la proteasa caspassa-3 i major presència de nuclis amb morfologia apoptòtica. Les proteïnes antiapoptòtiques FAIM i XIAP estaven disminuïdes en extractes totals de medul·la espinal de ratolí d'AME, tanmateix, en cultius de MNs es trobaven augmentades. Tot i així, la presència de caspassa-3 activa i de nuclis fragmentats, indica que l'expressió de FAIM-L i XIAP podria no ser suficient per contrarestar l'activació de l'apoptosi en MNs. Les vies de senyalització intracel·lular PI3K/Akt i ERK MAPK també estan alterades en les MNs AME. Es va observar una disminució de la fosforilació d'Akt i un increment de la fosforilació d'ERK. La inhibició d'aquestes vies en MNs va demostrar la seva implicació en la regulació transcripcional de SMN. Tot i així, la regulació endògena de SMN no va alterar la fosforilació d'Akt i ERK. L'estudi dels marcadors d'autofàgia va revelar un perfil d'expressió diferencial de les proteïnes analitzades entre els models cel·lulars d'AME. Així doncs, mentre que en múscul hi havia una disminució de la formació d'autofagosomes i un augment del flux d'autofàgia, en les MNs s'observava un increment d'autofagosomes i una disminució del flux. A més, les MNs AME presentaven un increment en la fosforilació de la proteïna mTOR, la qual participa en la inhibició de l'autofàgia. La fosforilació de mTOR i els canvis dels indicadors de l'autofàgia poden ser modulats per la inhibició farmacològica de la via ERK i per quelants de Ca^{2+} intracel·lular.

En conclusió, els nostres resultats demostren alteracions en vies de supervivència intracel·lular, en la senyalització per Ca^{2+}, i en els processos d'autofàgia i apoptosi en les MNs AME. Les observacions d'aquest treball suggereixen una connexió entre els nivells de Ca^{2+} intracel·lular i la disrupció de la via ERK MAPK, l'activació de la qual contribueix a la modificació de l'autofàgia en les MNs AME. La regulació del Ca^{2+} intracel·lular i de la via ERK MAPK podrien constituir dianes per restaurar els processos d'autofàgia alterats en les MNs i ser considerades en el desenvolupament futur de noves teràpies combinades pel tractament de l'AME.

RESUMEN

La Atrofia Muscular Espinal (AME) es una enfermedad neuromuscular degenerativa grave y la primera causa genética de muerte infantil. Se origina por la pérdida o mutación del gen *Survival Motor Neuron 1* (*SMN1*) y la disminución de la proteína Survival Motor Neuron (SMN). Los niveles de SMN contribuyen a la determinación del fenotipo y la gravedad de la enfermedad. La duplicación centromérica de este gen, *SMN2*, es el responsable de la producción de proteína SMN en la AME. La reducción sistémica de SMN resulta en la afectación de varios tejidos y células. Las motoneuronas (MNs) de la médula espinal son el tipo celular con mayores alteraciones. Para desarrollar nuevas terapias que impidan la degeneración de las MNs y la progresión de la enfermedad, es necesario conocer en profundidad los mecanismos celulares implicados en ésta. El objetivo de éste trabajo ha sido analizar las alteraciones de las vías de señalización de supervivencia neuronal PI3K/Akt y ERK MAPK, así como el estudio de marcadores de apoptosis y de autofagia en diferentes modelos de AME, centrando la investigación en la implicación de estas modificaciones en las MNs.

Los resultados mostraron que las MNs de los modelos de AME presentaban incremento en la degeneración neurítica, disminución en la supervivencia celular, aumento del corte de la proteasa caspasa-3 y mayor presencia de núcleos apoptóticos. Las proteínas antiapoptóticas FAIM y XIAP estaban reducidas en extractos totales de médula espinal de ratón de AME, mientras que en cultivos de MNs se encontraban elevadas. Aun así, la presencia de caspasa-3 activa y de núcleos fragmentados indica que la expresión de FAIM-L y XIAP podría ser insuficiente para contrarrestar la activación de la apoptosis en las MNs AME. Las vías de señalización PI3K/Akt y ERK MAPK también están alteradas en las MNs AME. Se observó una disminución de la fosforilación de Akt y un incremento de la fosforilación de ERK. La inhibición de estas vías en MNs demostró su implicación en la regulación transcripcional de SMN. No obstante, la regulación endógena de SMN no alteró la fosforilación de Akt y ERK. El estudio de los marcadores de autofagia reveló una expresión diferencial de las proteínas analizadas entre los modelos celulares de AME. Mientras que en músculo había una disminución de la formación de autofagosomas y un aumento del flujo de autofagia, en las MNs se observaba un incremento de autofagosomas y una disminución del flujo. Además, las MNs AME presentaban un incremento en la fosforilación de la proteína mTOR, la cual participa en la inhibición de la autofagia. La fosforilación de mTOR y los cambios de los indicadores de la autofagia pueden ser modulados por la inhibición farmacológica de la vía ERK y por quelantes de Ca^{2+} intracelular.

En conclusión, nuestros resultados demuestran alteraciones en vías de supervivencia intracelular, en la señalización por Ca^{2+}, y en los procesos de autofagia y apoptosis en las MNs AME. Las observaciones de este trabajo sugieren una conexión entre los niveles de Ca^{2+} intracelular y la disrupción de la vía ERK MAPK, la activación de la cual contribuye a la modificación de la autofagia en las MNs AME. La regulación del Ca^{2+} intracelular y de la vía ERK MAPK podrían constituir dianas para restaurar los procesos de autofagia alterados en las MNs y ser consideradas en el futuro desarrollo de nuevas terapias combinadas para el tratamiento de la AME.

ABSTRACT

Spinal Muscular Atrophy (SMA) is a severe degenerative neuromuscular disease and the first genetic cause of infant death. SMA is caused by the loss or mutation of the *Survival Motor Neuron 1* gene (*SMN1*) and the decrease of the Survival Motor Neuron (SMN) protein. SMN levels contribute to determining the disease phenotype and severity. A centromeric duplication of this gene, *SMN2*, is responsible for SMN protein production in SMA condition. The systemic decrease of SMN results in the alteration of various cells and tissues. Spinal cord motoneurons (MNs) are the cells with greatest dysregulations in SMA disease. To develop new therapeutic strategies for preventing MN degeneration and disease progression, studying the cellular and molecular mechanisms underlying the collapse of these cells is needed. The objectives of this work have been to analyze the alterations of the neuronal survival signaling pathways PI3K/Akt and ERK MAPK, as well as the study of apoptosis and autophagy markers in different SMA models, focusing the investigation on the involvement of these modifications in MNs.

Results showed that mouse and human SMA MNs showed higher percentage of neurite degeneration, decreased cell survival, increased caspase-3 cleavage, and incremented presence of nuclei with apoptotic morphology. The antiapoptotic proteins FAIM-L and XIAP were reduced in total extracts of SMA spinal cord. Conversely, in cultured MNs they were increased. However, the presence of active caspase-3 and fragmented nuclei indicates that FAIM-L and XIAP expression may not be sufficient to counteract apoptosis activation in SMA MNs. The intracellular signaling pathways PI3K/Akt and ERK MAPK are also altered in SMA MNs. A decrease in Akt phosphorylation and an increase in ERK phosphorylation was observed. The inhibition of these pathways in MNs demonstrated their involvement in SMN protein transcription. However, SMN endogenous regulation did not alter Akt or ERK phosphorylation. The study of autophagy markers revealed a differential expression profile of the analyzed proteins between SMA cellular models. Hence, while in muscle there was a decrease in autophagosome formation and an increase in autophagic flux, in MNs there was an increase in autophagosomes and a decrease in flux. In addition, SMA MNs showed increased mTOR phosphorylation, a protein which participates in autophagy inhibition. mTOR phosphorylation and changes in autophagy markers can be modulated by ERK MAPK pathway pharmacological inhibition and intracellular Ca^{2+} chelators.

In conclusion, our results demonstrate alterations in intracellular survival pathway, in Ca^{2+} signaling, and in autophagy and apoptosis processes in SMA MNs. This work's observations suggest a connection between intracellular Ca^{2+} levels and the disruption of the ERK MAPK pathway, the activation of which contributes to the modification of autophagy in SMA MNs. Intracellular Ca^{2+} and ERK MAPK pathway regulation could constitute targets to restore altered autophagic processes in MNs and may be considered in the future development of new combined therapies for SMA treatment.

ACKNOWLEDGMENTS

Ja fa dies que aplaço aquest moment de seure davant l'ordinador a escriure aquesta part de la tesi, per mi, la més difícil. Difícil perquè significa tancar i dir adeu a una etapa que ha marcat la meva vida en molts aspectes, tant personals com professionals. D'aquesta aventura que ha estat el doctorat m'enduc records inoblidables, persones que són per mi la meva segona família, i amistats que m'agradaria conservar per sempre, i a les que vull agrair que m'hagin acompanyat durant el camí. Arribar fins aquí no hagués estat possible sense tots i cada un de vosaltres, gràcies.

Per començar, m'agradaria agrair a les meves directores de tesi, la Rosa i l'Ana, per haver-me donat l'oportunitat de realitzar el doctorat amb vosaltres i acollir-me amb els braços oberts a la Unitat de Senyalització Neuronal des del TFG. Rosa, gràcies per creure en mi i participar en el meu creixement personal i com a científica. Gràcies per deixar-me explotar la meva creativitat i fer experiments submarinos, dels que n'han sortit coses molt interessants. Gràcies també per aguantar-me en els meus dies 'tontus', quan soc una 'peeeesaada' que et demana que signis mil documents del RAPI dels trons, i quan t'omplo el cap d'idees d'experiments sense posar-te en context, tornant-te boja! Ana, gràcies pel teu positivisme i per fer-me veure sempre el got mig ple quan tot ho veig negre. Gràcies per participar, incentivar i ser còmplice de les meves idees de 'bombero' quan vull provar de fer experiments submarino. Gràcies també per ensenyar-me a treballar amb les motoneurones humanes i a dissenyar primers, tot i que cada cop que ho he de fer de nou et vingui a demanar ajuda perquè no me'n recordo! Tot i els nostres alts i baixos, com a totes les bones famílies, la vostra MariSansi s'emporta al cor mil estones divertides; quan la Rosa ens va batejar com a les seves 'Nenes', el viatge a Santander per la tesi de l'Oriolet, el 'vino turbio' i els riures, els viatges a congressos, les estones de 'cotilleos' fent el cafè, i per últim però no menys important, el trosset de xocolata diari que ja s'ha convertit en tradició.

A mi Sandrix, compitrueno de experimentos, cultivos de motoneuronas (gracias por inventar la canción 'cortar cabezas es mi profesión'), y confesiones interminables. Gracias por haber sido una gran mentora, compañera y amiga, y por estar ahí siempre que lo he necesitado. ¡Recordaré siempre los ataques de risa en los seminarios, nuestro viaje al sur y las aventuras en los congresos, sobre todo cuando nos intentamos subir a aquellos osos en Berlín de vuelta de la disco! A la Núria, per mi Nuvigu3, que va ser la meva 'primera' estudiant i conillet d'índies. Gràcies per no pensar (gaire) que soc una antipàtica davant la meva serietat a l'hora de treballar, i també per aguantar les hores i hores de confessions i drames davant del confocal o una tassa de cafè... Però, som amigues? A mi MaPi, que aunque empezamos un poco con el pie izquierdo, te has convertido en alguien muy especial para mí. Gracias por aguantar que te

haga de mami y te eche bronquitas con amor, por haber sido un gran apoyo en los meses malos y apuntarte a todos los planes que te propongo. Echaré de menos tus abrazos que lo curan todo, espero que me guardes unos cuantos para cuando venga de visita. Marieta (Maria B), ets la persona més previsora que conec (junt amb l'Arabela), no m'hagués esperat mai que portessis unes tisores a la maleta de cap de setmana pel congrés; gràcies per fer de mami amb mi aquell dia! Gràcies també a l'Oriol (Oriolet), per la teva amistat tot i coincidir poc temps en el laboratori i per acceptar ser examinador extern de la tesi, com ja et vaig dir, et dec un sopar! Grazie anche a Gabriele (Finocchio) per essere diventato un grande amico in pochissimo tempo, mi mancherà la tua follia e fare lo stupido per strada; spero di rincontrarti presto!

L'experiència durant tots aquests anys no hagués estat la mateixa sense compartir laboratori amb els BQ: Kim, Elisa, Jordi, Fabien, Roser, Marta MC, Arabelita, Maria Pazos, Marta P i Elena. Al Kim, gràcies sobretot sobretot pels financers de xocolata (encara que a vegades servissin per demanar favors), i per les converses sobre la vida un dia qualsevol a les set de la tarda. Elisa i Jordi, gràcies per les converses en les estones de cafè, ha estat un plaer compartir laboratori amb vosaltres i discutir sobre ciència i no ciència. Ro, sense tu el laboratori seria una olla de grills, tens solucions a tots els problemes! Gràcies per transmetre'm sempre la teva energia, per donar un cop de mà sempre amb actitud positiva, i ensenyar-me a relativitzar les coses quan no veia més enllà. Fabien, aunque a veces no entienda tu humor francés y me meta mucho contigo, en el fondo te voy a echar de menos. A ti, a tus camisetas frikis, y cuando aguantas mis tonterías (junto a Marta MC) pegando la nariz contra el cristal de tu despacho. Arabelita, sempre tens un somriure a la boca i estàs disposada a ajudar tot i tenir mil coses a fer, no entenc d'on treus l'energia, i t'admiro moltíssim per això. Trobaré a faltar la teva sensibilitat i dolçor, la obsessió que compartim per les coses de color pastel, i que siguis la farmaciola particular del laboratori. Maria Pazos, gràcies per obrir-nos les portes de casa teva a Cabdella, apuntar-te sempre als plans d'esquí, i per ser la culpable de mil atacs de riure al laboratori. A la nova incorporació de BQ, Marta P, et passo el testimoni de 'pijilla' del laboratori; m'hagués agradat coincidir més temps amb tu, espero que gaudeixis moltíssim de l'experiència que és fer el doctorat. Elenuccia, mi Britti, mi italiana favorita. Aunque muchas tardes no te soportaba y te quisiera tirar por las ventana por tus 'eeeegh, eeeegh' interminables y tu risa de delfín, gracias por ser mi principal fuente de abrazos, por ser un osito amoroso, la mejor bailarina de reguetón del todo el IRB, y por dejarte hacer trenzas en el pelo en cualquier momento sin rechistar. A la futura Dra. Marta Medina-Carbonero, estic molt contenta d'haver compartit amb tu l'aventura del doctorat des dels drames del RAPI i el pla de recerca fins

escriure la tesi i lliurar-la. Gràcies per ser la millor companya de ploreres, rialles i coti-cotis, ser còmplice de 'gastera' i 'comprera', i per compartir l'humor estúpid que tenim les dues. Amb tu he trobat una gran amiga i còmplice, que espero mantenir durant molts anys; perquè no et lliuraràs de mi ni durant el PostDoc. Ja ens veig a Cali-beach surfejant onades vestides amb neoprè Roxy sobretot! T'estim bonica.

Al Joan Comella i a la Maria José, gràcies per acollir-me en el seu grup a Vall d'Hebron i ensenyar-me a fer RT-PCRs i a estimar FAIM-L. A les nenes de Barcelona, Elena, Isa, Rachi i Anna, gràcies per totes les estones divertides, les foto-papada i per afegir-me al pessebre de nadal. Als 'compis' de la 4a planta, Mario, Bruno, Àgueda, Núria i Estefanía, trobaré a faltar els vostres riures a les quatre de la tarda. EAE, gracias por los vermuts de Domingo y tu sonrisa contagiosa, aunque te guste la Mahou se te quiere igual. Irene i Turi, gràcies per les converses sobre futur i per ensenyar-me que hi ha vida després del doctorat. Sara, Sílvia, Alaó i Lídia, gràcies per deixar-me robar anticossos cada dos per tres, i per la vostra amabilitat i simpatia. A l'Anaïs, gràcies per la teva paciència i amabilitat sempre que he tingut dubtes amb el confocal, trobaré a faltar les vostres discussions sobre ocells amb la Marta a l'hora del cafè. Gràcies Isu per la paciència ensenyant-me a fer servir el CFX-96 i per les estonetes xerrant entre dinar i infusió. Vull agrair també a la resta de personal, estudiants, becaris i investigadors que han passat pel grup d'USN/BQ i/o per l'IRB, i han deixat empremta en mi; Lía, Anna V, Rosa P, Lucía, Marc L, Mariona, Marina, Ferran, Roberto, Marta R, Marta G, Marc T, Meri, Lara, Marc C, Fernando, Alba C, Marc E, Alba J, Ana A, Alex, Allison, Ivan, Tom, Emma, Alejandro, Coral, Marta Corral, Leila, Cristina P, Xavi D, Pasqual, Laia, Aurora, Àuria, i també als patoncs més malvats, Raúl i Cris, què tranquils que estaran el Pol i la Gisela sense vosaltres!

Alla mia famiglia Italiana; Serena, Marina, Corrado, Alessandro, Roberta, Giovanna, Daniela, Anna, Federica, Gianna, Sveva, Giorgia e Alessia. Grazie Marina e Alessandro per avermi dato l'opportunità di venire al NICO, imparare tanto e conoscere delle persone che porterò sempre nel mio cuore. Serena, sei stata uno scoprimento unico quest'ultimo anno. Sono felice di aver incontrato te e di sapere che continueremmo a lavorare insieme sia a Torino che a LA. Gio-puzzetta-399 e Dani, da grande vorrei essere come voi, grazie per la vostra amicizia e per essere un esempio a seguire; vi adoro. Annasita-Aniña-Giggia, grazie per essere sempre gioiosa e trasmettere la tua positività a tutte. Fede, mi italo-española adoptada, grazie per la tua amicizia incondizionata, ojalá nos reencontremos pronto, ya sea en Verona, en Madrid o en Bilbao; te quiero. Grazie a tutti per le serate condivise, per accogliermi come una di voi e fare così facile ed indimenticabile il mio periodo all'estero.

Gràcies a la meva família Biomed, els mitocondris (Martí, Aida, Anna, Moni, Cris, Adrià i Unai), per acompanyar-me durant tot Biomedicina i continuar sent partícips dels meus 'pinitos' en la ciència fent el doctorat. Gràcies a l'Aida, la meva mitolleidatana particular, espero que puguem mantenir el viatge anual juntes com a tradició. I un gran gràcies a la meva titi, la Cristina; portem juntes des de l'institut i no sé com encara m'aguantes. Espero que arribi el dia en que tornem a viure en la mateixa ciutat, però de moment ens haurem de conformar amb el títol de la peli: tu a Boston i jo a California. Gràcies també a les meves 'nenas' de Lleida; Patri i Judit, que estan aquí des de gairebé sempre i que han fet aquests quatre anys molt divertits, des de les nits de dissabte de sopar i 'lo que surja', fins a les nostres escapades de cap de setmana o les festes majors de pobles. Y a ti Javi, qué decirte que no sepas ya. Necesitaría más de una página pero voy a intentar ser breve. Gracias por haberte convertido en mi mejor amigo y en un pilar esencial en mi vida. Gracias por ser y por estar, por aguantar que sea tan cariñosa siendo tu tan 'gato', por nuestros momentos de 'sassyness' y todos los bailes y comilonas que nos hemos pegado en el piso de Ricard Vinyes. Gracias también por presentarme a María Mañica, a Marta y Elena Rojas, os habéis convertido en personitas importantes para mí en poco tiempo, y espero teneros en mi vida por muchos años.

Per últim, vull agrair especialment a tota la meva família. Pare i mare, gràcies per creure en mi des de petita i ajudar-me a arribar tant lluny, res d'això no hagués estat possible sense el vostre suport incondicional. Pare, no he acabat sent alcaldessa de Lleida, però espero que estiguis igualment orgullós de mi. Mare, gràcies per escoltar-me sempre amb paciència i admiració quan parlo dels experiments del laboratori, de l'Atròfia Muscular Espinal, de ratolins i de motoneurones, tot i que no entenguis res i et soni tot a 'chino'. Marc, bro, gràcies per alegrar-te com el que més quan vinc a casa explicant que m'han acceptat un article; encara que no ens ho diguem gaire, t'estimo molt i estic orgullosa de tu. Als tiets, tietes, cosins i cosines, gràcies pels dinars amb sobretaula interminables de diumenge i per estar al meu cantó durant tot aquest temps. Tata, gràcies per creure en mi i pels teus consells, has estat sempre i seràs un gran model a seguir. Als meus padrins, que tot i no entendre perquè segueixo estudiant encara, han estat sempre donant-me el seu suport i parlant amb orgull de la seva neta, la 'biòloga'. Vull dedicar un aquest últim paràgraf a la meva padrina, ja que aquest any no ha estat gens fàcil per ella. Padrina, de gran vull ser tan valenta, lluitadora i bona persona com tu; gràcies per obligar-me a venir a dinar a la torre quan estic sola a casa i per preparar fricandó cada dos per tres sabent que és el meu plat preferit, t'estimo moltíssim i tan de bo no em faltis mai.

INDEX

ABBREVIATIONS

3-MA – 3-methyladenine

6-OHDA – 6-hydroxydopamine

α-Syn – Alpha synuclein

Aß – Amyloid ß

AßPP – Amyloid ß protein precursor

AAV – Adeno-Associated Virus

AD – Alzheimer's Disease

ADCD – Autophagy-dependent Cell Death

AIF – Apoptosis Inducing Factor

Akt – Activated Kinase or Protein Kinase B

ALS – Amyotrophic Lateral Sclerosis

ANOVA – Analysis of Variance

ANS – Autonomic Nervous System

APAF1 - Apoptosis protease-activating factor-1

ApoE – Apolipoprotein E

APP – Amyloid precursor protein

ASO – Antisense Oligonucleotide

Atg – Autophagy-related genes

ATP – Adenosine triphosphate

ATP13A2 – ATPase type 13A2

BAK – Bcl-2 homologous antagonist killer

BAX – Bcl-2-associated X protein

BBB – Blood-Brain Barrier

Bcl-2 – B-cell leukemia/lymphoma 2 protein

Bcl-XL – Bcl-2- like protein extra-large

BDNF – Brain Derived Neurotrophic Factor

bFGF – Bovine Fibroblast Growth Factor

BIR – Baculovirus Inhibitor of Apoptosis Repeat

BIRC – Baculovirus IAP repeat-containing protein

BPAN – β-propeller protein-associated neurodegeneration

BSA – Bovine Serum Albumin

C1-C7 – Cervical spinal cord segments

Ca^{2+} – Calcium

CAD – Caspase-activated deoxyribonuclease

CaMKII – Calmodulin Kinase II

CBs – Cajal Bodies

C. elegans – Caenorhabditis elegans

ChAT – Choline Acetyl Transferase

CHMP2B – Charged multivesicular body protein 2B

cIAP – Cellular Inhibitor of Apoptosis Protein

CMT2 – Charcot Marie Tooth disease type 2

CMYC – MYC proto-oncogene

CNTF – Ciliary Neurotrophic Factor

CNS – Central Nervous System

CT-1 – Cardiotrophin 1

CTCF – Corrected Total Cell Fluorescence

CTRP3 – C1q/TNF-Related Protein 3

DIAP – Drosophila Inhibitor of Apoptosis Protein

DIV – Days In Vitro

DMEM – Dulbeco's Modified Eagle Medium

DMSO – Dimethyl sulfoxide

DNA – Deoxyribonucleic Acid

DRG – Dorsal Root Ganglia

DTT – Dithiothreitol

E12.5, E13, E18 – Embryonic day 12.5, 13, 18

EMA – European Medicine Agency

ER – Endoplasmic Reticulum

ERK – Extracellular Regulated Kinase

ESS – Exonic Splicing Sliencer

EV – Empty Vector

FADD – Fas Associated Death Domain

FAIM-L – Fas Apoptosis Inhibitory Molecule Long

Fas – Protein with a cell death domain

FasL – Fas ligand

FDA – Food and Drug Administration

FF – Fast-twitch Fatigable

FFR – Fast-twitch Fatigable-Resistant

GAPDH – Glyceraldehyde-3-Phosphate dehydrogenase

GFP – Green Fluorescent Protein

GDNF – Glial cell line Derived Neurotrophic Factor

KCl – Potassium chloride

Grm7 - Glutamate Metabotropic Receptor 7

HB9 – Homeobox transcription factor B9

HD – Huntington Disease

HDACs – Histone deacetylases

HEK 293T – Human Embryonic Kidney Cell Line

HGF – Hepatocyte Growth Factor

hiPSCs – Human Induced Pluripotent Stem Cells

HFMSE – Hammersmith Functional Motor Scale Expanded

hnRNPs – Heterogenous nuclear ribonucleoproteins

HRP – Horse Radish Peroxidase

HS – Horse Serum

HSC70 – Heat Shock Protein 70

HSP – Hereditary spastic paraplegia

Htt – Huntingtin

HU – Hydroxyurea

HuR – Hu antigen R

I3P – Inositol (1,4,5)P3

IAPs – Inhibitor of apoptosis proteins

IBMs – IAP-binding motifs

ICAD – Inhibitor of Caspase-activated deoxyribonuclease

IGF-1 – Insulin-like Growth Factor 1

IkB – Inhibitory kappa B

IntDen – Integrated Density

JAK/STAT – Janus Kinase signal transduced and activator of transcription

JNK – c-Jun NH2-Terminal Kinase

K^+ – Potassium

KCl – Potassium chloride

LAMP-1 – Lysosomal-associated membrane protein 1

LAMP-2A – Lysosomal-associated membrane protein 2A

LB – Luria Broth

LC3 – Microtubule-associated protein light chain 3

LCDC - Lysosome-dependent cell death

LIR – LC3-interacting region

LRRK2 – Leucine Rich Repeat Kinase 2

LSD – Lysosomal storage disease

LY – LY294002

MAPK –Mitogen Activated Protein Kinase

MCL-1 – Myeloid Cell Leukemia 1

MEM – Minimum Eagle's Medium

miRNA – microRNA

ML-IAP – Melanoma Inhibitor of Apoptosis Protein

MLKL – Mixed Lineage Kinase domain-Like Protein

MNs – Motoneurons

MNPs – Motoneuron Progenitors

MOM – Mitochondrial Outer Membrane

MOMP – Mitochondrial Outer Membrane Permeabilization

mRNA – messenger RNA

mTOR – Mammalian Target of Rapamycin

mTORC1 – mTOR Complex 1

mTORC2 – mTOR Complex 2

mutSMA – $Smn^{-/-}$; $SMN2^{+/+}$ mice

Na^+ - Sodium

NAIP – Neuronal Apoptosis Inhibitory Protein

NDs – Neurodegenerative diseases

NEAA – Non essential amino acids

NEPI – Neuroepithelial

NGF – Nerve Growth Factor

NF-M – Neurofilament M

NFkappaB – Nuclear Factor kappa B

NSC34 – Neuroblastoma x Spinal Cord-34

NTFs – Neurotrophic Factors

OCT4 – Octamer-binding transcription factor 4

OpIAP: Baculovirus Inhibitor of Apoptosis Protein

ovSMN – overexpressed SMN

p62/SQSTM1 – Sequestrosome 1

PBS – Phosphate Buffered Saline

PCD – Programmed cell death

PCR – Polymerase Chain Reaction

PD – Parkinson Disease

PDK1 – 3-Phosphoinositide-dependent kinase 1

PEI – Polyethyleneimine

PFA – Paraformaldehyde

PI – Phosphatidylinositol

PI3K – Phosphatidylinositol-3-kinase

PICALM – Phosphatidylinositol-binding clathrin assembly protein

PIP2 – Phosphatidylinositol-2-hosphate

PIP3 – Phosphatidylinositol-3-hosphate

PLCy – Phospholypase C

PLS3 – Plastin 3

PMSF – Phenylmethylsulfonyl fluoride

pNF-H – phosphorylated neurofilament heavy

PNS – Peripheral Nervous System

PRL – Prolactin

PS1 – Presenilin 1

PVDF – Polyvinylidene difluoride

RA – Retinoic Acid

RBPs – mRNA Binding Proteins

RCF – Relative centrifugal force

RING – Really Interesting New Gene

RIPK3 – Receptor-interacting serine/threonine-protein kinase 3

RISC – RNA-Induced Silencing Complex

RNA – Ribonucleic Acid

RNAi – RNA interference

RNP – Ribonucleoprotein

rRNA – Ribosomal RNA

RSK – Ribosomal S6 kinase

RTK – Tyrosine Kinase Receptor

RT-qPCR – Reverse Transcriptase quantitative Polymerase Chain Reaction

scAAV – Self-complementary adeno-associated virus

S. cerevisiae – Saccharomyces cerevisiae

SD – Standard Deviation

SDS – Sodiumdodecylsulfate

SDS-PAGE – SDS polyacrylamide gel electrophoresis

SEM – Standard Error of the Mean

SERF1 – Small EDRK-Rich Factor 1

SFR – Slow-twitch Fatigable-Resistant

Shh – Sonic Hedgehog

shRNA – Short hairpin RNA

shSmn – Short hairpin Smn

SIGMAR1 – Sigma non-opioid intracellular receptor 1

siRNA – Small interfering RNA

SMA – Spinal Muscular Atrophy

SMAC – Second Mitochondrial Activator of Caspases

SMN – Human Survival Motor Neuron Protein

SMN – Human Survival Motor Neuron Gene

Smn-1 – SMN gene in C.elegans

SMN1 – Telomeric gene for SMN

SMN2 – Centromeric gene for SMN

SMNΔ7 – SMN gene without exon 7

SMNdelta7 – $Smn^{-/-}$; $SMN2^{+/+}$; $SMN\ 7^{+/+}$ mouse model

snoRNAs – Small nucleolar RNAs

snRNP – Small nuclear ribonucleoprotein

SOD1 – Superoxide Dismutase 1

SOX2 – Sex determining region Y)-box

S. pombe – Schizosaccharomyces pombe

τ - Tau protein

TBST – Tris Buffered Saline with Tween 20

TFEB – Transcription factor EB

TNF – Tumor Necrosis Factor

TTC – Tetanus Toxic Chain

TU – Transducing units

TUNEL – Terminal Deoxynucleotidyl Transferase Mediated deoxy uridine triphosphate Nick-End Labelling

U0 – U0126

Uba 1 – Ubiquitin activating enzyme 1

ULK1 – unc-51-like autophagy-activating kinase 1

UPS – Ubiquitin Proteasome System

VGCC – Voltage gated calcium channel

VPA – Valproic Acid

WNT – Wingless-type MMTV integration protein

WT – Wild Type

WIPI4 – WD repeat domain phosphoinositide-interacting protein 4

XIAP – X-linked Inhibitor of Apoptosis Protein

YFP – Yellow Fluorescent Protein

INDEX OF FIGURES AND TABLES

1. Index of Figures

2. Index of Tables

INTRODUCTION

1. SPINAL MUSCULAR ATROPHY (SMA)

Spinal Muscular Atrophy (SMA) is an hereditary autosomal recessive neuromuscular disease. The term SMA encompasses a group of genetic disorders with one common feature, the degeneration of the alpha motoneurons (**MNs**) in the anterior horn of the spinal cord and proximal muscular atrophy (**Figure 1**) (Lewelt et al., 2012). The disease was first described by Dr Guido Werdnig and Dr Johann Hoffman at the beginning of the 1890s, describing a progressive weakness of skeletal and respiratory muscles, which lead to pulmonary problems, spine deformities, swallowing complications and gastrointestinal dysfunction (Kolb & Kissel, 2015). Nevertheless, multiple described phenotypes with different clinical severity were observed and formalized into a classification scheme at an International Consortium on Spinal Muscular Atrophy in 1991 (Kolb & Kissel, 2015).

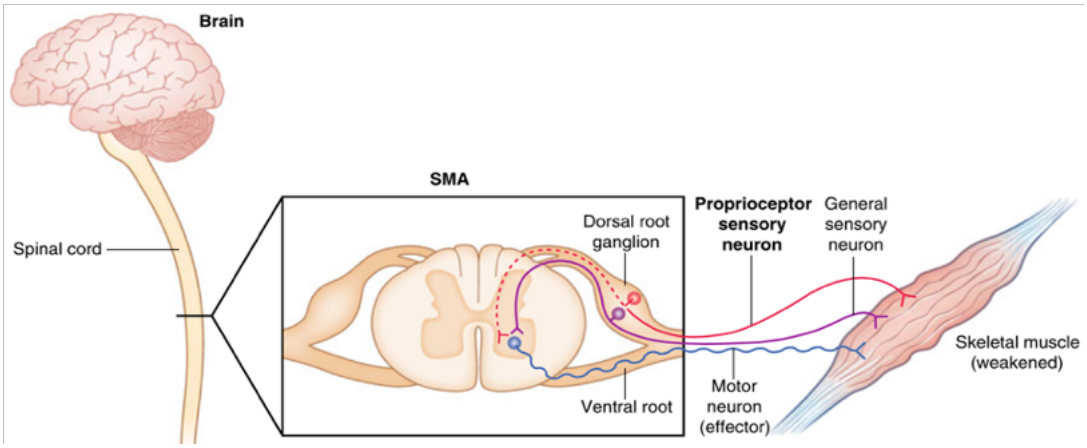

Figure 1 | MN degeneration and muscular atrophy are pathological hallmarks of SMA disease. Adapted from (Lewelt et al., 2012). Reproduced with permission from Springer Nature.

It was not until 1990 when the neuropediatric and researcher Judith Melki discovered that SMA was caused by the deletion or mutation of the *Survival Motor Neuron 1* (*SMN1*) gene, located on chromosome 5q13.1 (Melki et al., 1990). *SMN1* gene is located in a region with a high degree of genomic instability, where a 500-kb duplication appeared about five million years ago in a primate ancestor, conferring them 2 to 7 identical copies of *SMN* (Rochette et al., 2001). A sequence variation evolved in humans, originating a near-duplication of *SMN1*, called *SMN2*, and slightly differs from *SMN1* in several nucleotides. The most important nucleotide change is from a cytosine to a thymine in exon 7 of *SMN2* gene. This modification results in the exclusion of exon 7 in the 90% of the transcripts from *SMN2* (Cartegni & Krainer, 2002; Young et al., 2000). The majority of the translated protein is not functional and gets degraded rapidly. Without *SMN1*, protein translated from *SMN2* copies is not enough to maintain MNs survival

(Lefebvre et al., 1997; Wirth, 2000), and the severity of the disease relies on the copy number of *SMN2* gene (Mailman et al., 2002), although it is not the only phenotypic modifier described (Prior et al., 2009).

1.1. SPINAL CORD MNs

MNs are the cells of the central nervous system (CNS) in charge of the generation and transmission of the nerve impulses to produce the muscular contraction. These cells are divided in two types, the **upper MNs** that originate from the cerebral cortex, and the **lower MNs** that are located in the brainstem and spinal cord.

- **Upper MNs** are located in the pre-motor and primary motor region of the cerebral cortex and are responsible for planning and directing body movements by stablishing glutamatergic connections with the lower MNs in the spinal cord (Purves et al., 2003).
- **Lower MNs** are cholinergic cells located in the nuclei of the cranial nerves in the brainstem and in the ventral horn of the spinal cord. These cells receive inputs from the upper MNs (complex circuits), sensory neurons and interneurons (local circuits), and project their axonal extensions outside the CNS to control muscle contraction directly by performing synapses with skeletal muscle or indirectly through dorsal root ganglia (DRG)(Purves et al., 2003).

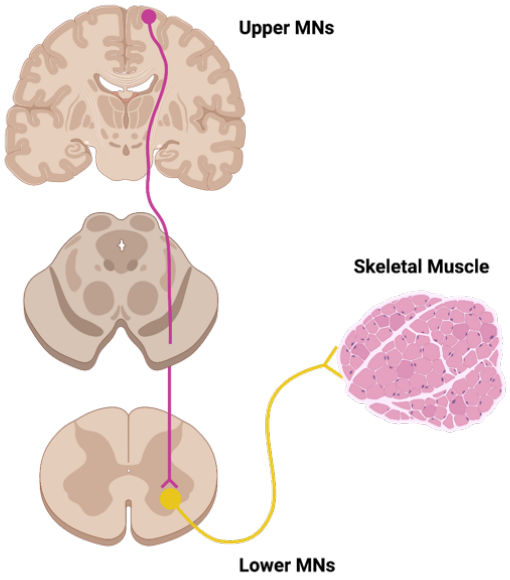

Figure 2 | Simplified schematic representation of the localization and function of the upper MNs and the lower MNs. Upper MNs (pink) from the motor cortex control body movements by stablishing connections with lower MNs (yellow) in the spinal cord. Based on (Purves et al., 2003). Created with BioRender.com.

1.2. Classification of the Lower MNs

Lower MNs are subclassified into three groups depending on the type of target they innervate:

1. **Branchial MNs:** These MNs are located principally in the brainstem and together with the sensory neurons form the following cranial nerves to innervate the facial and neck muscles; the trigeminal (V), the facial (VII), the glossopharyngeal (IX), the vagus (X), and the accessory (XII) (Chandrasekhar, 2004).
2. **Visceral MNs:** The visceral MNs belong to the autonomic nervous system (ANS). These cells transmit their signal indirectly through the ganglionic neurons of the peripheral nervous system (PNS), which in turn target smooth muscle and glands (Purves et al., 2003).
3. **Somatic MNs (Spinal Cord MNs):** These cells are located in the ventral horn of the spinal cord, controlling skeletal muscle contraction. They are characterized by a long axonal extension, which is a unique anatomical feature. Each MN forms a motor unit with the muscular fiber that innervates, and depending on the muscle fiber type, somatic MNs can be divided into three groups: alpha, beta and gamma (Kanning et al., 2010; Stifani, 2014).

1.3. Classification of the spinal cord MNs

Spinal cord MNs are divided into three groups depending on the muscular type they innervate:

1. **Alpha MNs (α-MNs):** are the most abundant type of MNs, morphologically characterized by a large soma. These cells receive monosynaptic innervation directly from sensory neurons and exclusively innervate extrafusal muscle fibers forming the neuromuscular junction (NMJ). Alpha MNs are subclassified based on the contractile properties of the extrafusal fiber that they innervate, their size, conductivity and neuronal excitability:
    a. **Slow-twitch fatigable-resistant (SFR) MNs** are cells with smaller somas and short axons responsible for the maintenance of the body posture by establishing their NMJ with slow contraction muscle fibers, which respond to a lower stimulation threshold and are capable of maintain their activity after the cease of stimulation (R. H. Lee & Heckman, 1998).
    b. **Fast-twitch fatigable (FF) MNs** are cells with larger somas, higher rates of dendritic arborization and abundant presynaptic terminals (Cullheim et al., 1987). These MNs innervate fibers of rapid contraction, activating movements that require short impulses but strong contractions. In ALS and SMA diseases, and in aging FF MNs

are considered more vulnerable since these cells degenerate earlier than MNs innervating slow muscles (Kanning et al., 2010; Schweingruber & Hedlund, 2022).

c. **Fast-twitch fatigable-resistant (FFR) MNs** are cells that have intermediate characteristics between FF and SFR MNs, although its specific physiology is still unknown.

2. **Beta MNs (ß-MNs):** are smaller and less abundant than other MN subtypes. They control both muscle contraction and responsiveness of the sensory feedback from muscle spindles by innervating both intrafusal and extrafusal muscle fibers (Bessou et al., 1965; Stifani, 2014). These cells are subdivided into two subtypes based on the intrafusal fiber type that they innervate:
    a. **Static beta MNs** innervate nuclear chain fibers and increase the firing rate of sensory fibers at a given muscle length.
    b. **Dynamic beta MNs** innervate the nuclear bag fibers of muscle spindles and increase the stretch-sensitivity of the sensory fibers.
3. **Gamma MNs (γ-MNs):** are characterized by slow axonal conduction due to their smaller axon diameter, and are responsible for controlling the sensitivity of muscle spindles, regulating complex functions in motor control even if they don't have any particular motor function. γ-MNs don't receive innervation from proprioceptive sensory neurons. These cells contribute to the modulation of muscle contraction through direct stimulation of the intrafusal fibers. Hence, they increase fibers' tension and mimic the stretch of the muscle. Gamma MNs are divided into two subtypes:
    a. **Static gamma MNs** innervate nuclear chain fibers and static nuclear bag fibers.
    b. **Dynamic gamma MNs** innervate dynamic nuclear bag fibers.

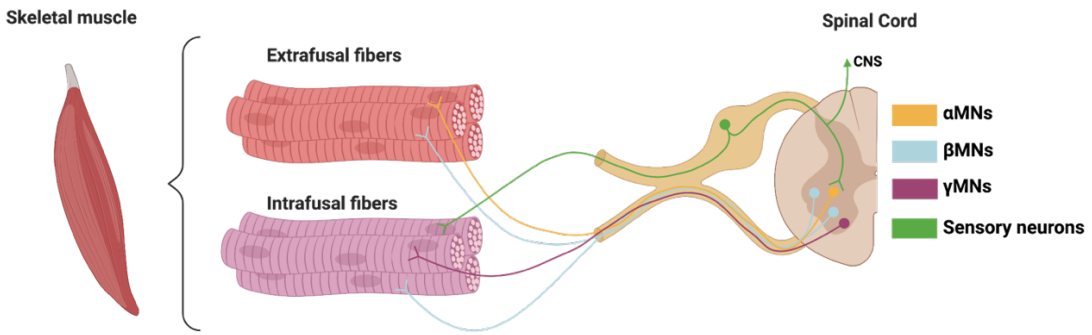

Figure 3 | Classification and schematic representation of the Somatic MNs and the type of muscle they innervate. Alpha MNs (yellow) innervate extrafusal muscle fibers. Beta MNs (blue) innervate both types of muscle fibers. Gamma MNs (purple) innervate intrafusal fibers. Sensory neurons (green) carry information from the intrafusal fibers to the CNS and to the somatic MNs. Based on (Stifani, 2014). Created with BioRender.com.

1.4. Epidemiology of SMA

SMA is known to be the most common neuromuscular disease in infants, and the leading cause of infant mortality by a genetic disorder, with an incidence of 1 in 6,000-11,000 live births, and the carrier frequency is of 1 in 54 for the world population (Sugarman et al., 2012), and 1 in 35 for the European population (Verhaart et al., 2017).

1.4.1. Clinical classification of SMA

Multiple described phenotypes of SMA have been associated to the disease severity. Thus, a classification based on the age of onset and the maximum motor function achieved was created and has been adapted through years (see **Table 1**).

The disease diagnosis and classification are first made by clinical parameters and onset symptomatology, observing muscle atrophy, tremor and weakness, loss of reflexes, abnormal tongue movements and denervation on an electromyogram. A genetic test confirms the SMA subtype depending on the *SMN2* gene copy number (Kolb & Kissel, 2015; Russman, 2007). An additional classification to assess the patient current functional status and response to therapies has been proposed, classifying the patients into nonsitters, sitters and walkers, independently from their SMA subtype (**Figure 6**) (Wirth et al., 2020).

Table 1 | Classification of human SMA types. SMA is classified into 5 types (Type 0 to IV) based in the age of onset symptoms, maximum motor function achieved and clinical severity.

SMA Type	Motor milestones achieved	Subtype	Onset	Estimated SMN2 copies	Estimated SMA proportion
SMA0	-	0	Prenatal	1	<1%
SMAI	Never sit	1A	<1 months	1 or 2 (80%)	60%
		1B	1-3 months		
		1C	3-6 months		
SMAII	Sits but never stands	2A	>6 months	3 (>70%)	27%
		2B	≥12 months		
SMAIII	Stands and walks	3A	18-36 months	3 or 4 (95%)	12%
		3B	>3 years		
SMAIV	Stands and walks	None*	2nd-3rd decade of life	4 or more (>90%)	1%

Type 0 SMA or prenatal

Type 0 SMA is a classification for patients with a prenatal onset. Neonates present severe weakness, hypotonia and decreased fetal movements. Patients require of respiratory assistance, suffer from autonomic dysfunction and can present in some cases congenital heart defects. Lifespan is reduced; most of the children are unable to survive beyond 6 months of age (Dubowitz, 1999; Kolb & Kissel, 2015).

Type I SMA or infantile (Werdnig-Hoffman disease)

Type I SMA or Werdnig-Hoffman disease patients present symptomatology, evidenced before 6 months of age: hypotonia, poor head control, reduced or absent tendon reflexes and tongue and swallowing weakness. The weakness in intercostal muscles produces a bell-shaped chest. Infants with type 1 SMA usually develop respiratory failure before 2 years of life (Kolb & Kissel, 2015). Survival prognosis varies depending on the symptoms severity. Nutritional and respiratory support help to prolong life expectancy (Finkel et al., 2014; Thomas & Dubowitz, 1994).

Type II SMA or intermediate

Type II SMA patients present progressive proximal leg weakness greater than in the arms, with hypotonia and areflexia, scoliosis, joint contractures and ankylosis of the mandible; with the appearance of symptomatology between 6 and 18 months of age. SMAII children manage to sit unassisted, but never to walk independently. The combination of intercostal muscular weakness, thorax abnormalities, and scoliosis can cause severe respiratory insufficiency, resulting in the need of supportive care (Kolb & Kissel, 2015). Although life expectancy is reduced, survival and disease progression can variate depending on the supportive care that patients receive (Mercuri et al., 2016).

Type III SMA or juvenile (Kugelberg-Welander disease)

Type III SMA or Kugelberg-Welander disease patients are subdivided depending on the disease onset; Type 3a for patients with an onset between 18 months and 3 years, and Type 3b for patients with an onset between 3 and 21 years of age. SMA Type III patients are able to walk unassisted. Nonetheless, they present difficulties when running, climbing steps or rising when they are sat on a chair. The progressive proximal leg weakness results in the eventual need of a wheelchair. Scoliosis and respiratory muscle weakness are also present in these patients. Life expectancy is not normally altered in these patients if given a good supportive care (Mercuri et al., 2016).

Type IV SMA or adult

Type IV SMA patients represent around the 1% of SMA cases and have the mildest form of the disease, mainly occurring in males. They present similar comorbidities as SMA Type 3 patients, however, onset is in adulthood after the age of 21. Gradual proximal weakness of the limbs is present but other complications such as swallowing and respiratory dysfunction can appear. Life expectancy is not affected but patients eventually require the use of a wheelchair to move (Piepers et al., 2008).

1.5. Molecular genetics of SMA

1.5.1. SMN genes

SMN1 and *SMN2* genes, identified by Judith Melki's group in the early 1990s (Melki et al., 1990), are located in the region q11.2-13.3 of chromosome 5, with a 99.9% identical sequence. The locus contains a tandem chromosomal duplication in the centromeric region of more than 500 kb with multiple repeated sequences. This characteristic makes the region more prone to suffer deletions (Melki et al., 1994).

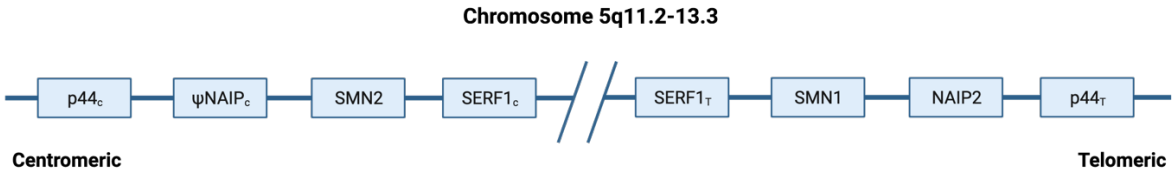

Figure 4 | Duplicated chromosomal region 5q11.2-13.3. This region contains the genes p44, NAIP (Neuronal Apoptosis Inhibitory Protein), SMN and SERF1 (Small EDRK-Rich Factor 1). Based on (Lefebvre et al., 1995). Created with BioRender.com.

Each *SMN* copy is about 34 kb long and contains 10 exons (exons 1, 2a, 2b, 3, 4, 5, 6a, 6b, 7 and 8). The two *SMN* genes differ by only five nucleotides, but only a C>T transition at position +6 in exon 7 (c.840C>T) is within the coding region. Despite it is a silent variant that causes no amino acid exchange, it creates an exonic splicing silencer site (ESS), thus altering the splicing of exon 7 and generating a truncated protein (Lefebvre et al., 1995; Lorson et al., 1999).

SMN1 is generally correctly spliced and produces full-length transcripts and protein. *SMN2* mainly produces alternatively spliced variants lacking exon 7 (*SMN2*Δ7), and only approximately 10% of the transcripts are properly spliced and are able to generate a full-length protein (Kashima and Manley 2003; Lorson, 2000). The resultant SMNΔ7 protein functions partially and oligomerizes less efficiently, which results in higher protein instability and rapid

degradation (Lorson et al., 1999; Monani, Sendtner, et al., 2000). In SMA patients both alleles of the *SMN1* are lost or mutated. Homozygous absence of *SMN2*, which is found in about 5% of controls has no clinical phenotype (Wirth, 2000). In SMA patients, SMN protein production derives entirely from the *SMN2* gene. The sole 10% of protein produced cannot compensate *SMN1*, resulting in reduced levels of SMN protein in the cells (**Figure 5**).

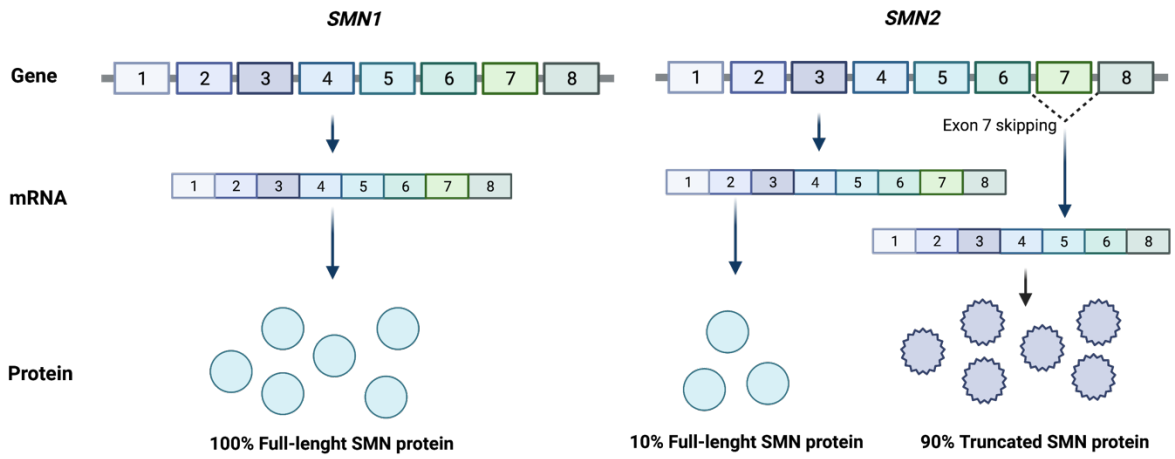

Figure 5 | Schematic representation of the transcription of *SMN1* and *SMN2* genes. In the *SMN1* gene all the transcripts encode for the full-length SMN protein. In contrast, in the *SMN2* gene, about 90% of the transcripts encode for a truncated protein (SMNΔ7), which is unstable and rapidly degraded. Only around a 10% of the transcripts from *SMN2* produce the full-length SMN protein, which results in low levels of SMN. Created with BioRender.com

Ninety-six percent of SMA patients show homozygous absence of *SMN1* exons 7 and 8 or exon 7 only, while 3.6% of the patients present a mutation on one chromosome and a deletion or gene conversion on the other chromosome. The most frequent mutation on *SMN1* gene is the Y272C missense mutation, corresponding to a 20% of the cases (Wirth, 2000).

1.5.2. Genotype-phenotype correlation

SMA severity phenotype is mainly influenced principally by the *SMN2* copy number; the higher the copy number, the milder the phenotype. Hence, as the number of *SMN2* copies increase, more quantity of stable full-length SMN protein is produced. Despite it is strong, this correlation is not absolute. There is heterogeneity of *SMN2* copy numbers in each SMA subtype; as an example, the 73% of patients with SMA type I have 2 *SMN2* copies, whereas there is a 20% of patients that carry three copies of the gene. Likewise, SMA type 2 patients carry three copies of *SMN2* in the 78% of the cases, but 16% carry only 2 copies of *SMN2*, having

a milder phenotype than patients with SMA type I (**Figure 6**) (Wirth et al., 2020). Therefore, although the number of *SMN2* copies modulates the SMA phenotype, it should not be used for prediction of SMA severity.

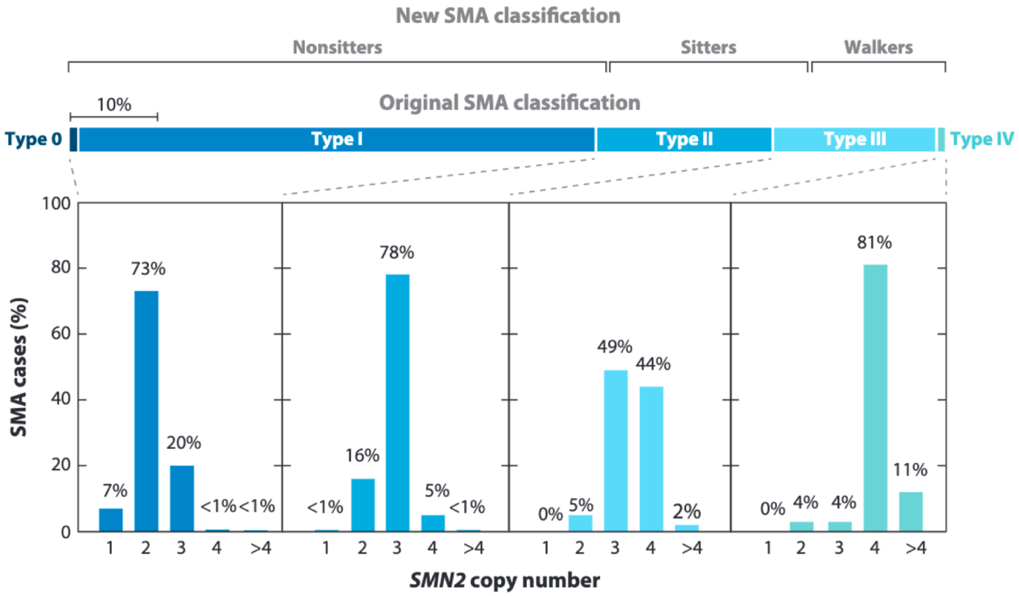

Figure 6 | New SMA classification and Original SMA classification. Nonsitters: All type 0 and type I patients and some type II patients. Sitters: the remaining type II and some type III patients who are able to walk independently. Walkers: the remaining type III patients and all type IV patients. The correlations between clinical severity and *SMN2* copy numbers are taken from the most recent compiled study of SMA (Calucho et al., 2018). Type 0 SMA cases reported so far carry one copy of *SMN2* gene (Wirth et al., 2020). Reproduced with permission from Annual Reviews, Inc.

1.5.3. SMA modifiers

1.5.3.1. SMN-dependent modifiers

As aforementioned, *SMN2* copy number determines the severity of SMA disease, and *SMN2* is used to determine the patient eligibility to receive certain therapies (Glascock et al., 2018, 2020). However, not all *SMN2* copies are identical and able to produce equal amounts of SMN protein, as *SMN2* copies can be truncated or mutated, affecting the splicing or the protein function (Wirth, 2021). Moreover, multiple trans-regulatory factors such as *Tra2-ß1* and several hnRNP proteins have been reported to influence on SMN2 exon 7 inclusion or exclusion (Kannan et al., 2020; Wirth, 2021; Wirth et al., 2020). Another known modifier of the disease is the Neuronal Apoptosis Inhibitory Protein (*NAIP*); NAIP gene is placed within the *SMN1* locus, and is deleted in 67% of SMA type I patients, and around a 42% in SMA type II and III patients (Roy et al., 1995). Furthermore, *NAIP* deletion is associated with an early onset, severe hypotonia, and worse outcome in SMA patients with homozygous *SMN1* deletion (Ahn et al.,

2017). Hence, relying solely on the number of *SMN2* copies to predict SMA severity should not be the only condition to take into consideration when treating SMA patients.

1.5.3.2. SMN-independent modifiers

In humans, two SMN-independent protective modifier genes have been described to influence disease severity in phenotypically discordant SMA families; *Plastin 3* (*PLS3*) and *Neurocalcin Delta* (*NCALD*). *PLS3* is localized in the X-chromosome, and is upregulated in unaffected *SMN1*-deleted females blood (Oprea et al., 2008), and in *SMN1*-deleted iPSCs-derived MNs from asymptomatic women (Heesen et al., 2016). *NCALD* is a Ca^{2+}-dependent negative regulator of endocytosis and is downregulated in lymphoblastoid cell lines of asymptomatic individuals when compared to SMA patients (Riessland et al., 2017). Moreover, a significant number of SMA-independent modifiers have recently been identified by various genetic screenings in SMA animal models (Wirth, 2021; Wirth et al., 2017).

1.6. SMN protein

Human SMN protein, expressed in all cell types, contains 294 amino acids, with a molecular weight of around 38 kDa in western blot analysis (Coovert et al., 1997; Lefebvre et al., 1997). The protein localizes to both nuclear and cytosolic compartments and it is implicated in a wide range of cellular processes (R. N. Singh et al., 2017). SMN can bind to several proteins and participate in different physiological processes, but the specific function that is critical for MNs and other cell types when SMN proteins levels are low is still unclear.

At structural level, SMN protein harbors multiple domains, from N-terminal to C-terminal (**Figure 6**):

- **Basic/lysine-rich domain:** Mainly encoded by exon 2 and responsible for the interaction between SMN and RNA in the Gems structures, like Gemin2 (Lorson et al., 1998).
- **Tudor domain:** A highly conserved motif that mediates SMN interaction with other proteins facilitating processes like the assembly of spliceosomes and the nuclear localization of the protein (Selenko et al., 2001).
- **Proline-rich domain:** Encoded by exons 4, 5 and 6, allows the binding of SMN protein with profilins, thus regulating actin dynamics (Giesemann et al., 1999).
- **YG box or tyrosine/glycine-rich region:** Plays a role in SMN stability by regulation of SMN self-oligomerization (Lorson et al., 1998). The domain is important for post-transcriptional

modifications that will determine SMN location (i.e. the Cajal Bodies (CBs) or the cytoplasm) and function.

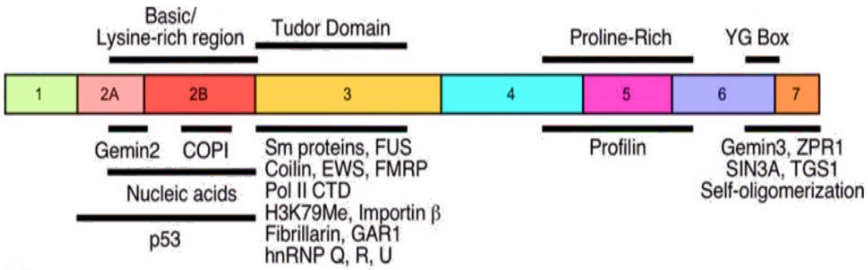

Figure 7 | Diagrammatic representation of the SMN protein. The numbers in the colored boxes indicate the exon. Domains are indicated above the boxes and proteins interacting with SMN are shown below (R. N. Singh et al., 2017). Reproduced with permission from Elsevier.

Alternative splicing of *SMN1* and *SMN2* generates several transcripts, including the full-length *SMN* and the *SMNΔ7* mRNA transcripts (R. N. Singh et al., 2017). One of the other isoforms codes for axonal-SMN (a-SMN), which plays a developmental role in mammalian brain, promoting axonal growth, stimulating cell motility and regulating chemokine expression (Locatelli et al., 2012). The functions of the other SMN protein isoforms generated from these alternative transcripts are still unknown.

1.6.1. SMN functions

1.6.1.1. SMN in RNA metabolism

SMN protein is described to be involved in several aspects of the RNA metabolism:

Spliceosome small nuclear ribonucleoprotein (snRNP) assembly: snRNP assembly is executed by SMN complex; formed by SMN (also known as Gemin1), Gemin proteins from 2 to 8, and Unrip (UNR). The snRNPs are RNA-protein complexes required for the spliceosome formation, a machinery that removes intronic sequences from the pre-mRNA. The composition of a snRNP consists on a U snRNA (U1, U2, U4, U5, U11 or U12) bound to a set of 7 Sm proteins (Matera & Wang, 2014), which requires the mediation of the SMN complex (Pellizzoni et al., 1999). In the cytoplasm, SMN monomers self-associate to form SMN oligomers, which in turn form a macro complex with all the other Gemins and UNR; the assembly reaction is ATP dependent (Bühler et al., 1999; Fischer et al., 1997). Then, the SMN complex promotes the Sm heptameric ring assembly to the snRNAs and the whole complex is translocated to the nucleus (where is called 'Gem') into the CBs, where the snRNAs go through a final maturation (R. N. Singh et al., 2017). SMA type I patient's MNs show reduced number of Gems (Lorson et al.,

1998). Additionally, SMN has also been associated with the participation in the assembly and metabolism of other ribonucleotide complexes like snoRNPs (RNP complexes that perform posttranscriptional modifications to ribosomal RNAs (rRNAs) and to snRNAs (Pellizzoni, Baccon, et al., 2001).

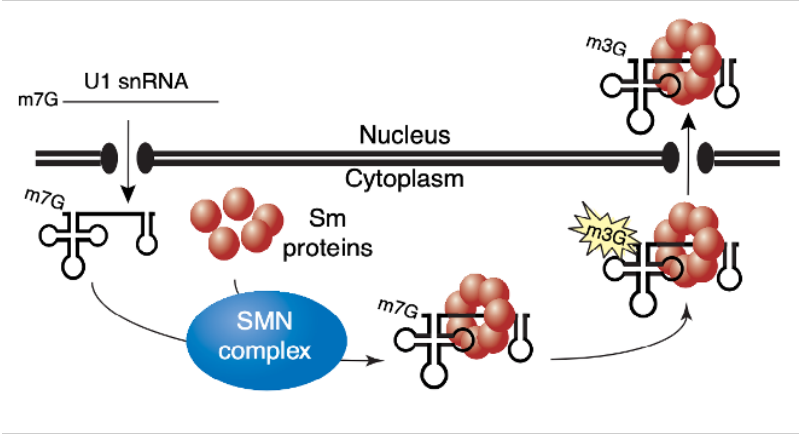

Figure 8 | SMN function in the snRNP assembly. SMN (as part of the SMN complex) participates in the formation of spliceosomal U snRNPs. Initially, the U snRNA that is transcribed in the nucleus is transported to the cytoplasm where it assembles with Sm proteins with the assistance of SMN complex. After Sm assembly the U snRNA suffers modifications and reenters into the nucleus (Eggert et al., 2006). Reproduced with permission from Elsevier.

Pre-mRNA splicing: The exact mechanism by which SMN complex acts modulating the splicing of pre-mRNAs is not fully understood. SMN is described to interact with RNA helicases (Gemin3, DDX1, DDX3 and DDX5), suggesting that this protein can modulate its own splicing as well as other transcripts through these interactions (Charroux et al., 1999; Shafey et al., 2010; R. N. Singh et al., 2017).

mRNA stabilization and trafficking: Several investigations support the hypothesis that SMN is involved in mRNA trafficking; it has been detected by electron microscopy in the dendrites, axons and growth cones of cultured MNs (Pagliardini et al., 2000). Moreover, bi-directional transport of SMN along the axons has also been observed *in* vivo (H. L. Zhang et al., 2003). There are two different trafficking mechanisms in which SMN is involved:

– SMN binds to a protein from Golgi-derived vesicles, alpha-COP. Golgi-derived vesicles are involved in intracellular trafficking in neurites, and play a crucial role in the maturation of these neural cell processes (Peter et al., 2011). This association suggests that SMN could be involved in neuronal outgrowth and axonal formation. As an example of this process,

SMN contributes to the localization of ß-Actin mRNA in the growth cones (Rossoll et al., 2003).

- SMN binds to mRNA-binding proteins (RBPs) to promote mRNA transport along the axon, which is important to provide rapid protein turnover in distal regions of the neurons (Fallini et al., 2012; Glock et al., 2017).

mRNA transcripts transcription and translation: SMN complex also participates in mRNA translation (Fallini et al., 2016), by its association to polyribosomes, and regulating the availability of ribosomal units for local translation (Sanchez et al., 2013).

1.6.1.2. SMN in cytoskeleton dynamics modulation

SMN protein has been linked to the cytoskeleton dynamics modulation through the following mechanisms:

- Transport and localization of the ß-Actin mRNA in the growth cones, an essential protein for cytoskeletal dynamics and growth cone formation (Rossoll et al., 2003).
- Colocalization with Profilin 2a, a neuron-specific actin-binding protein that participates in the regulation of actin turnover by promoting its polymerization (Nölle et al., 2011; Sharma et al., 2005).

1.6.1.3. SMN in maintaining cellular homeostasis

SMN protein level reduction has been related to dysregulations of multiple cellular processes:

- SMN association with the RNA polymerase II suggests its role as a transcription factor in the cell (Pellizzoni, Charroux, et al., 2001).
- Low SMN levels result in the increased activity of the c-Jun NH_2-Terminal Kinase 3 (JNK3) through an unknown mechanism, which contributes to an increase of MN degeneration (Genabai et al., 2015).
- The ubiquitin homeostasis is compromised in the spinal cord and gastrocnemius muscle of severe SMA mice (Wishart et al., 2014); SMN reduction leads to decreased Uba1 (ubiquitin activating enzyme 1) levels and the dysregulation of the ubiquitination process (Wishart et al., 2014).
- Studies in several SMA mouse models have revealed endosomal trafficking defects in neuronal and non-neuronal tissue (Dimitriadi et al., 2016). Similarly, an increase in the number of autophagosomes has been observed in SMN-reduced models, and the use of

autophagy modulators can influence on SMN protein levels (de la Fuente et al., 2018; Garcera et al., 2013; Periyakaruppiah et al., 2016; Piras et al., 2017).

- Low SMN protein levels are linked to a dysregulation in anti-apoptotic proteins like Bcl-2 and Bcl-XL in some neuronal models (D. A. Kerr et al., 2000; Soler-Botija et al., 2003).
- SMN deficiency is associated to changes in oxidative stress, mitochondrial malfunction and transport, and bioenergetic pathway impairments (Chaytow et al., 2018).

To date none of the roles in which SMN has been described to participate has been identified as uniquely responsible for SMA pathophysiology.

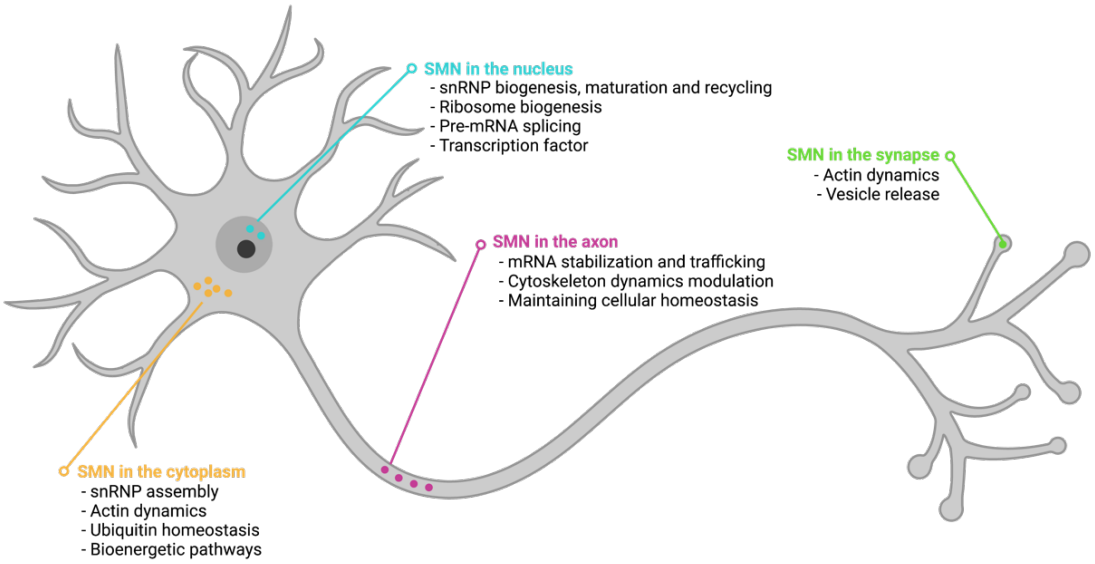

Figure 9 | Localization of SMN protein in MNs and its cellular functions. Based on (Bowerman et al., 2017; R. N. Singh et al., 2017). Created with BioRender.com.

1.7. SMA pathology

1.7.1. MN alteration and degeneration

The main alterations observed in SMA patients in the nervous system is the specific loss of function of the MNs from the ventral horn of the spinal cord. Other alterations have also been observed in these cells; altered positioning of the MNs in the ventral white matter (Simic et al., 2008), chromatolysis, swelling, and accumulation of phosphorylated neurofilaments, vesicles and ribosomes in the MNs somas. These pathological features of SMA are usually described only from the analyses of autopsy tissue samples from patients with severe forms of the disease. Thus, the changes observed are only reflecting the final stages of the disease (Crawford & Pardo, 1996), suggesting that MN loss could be the consequence of neurodegenerative processes previously occurring in these cells.

Several animal models have been generated to study the alterations occurring in the early stages of SMA disease. Interestingly, a reduction of 20-35% in MN number has only been observed at post-symptomatic stages in SMA affected mice, despite the severe neuromuscular degeneration observed in those animals (Hsieh-Li et al., 2000a; Le et al., 2005; Monani, Sendtner, et al., 2000). Further investigations suggest that synaptic abnormalities followed by axonal degeneration may be the disease's early pathogenic feature (Kariya et al., 2008; Monani, 2005; Tarabal et al., 2014). NMJ defects have been observed at both pre- and post-synaptic terminals characterized by impaired neurotransmitters release, accumulation of neurofilament proteins, nerve terminal loss and reduced maturation of acetylcholine receptor clusters, together with truncated and branched axons (Cifuentes-Diaz et al., 2002; Dachs et al., 2011; Kariya et al., 2008; Kong et al., 2009; Mcgovern et al., 2008; L. M. Murray et al., 2008; Tarabal et al., 2014). All these changes observed suggest that the loss of MN somas occur as a result of anomalies in MN function at their distal end.

1.7.2. SMA as a MN disease: one protein and two hypothesis

Though it has been described that the specific loss of SMN in MNs can cause SMA disease (Park et al., 2010), the precise mechanism that leads to MN degeneration is still unclear. Two hypotheses have raised to explain the specific vulnerability of MNs due to SMN reduction in SMA disease (**Figure 10**). The first hypothesis sustains that SMA disease is produced as a direct consequence of an altered snRNP biogenesis and pre-mRNA splicing, while the second withstands that the MN disease is due to defects of SMN function in axonal trafficking of specific mRNAs.

Hypothesis 1. Altered snRNPs biogenesis: Lower SMN protein levels wouldn't be sufficient for the maintenance of snRNP assembly and pre-mRNA splicing in MNs due to their high cellular energy requirements in contrast with other cell types, which are less affected (Simic et al., 2008). Nonetheless, there is contradictory evidence regarding this hypothesis. While there are several studies that show reduced levels of snRNPs and splicing defects in SMA cells (Gabanella et al., 2007; Wan et al., 2005; Z. Zhang et al., 2008), these alterations do not occur in other cell types with a high RNA turnover such as hepatocytes and other types of neurons, which don't appear to be affected in the disease. These deficits in snRNP maturation and abnormal splicing don't seem to be sufficient for the initiation of SMA pathogenesis (Bäumer et al., 2009; Rajendra et al., 2007), because no differences in snRNP assembly activity were observed when comparing two severe SMA mouse models with differential lifespan (Gabanella et al., 2007).

Hypothesis 2. Axonal transport defects: SMN has a specific function in MN axons and growth cones, as it has been detected in these structures without being associated with the Sm heptamers and the snRNPs. Furthermore, SMN protein is reported to be actively transported through the axon in cultured MNs (Rossoll et al., 2003), and different animal models for SMA disease present axonal defects in cultured MNs like: short or truncated and branched axons, smaller growth cones and a reduction of ß-actin mRNA transport (McWhorter et al., 2003; Rossoll et al., 2003). Nevertheless, whether the MN axonal defects result from the loss of a specific function of SMN in these cells or as a consequence of an altered snRNP biogenesis is still unclear. Moreover, other neuron types with long axonal prolongations don't seem to be affected by SMN loss.

Altogether, the two hypothesis converge in a final alteration of the synapse and axonal degeneration, suggesting that the altered splicing of specific genes due to low levels of SMN and snRNPs could lead to reduced expression of specific genes at the synapse and thus, to its alteration and degeneration (**Figure 10**) (Burghes & Beattie, 2009).

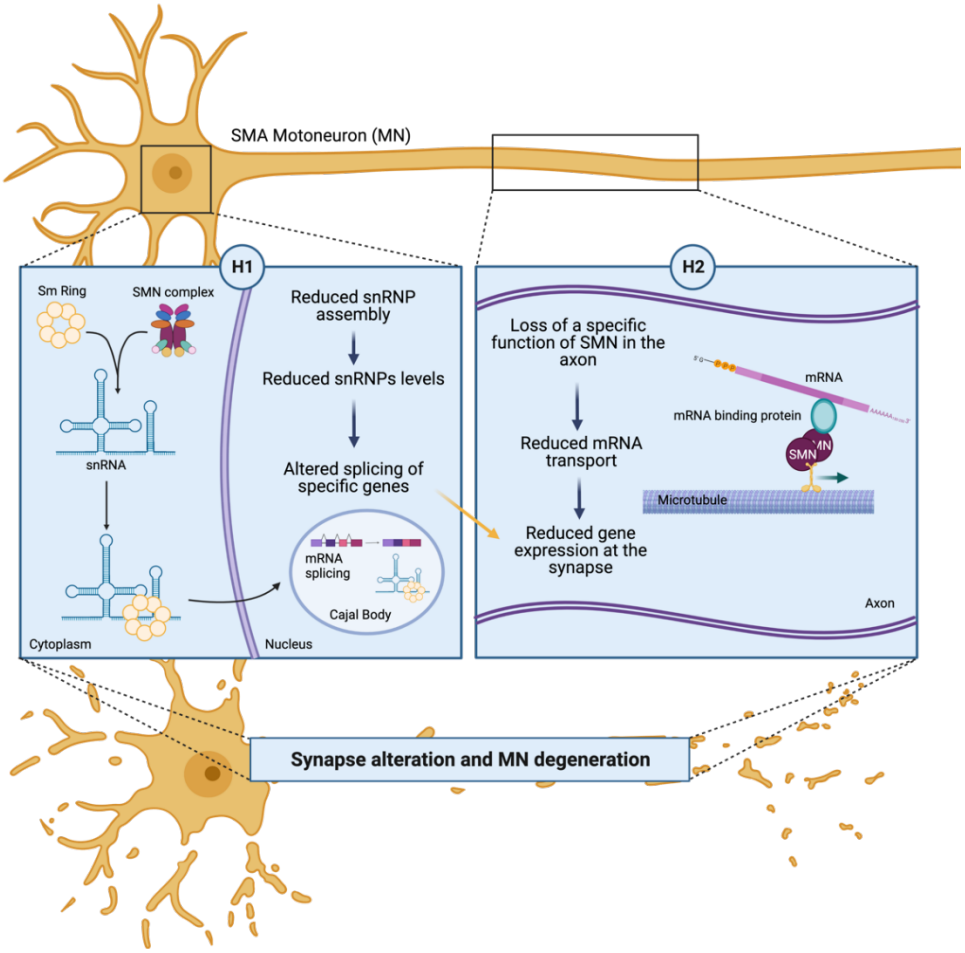

Figure 10 | Hypotheses proposed to explain the specific vulnerability of MNs to low SMN levels. The yellow arrow connects the two hypotheses, where the reduction of snRNP assembly causes a decrease in the splicing of targeted genes critical for the transport of mRNA to the MN synapse. Based on (Burghes & Beattie, 2009; Talbot & Davies, 2008). Created with BioRender.com.

1.7.3. SMA as a multisystemic disease

The ubiquitous expression of SMN protein and the presence of non-motor abnormalities in severe forms of SMA led to the hypothesis that SMN protein deficiency may have other systemic consequences that could contribute to the disease development (A. Nash et al., 2017; Hamilton & Gillingwater, 2013). Thus, there is a gradient of susceptibility to SMN reduction (the 'threshold hypothesis'), where MNs are the first cells affected, and additional tissues such as bone, heart, and sensory neurons become affected as protein levels are further reduced (Hamilton & Gillingwater, 2013; Sleigh, Gillingwater, et al., 2011) (**Figure 11**).

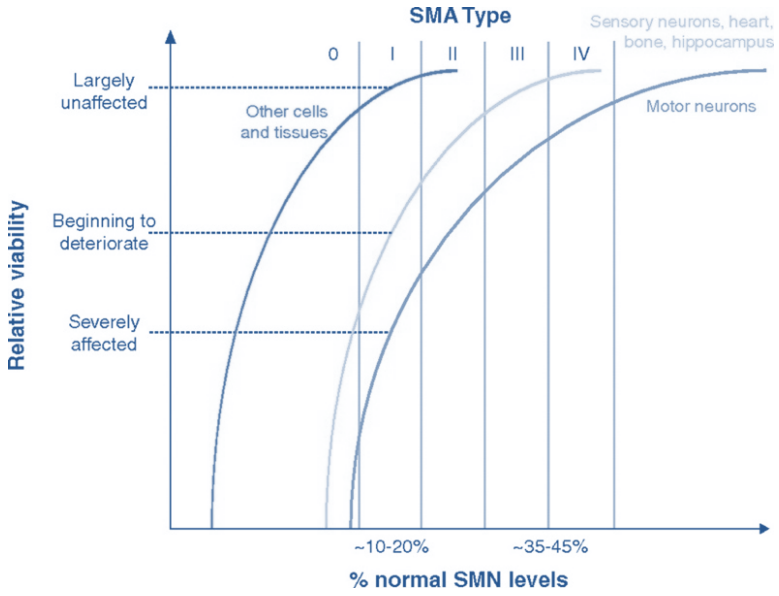

Figure 11 | Representative image of the 'threshold hypothesis' in SMA disease. MNs are the most severely affected by SMN depletion and are thus at one end of a vulnerability-resistance spectrum. When protein levels are further reduced, other tissues like bone, heart and sensory neurons become affected, while other cells and tissues remain unaffected. Adapted from (Sleigh, Gillingwater, et al., 2011).

The affectation of other cell types rises the concern of the need to find a systemic rise of SMN protein levels when developing new therapies. Alterations in SMA tissues and systems are described below, pointing out SMA as a multisystemic disease rather than a MN-specific pathology (**Figure 12**).

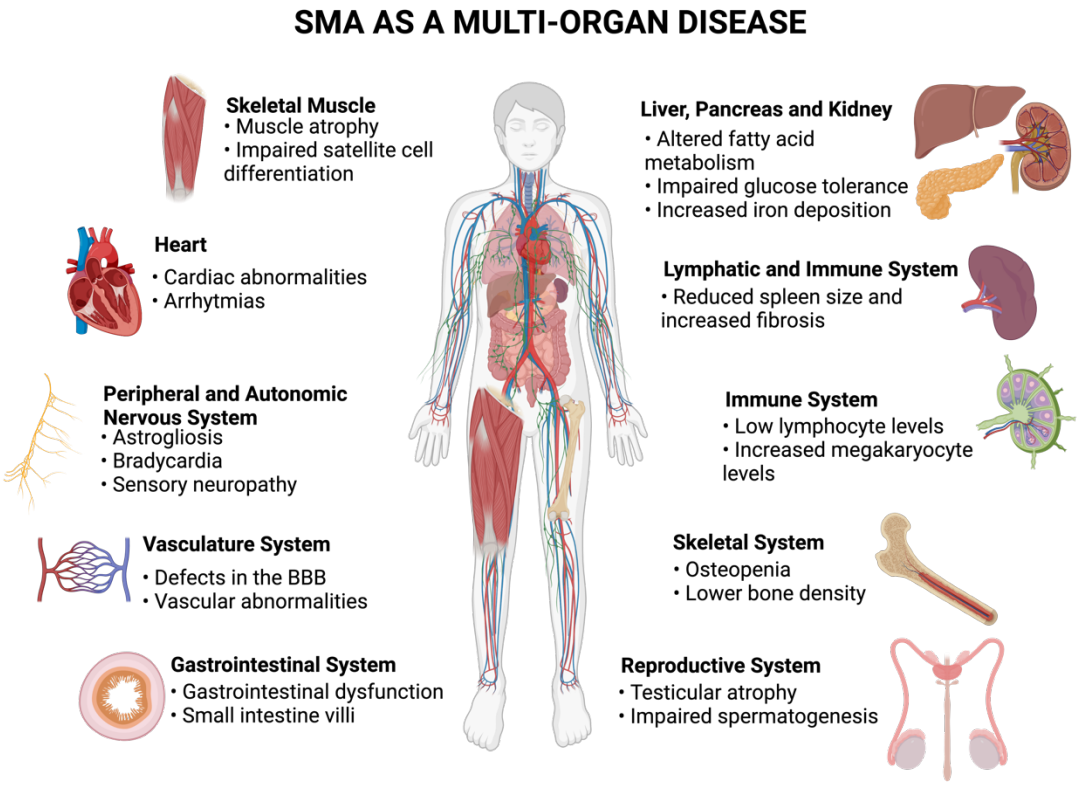

Figure 12 | SMA as a multi-organ disease: overview of the systemic alterations in SMA disease. Besides the MN degeneration and the muscular atrophy, several tissues and organs are described to be affected during the development of the disease. Based on (A. Nash et al., 2017; Jing et al., 2020). Created with BioRender.com.

Skeletal Muscle: Patients with SMA Type 1 have tiny, disordered myotubes with delayed maturation and impaired acetylcholine receptor expression (Arnold et al., 2004; Martínez-Hernández et al., 2009). Patients with SMA Type I-III show mitochondrial dysfunction in skeletal muscle (Ripolone et al., 2015). Adult patients with SMA have a pattern of progressive atrophy of specific skeletal muscles over time similar to the muscular atrophy pattern seen in SMA rodent models (Durmus et al., 2017). SMN deficiency has been suggested to directly cause skeletal muscle pathology, as pathological changes in muscle occur independently and prior to nerve degeneration (L. M. Murray et al., 2008; Mutsaers et al., 2011). In SMA mice, the targeted depletion of SMN in mature muscle fibers lead to muscle degeneration (Cifuentes-Diaz et al., 2001). Likewise, the *in vitro* knock-down of SMN resulted in reduced cell proliferation and myotube fusion defects (Boyer et al., 2013; Bricceno et al., 2014; Hayhurst et al., 2012; Shafey et al., 2005). Nevertheless, the overexpression of SMN in skeletal muscle alone doesn't rescue the SMA phenotype (Gavrilina et al., 2008), suggesting that increasing SMN in muscle is not sufficient to reverse the SMA phenotype and reinforcing the need for a systemic increase of the protein.

Cardiovascular System: Congenital heart defects are reported in every 3 out of 4 screened patients with SMA type 0, suggesting that SMN plays a crucial role in cardiac development (Rudnik-Schöneborn et al., 2008). Conversely, SMA type II and III patients do not present these observed cardiac abnormalities (Bianco et al., 2015). These structural heart defects may be due to dysregulation of specific genes involved in cardiac development (Sheng et al., 2018), and in heart failure (Alves et al., 2019) observed in SMA disease, or due to specific functions of SMN protein in the heart.

Peripheral Nervous System: Mouse and human SMA tissues present astrogliosis (Kumagai & Hashizume, 1982; Tarabal et al., 2014). The restoration in astrocytes of SMN levels in SMA mouse models increased life expectancy, improved the motor unit function, and restored the NMJ defects, even though it could not counteract the MN degeneration (Rindt et al., 2015). Schwann cells (Hao et al., 2015) and DRG neurons are also altered in SMA disease (Fletcher et al., 2017; Mentis et al., 2011; Tisdale & Pellizzoni, 2015).

Autonomic Nervous System: Signs of Autonomic Nervous System (ANS) dysfunction, bradycardia, reduced heart innervation, unusual vasodilation responses to cold, blood pressure fluctuations, and fingers and toes necrosis have been reported in severe SMA disease (Araujo et al., 2009; Bach et al., 2007; Hachiya et al., 2005; Heier et al., 2010). SMA type II, III and IV patients do not show alterations in the ANS.

Vascular System: SMA patients and animal models have present vasculature defects and capillary bed depletion, resulting in spinal cord hypoxia and defects in the blood brain barrier (BBB) (Somers et al., 2016), contributing to the MN degeneration. Some SMA patients are more likely to be diagnosed with vascular abnormalities before showing any signs of neuromuscular dysfunction (Lipnick et al., 2019).

Gastrointestinal System: SMA patients and mice present defects in the enteric nervous system (Davis et al., 2014). Moreover, besides presenting autonomic dysfunction, reduced number of abnormal small intestine villi have been seen in severe SMA mouse models (Sintusek et al., 2016).

Liver, Pancreas, Kidney and Metabolism alterations: SMA mice and human SMA patients show impaired liver (Crawford et al., 1999; Deguise et al., 2019; Hua et al., 2011; Yesbek Kaymaz et al., 2016), pancreatic (Bowerman, Swoboda, et al., 2012) and kidney functions, resulting in overall metabolism alterations (A. Nash et al., 2017; Jing et al., 2020).

Lymphatic and Immune System: Spleens from patients with SMA type I present morphological alterations, including decreased size, lack of lymphocytes, and elevated megakaryocyte levels (Khairallah et al., 2017). Besides, the severe SMA Taiwanese mouse model spleen is smaller and has an altered morphology. Moreover, it presents increased fibrosis, lack of cellular proliferation, reduced lymphocyte and increased megakaryocyte levels, and increased apoptosis. (Thomson et al., 2017).

Skeletal System: SMA type I, II and III patients have significantly lower bone mineral density (BMD) than their age-matched controls (Khatri et al., 2008; Poruk et al., 2012). SMA type II and III patients present higher rates of bone fractures and bone resorption compared to controls (Vai et al., 2015; Vestergaard et al., 2001). In SMA mice, the *Smn*$^{-/-}$;*SMN2* mouse model showed significant decrease in bone volume, density and trabecular number when compared to controls. Additionally, mice showed an increase in the number of bone resorbing cells and a decrease in bone matrix and bone differentiation markers (Shanmugarajan et al., 2009).

Reproductive System: Intermediate SMA mouse models are used to study and report the effects of SMN deficiency on fertility, as the severe SMA mouse models do not normally reach an age for reproduction. A study with a SMA mouse model that produces around a 25-50% of normal Smn protein levels, revealed that males had significantly smaller testis, a substantial reduction in sperm count, degenerated seminiferous tubules and increased levels of apoptosis and DNA fragmentation. These findings suggest that SMN loss causes an abnormal reproductive phenotype in males, despite the fact that this data has not yet been validated in humans (Ottesen et al., 2016).

1.8. SMA models

SMA disease is a pathology observed only in humans, and since the complete deletion of *Smn* gene in animals is embryonic lethal (Schrank et al., 1997), the generation of SMA models requires a minimum level of SMN protein to ensure their survival.

1.8.1. Schizosaccharomyces pombe

Schizosaccharomyces pombe (*S. pombe*) is used as a yeast model to study SMA disease as it has an ortholog of the human *SMN* gene (*Yab8* or *ySMN*) (Owen et al., 2000). The *ySMN* gene translates for a similar protein to the human SMN at the carboxy-terminal level, but shows poor internal homology as it lacks the RNA binding domain (Talbot et al., 1997). The ySMN protein is located both in the nucleus and the cytoplasm of the *S. pombe* cell. Although ySMN can form

complexes with the human SMN protein, its downregulation cannot be rescued by expressing human SMN (Paushkin et al., 2000). This model has been used to study SMN protein interactome.

1.8.2. Caenorhabditis elegans

Caenorhabditis elegans (C. elegans) contains a single *Smn* gene (*Smn-1*) which encodes for a protein with a 36% similarity to the human ortholog (Bertrandy et al., 1999). The removal of the *Smn-1* coding region causes severe defects such as developmental arrest, lifespan reduction and progressive loss of motor functions (Briese et al., 2009). A point mutation in *Smn-1*, mimicking the alteration produced in human SMA disease, causes minor disturbances, such as weak motor defects and a slightly reduced lifespan (Sleigh, Buckingham, et al., 2011). This model is usually used for the identification and testing large amounts of disease modifying genes as potential therapeutic targets for SMA (Dimitriadi et al., 2010).

1.8.3. Drosophila melanogaster

Drosophila melanogaster contains an orthologous copy of the human *SMN* gene (*Smn*) with a 41% of sequence homology. The expression of truncated forms of Smn in Drosophila causes developmental arrest and death of the pups (Miguel-Aliaga et al., 2000). Moreover, introducing mutated forms of the human *SMN1* gene causes reduction in excitatory postsynaptic signaling, loss of glutamate receptors in the NMJs and compromised motor capacities (Chan et al., 2003). Due to its short reproductive cycle, size and simplicity, the Drosophila model is widely used to study Smn interactome,being a good model to identify potential therapeutic approaches.

1.8.4. Danio rerio

Zebrafish (*Danio rerio)* Smn protein shares a 49% homology with its human ortholog. Reduction of Smn levels with an antisense morpholino produces MN defects, such as truncation and ectopic branching of motor axons (McWhorter et al., 2003). Endogenous Smn mutations produces reduced overall size and a decrease in a synaptic vesicle protein (SV2) (Boon et al., 2009). A transgenic zebrafish model generated by expressing the human *SMN2* gene together with endogenous mutated *Smn* gene has been created to produce a genetically comparable model for the study of SMA pathology (Hao et al., 2011). This animal model is a great tool to widen the knowledge of SMA disease development and progression as well as for drug

screening due to its easy genetic manipulation and its short life cycle (zebrafish reach adulthood at around 90 days).

1.8.5. Mus musculus

Mus musculus contains a single *Smn* gene similar to the human *SMN1* gene, with an 82% amino acid identity (Bergin et al., 1997; DiDonato et al., 1997; Viollet et al., 1997). Homozygous removal of *Smn* gene in mice leads to a massive embryonic cell death before implantation (Schrank et al., 1997). Since heterozygous mice don't present a severe clinical phenotype, multiple approaches have been developed to produce mice with low Smn levels but enough protein to survive. To this end, several mice have been obtained to allow molecular and phenotypic analysis, and the development of therapeutic trials; from tissue-specific *Smn* knockout to human *SMN2* transgene introduction (Sleigh, Gillingwater, et al., 2011), and are summarized in **Table 2**. Further information of the mouse models used in this study is detailed in the 'Materials and Methods' section and are indicated in **Table 2** with an asterisk (*).

Table 2 | Mouse models of SMA.

Genotype	Information	References
***Smn*$^{-/-}$**	Death prior to uterine implantation	(Schrank et al., 1997)
***Smn*$^{+/-}$**	Early acute loss of lumbar spinal cord MNs with subsequent slow and progressive reduction over time	(Balabanian et al., 2007; Jablonka et al., 2000)
***Smn*$^{+/\Delta 7}$*;NSE-Cre*$^{+}$**	*Smn*$^{+/}$Δ7 mice with Cre-*loxP*-mediated deletion of *Smn* exon 7 in neuronal tissue; lifespan 25 days	(Cifuentes-Diaz et al., 2002; Frugier et al., 2000)
***Smn*$^{+/+}$*;NSE-Cre*$^{+}$**	*Smn*$^{+/+}$ mice with Cre-*loxP*-mediated deletion of *Smn* exon 7 in neuronal tissue; lifespan 31±2 days.	(Ferri et al., 2004)
***Smn*$^{+/\Delta 7}$*;HSA-Cre*$^{+}$**	*Smn*$^{+/}$Δ7 mice with Cre-*loxP*-mediated deletion of *Smn* exon 7 in skeletal muscle tissue; lifespan 33 days	(Cifuentes-Diaz et al., 2001)
***Smn*$^{+/+}$*;Alfp-Cre*$^{+}$**	*Smn*$^{+/+}$ mice with Cre-*loxP*-mediated deletion of *Smn* exon 7 in hepatocytes. Embryonic lethality at E18	(Vitte et al., 2004)
***Smn*$^{-/-}$*;SMN2(2Hung)*$^{+/+}$**	Includes human *SMN2, SERF1* and part of *NAIP* Transgene copy number varies and correlates with disease severity; lifespan:1 week to normal survival	(Hsieh-Li et al., 2000b)
***Smn*$^{-/-}$*;SMN2(89Ahmb)*$^{+/+}$ (*)**	Includes human *SMN2* Transgene copy number varies and correlates with disease severity; lifespan from 4 to 6 days	(Monani, Sendtner, et al., 2000)
***Smn*$^{-/-}$*;SMN2(89Ahmb)*$^{+/-}$*;SMN1(A2G)*$^{+/-}$**	Heterozygous deletion of *Smn* and *Gemin2* Display an accelerated loss of MNs	(Jablonka et al., 2002)
***Smn*$^{-/-}$*;SMN2(89Ahmb)*$^{+/+}$*; SMNΔ7*$^{+/+}$ (*)**	Includes the human transgene *SMNΔ7;* mean lifespan 13.3±2 days	(Le et al., 2005)
***Smn*$^{-/-}$*;SMN2*$^{+/+}$*; SMN1(A111G)*$^{+/-}$**	Includes human *SMN1* allele of Type I and II SMA patients	(Workman et al., 2009)
***Smn*$^{-/-}$*;SMN2*$^{+/+}$*; SMN1(VDQNQKE)*$^{+/-}$**	Includes human *SMN1* exons 1-6 with an additional motif	(Workman et al., 2009)
***Smn*$^{2B/-}$**	Smn transgene with three nucleotide substitutions within the exonic splicing enhancer of exon 7; mean lifespan 28 days	(Bowerman et al., 2009)
***Smn*$^{-/-}$*;SMN2(N11)*$^{+/-}$*; SMN2(N46)*$^{+/-}$**	Mice with trhee copies of the human *SMN2*; mean lifespan 15.2±0.4 days	Michaud (Michaud et al., 2010)
***Smn*$^{+/-}$*;SMN2(89Ahmb)*$^{+/+}$*;Olig2-Cre*$^{+}$**	Cre-*loxP*-mediated deletion of *Smn* exon 7 in MN progenitor cells Extended survival up to 12 months	(Park et al., 2010)
***Smn1*$^{tm1Cdid/tm1Cdid}$*;Cre*^{Esr1} *and* *Smn1*$^{tm2Cdid/tm2Cdid}$*;Cre*^{Esr1}**	Inducible *Smn* alleles that mimic *SMN2* splicing with a Cre recombinase; excising intron 7 and producing full-length Smn	(Hammond et al., 2010)

1.8.6. Other animal models: Pigs and Monkeys

Larger animal models like pigs and monkeys are usually used for drug efficiency and safety analysis (Meyer et al., 2015; Passini et al., 2015). Pigs are used as a model organism for preclinical trials due to their size and the similarity of their spinal cords to humans (Federici et al., 2011). For instance, they are used to test the efficiency of scAAV vector serotypes for spinal cord MN transduction (Snyder et al., 2011), or to test functional outcomes of SMN gene therapy (Duque et al., 2015). Likewise, monkey models have been used to validate the efficiency and the optimal route of administration of scAAV9-mediated SMN gene therapy (Passini et al., 2015).

1.8.7. Cellular models

The impossibility to directly study MNs in individuals affected by neurological disorders such as SMA and Amyotrophic Lateral Sclerosis (ALS) makes more difficult to understand the basic pathological mechanisms occurring in the disease process. Thus, the use of cell cultures helps unravelling the molecular basis of these pathologies and their phenotypical alterations. Moreover, cell cultures allow the analysis of drugs pharmacokinetics and pharmacodynamics for future applications *in vivo*. For instance, neuronal cell lines like the NSC34 (Cashman et al., 1992) have been used to better understand the molecular mechanisms undergoing in SMN-reduced neuron-like cells. Other approaches like primary MN cultures from chicken and mouse models have been developed (Garcera et al., 2011; Gou-Fabregas et al., 2009; Pérez-García et al., 2008) due to their capacity to replicate in vivo physiological conditions. Finally, fibroblasts from SMA patients can also be obtained and immortalized, being purchased by companies like Coriell Institute. These cells can serve as SMA human models to study the disease mechanisms in non-neuronal cell types (Rashnonejad et al., 2016).

1.8.8. Human induced pluripotent stem cells (hiPSCs)

The discovery that mouse and human fibroblasts can be reprogrammed into becoming embryonic stem cells has significantly advanced the area of stem cell and neurodegenerative disease research (Ebert & Svendsen, 2010). These newly generated cells, termed induced pluripotent stem cells (iPSCs) can form teratomas and become lineage restricted into various cell types (Stem Cell Model of Spinal Muscular Atrophy, 2010; Müller et al., 2009). As these iPSCs can be derived from patients, the technique allows the analysis of the disease in the cell types specifically affected, like MNs in SMA and ALS patients (S.-H. Du et al., 2015; Ebert et al., 2009). iPSCs can also be differentiated to other cell types, allowing the study of other SMA

affected tissues alone or in co-culture systems, mimicking the dynamic interactions occurring in human bodies (De Vos et al., 2016). Additionally, iPSCs can also be used to generate endothelial cells (Lippmann et al., 2014) to model the blood-brain barrier (BBB) and study drug capacity to cross the BBB in SMA conditions. iPSCs can be generated from patients with diverse SMA clinical subtypes, contributing to the analysis of small changes in SMN expression at a cellular level, and the identification of disease modifiers in those patients genotypically matching but discordant for the SMA phenotype (Boza-Morán et al., 2015). Thus, iPSC-based models can give new insights into disease mechanisms and serve as a screening and validation tool for potential therapies.

1.9. SMA therapies

Although there is still a long way to go in discovering the cure for SMA, there are several treatments that help control the symptoms of the disease (**Table 3** and **Figure 13**) (Finkel et al., 2018; Mercuri et al., 2018). In recent years, multiple experimental therapies are being approved by the Food and Drug Administration (FDA) and the European Medicines Agency (EMA).

1.9.1. Symptomatology treatment

Muscle weakness and atrophy is one of the hallmarks of SMA disease. To maintain muscle strength, reduce stiffness and scoliosis progression, physiotherapy and exercise are recommended. With disease development, orthopaedical supports and walking assistance devices are normally required. Most severe cases require surgical intervention (Finkel et al., 2018; Mercuri et al., 2018). Involuntary muscles are also affected, producing gastrointestinal dysmotility and nutritional problems. These issues are addressed with regulated diets and feeding tubes in the most severe cases (Finkel et al., 2018; Mercuri et al., 2018). Decrease in the respiratory function in SMA patients is a potential cause of death due to breathing failure. Breathing exercises and vaccination against flu are recommended. The most severe cases also require assisted ventilation (Finkel et al., 2018; Mercuri et al., 2018).

1.9.2. SMN-dependent therapies

1.9.2.1. Nusinersen or Spinraza®

Nusinersen (ISIS SMNRx, nusinersen, Spinraza®; Ionis Pharmaceuticals and Biogen) is an antisense oligonucleotide (ASO) chemically modified with a 2-methoxyethyl. ASOs are short

synthetic nucleotide chains designed to bind specific mRNAs. Specifically, Nusinersen binds to the ISS-N1 region in *SMN2* and blocks the recruitment of the splicing repressor hnRNP-A1, facilitating the correct splicing of *SMN2* mRNA and increasing the production of full-length SMN protein (Hua et al., 2008; Wirth, 2021).

Nusinersen is the first drug ASO-based therapy approved to treat a genetic disorder, and the first treatment approved for SMA disease (FDA December 2016 EMA June 2017). The compound, unable to cross the blood-brain barrier, is injected intrathecally three times as loading dose and every 4 months. Clinical trials showed motoric improvement and prolongation of survival. However, patients show different response to the treatment depending on the age and the disease stage (De Vivo et al., 2019; Finkel et al., 2018; Mercuri et al., 2018).

1.9.2.2. Risdiplam or Evrysdi®

Risdiplam (RG7916, Risdiplam, Evrysdi®; Genentech and Roche) is a small molecule which acts as a *SMN2* mRNA splicing modifier by facilitating the recruitment of U1-snRNP particles to the splice donor site of intron 7, thus increasing SMN protein expression (Ratni et al., 2018).

Risdiplam was first approved by the FDA on August 2020 for the treatment of adults and children from 2 months old. The compound is orally bioavailable, which allows a daily administration without the need for hospitalization. Several clinical trials show significant improvements amongst all SMA types. FIREFISH (NCT02913482) (Baranello et al., 2021) and SUNFISH (NCT02908685)(Mercuri et al., 2022) trials are investigating efficacy in SMA type I, II and III, safety, tolerability, and pharmacodynamics and kinetics. JEWELFISH (NCT03032172) (Chiriboga et al., 2022) and RAINBOWFISH (NCT03779334) trials are currently investigating the long-term efficacy of Risdiplam in patients who previously received another SMA treatment and infants from birth until 6 weeks of age, respectively.

1.9.2.3. Branaplam

Branaplam (LMI070; Novartis) is a small molecule which acts as a mRNA splicing modifier, thereby rising SMN protein expression (Palacino et al., 2015). The compound is orally bioavailable, and is currently in a phase I/II clinical trial (NCT02268552) for infants with SMA type I with 2 copies of *SMN2* to evaluate safety, tolerability, pharmacokinetics and pharmacodynamics and efficacy, after 13 weeks of Branaplam treatment. This treatment has received an FDA Fast Track designation for SMA type I and Huntington's disease (HD)

(NCT05111249) to facilitate and accelerate the development of Branaplam as a treatment for these pathologies.

1.9.2.4. Onasemnogene abeparvovec or Zolgensma®

Onasemnogene abeparvovec (SMN-AVXS-101, omasemnogene abeparvovec-xioi, **Zolgensma®**; AveXis and Novartis) is a genetically modified adeno-associated virus (AAV9) containing the complementary DNA copy of the *SMN1* gene under the control of the cytomegalovirus (CMV) enhancer/chicken-beta-actin hybrid promoter (Rao et al., 2018).

Zolgensma was first approved by the FDA in May 2019 for all children of at least 2 years old and above, and conditionally EMA approved in May 2020 for all patients with three or fewer *SMN2* copies and less than 21kg. The compound is administered by intravenous injection in a one-time dose of 1.1×10^{14} vector genomes per kg of body weight (Stevens et al., 2020). Clinical trial results are showing promising results; STR1VE trial (NCT03306277) (Day, Finkel, et al., 2021), concluded in November 2019, shows that patients achieved rapid and sustained improvement in motor function. SPR1NT trial (NCT03505099) (Day, Mendell, Mercuri, et al., 2021) is evaluating the safety and efficacy of a one-time intravenous infusion in pre-symptomatic SMA type I patients. Other trials like START Long Term Follow Up (NCT03421977) aim to estimate long-term safety on patients who completed the study START (Day, Mendell, Al-Zaidy, et al., 2021).

1.9.2.5. Valproic Acid (VPA)

Valproic acid is a molecule known to participate in the inhibition of histone deacetylases (HDACs), which are proteins that repress gene transcription by chromatin condensation, including *SMN2*. The drug promotes the transcriptional upregulation of *SMN2* gene, and potentiates ASO's upregulation of exon 7 inclusion when administered in combination (Marasco et al., 2022). The compound is orally administered altogether with levocarnitine (to prevent liver toxicity) in a daily dose and is currently in a phase III study (NCT01671384; All India Institute of Medical Sciences, New Delhi) with SMA patients from 2 to 15 years old. Studies revealed that beneficial effects of VPA treatment were only observed in SMA type II patients. Interestingly, non-responder patients had higher levels of CD36, a fatty acid translocase known to prevent SMN expression (Garbes et al., 2013). In another concluded study, the SMA CARNIVAL trial (NTC0227266), although VPA treatment showed weight gain, it was not effective in improving strength or function in SMA children (Kissel et al., 2011; Swoboda et al., 2010). Thereby, combinatorial therapy along with ASOs may produce more

beneficial effects than VPA alone administration, which seems insufficient for improving SMA patients' symptoms (Marasco et al., 2022).

1.9.2.6. Hydroxyurea

Hydroxyurea (HU) is a histone deacetylase (HDAC) inhibitor, promoting the transcriptional upregulation of *SMN2* gene (Grzeschik et al., 2005; Liang et al., 2008). The compound, used for treating thalassemia and sickle cell disease, is orally administered daily at a dose of 30mg/kg in a phase II and III clinical trial study (NCT00485511; Ksohsiung Medical University Chung-Ho Memorial Hospital) for SMA type II and III patients to evaluate the drug efficacy and safety.

1.9.3. SMN-independent therapies

1.9.3.1. Muscle enhancing therapies

Muscular weakness and atrophy is one of the hallmarks of SMA. Therapeutic approaches focused on muscle protection can be crucial to slow down the disease progression. Currently, there are two muscle enhancing therapies undergoing clinical trials: Reldesemtiv and Apitegromab (Parente & Corti, 2018).

Reldesemtiv, also known as Tirasemtiv or CK-2127107 (Cytokinetics, California, USA), is a small molecule troponin complex activator. Its mechanism of action is based on slowing the rate of calcium (Ca^{2+}) release from fast skeletal muscle, thus sensitizing the sarcomere to Ca^{2+}. In consequence, muscle contraction and function is reinforced and improved (Collibee et al., 2021; Messina & Sframeli, 2020). The compound is orally bioavailable, allowing administration without hospitalization. A phase II clinical trial (NCT02644668) in patients with SMA type II to IV showed a trend towards an increase in motor function and respiratory performance (Rudnicki et al., 2021). The drug is also undergoing a phase III clinical trial (NCT04944784) in ALS patients to evaluate efficacy and safety.

Apitegromab, or SRK-105 (Scholar Rock), is a monoclonal antibody against myostatin, a protein involved in preventing or inhibiting muscle growth. This molecule binds and inhibits myostatin, thereby promoting muscle cells growth and differentiation. Moreover, studies in SMA mice demonstrated that SRK-105 was able to improve muscle force in the affected animals (Z. Feng et al., 2016; Long et al., 2019). The compound is administered by intravenous injection at a dose of 20mg/kg every four weeks during one year. A phase I clinical trial in 2018 (NCT02644777) verified its safety and tolerability. The clinical trial TOPAZ (NCT03921528), concluded in the end of 2020, involved SMA type II and III patients. The drug was given as a

monotherapy or in combination with Nusinersen (Scholar Rock, 2021). The majority of patients maintained or improved their motor function, and with these promising results, the company has recently started a phase III clinical trial (SAPPHIRE, NCT05156320).

Sarconeos (BIO101) or 20-hydroxyecdysone (Biophytis, France) is a steroid hormone that activates the MAS receptor in muscle cells, promoting muscle anabolism. Ecdysteroids are natural compounds found in insects and plants which increase protein synthesis in mammals, improving skeletal muscle strength and endurance. The compound is orally bioavailable and it is currently undergoing a phase II clinical trial (SARA-INT; NCT03452488) to evaluate the benefits of the drug on patients suffering from age-related sarcopenia. BIO101 is being proposed to use in combination with existing SMN-dependent therapies such as Spinraza®, Evrysdi®, or Zolgensma®, in responder patients to improve muscle fatigue resistance and moving capacity (Bezier et al., 2022; Latil et al., 2019). The authors also suggest the administration of BIO101 as a monotherapy for non-responder and or untreated SMA patients (Bezier et al., 2022; Latil et al., 2019).

Amifampridine or 3,4-diaminopyridine is a voltage-dependent K^+ channel blocker that prolongs presynaptic NMJ terminal depolarization, enhancing neuromuscular transmission. It orally administered and is undergoing a phase II clinical trial (SMA-001; NCT03781479; EUDRACT 2017-004,600-22) for treating ambulatory SMA type III patients. Results revealed an improvement in the Hammersmith Functional Motor Scale Expanded (HFMSE) compared to placebo treatment (Bonanno et al., 2022).

1.9.3.2. Neuroprotection therapies

Olesoxime, (TRO19622; Hoffman-La Roche) is a cholesterol-like compound with a neuroprotective effect independent from *SMN* regulation. It is believed to interact with mitochondrial components, preventing an excessive membrane permeability under stress conditions, preserving mitochondrial function and counteracting apoptosis (Bordet et al., 2010). The compound is orally administered. Although it showed promising results in SMA mouse models and later in a phase I clinical trial (NCT01302600) (Bertini et al., 2017), the phase II clinical trial (NCT02628743) (Wadman et al., 2019) was stopped as deterioration of motor function was observed.

Mestinon or Pyridostigmine bromide (UMC, Utrecht), is a molecule which acts as a reversible inhibitor of the acetylcholinesterase enzyme, a protein responsible for the degradation of acetylcholine. It induces an increase in acetylcholine levels and prolongs the signaling

transmission at the neuromuscular junction (NMJ). The compound, which is already used for the treatment of the Myasthenia Gravis disease (Maggi & Mantegazza, 2011), is orally administered in four daily doses and it is undergoing a phase II clinical trial (SPACE trial; NCT02941328) including patients with SMA type II, III and IV (Stam et al., 2018).

1.9.3.3. Stem Cell Therapy

Mesenchymal Stem Cells (MSCs) are cells capable of maturing into many other cell types, and are increasing interest as a potential therapeutic approach for treating diseases like SMA, as they have immunosuppressive, anti-inflammatory, neuroprotective and regenerative properties. MSCs can potentially protect MNs from death through the delivery of neurotrophic factors (NTFs), thereby slowing disease progression.

Currently, a phase I clinical trial in Iran (NCT02855112; Tehran University of Medical Sciences) is evaluating the safety and effectiveness of treating SMA type I with a subpopulation of fat tissue-derived MSC. The treatment consists in three intrathecal injections of 1 million cells per kilogram of weight; each injection separated by three weeks. Results published in April 2021, showed that after the third injection, all infants presented increased motor response and a trend for extended survival, although only one of the five treated patients was still alive after four years (Mohseni et al., 2022). These findings suggest that treatment with MSCs may promote some benefit in SMA type I patients, although further research should focus on developing improved stem cell therapies and testing them in multi-center studies.

Table 3 | Main available therapies in SMA undergoing clinical trials.

Compound	Mechanism	Administration	SMA Type	Trials' Phase	FDA Approval
Splicing modifiers of *SMN2* gene					
Nusinersen	ASO	Intrathecal	I, II, and III	I, II and III	X
Risdiplam	Small molecule	Oral	I, II, and III	I, II and III	X
Branaplam	Small molecule	Oral	I	I and II	-
Replacing *SMN1* gene					
Zolgensma	AAV9	Intravenous	I, II	I, II and III	X
Transcriptional upregulation of *SMN2* gene					
Valproic Acid + Levocarnitine	HDAC inhibitor	Oral	II	III	-
Hydroxyurea	HDAC inhibitor	Oral	II and III	II and III	-
Muscle enhancing drugs					
Reldesemtiv	Troponin activator	Oral	I and II	II, III and IV	-
Apitegromab	Myostatin inhibitor	Intravenous	I and II	II and III	-
Sarconeos	MAS receptor activator	Oral	-	-	-
Amifampridine	Voltage-dependent K^+ channel blocker	Oral	III	II	-
Neuroprotection					
Olesoxime	Anti-apoptotic	Oral	II and III	I and II	-
Mestinon	Cholinesterase inhibitor	Oral	II, III and IV	II	-
Stem Cell therapy					
MSCs	Mesenchimal Stem Cells	Intrathecal	I	I and II	-

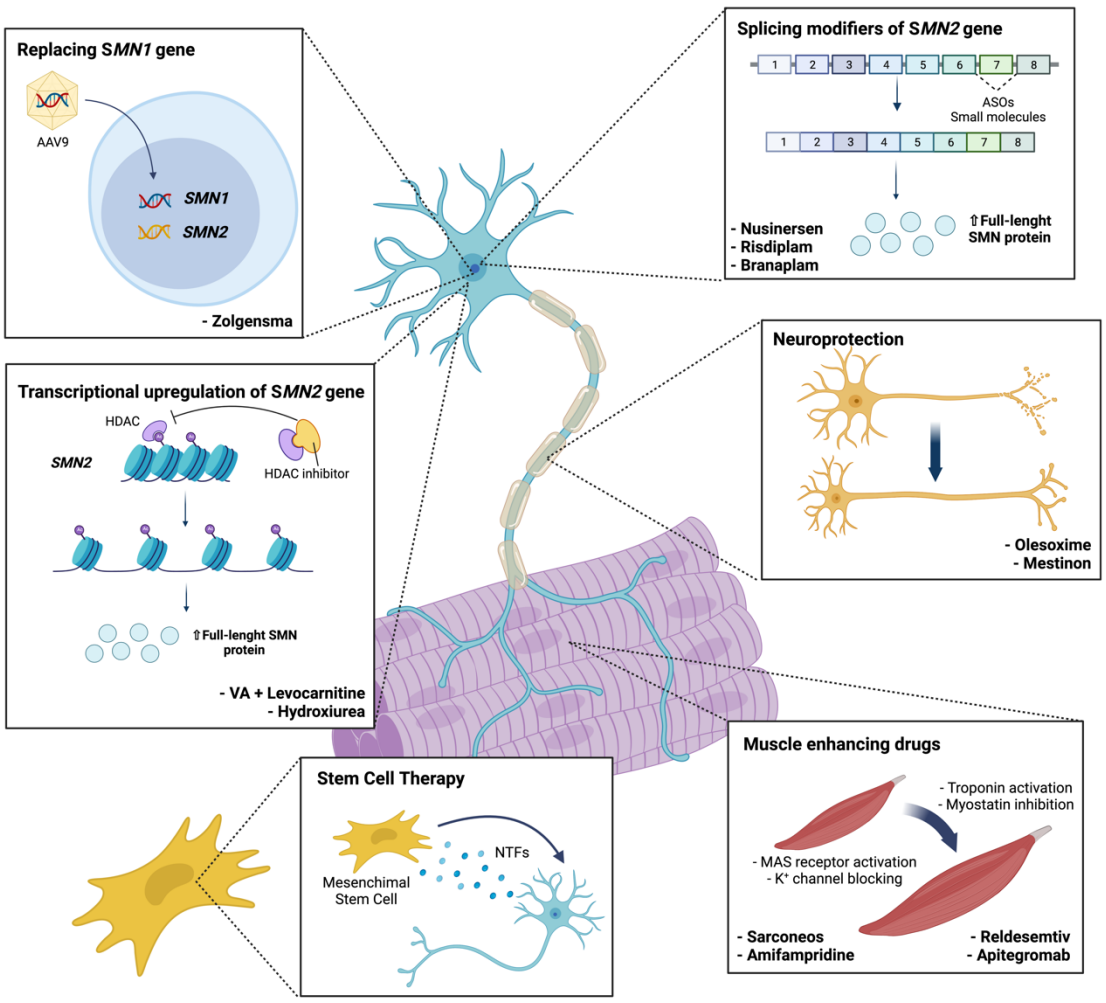

Figure 13 | Main available therapeutic approaches undergoing clinical trials and their mechanisms of action. *SMN1 = Survival Motor Neuron 1*; *SMN2 = Survival Motor Neuron 2*; AAV9 = Adeno-associated virus 9; ASOs = Antisense Oligonucleotides; HDAC = Histone Deacetylase; VA = Valproic Acid; NTFs = Neurotrophic Factors. Based on (Chiriboga, 2022; Messina et al., 2021; Messina & Sframeli, 2020; Wirth, 2021). Created with BioRender.com.

1.9.4. Future perspectives in SMA therapies

Promotion of transcriptional upregulation

Transcriptional upregulation of *SMN2* has become a potential target to treat SMA patients. The hormone Prolactin (PRL), a drug approved for the treatment of lactation deficient mothers (Powe et al., 2010), is able to cross the blood brain barrier (BBB) and induces the transcription of *SMN2* gene by the activation of the JAK2/STAT5 signaling pathway (F. Farooq et al., 2011). Due to its characteristics and since it is already tested for clinical safety, it could be a potential therapy for SMA patients.

Full length SMN transcript stabilization

In the recent years, two approaches to promote full length SMN mRNA stabilization have been developed.

- Inhibitors of the RNA degradation machinery (F. T. Farooq et al., 2013; J. Singh et al., 2008; Van Meerbeke et al., 2013), i.e. **Celecoxib** or the **Scavenger decapping enzyme (DcpS)**, block the breakdown of *SMN2* mRNA and increase SMN protein levels.
- Activation of p38 signaling pathway with **Anisomycin** results in the binding of the HuR protein to *SMN2* mRNA and the stabilization of the transcript, increasing SMN protein levels (F. Farooq et al., 2009).

SMN protein stabilization - Bortezomib

SMN protein turnover has been associated to different pathways like the proteasome system (Burnett et al., 2009). Targeting the ubiquitin-proteasome pathway can be an alternative therapeutic approach. **Bortezomib** is a small molecule known to inhibit the proteasome system and SMN protein degradation through this pathway. The use of Bortezomib in SMNdelta7 mice did not extend mice lifespan but improved muscle function and the morphology of the NMJ. However, this molecule is not able to cross the BBB and combinatorial therapies have been developed to achieve better outcomes. For instance, Bortezomib in combination with a HDAC inhibitor (trichostatin A), extended mouse survival and increased SMN levels in the CNS and peripheral tissues (Kwon et al., 2011).

Actin dynamics modulation

Dysregulated levels of proteins involved in actin dynamics have been reported in SMA. SMN directly interacts with Profilin2a, a small actin binding protein specifically expressed in neurons (Giesemann et al., 1999; Hensel & Claus, 2018; Nölle et al., 2011; Sharma et al., 2005). SMN reduction increases Profilin2a accessibility, which is hyper-phosphorylated by ROCK (Rho-associated protein kinase), an upstream regulator, causing a neuron-specific dysregulation of the actin cytoskeleton (Bowerman et al., 2009; Hensel & Claus, 2018; Nölle et al., 2011). Interestingly, ROCK pharmacological inhibition showed increased lifespan and improved disease phenotype in a mild SMA mouse model, improving NMJs independently of SMN levels (Bowerman et al., 2010; Bowerman, Murray, et al., 2012).

Nonetheless, ROCK inhibition treatment did not increase lifespan in a severe mouse model (Hensel et al., 2017). These distinct outcomes between SMA models highlight the existing

diversity of molecular alterations within the SMA types, reinforcing the need for designing personalized therapies based on their specific molecular patient's alterations.

Muscle enhancing drugs

SMN upregulation therapies like ASOs have shown to improve neuromuscular transmission, (reviewed in (Boido & Vercelli, 2016)). Muscle enhancing drugs like **Reldesemtiv**, **Apitegromab**, **Sarconeos** or **Amifampridine**, have shown beneficial results in SMA, but further research is undergoing to discover new therapeutic approaches. For instance, targeting NMJ has become an object of study in SMA disease. **Agrin**, a crucial molecule for NMJ formation and acetylcholine receptor cluster stabilization (Witzemann, 2006), is abnormally expressed in SMA models (Arnold et al., 2004; Z. Zhang et al., 2013). A recent study showed that direct administration of an active splice variant form of Agrin (NT-1654) had beneficial effects on muscle fibers and NMJs stabilization, delaying muscular atrophy, improving motor performance and extending survival in SMA mice (Boido et al., 2018). These results suggest that NMJ preservation in addition to enhancing SMN level could be an interesting approach to take into consideration for future clinical trials.

Apoptosis and autophagy modulation

Apoptotic features and altered apoptosis molecules such as Bcl-2 (B-cell leukemia/lymphoma 2 protein) and Bcl-XL (Bcl-2- like extra-large) reduction (Soler-Botija et al., 2003) have been observed in SMA pathogenesis. Targeting these alterations may contribute to preventing MN degeneration and death in SMA. For instance, SMN protein reduction promoted apoptosis in an *in vitro* SMA model (Parker et al., 2008). Over-expression of the antiapoptotic protein Bcl-XL rescued MNs from neurite degeneration and cell death *in vitro* (Garcera et al., 2011), and ameliorated motor function and lifespan in a SMA mouse model (L. K. Tsai et al., 2008). Besides, removing Bax-dependent apoptosis showed beneficial effects in a SMA model (M. S. Tsai et al., 2006). The c-Jun NH2-terminal kinase (JNK) pathway is activated in SMNΔ7 mice and in SMA patients (Genabai et al., 2015), and is linked to a pro-apoptotic role. Its pharmacological inhibition ameliorated morphological features, motor performances and lifespan of SMA mice (Schellino et al., 2018). Finally, administration of the neuroprotective drug loganin decreased apoptotic cell number and neurite damage in a SMA cell model and stimulated SMN, Gemin2, Akt and Bcl-2 expression (Tseng et al., 2016).

In vitro and *in vivo* studies have reported a dysregulation of autophagy-related proteins in SMA cells, suggesting that autophagy impairment might alter intracellular trafficking, leading to cytotoxicity (de la Fuente et al., 2018, 2020; Nishimura et al., 2004; Periyakaruppiah et al., 2016;

Piras et al., 2017; Tripathi et al., 2021). Using the autophagy inhibitor 3-methyladenine (3-MA) ameliorated autophagic features, increased lifespan and improved motor performances in SMA mice. Moreover, 3-MA administration also reduced apoptotic death observed in the lumbar spinal cord of SMA mice (Piras et al., 2017). Intramuscular injections of the neurotrophic factor tetanus toxin heavy chain (TTC) have also been described to reduce the expression of several autophagy makers in SMA mice without effects on weight and survival time (Oliván et al., 2016). Finally, autophagy inhibition with the pharmacological approach calpeptin (calpain inhibitor) has been shown to reduce the expression of the LC3-II autophagy marker in neurites *in vitro,* and to improve motor function and extend lifespan in two SMA mouse models (de la Fuente et al., 2020). Moreover, calpeptin treatment increased the levels of SMN protein and reduced its cleavage by calpain in mouse SMA MNs, suggesting that the treatment not only produced a modulation on the autophagy process but also an upregulation of SMN protein level (de la Fuente et al., 2018, 2020).

Overall, these studies results suggest that autophagy and apoptosis may be dysregulated in SMA disease and pharmacologically targeting these processes could ameliorate SMA phenotype, although additional evidence is needed before clinical translation of new molecules acting on these pathways.

2. MECHANISMS OF NEURONAL CELL DEATH

2.1. Types of Cell Death

The classifications of cell death and the types included within that term have evolved through time. The Nomenclature Committee on Cell Death (NCCD) first proposed three criteria for the identification of dead cells: (1) the cell loses its plasmatic membrane integrity, (2) the cell breaks into discrete fragments, referred to as apoptotic bodies, and (3) the cellular body fragments are engulfed by phagocytes or other cellular types with phagocytic activities (Kroemer et al., 2009). Currently, cell collapse can be divided in two main types according to the (NCCD) (Galluzzi et al., 2015, 2018):

- **Accidental Cell Death (ACD):** An instantaneous demise of cells exposed to severe insults of physical, chemical or mechanical nature. Cells exposed to these stimuli die in an uncontrollable manner as a result of their structural breakdown, being insensitive to any pharmacological or genetical interventions.
- **Regulated Cell Death (RCD):** Includes types of cell death which are part of physiologic programs, or are activated by adaptative responses to perturbations of the extracellular or intracellular microenvironment. It involves genetically encoded molecular machinery and can be altered by pharmacologic and genetic interventions.

2.2. Types of Regulated Cell Death

The field of cell death is continuously evolving and including novel signaling pathways that orchestrate RCD. Currently, the following types of recognized RCD are collected in (Galluzzi et al., 2018) and **Table 4**. Each type of RCD can manifest within an entire spectrum of morphological features, presenting itself as fully necrotic to fully apoptotic (**Figure 14**) (Edinger & Thompson, 2004; Galluzzi et al., 2018). In this work we have focused on the apoptosis and the autophagy pathways in the context of SMA disease.

Table 4 | Types of RCD.

Programmed Cell Death (PCD)	Phenomenon that occurs as part of a developmental program or to preserve physiologic tissue homeostasis.
Apoptosis	A programmed phenomenon which can be initiated by diverse physiological or pathological external (**extrinsic apoptosis**) or internal (**intrinsic apoptosis**) stimuli.
Anoikis	Specific variant of intrinsic apoptosis initiated by the loss of integrin-dependent anchorage.
Autophagy-dependent cell death (ADCD)	RCD that mechanistically depends on the autophagic machinery.
Autosis	A specific type of autophagy-dependent cell death that critically relies on the plasma membrane Na^+/K^+-ATPase.
Entotic cell death	Originated from actomyosin-dependent cell-in-cell internalization executed by lysosomes.
Ferroptosis	Initiated by oxidative perturbations of the intracellular microenvironment that can be inhibited by iron chelators and lipophilic antioxidants.
Lysosome-dependent cell death (LDCD)	Starts with the lysosomal membrane permeabilization and the liberation of cathepsins.
Necroptosis (Necrosis)	Started by cellular homeostasis perturbations that depend specifically on the proteins MLKL and RIPK3.
NETotic cell death	A ROS-dependent type of RCD restricted to cells with hematopoietic lineage.
Mitochondrial permeability transition-driven necrosis	Proceeds with the loss of the impermeability of the inner mitochondrial membrane due to intracellular perturbations such as severe oxidative stress and cytosolic Ca^{2+} overload.
Parthanatos	Initiated by PARP1 hyperactivation followed by AIF-dependent and MIF-dependent DNA degradation.
Pyroptosis	Depends on the formation of pores in the plasma membrane.

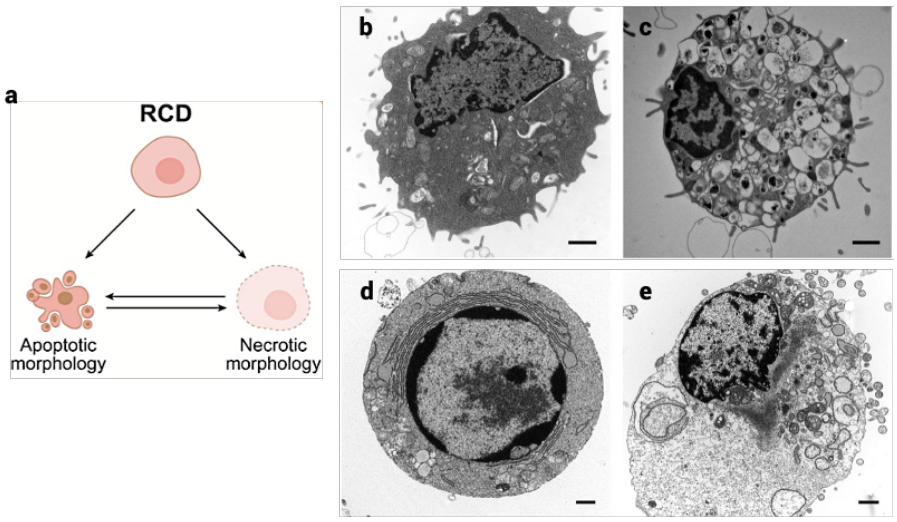

Figure 14 | Representation of the different morphological forms or RCD. (a) RCD morphologies. **(b, c, d and e)** Electronic microscopy images of the morphological features of **(b)** normal, **(c)** autophagic, **(d)** apoptotic and **(e)** necrotic cells. Adapted from (Edinger & Thompson, 2004; Galluzzi et al., 2018). Adapted with permission from Elsevier (Edinger & Thompson, 2004).

2.3. Programmed cell death during MN development

The concept of PCD was first introduced in 1965 (Lockshin & Williams, 1965) to describe a pattern by which insects cells died during their development (reviewed in (Bredesen et al., 2006)). Currently, PCD is referred to the cellular death that occurs in specific anatomical areas and in determined periods of time during the development (Yamamoto & Henderson, 1999), and it has a critical function during the nervous system development (J. F. R. Kerr et al., 1972). There, it proceeds in two stages; the first one affects immature neuronal precursors at proliferation zones and postmitotic neuroblasts (Yeo & Gautier, 2004). The second one involves principally postmitotic neurons (Blaschke et al., 1998) and is regulated through the competition for limited amount of nerve growth factor (NGF) that innervated cells and tissues release (Levi-Montalcini, 1987; Yeo & Gautier, 2004). During this process, around the 50% of all neurons undergo cell death, resulting crucial for the establishment of a definitive pattern of neuronal connections.

The stages of PCD in spinal cord MNs proceed differently depending on the species. In the mouse spinal cord, MN PCD is produced between the embryonic day 13 (E13) and E18 (Sun et al., 2005), initiating from the cervical and ending in the sacral region, though the process does not follow a rostro-caudal pattern (Yamamoto & Henderson, 1999). This process usually concurs with the MN acquisition of **neurotrophic dependency** and muscle innervation.

2.4. Apoptosis

The term 'apoptosis' was first described in 1972 by J.F.R. Kerr and colleagues (J. F. R. Kerr et al., 1972), who defined the process as an inherently programmed process which could be initiated or inhibited by diverse physiological and pathological stimuli. Kerr and colleagues described the phenomenon as structural changes that take place in two stages. The first step consists in the nuclear and cytoplasmic condensation with the breaking up of the cell into a number of membrane-bound fragments called apoptotic bodies. These morphological changes appear as a result of activation of cysteine-proteases called caspases. In the second stage, these apoptotic bodies are taken up by other cells where they are degraded in autophagolysosomes by the lysosomal enzymes.

2.4.1. Extrinsic Apoptosis

Extrinsic apoptosis can be initiated by activation of death receptors of the Tumor Necrosis Factor (TNF) family located in the plasma membrane. These receptors contain an internal death domain, activated by the binding of specific ligands. Following the ligand binding, the Fas Associated Death Domain (FADD) is recruited to initialize the formation of the Death Inducing Signaling Complex (DISC), composed principally by FADD and the initiator pro-caspases 8 and/or 10. These proteases produce the cleavage and activation of the executioner pro-caspases-3 and 7, resulting in active caspase-3/7, which will in turn activate the DNA fragmentation, producing apoptotic cell death (**Figure 15**) (Galluzzi 2012, Ichim and Tait, 2016).

2.4.2. Intrinsic Apoptosis

Intrinsic apoptosis is initiated due to diverse stimuli such as cytokine deprivation, DNA damage, endoplasmic reticulum stress, hypoxia, and metabolic stress among others. These perturbations trigger the activation of BH3-only proteins (pro-apoptotic proteins with a BH3 domain) that will promote the stimulation of BAX/BAK proteins, causing the mitochondrial outer membrane permeabilization (MOMP) (Galluzzi et al., 2011; Ichim et al., 2016).

Following mitochondrial permeabilization, the cytochrome C protein is released in the cytoplasm, promoting the formation of a complex with Apoptosis protease-activating factor-1 (APAF1) and pro-caspase-9 called apoptosome. This structure produces caspase-9 activation, which in turn promotes the cleavage and activation of the effector caspases 3 and 7, leading to apoptotic cell death (**Figure 15**) (Galluzzi et al., 2011; Ichim et al., 2016). On the other hand, MOMP stimulates the release of the Second Mitochondria-derived Activator of Caspases

(SMAC or DIABLO). SMAC acts as a pro-apoptotic protein, promoting the degradation of the X-linked Apoptosis Inhibitor Protein (XIAP) (a potent inhibitor of pro-caspases and active caspases) (Qin et al., 2016; Scott et al., 2005) through the proteasome. Therefore, SMAC release exacerbates the activation of caspase-3 and 7 and the apoptotic death (Ichim et al., 2016).

2.4.3. Convergence of intrinsic and extrinsic apoptosis

Both extrinsic and intrinsic apoptotic pathways can converge through the cleavage of the BH3-Interacting Death Domain agonist (BID) into tBID (truncated BID) by activated caspases 8 and 10. tBID promotes BAX and BAK stimulation of the MOMP, thus triggering the activation of caspase-3 and 7 through both intrinsic and extrinsic pathways (Ichim et al., 2016). The activation of executioner caspases leads to cleavage of several substrates that will lead to molecular and morphological alterations and end with apoptosis of the cell (**Figure 15**) (Fischer et al., 2003). For instance, cleavage of ICAD (Inhibitor of Caspase-activated deoxyribonuclease) by caspase-3 liberates the CAD nuclease that mediates apoptotic DNA fragmentation (Enari et al., 1998; X. Liu et al., 1997).

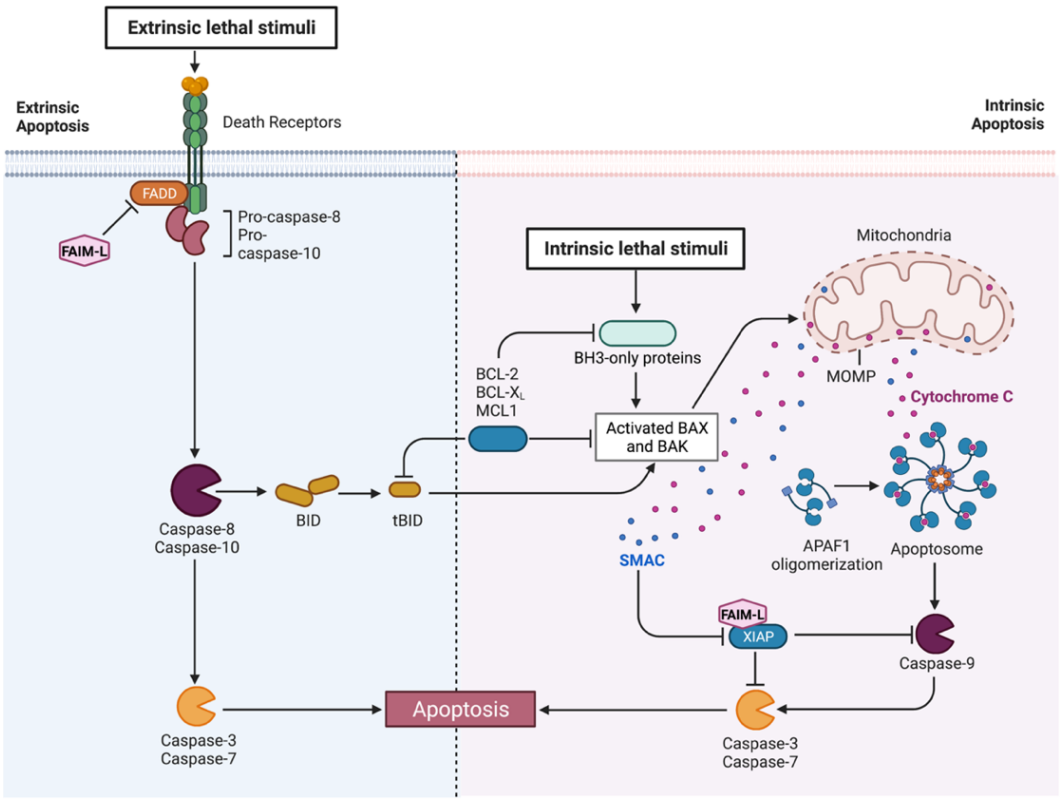

Figure 15 | Schematic representation of Intrinsic and Extrinsic Apoptosis pathways. Based on (Galluzzi et al., 2011; Ichim et al., 2016). Created with BioRender.com.

Apoptotic morphology can be detected in cells with diverse techniques; at nuclear level with the DNA dye with bisbenzimide (Hoechst) or the Terminal Deoxynucleotidyl Transferase Mediated deoxy uridine triphosphate (dUTP) Nick-End Labelling (TUNEL) technique, and at cytoplasmic level, by immunodetection of activated caspases and their cleaved substrates.

2.4.4. Apoptosis Modulation Molecules

Apoptosis can be counteracted by different proteins by directly inactivating caspases or inhibiting other pro-apoptotic related proteins.

2.4.4.1. The Bcl-2 family

Bcl-2 family proteins play a crucial role in regulating mitochondrial integrity and the response to the apoptotic signals. Proteins are included in the Bcl-2 family based on sequence homology to the Bcl-2 founding member (Giménez-Cassina & Danial, 2015; Shamas-Din et al., 2013). Most members of the Bcl-2 family proteins contain a membrane-binding region on their carboxyterminal end that facilitates binding and localization of these proteins to the MOM or to the endoplasmic reticulum (ER) membrane (Giménez-Cassina & Danial, 2015). Members of Bcl-2 family are classified in two subgroups, containing proteins that either inhibit or promote apoptosis (**Figure 16**):

- Proapoptotic proteins:
    - **Proapoptotic multidomain proteins:** Proteins that oligomerize and permeabilize the mitochondrial outer membrane (i.e. Bax and Bak).
    - **BH3-only proteins:** These molecules only have a BH3 domain and their specific function is to inhibit the antiapoptotic proteins (i.e. Bid, Bim, Bad and Noxa).
- **Antiapoptotic multidomain proteins:** These proteins contain 3 to 4 homology domains (BH) and can interact with pro-apoptotic members of the same family preventing their function (i.e. Bcl-2 and Bcl-XL).

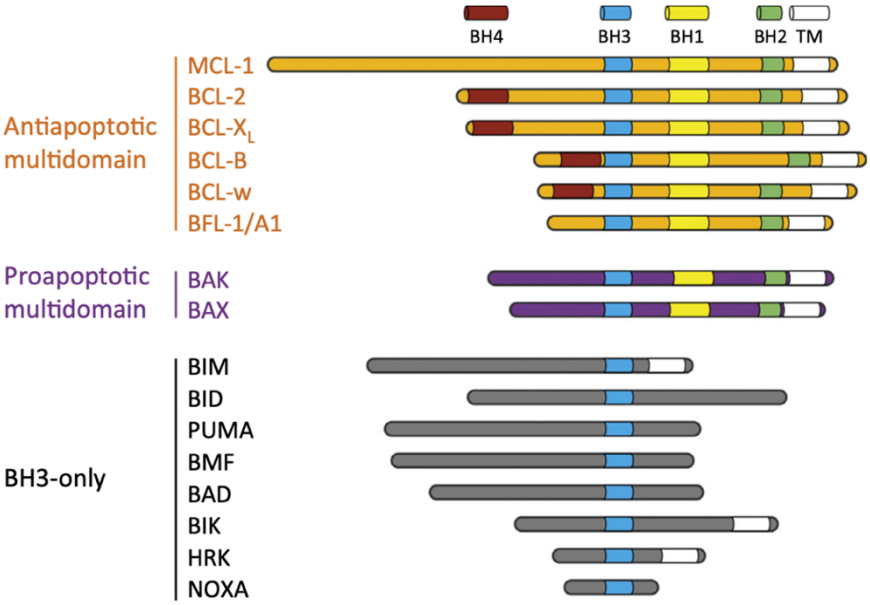

Figure 16 | Structural and functional classification of Bcl-2 proteins according to conserved BH domains. Abbreviations: MCL-1: Myeloid Cell Leukemia 1; BCL-2: B cell lymphoma 2; BCL-XL: B Cell Lymphoma Extra Large; BCL-B: Bcl-2 like B; BCL-w: Bcl-2 like 2; BAX: Bcl-2 Associated X protein; BAK: Bcl-2 Homologous Antagonist Killer; BIM: Bcl-2 like protein 11; BID: BH3-Interacting Death Domain agonist; PUMA: p53 Upregulated Modulator of Apoptosis; BMF: Bcl-2 Modifying Factor; BAD: Bcl-2 Associated Agonist of Cell Death; BIK: Bcl-2 Interacting Killer; HRK: Harakiri; TM: Transmembrane Domain. Reproduced from (Giménez-Cassina & Danial, 2015) with permission from Elsevier.

2.4.4.2. Inhibitors of Apoptosis Proteins (IAPs)

The apoptotic process can be counteracted by the IAPs family, which represent a group of negative regulators of caspases and cell death. These proteins function as E3 ubiquitin (Ub) ligases by mediating the transfer of Ub to targeted substrates for they degradation by the proteasome (Silke & Meier, 2013).

IAPs are a set of proteins defined by the presence of several domains of the Baculovirus Inhibitor of Apoptosis Repeat (BIR), which mediates protein-protein interactions. In humans, there are eight IAP types, which carry one to three copies of the BIR domain (**Figure 16**). Some BIR domains can confer IAPs specific binding capacities. Type 1 BIR domains link IAPs to specific signaling processes, whereas type 2 BIR regions can bind to IAP-binding motifs (IBMs) present in caspases and in IAP-antagonists such as SMAC (Silke & Meier, 2013; G. Wu et al., 2000). IAPs can also contain an Ub-associated and a Really Interesting New Gene (RING) domain to bind poly-Ub chains and have E3 ligase activity, labelling proteins of interest for their degradation in the proteasome (**Figure 17**) (Silke & Meier, 2013).

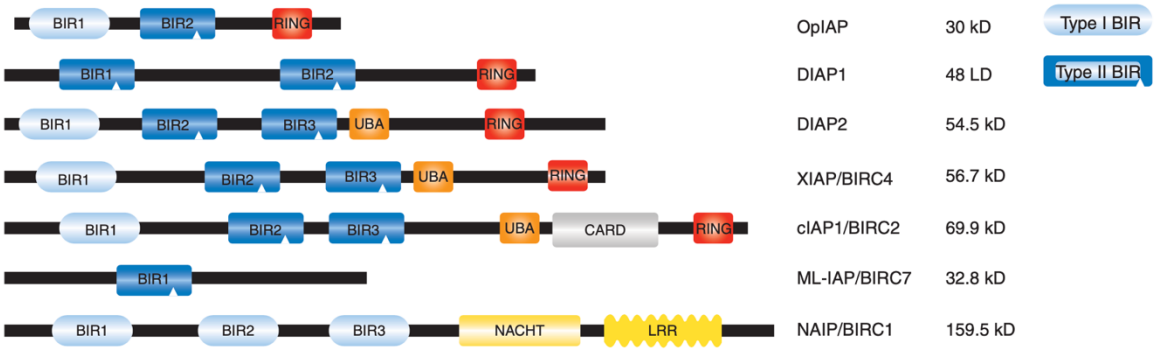

Figure 17 | Domain architecture of IAPs and different types of IAPs in humans. Abbreviations: OpIAP: Baculovirus Inhibitor of Apoptosis Protein; DIAP1: Drosophila IAP1; DIAP2: Drosophila IAP2; XIAP/BIRC4: X-linked inhibitor of apoptosis protein / Baculoviral IAP repeat-containing protein 4; cIAP1/BIRC2: Cellular Inhibitor of Apoptosis 1 / Baculoviral IAP repeat-containing protein 2; ML-IAP/BIRC7: Melanoma Inhibitor of Apoptosis Protein / Baculoviral IAP repeat-containing protein 7; NAIP/BIRC1: Neuronal Apoptosis Inhibitory Protein / Baculoviral IAP repeat-containing protein 1. Adapted from (Silke & Meier, 2013); Copyright 2013 by Cold Spring Harbor Laboratory Press. Adapted with permission.

2.4.4.3. The X-linked Inhibitor of Apoptosis Protein (XIAP) and the Long form of Fas Apoptosis Inhibitory Molecule (FAIM-L)

XIAP is known as a potent caspase inhibitor due to its structural properties. It contains two distinct Type 2 BIR domains that allow the inhibition of both initiation and executioner caspases; BIR2 domain inhibits caspase-3 and -7 while the BIR3 domain inhibits caspase-9 (Scott et al., 2005). This IAP contains a RING domain that acts as an E3 ubiquitin ligase and promotes the proteasomal degradation of caspases, SMAC and XIAP itself (Scott et al., 2005; Silke & Meier, 2013). Hence, this protein constitutes a pan-caspase inhibitor (**Figure 18a**) that can be inhibited and degraded by the proteasome through SMAC interaction (**Figure 18b**) (Moubarak et al., 2013).

FAIM-L is a 23 kDa protein which expression is limited to the CNS, including the spinal cord, the midbrain, the hindbrain, the cortex, the cerebellum and the hippocampus (Segura et al., 2007; Sole et al., 2004). The protein acts as an apoptosis inhibitor through both the extrinsic and the intrinsic pathways. FAIM-L interacts with death receptors, avoiding FADD binding and inhibiting caspase-8 and -10 activation. FAIM-L also binds to XIAP through the BIR2 domain, preventing SMAC binding and XIAP degradation through the proteasome (**Figure 18a**) (Planells-Ferrer et al., 2016). Therefore, FAIM-L acts as a XIAP stabilizer, promoting its IAP activity (**Figure 18b**) (Moubarak et al., 2013).

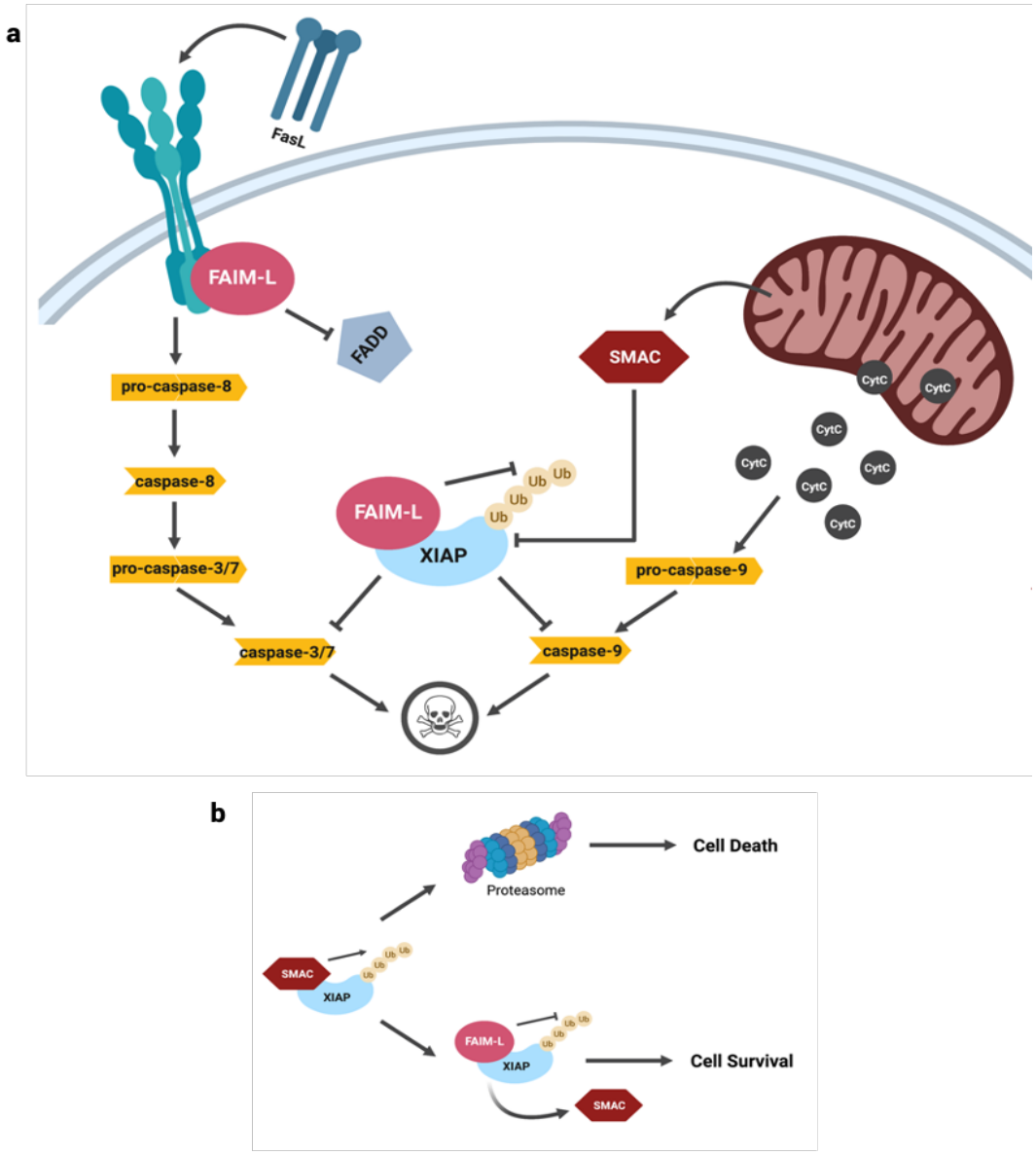

Figure 18 | Role of XIAP and FAIM-L in extrinsic and intrinsic apoptosis and their contribution to preventing cell death. (a) Upon an extrinsic apoptotic stimulus, FAIM-L prevents FADD binding with the death receptor, blocking the activation of initiator caspases and the execution of apoptosis. **(a and b)** Upon an intrinsic stimulus and after cytochrome C and SMAC release from the permeabilized mitochondria, FAIM-L binding to XIAP prevents its degradation through the proteasome, thus promoting cell survival. Based on (Moubarak et al., 2013; Planells-Ferrer et al., 2016). Created with BioRender.com.

2.5. Autophagy

The concept of autophagy was first minted in Christian de Duve's (awarded with a Nobel prize in 1974) laboratory as a result of their observations of the degradation of mitochondria and other intracellular structures within lysosomes of rat liver perfused with glucagon (Deter & De Duve, 1967). This process has been widely studied and characterized mostly in yeast by Yoshinori Ohsumi and colleagues, who described several autophagy related proteins (ATGs), essential for the delivery of cargo proteins to the vacuole (equivalent to the lysosome in mammalian cells) (Dikic & Elazar, 2018; Tsukada & Ohsumi, 1993). Thanks to these discoveries, which were awarded with a Nobel Prize in 2016, nowadays it is known that the pathway involves the formation of unique structures that sequester and engulf specific cargos to finally deliver them into the lysosome for degradation (Dikic & Elazar, 2018; Ravanan et al., 2017).

The main physiological functions of autophagy are providing nutrients for vital cellular functions during fasting, to selectively eliminate unwanted and potentially harmful cytosolic material, like damaged mitochondria or protein aggregates, and to secrete cytoplasmic constituents (Dikic & Elazar, 2018). The autophagic process has been reported to participate in the regulation of processes like the maintenance of stem cell self-renewal potential (Chen et al., 2018; Dong et al., 2021), the cellular plasticity and differentiation (Boya et al., 2018; Clarke & Simon, 2019), the defense against pathogens, or the regulation of oxidative stress and nutritional starvation (Badadani, 2012). Autophagy is also considered a form of RCD. Autophagy-dependent cell death (ADCD) does not refer to sceneries where the autophagic machinery is activated alongside RCD, but it rather precipitates the process. ADCD can favor the engagement of other RCD types such as ferroptosis, extrinsic apoptosis or necroptosis (reviewed in (Galluzzi et al., 2018)). Autophagy dysregulation can contribute to the development of several pathologies, including cancer, infectious diseases and neurodegeneration (reviewed in (Dikic & Elazar, 2018)).

There are three defined types of autophagy: **micro-autophagy**, **chaperone-mediated autophagy** and **macro-autophagy**, all of which promote proteolytic degradation of cytosolic components at the lysosome (**Figure 19**).

- **Micro-autophagy:** the cytosolic components are directly taken up by the lysosome through the invagination of the lysosomal membrane.
- **Chaperone-mediated autophagy (CMA):** the targeted components, which must specifically contain a common aminoacidic sequence (KFERQ), are translocated to the lysosomal

membrane forming a complex with the chaperone protein Hsc-70. The protein-chaperone complexes are recognized by the lysosomal membrane receptor LAMP-2A (lysosomal-associated membrane protein 2A), which allows the engulfment and degradation of the complex inside the lysosome.

– **Macro-autophagy:** the cytoplasmic cargo is delivered to the lysosome through the formation of double-membrane vesicles called autophagosomes, which sequester cellular contents and targeted proteins to eventually fuse with the lysosome, forming a structure called auto-phagolysosome. Macro-autophagy is usually referred to as autophagy or canonical autophagy because it is the one most used by cells. This process can proceed in a nonselective manner (known as "bulk autophagy"), or involve a tightly regulated elimination of individual cellular components (known as "selective autophagy") (Dikic & Elazar, 2018; Klionsky, Petroni, et al., 2021; Parzych & Klionsky, 2014; Yang & Klionsky, 2009).

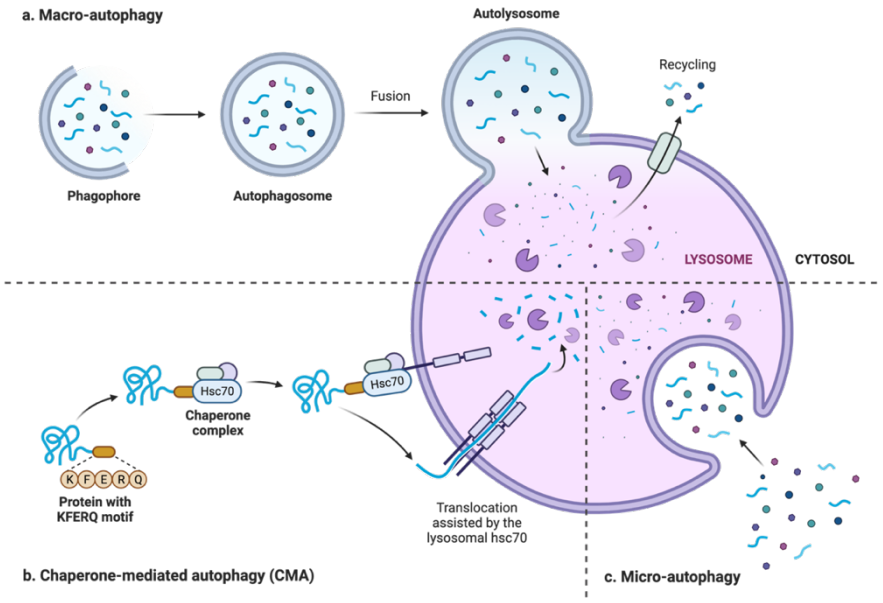

Figure 19 | Schematic representation of the three autophagy types in mammalian cells. A. Macro-autophagy is based on the formation of double-membrane cytosolic vesicles that sequester and transport the cargo to the lysosome. B. Chaperone-mediated autophagy degrades individual proteins with a KFERQ sequence by HSC70 recognition and interaction with the LAMP-2A membrane receptor. C. Micro-autophagy is based on the direct uptake of the cargo through invagination of the lysosomal membrane without vesicular transport. Based on (Ho et al., 2019). Created with BioRender.com.

2.5.1. The autophagy process

The morphological feature that distinguishes macro-autophagy (from now on referred to as autophagy) from other intracellular vesicle-mediated trafficking processes is that the autophagosomes are formed de novo rather than through membrane budding from a preexisting organelle (Yang & Klionsky, 2009). In mammalian systems, autophagosome generation is initiated at multiple sites throughout the cytoplasm (Itakura & Mizushima, 2010).

Once an autophagy activation signal is induced, the process is divided into five stages; **initiation**, phagophore **nucleation**, phagophore **elongation**, **fusion with the lysosome** and **degradation and recycling** by lysosomal proteases (**Figure 20**).

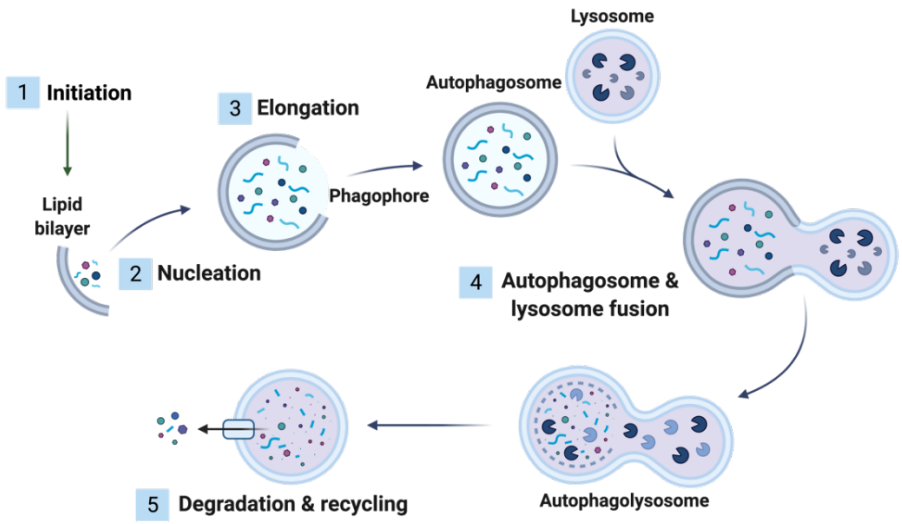

Figure 20 | Schematic representation of the autophagy process. 1. Initiation of the process by activation of the autophagy signaling pathways. 2. Autophagosome nucleation. 3. Elongation and capture of the cytoplasmic components; formation of the autophagosome. 4. Fusion of the autophagosome with the lysosome. 5. Degradation of the cargo by hydrolases and proteases from the lysosome and recycling of some components. Based on (Ho et al., 2019). Created with BioRender.com.

Initiation

The initiation of the autophagic cascade is normally subjected to the repressive control of mTOR (mechanistic target of rapamycin kinase) complex 1 (mTORC1) through direct interaction with the ULK1 (unc-51-like autophagy-activating kinase 1; autophagy related protein 13; RB1-inducible coiled-coil protein 1; autophagy related protein 101) complex, which is responsible for the initiation of the autophagic pathway downstream of mTORC1 (Klionsky, Petroni, et al., 2021).

- Under growth promoting conditions mTORC1 is activated by several upstream stimuli (like the NFkappaB, the PI3K/Akt and the MAPK/ERK pathways) (Melick & Jewell, 2020; Tchevkina & Komelkov, 2012) to inhibit autophagy and promote growth through induction of protein translation and expression. This inhibition is produced by direct interaction and phosphorylation of the ULK1 complex.
- Conversely, during starvation conditions mTORC1 is inhibited by the TSC1/TSC2 (Tuberous sclerosis complex 1 and 2) complex, thereby letting ULK1 autophosphorylation and the phosphorylation of the other associated proteins, to initiate the autophagy process (Ganley et al., 2009; Hosokawa et al., 2009; Jung et al., 2009; Sarkar, 2013).

Autophagy initiation is also regulated by mTORC1 independent pathways. For instance, increased levels of inositol triphosphate (I3P) or cAMP (cyclic adenosine monophosphate) have been related to an inhibition of the autophagosome synthesis (Noda & Ohsumi, 1998; Sarkar et al., 2005).

Nucleation

Once the ULK1 complex is activated, it triggers the phagophore nucleation by facilitating the phosphatidylinositol-3-kinase activity of a multiprotein complex (PI3KC3 complex) formed by: BECLIN1; VPS34 (phosphatidylinositol-3-kinase catalytic subunit type 3; VPS15 (phosphoinositide-3- kinase regulatory subunit 4); ATG14; NRBF2 (nuclear receptor binding factor 2); AMBRA1 (activating molecule in BECLIN1 regulated autophagy protein 1); and p115 (general vesicular transport factor (p115) (Dikic & Elazar, 2018; Hurley & Young, 2017; Klionsky, Petroni, et al., 2021). VPS34 uses phosphatidylinositol (PI) as a substrate to generate PI triphosphate (PI3P), an essential component for the nucleation of the phagophore recruitment and other ATG proteins (Nascimbeni et al., 2017). Interestingly, the activation of the PI3KC3 complex can be inhibited by the antiapoptotic protein Bcl-2 (Yang & Klionsky, 2009), suggesting that apoptosis and autophagy are linked processes.

Several studies suggest that endoplasmic reticulum (ER)-associated structures may serve as initiation sites to form autophagosomes in mammals (Hayashi-Nishino et al., 2009; Ylä-Anttila et al., 2009), although the source of the autophagosome membrane is still in investigation.

Elongation

The elongation phase, where the double-membrane expands to engulf the intracellular cargo, is promoted by two distinct ubiquitin-like conjugation modules, the Atg5-Atg12 conjugation and the LC3 processing (Glick et al., 2010; Kirkin et al., 2009):

a. **ATG5-ATG12 conjugation:** The activity of ATG7 and ATG10 proteins enables the buildup of a complex formed by ATG5, ATG12 and ATG16L1 (autophagy-related 16-like 1). This complex associates with the extending phagophore to promote its bending. The formation of this complex is essential for LC3 lipidation (Otomo et al., 2012). Once the autophagosome is formed, the ATG5-ATG12-ATG16L1 complex dissociates from the membrane in order to be degraded (Glick et al., 2010).
b. **LC3 processing:** The processing of pro-LC3 (microtubule-associated protein light chain 3) starts with the proteolytical cleavage of the c-terminal end by ATG4, thus generating LC3-I, which has an exposed glycine residue. This residue allows the conjugation of phosphatidylethanolamine (PE) to LC3-I by ATG7-ATG3, generating a membrane-anchored lipidated form of LC3 (named **LC3-II**) (Eskelinen, 2004).

For an efficient LC3 recruitment, ATG3 requires stimulation from the ATG5-ATG12-ATG16L1 complex (Otomo et al., 2012). Once processed, LC3-II is recruited and integrated into the inner and outer surface of the growing phagophore, inducing the elongation and sealing the phagophore to form the autophagosome. LC3-II also serves as a receptor for LC3-interacting region (LIR)-containing proteins, including autophagy receptors and substrates such as p62/SQSTM1 (Sequestrosome 1). Hence, LC3-II is also necessary to select the cargo for degradation (Klionsky, Petroni, et al., 2021).

– p62/SQSTM1 is a cargo protein for ubiquitinated proteins that can be degraded by autophagy and/or by the proteasome. It possesses a LIR region that facilitates interaction with LC3 and therefore, p62 is normally degraded by autophagy. Accumulation of this protein is produced upon autophagy inhibition, whereas p62 level decrease is associated with autophagy activation. The level of p62 can be monitored by western blotting and serves as an indicator of the autophagy flux (reviewed in Bjørkøy et al., 2009).

LC3-II formation is increased during the autophagy process, and the lipidated protein remains associated with the autophagosome membrane until the fusion with the lysosome occurs. Then, LC3-II from the inner surface is degraded together with the cargo, whereas the LC3-II from the outer surface dissociates and degrades through the proteasome. Due to these characteristics, measuring LC3-II levels is widely used for quantifying autophagy (Glick et al., 2010; Klionsky, Abdel-Aziz, et al., 2021).

Lysosomal fusion and degradation

Upon closure of the phagophore, the resulting autophagosome fuses with a lysosome to form an autophagolysosome, culminating with the degradation of autophagic substrates by acidic lysosomal hydrolases (Parzych & Klionsky, 2014). It has been suggested that prior to the fusion with the lysosome, the autophagosome fuses with early and late endosomes (formatting structures called amphisomes) to acquire the machinery and pH conditions required for the fusion with the lysosome (Eskelinen, 2004). Once fused, lysosomal acid proteases and hydrolases degrade indistinctly the inner membrane of the autophagosome and all the components inside the cytoplasmic region of the autophagolysosome. Some of the proteins involved in this process are cathepsin proteases B and D (Koike et al., 2005), and LAMP-1 and LAMP-2 (Lysosomal-associated membrane protein 1 and 2). LAMPs are type-1 transmembrane proteins that target to the lysosomes, and LAMP-1 is the most abundant endolysosome membrane protein (Saftig & Klumperman, 2009). Deletion of LAMP proteins inhibits the degradation process (Tanaka et al., 2000). Finally, amino acids and other monomeric molecules are exported to the cytosol to be reused (reviewed in (Ho et al., 2019)).

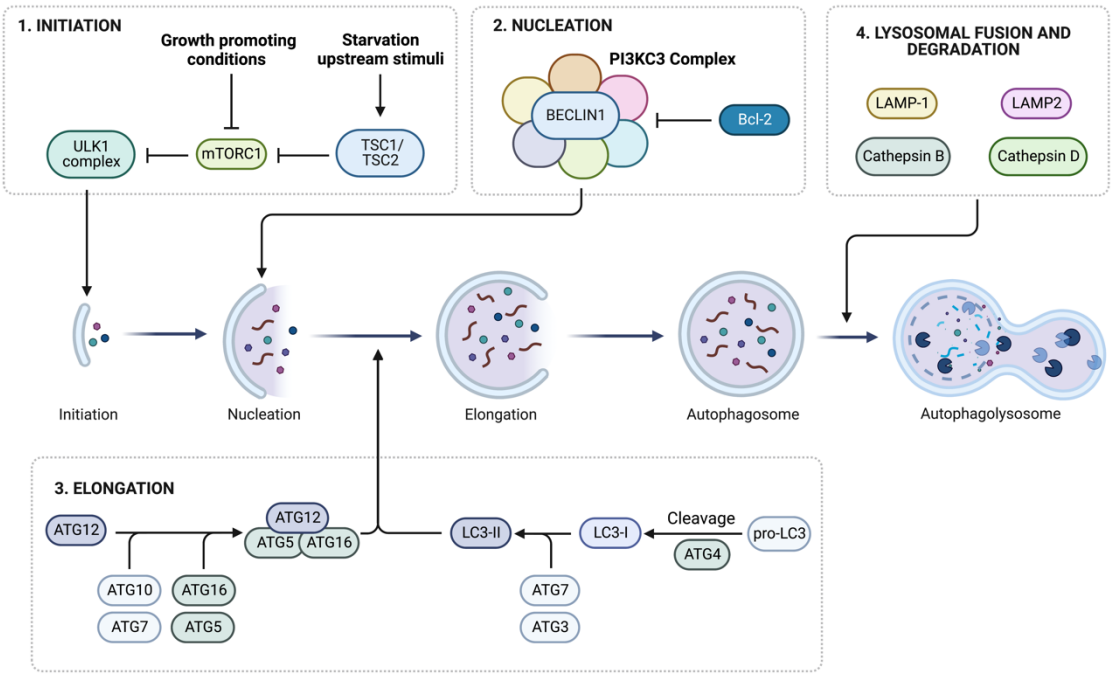

Figure 21 | Schematic representation of the molecules involved in the autophagy process. Based on (Klionsky, Petroni, et al., 2021). Created with BioRender.com.

3. MECHANISMS OF NEURONAL SURVIVAL

Neuronal cell survival regulation is complex and multifactorial, involving multiple variables and signaling pathways. Neurons receive extracellular signals from other neuronal and non-neuronal cell types such as electrical signals, neurotransmitters, neurotrophins, hormones and cytokines, which they use to adapt to the different physiological and pathological situations. These stimuli promote intracellular signaling pathways activation and ion mobilization, such as K^+ and Ca^{2+}, having a crucial role in the maintenance and regulation of neuronal survival.

3.1. Neurotrophic Factors Regulating neuronal survival and differentiation

Neurotrophic factors (**NTFs**) are signaling molecules that bind to specific membrane receptors present in the plasma membrane of neurons, including neurotrophins, hormones, and cytokines. They induce the stimulation of signaling pathways that lead to the translocation of transcription factors into the nucleus, and activating transcription of genes involved in cell survival and in the prevention of RCD processes (Frebel & Wiese, 2006; Kaplan & Miller, 2000).

The first NTF discovered was the Nerve Growth Factor (NGF) thanks to the work of Viktor Hamburger, Rita Levi-Montalcini and Stanley Cohen, who stablished the basis of the NTF theory (Levi-Montalcini, 1987). NGF is produced by the targeted tissue that is going to be innervated by sensory neurons, and this growth factor is retrogradely transported from the axonal terminal to the soma. Moreover, NGF is essential for neuronal *in vitro* and *in vivo* survival (Levi-Montalcini, 1987). Hence, this theory proposes that innervated tissues produce a signal for the innervating neurons, limiting the neuronal cell death occurring during the development, and that molecules similar to NGF may be capable of rescuing other neuronal populations (Korsching, 1993).

From these studies, several NTF molecules have been identified and classified into different groups depending on their structural homologies such as; neurotrophins, GDNF family ligands, cytokines and other NTFs (**Table 5** and **Figure 22**). Due to their properties, NTFs cocktails are used to maintain and regulate the survival of primary MN cultures and differentiated human MNs derived from iPSCs.

Table 5 | NTFs Regulating neuronal survival and differentiation.

Neurotrophins	Nerve Growth Factor (NGF)	(Levi-Montalcini, 1987)
	Brain Derived Neurotrophic Factor (BDNF)	(Barde et al., 1982)
	Neurotrophin 3 (NT-3)	(Rosenthal et al., 1990)
	Neurotrophin 4/5 (NT-4/5)	(Berkemeier et al., 1991; Ip et al., 1992)
GDNF Family Ligands	Glial cell line-Derived Neurotrophic Factor (GDNF)	(L. F. H. Lin et al., 1993)
	Neurturin (NRTN)	(Kotzbauer et al., 1996)
	Persephin (PSP)	(Chadwick et al., 1998; Milbrandt et al., 1998)
	Artemin (ARTN)	(Baloh et al., 1998)
Cytokines	Ciliary Neurotrophic Factor (CNTF)	(Varon et al., 1979)
	Cardiotrophin-1 (CT-1)	(Latchman, 1999)
	Leukemia inhibitory factor (LIF)	(Oppenheim, 1989)
Others	Hepatocyte Growth Factor (HGF)	(Nakamura et al., 1984; Nakamura & Mizuno, 2010)
	Insulin Growth Factor (IGF-1)	(Laron, 2001)
	Vascular Endothelial Growth Factor (VEGF)	(Ferrara & Adamis, 2016)
	Pleiotrophin	(Merenmies & Rauvala, 1990)
	Neuropoietin	(Derouet et al., 2004)
	Mullerian Inhibiting Substance (MIS)	(Price et al., 1977)
	Growth Differentiation Factor-15 (GDF-15)	(Lawton et al., 1997)
	Progranulin	(Van Damme et al., 2008)
	Angiogenin	(Kieran et al., 2008)

Neurotrophins

Neurotrophins are NTFs that exert diverse functions depending on the neuronal population. For instance, BDNF promotes MN and sensory neuron survival whereas NGF only produces beneficial effects on sensory neurons (Gutierrez et al., 2005). Neurotrophins bind to either Trk or $p75^{NTR}$ membrane receptors, promoting its dimerization and activation of survival signaling pathways (Kaplan & Miller, 2000) such as PLCy (Phospholipase C) (Patapoutian & Reichardt, 2001), JNK (Janus Kinase) (Dolcet et al., 2001), NFkappaB (Nuclear Factor kappa B) (Arumugam et al., 2018; Mincheva et al., 2011), PI3K/Akt (Phosphatydilinositol-3-kinase/Protein Kinase B) (Holgado-Madruga et al., 1997; Nguyen et al., 2009) and ERK MAPK (Extracellular Regulated Kinase / Mitogen Activated Protein Kinase)(Marshall, 1995).

GDNF Family Ligands

GDNF family ligands (GFLs) are NTFs synthetized as precursors that bind to GFRα (GDNF Family Receptor alpha, 1-4) receptors. GFRα receptors dimerize and trigger the activation and homodimerization of the Ret (Receptor tyrosine-kinase proto-oncogene) receptor. (Airaksinen & Saarma, 2002). This receptors group together and their activation regulates survival signaling pathways such as PI3K/Akt (Gould et al., 2008; Soler et al., 1999) and ERK MAPK (Vega et al., 1996). Interestingly, GDNF is expressed before the PCD period in MNs, and its depletion can cause a loss of around 20 to 30% of the MNs (Gould et al., 2008).

Cytokines

Cytokines family has been described as one of the most important for regulating cell survival both *in vitro* and *in vivo* (Arakawa et al., 1990; Oppenheim et al., 1991; Sendtner et al., 1991). These proteins interact with an heterodimeric receptor (gp130/LIFRß) and a co-activator receptor to trigger the activation of several survival pathways including; JAK/STAT, PI3K/Akt, ERK MAPK (Dolcet et al., 2001), and NFkappaB (Middleton et al., 2000). These NTFs have neuroprotective effects (Lesbordes et al., 2003; Sendtner et al., 1990), and their deletion can produce MN loss and muscular atrophy (Sendtner et al., 1990, 2000; Simon et al., 2010).

Other NTFs - HGF

The Hepatocyte Growth Factor (HGF) is a NTF that regulates activation of survival signaling pathways through the specific binding to the mesenchymal-epithelial transition factor (c-Met or HGF receptor) (Nakamura & Mizuno, 2010). HGF *in vitro* administration promotes MN survival (Schaller et al., 2017).

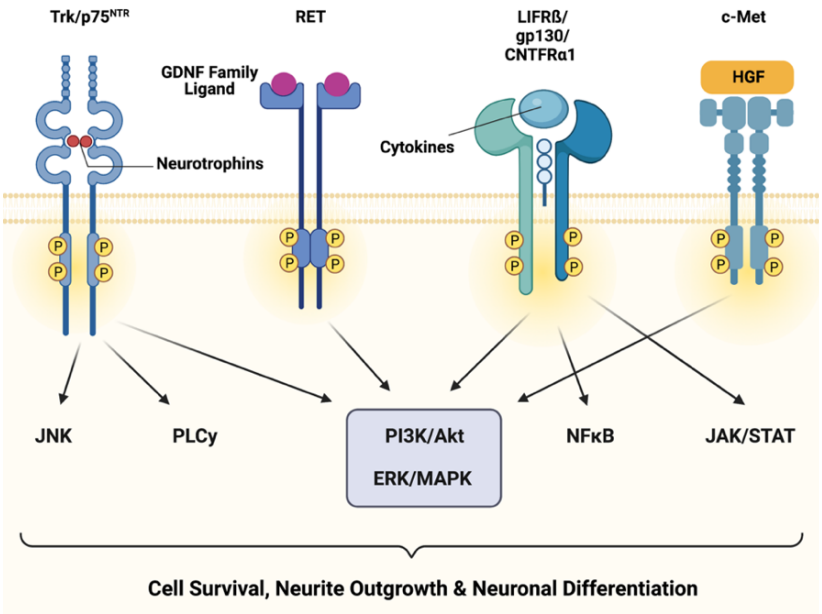

Figure 22 | Schematic representation of different NTF receptors activation by their ligands and the signaling pathways that they activate. NTFs promote cell survival, neurite outgrowth and neuronal differentiation. Created with BioRender.com.

3.2. Signaling pathways involved in MN survival

NTFs and ion mobilization (K^+ and Ca^{2+}, principally) are the major regulators of the activation of survival signaling pathways in MNs. Notwithstanding the origin diversity, the majority of the signals converge in the activation of survival pathways. The most known and studied, and the principal effectors involved in neuronal survival and differentiation are the PI3K/Akt and the ERK MAPK signaling pathways.

3.2.1. The PI3K/AKT pathway

The PI3K/Akt pathway is a key regulator of cell cycle proliferation, growth, survival, protein synthesis, and glucose metabolism (Yung et al., 2011). Akt is the major downstream target of PI3 kinase (PI3K), which is activated by receptor tyrosine kinases (RTKs). PI3 kinase is an heterodimeric protein constituted by two subunits: the regulator or p85, and the catalytic subunit or p110. This protein is activated by the phosphorylation of two tyrosine residues from the regulator subunit, which produces a conformational change in the catalytic subunit and PI3K activation. Once active, PI3K catalyzes the phosphorylation of phosphatidylinositol 2-phosphate (PIP_2) to phosphatidylinositol 3-phosphate (PIP_3) (Cantrell, 2001). This process promotes the recruitment of the 3-Phosphoinositide-dependent kinase 1 (PDK1), which phosphorylates the threonine 308 (Thr308) of Akt protein. Akt also requires the phosphorylation of the serine 473 (Ser473) by mTORC2 or a DNA-dependent protein kinase (Yung et al., 2011) for its activation. Finally, active Akt phosphorylates RXRXX(S/T) sequences of transcription factors, controlling apoptosis and the transcription and translation of pro-survival molecules (**Figure 23**) (Frebel & Wiese, 2006; LoPiccolo et al., 2008).

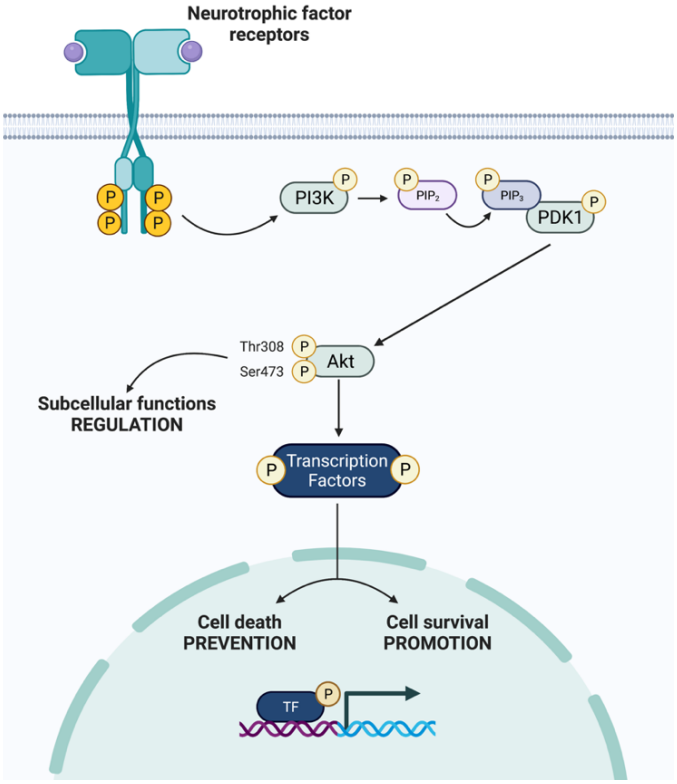

Figure 23 | Schematic representation of PI3K/Akt signaling pathway. Based on (T. A. Yap et al., 2008). Created with BioRender.com.

PI3K/Akt pathway main function is to promote neuronal survival. Several proteins are susceptible of being phosphorylated by Akt, including cytoplasmic proteins and transcription factors that regulate cell proliferation, growth, protein synthesis and anti-apoptotic gene expression (Sánchez-Alegría et al., 2018; T. A. Yap et al., 2008).

- Akt is known to phosphorylate BAD protein, thus promoting the liberation of the anti-apoptotic proteins Bcl-2 and Bcl-XL (Datta et al., 2000; Vauzour et al., 2007).
- Caspase-9 phosphorylation by Akt can inhibit the apoptosis process (Cardone et al., 1998).
- Akt phosphorylation of the Forkhead transcription factor prevents its nuclear translocation and the transcription of pro-apoptotic genes such as Bim (Frebel & Wiese, 2006).
- CREB phosphorylation by Akt induces the expression of the anti-apoptotic Bcl-2 gene (K. Du & Montminy, 1998).
- IKKß phosphorylation by Akt liberates the NFkappaB transcription factor, promoting its nuclear translocation and the expression of antiapoptotic proteins such as Bcl-XL (Madrid et al., 2000; Ozes et al., 1999).
- Akt controls cell survival and autophagy by phosphorylating TSC and activating mTORC1 protein (Melick & Jewell, 2020).

The pro-survival effect of PI3K/Akt pathway has been observed on several neuronal populations, including MNs (Dolcet et al., 1999, 2001), cortical neurons (Hetman et al., 1999), sympathetic neurons (Creedon et al., 1997) and hippocampal neurons (Righi et al., 2000). Besides promoting survival, PI3K/Akt pathway is also involved in neurite elongation and axonal arborization (reviewed in (Dijkhuizen & Ghosh, 2005; Markus et al., 2002)).

3.2.2. The ERK MAPK pathway

ERK MAPK is a signaling pathway that promotes neuronal survival after the activation initialized by NTF binding to their specific receptors, and has been the best characterized MAPK signaling pathway (Wei & Liu, 2002). The activation of RTKs by NTFs provokes the activation of MAPKs in a multistep process that involves many proteins. Essentially, first the Ras GTPase activation is produced. Then, Ras binds to Raf (MAPKKK) kinase, which phosphorylates MEK1 and MEK2 (MAPKK) kinases. These two proteins then phosphorylate ERK1 (p44 MAPK) and ERK2 (p42 MAPK), thereby increasing their enzymatic activity. The activated ERKs can translocate to the nucleus acting as transcription factors promoting the

gene expression, or remain in the cytoplasm regulating subcellular functions via the ribosomal S6 kinase (RSK) (**Figure 24**), or other cytosolic proteins (Bodart, 2010; LoPiccolo et al., 2008; Melick & Jewell, 2020). Inside the nucleus, ERK phosphorylates different transcription factors including c-Myc, Ets1, c-Jun, E-twenty-six Like 1 (Elk-1), which has been shown to participate in promoting SMN transcription (Demir et al., 2011). Like Akt, ERK can phosphorylate BAD to liberate Bcl-2 and Bcl-XL (Datta et al., 2000; Vauzour et al., 2007), and RSK to regulate mTORC1 protein and control cell survival and autophagy process (Melick & Jewell, 2020). RSK protein can also phosphorylate transcription factors such as IkBα or CREB (Wei & Liu, 2002), which in turn regulate gene expression. For instance, CREB phosphorylation leads to Bcl-2 expression (K. Du & Montminy, 1998).

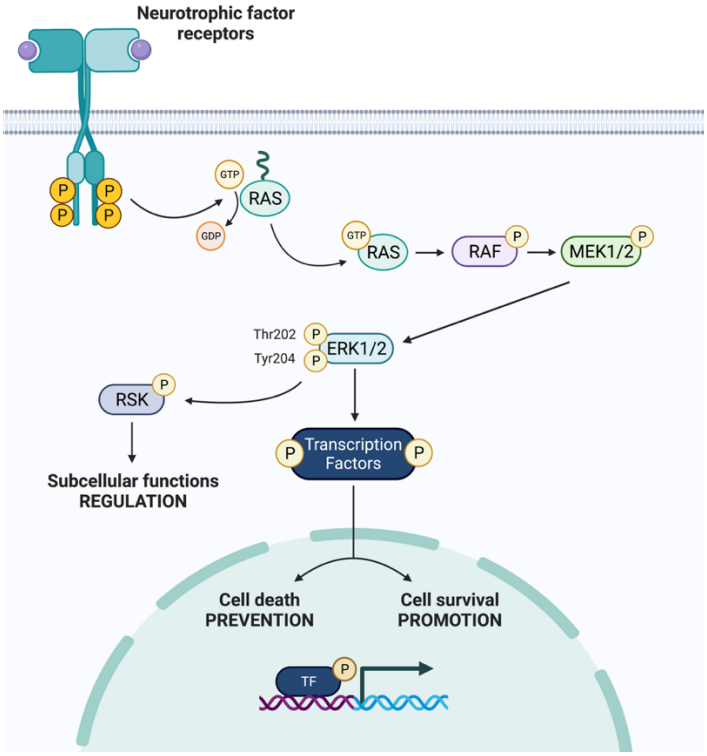

Figure 24 | Schematic representation of ERK MAPK signaling pathway. Based on (F. Liu et al., 2018; Melick & Jewell, 2020). Created with BioRender.com.

3.2.3. Intracellular calcium as neuronal survival modulator

Calcium (Ca^{2+}) is one of the most common intracellular messenger in neuronal populations. Transient increases of intracellular calcium concentrations can be produced by several stimuli, promoting the activation of proteins with Ca^{2+} binding domains and signaling pathways which activity relies on the amount of intracellular Ca^{2+} levels, and regulating multiple events such as cell cycle, survival and differentiation (reviewed in Clapham, 2007).

Intracellular Ca^{2+} concentrations are usually low (50 – 100nM), whereas in the extracellular space they can reach mM levels. Both NTFs (De Bernardi et al., 1996; Pérez-García et al., 2004) and neuronal activity (membrane depolarizations) (Franklin & Johnson, 1992; Soler et al., 1999) are capable of producing transient intracellular Ca^{2+} increases. The cells use several mechanisms to maintain intracellular Ca^{2+} homeostasis:

- ATPases, ligand dependent Ca^{2+} channels, voltage dependent gated Ca^{2+} channels (VGCC), and Na^{+}/Ca^{2+} exchangers in the cytoplasmic membrane regulate the intracellular Ca^{2+} concentrations.
- ER and mitochondria are Ca^{2+} stores which liberate the ions to participate in intracellular signaling pathway activation.
- Proteins with Ca^{2+} binding sites that buffer Ca^{2+} by reversibly binding to it and releasing the ion when necessary.

In pathological conditions and during aging, neurons capability to buffer Ca^{2+} can be compromised, becoming a mechanism related to neurodegenerative diseases (Zündorf & Reiser, 2011). For instance, both high and low intracellular calcium concentrations have been associated to neuronal cell death (Franklin & Johnson, 1992).

4. SPECIFIC VULNERABILITY OF SPINAL CORD MNs

MNs are highly polarized cells with a big soma, short dendrites and a single axon that can reach up to 1m length in humans (Ragagnin et al., 2019). αMNs of different classes are grouped into motor pools, each of which innervates a single skeletal muscle (Kanning et al., 2010). Interestingly, in ALS and SMA diseases, and in aging fast-twitch fatigable MNs degenerate earlier than MNs innervating slow muscles, and are therefore, more vulnerable (Kanning et al., 2010; Schweingruber & Hedlund, 2022). Studies have demonstrated that resilient MN subpopulations present differential gene regulation and protein content, and these features are being investigated to provide protection to more vulnerable cells (Nichterwitz et al., 2020; Schweingruber & Hedlund, 2022).

The specific MN morphology relies on the cytoskeletal organization, and can confer specific vulnerability to these cells as most of the proteins are synthesized in the soma and transported along the axon to the synaptic terminals. Some MN disorders are caused by genetic mutations of ubiquitous proteins, such as SMA and ALS in around 5-10% of the cases (Berdyński et al., 2022; Jablonka et al., 2000). These molecules could have essential roles in MNs, hence, the loss of function of specific proteins may compromise MNs in a major grade than other tissues and cells. This loss of functionality can favor the emergence of several defects in these cells leading to MN degeneration and death such as: defects in the neuronal cytoskeleton, defects in the molecular machinery of axonal transport, disruption of endosomal trafficking, mitochondrial toxicity, low intracellular Ca^{2+} buffering capacity and survival intracellular survival pathways deregulation. Moreover, alterations in the MN environment have also been reported to participate and/or influence in MN diseases progression (reviewed in Lambrechts et al., 2007).

Defects in the MN cytoskeleton: MN cytoskeletal organization and integrity is vital for these cells. Many proteins synthetized in soma and mRNAs are transported along the axon to exert specific functions at the synaptic terminal. Disrupted axonal transport causes MN degeneration. Neurofilaments (NF) are the most abundant structural proteins in neurons, and accumulations of these NF have been observed in SMA and ALS models (Cifuentes-Diaz et al., 2002; L. M. Murray et al., 2008; Zucchi et al., 2020). Besides, phosphorylated neurofilament heavy (pNF-H) is elevated in SMA infants plasma, and it decreases upon treatment with Nusinersen (Darras et al., 2019). Therefore, pNF-H may be a promising marker of disease activity and treatment response in SMA patients.

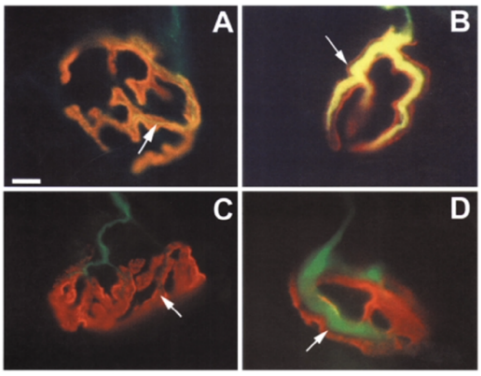

Figure 25 | Accumulation of neurofilaments in terminal axons of Smn mutant mice. Immunostaining of NMJ of muscle fibers from control (A,C) and Smn mutant mice (B,D). AChR (red) and NF-M (A,B, green) or phosphorylated NF-H (C,D, green) labeling revealed terminal axons filled with NF in mutant mice (B,D, arrows). Adapted from (Cifuentes-Diaz et al., 2002) with permission from Oxford University Press..

Mitochondrial dysfunction and toxicity: Mitochondria are essential organelles due to their specific functions in the cell such as ATP production, intracellular Ca^{2+} levels regulation and control of the oxidation levels. MNs are major energy consumers due to their morphology, and they are highly dependent of a proper mitochondrial function. SMN silencing in NSC-34 cell lines induces an increase in cytochrome c oxidase activity (Rage et al., 2013); and mitochondria number and axonal transport are altered in human SMA iPSCs (Xu et al., 2016). Besides, murine SMA models show alterations in mitochondrial respiration, membrane potential and mobility and increased oxidative stress level (reviewed in Stanga et al., 2020).

Low Ca^{2+} buffering capacity: Intrinsic capability of buffering Ca^{2+} ions is low in MNs (Krieger et al., 1994). These cells express low amounts of Ca^{2+} binding proteins such as calbindin and parvalbumin. In physiological conditions, this characteristic facilitates rapid relaxation in response to Ca^{2+} fluxes during high-frequency rhythmic activities. However, in pathological conditions this feature can accelerate mitochondrial disruption and excitotoxic damage. For instance, in ALS the most affected subpopulations of MNs are those with lower Ca^{2+} buffering capacity (reviewed in Von Lewinski & Keller, 2005), and conversely, those less affected present higher parvalbumin concentrations (Reiner et al., 1995).

Alterations in MN environment: Besides cell-autonomous toxicity, the cellular environment such as glial-mediated inflammation can negatively impact on MN survival, promoting progression and propagation of the degenerative process by the activation of apoptotic cascades. In SMA, gliosis has been linked to MN degradation in the spinal cord and brain stem (reviewed in Papadimitriou et al., 2010). Skeletal muscle can participate in maintaining MN survival; it releases signaling molecules that modulate survival, axonal growth and synaptic connection. NTFs released by these cells are crucial for maintaining MN integrity, and altered levels of several NTFs have been described in ALS and SMA patients and mouse models in cerebrospinal fluid and muscle tissue (Ekestern, 2004; L. M. Murray et al., 2008). Skeletal and

heart muscle cells are affected in SMA disease, and alterations in the mitophagy process have been described (Borgia et al., 2017). Nevertheless, it is still unclear whether the peripheral abnormalities precede MN degeneration or, on the contrary, MN degeneration derives in these peripheral dysfunctions.

5. APOPTOSIS, AUTOPHAGY, AND SURVIVAL SIGNALING PATHWAYS ALTERATIONS IN SMA AND MN DISORDERS

The lack of SMN in MNs, which has with multiple functions involved in RNA biosynthesis, metabolism and transport, can conduct to major alterations in these cells. These deregulations may involve decompensated signaling of survival intracellular pathways, leading to impairment of cellular and molecular mechanisms such as autophagy and ending in the collapse of these cells.

5.1. Survival signaling pathways in SMA and neurodegenerative diseases

PI3K/Akt Signaling Pathway

The PI3K/Akt pathway is a major regulator of cell survival, but it is also related to the regulation of neurite elongation and axonal arborization processes (reviewed in (Dijkhuizen & Ghosh, 2005; Markus et al., 2002)). Akt phosphorylates proteins including Bcl-2 family members (Datta et al., 2000; Vauzour et al., 2007) and protein kinases such as Raf (Zimmermann & Moelling, 1999) or IkappaB (Inhibitory kappa B) kinase (Ozer et al., 1999), Reviewed in (Nand Rai et al., 2019). In pathological situations, Akt phosphorylation pattern may undergo changes and contribute to disease development, such as ischemia (Sakurai et al., 2001), ALS (Wagey et al., 1998), HD (Humbert et al., 2002), AD (H. K. Lee et al., 2009; Nand Rai et al., 2019) and SMA (Biondi et al., 2015; Branchu et al., 2013):

- Both PI3K and Akt mediate growth factor-induced neuronal survival after cerebral ischemia in a MN axonal injury rodent model (Sakurai et al., 2001).
- In ALS, postmortem particulate fractions of spinal cord tissue showed increased levels of PI3K compared with control subjects, although there was not an upregulation in the activities of Akt and S6K. These results suggested an impairment in signal transduction mediated by PI3K in this disease (Wagey et al., 1998).
- In HD, Akt is altered in HD patients and IGF-1 neuroprotective effects required huntingtin (Htt) protein to be phosphorylated by Akt (Humbert et al., 2002).
- In Alzheimer's disease (AD), both PDK and Akt showed reduced activity in AD brains compared to controls (H. K. Lee et al., 2009). PI3K/Akt signaling pathway is an upstream effector of mTORC1, which in turn regulates autophagy (Melick & Jewell, 2020), and amyloid protein presence in neuronal tissue is suggestive of disrupted autophagy (reviewed in (Nand Rai et al., 2019).

- In SMA disease, Akt phosphorylation is reduced in spinal cord and muscle tissue protein extracts from a severe SMA mouse model (Biondi et al., 2015; Branchu et al., 2013).

ERK MAPK Signaling Pathway

ERK activation involvement in neuronal survival suggest an ambivalent role of this molecule. It may promote cell survival or cell death depending on the disease context and the experimental models used (reviewed in (Nand Rai et al., 2019)). Most neurodegenerative diseases hallmarks rely on abnormal fibrillary deposition in the CNS, and some of these components are cytosolic targets of ERK. These observations suggest the involvement of ERK MAPK pathway in the disease development (Gerfen et al., 2002; Spillantini et al., 1998):

- Inhibition of the p44/42 MAP kinase pathway protected hippocampal neurons in a cell-culture model of seizure activity (Sugino et al., 2000), whereas in a model of hippocampal ischemia ERK inhibition reduced cytotoxicity (B. Murray et al., 1998).
- Phosphorylated ERK has been found in aggregates in the substantia nigra of Parkinson's disease (PD) patients, suggesting that ERK activation may be related to neuronal cell death mechanisms in PD (J. H. Zhu et al., 2002). In a PD cellular model, the neurotoxin 6-OHDA (6-hydroxydopamine) induced dopaminergic cell death through chronic ERK activation, and MEK blocking conferred protection against the pharmacological induced cytotoxicity (Kulich & Chu, 2001), suggesting that ERK activation was promoting cell death. Conversely, hydrogen peroxide-induced cell death, which also produces ERK activation, was not counteracted by MEK blockers, suggesting that the specific ERK-dependent mechanism of neuronal death was different depending on the toxic agent used (Kulich & Chu, 2001).
- Numerous studies have reported a relationship between increased ß-amyloid and ERK activity, proposing a link between ERK activation and AD. ß-amyloid peptides are found elevated in AD patients brain samples, being the principal component of amyloid plaques. ERK sustained activation was observed in acute and organotypic hippocampal slides from an AD mouse model (X. Zhu et al., 2002). Additionally, increased phosphor-ERK was also found in AD patients brain extracts (C. Russo et al., 2002).
- In SMA disease, ERK phosphorylation is increased in spinal cord and muscle tissue protein extracts from a severe SMA mouse model (Biondi et al., 2015; Branchu et al., 2013; T. L. Lin et al., 2016). Moreover, ERK pharmacological inhibition in vivo extended

mouse lifespan (Branchu et al., 2013), suggesting that ERK pathway plays an important role in the pathology progression.

Other Survival Signaling Pathways

The Nuclear Factor kappa B (NFkappaB) is a neuron survival pathway described to be deregulated in neurodegenerative diseases. NFkappaB pathway, which is altered in Duchenne muscular dystrophy (Branchu et al., 2013), is also involved in SMA pathogenesis. This pathway modulated cell survival in mice spinal cord motor neurons induced by neurotrophic factors and its inhibition caused SMN reduction in cultured SMA MNs (Arumugam et al., 2018; Mincheva et al., 2011). Interestingly, NFkappaB pathway is also related to the modulation of protein level of molecules forming the SMN complex, such as Gemin3 (Curmi & Cauchi, 2018; Shin et al., 2014; Shpargel & Matera, 2005).

Dysregulation of Ca^{2+} signaling in neurodegenerative diseases

Ca^{2+} has a crucial role in maintaining neuronal function. The involvement of defective Ca^{2+} signaling in neuronal diseases has been widely described in a vast collection of neuronal pathologies, including neurodegenerative processes such as ALS, HD, AD, PD, Ataxias, and migraine (reviewed in Brini et al., 2014). For instance, intracellular free Ca^{2+} could be increased in the neurons of patients who develop ALS (Choi, 1988; Regan & Choi, 1991).

In SMA pathogenesis, Ca^{2+} signaling alterations have been described. iPSC derived SMA astrocytes revealed disrupted Ca^{2+} signaling altogether with increased ERK phosphorylation (Mcgivern et al., 2013). SMN-reduced MNs are electrically hyperexcitable and exhibit enhanced Na^{+} channels activity (Arumugam et al., 2017; H. Liu et al., 2015; Mentis et al., 2011). Moreover, cultured embryonic MNs from a Spinal and Bulbar Muscular atrophy mouse model showed disturbances in ER-associated Ca^{2+} homeostasis and increased ER stress (Montague et al., 2014). On the other hand, abnormal amounts of Ca^{2+}-dependent asynchronous release was detected in *ex vivo* muscles of SMNdelta7 mutant mice, suggesting an alteration in Ca^{2+} concentration in SMA synapses (Ruiz et al., 2010). Interestingly, a Ca^{2+} dependent protease named calpain is overactivated in two SMA mouse models (de la Fuente et al., 2020). Furthermore, calpain inhibition showed increased SMN protein level, decreased LC3-II accumulation, and extended mice lifespan and motor functions (de la Fuente et al., 2018, 2020).

5.2. Autophagy in SMA and neurodegenerative diseases

The appearance of a diseased state associated with autophagy dysregulation can be a result of alterations in these process. Interestingly, post-mitotic/quiescent cells like MNs exhibit higher sensitivity to loss of autophagy competence (reviewed in (Klionsky, Petroni, et al., 2021)).

The ubiquitous deletion of core autophagy genes in various animal models emphasizes the importance of autophagy in neuronal viability (Klionsky, Petroni, et al., 2021). In the absence of autophagy, these models undergo from embryonic lethality to a neurodegenerative phenotype characterized by ubiquitylated protein aggregate accumulation, axonal swelling, and neuronal death (Hara et al., 2006; Komatsu et al., 2006). During aging the proteasome activity deteriorates and overloads the autophagy system (Dikic & Elazar, 2018), inducing accumulation of intraneuronal aggregates of misfolded proteins (Ravikumar et al., 2002). Furthermore, autophagosome accumulation has been observed in several neurodegenerative diseases, including AD, spongiform encephalopathies, PD and HD (reviewed in (Rubinsztein et al., 2007; Williams et al., 2006)). These observations suggest that autophagy dysregulation may play a crucial role in neurodegenerative disorders where an accumulation of misfolded proteins is a hallmark of the disease, such as ALS, PD, AD, and HD (**Figure 26**) (Menzies et al., 2015).

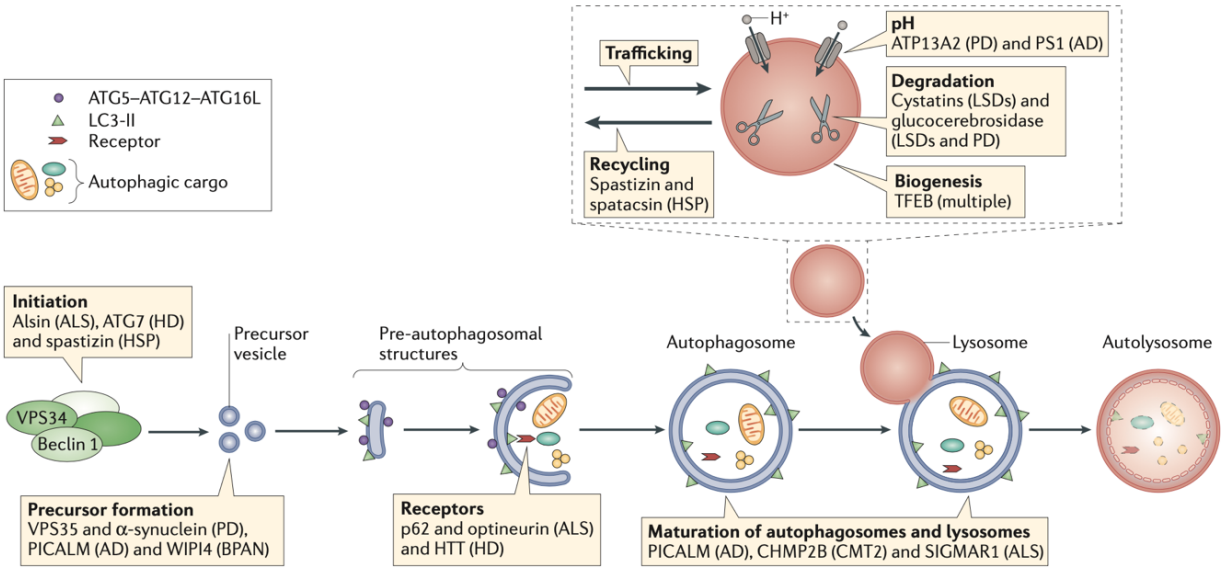

Figure 26 | Overview of the autophagy pathway and the sites of action of disease-associated proteins. Perturbations throughout the pathway, from initiation of autophagosome formation to degradation in the autolysosomes, have been suggested to be involved in neurodegenerative diseases. AD, Alzheimer disease; ALS, amyotrophic lateral sclerosis; ATG, autophagy protein; ATP13A2, ATPase type 13A2; BPAN, β-propeller protein-associated neurodegeneration; CHMP2B,

charged multivesicular body protein 2B; CMT2, Charcot–Marie–Tooth disease type 2; HD, Huntington disease; HSP, hereditary spastic paraplegia; HTT, huntingtin; LC3, microtubule-associated protein 1 light chain 3; LSD, lysosomal storage disease; PD, Parkinson disease; PICALM, phosphatidylinositol-binding clathrin assembly protein; PS1, presenilin 1; SIGMAR1, sigma non-opioid intracellular receptor 1; TFEB, transcription factor EB; WIPI4, WD repeat domain phosphoinositide-interacting protein 4 (Menzies et al., 2015) Reproduced with permission from Springer Nature.

In SMA pathogenesis, dysregulation of autophagy related proteins in SMA cells and mouse models has been described (Custer & Androphy, 2014; de la Fuente et al., 2018, 2020; Garcera et al., 2013; Periyakaruppiah et al., 2016; Piras et al., 2017; Rodriguez-Muela et al., 2018). Interestingly, SMN-reduced cells showed autophagic vesicles accumulation *in vitro* (**Figure 27**) (Custer & Androphy, 2014; Garcera et al., 2013; Periyakaruppiah et al., 2016). Moreover, these cultured SMA MNs exhibited increased neurite degeneration when compared to the control condition (de la Fuente Ruiz, 2020).

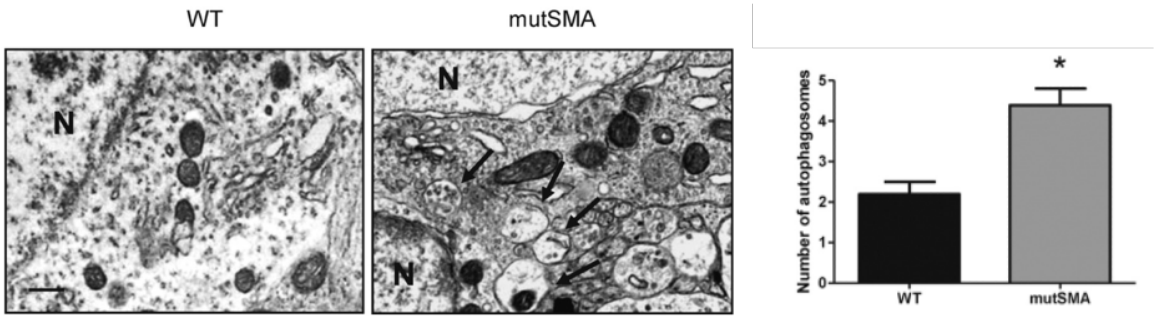

Figure 27 | Ultrastructural analysis of spinal cord MNs from postnatal SMA mice showing autophagosome and autolysosome accumulation compared to WT mice. The autophagosomes and autolysosomes were identified in MNs cytoplasm (arrows) (Periyakaruppiah et al., 2016). Reproduced with permission from Elsevier.

The autophagosome and autophagy markers accumulation observed in different SMA mouse models was counteracted by pharmacological inhibition of the process. On one hand, 3-MA administration reduced LC3-II autophagic marker levels, increased MN count and lifespan, and improved motor performances in SMA mice. Moreover, 3-MA administration also reduced apoptotic death observed in the lumbar spinal cord of SMA mice (Piras et al., 2017). On the other hand, calpain inhibition, a negative regulator of autophagy, reduced the levels of LC3-II protein in neurites *in vitro,* improved motor function and extended lifespan in two SMA mouse models (de la Fuente et al., 2020). Moreover, calpeptin treatment increased the levels of SMN protein and reduced its cleavage by calpain in mouse SMA MNs, suggesting that the treatment

not only produced a modulation on the autophagy process but also an upregulation of SMN protein level (de la Fuente et al., 2018, 2020).

Taken together, evidences indicate the important role of autophagy and its dysregulation in the pathogenesis of neurodegenerative diseases. However, the exact mechanism/s of autophagy alterations in SMA MNs and other tissues, and its regulation in this disease remain unclear. Moreover, the presence of autophagosomes in dying cells is not sufficient to distinguish cell death with autophagy from cell death produced by autophagy impairment.

5.3. Apoptosis in SMA and neurodegenerative diseases

Under pathological situations, apoptosis can take part in the loss of neurons associated with neurodegenerative diseases (reviewed in (Ghavami et al., 2014)).

In AD, toxic accumulation of ß-amyloid (Aß) is manifested with ROS generation, apoptosis induction and impaired memory (Lustbader et al., 2004). Extracellular Aß can cause mitochondrial dysfunction; *in vivo* and *in vitro* experiments showed that soluble Aß decreased cytochrome oxidase activity and increased hydrogen peroxide generation (Manczak et al., 2006). In an AD cellular model, Aß accumulation in mitochondria induced cytochrome c release and neuronal death (Cha et al., 2012). Furthermore, Aß peptide induced caspase-3-dependent apoptosis in primary culture of astrocytes due to APP (amyloid precursor protein) aggregation in mitochondria (Bartley et al., 2012).

In PD, aggregation of alpha-synuclein (α-syn) in Lewy bodies is a hallmark of the disease. α-syn can downregulate the expression of an oxidative stress-sensitive kinase that suppresses dopaminergic cell death (Jin et al., 2011). On the other hand, LRRK2 (Leucine Rich Repeat Kinase 2) protein, which is highly expressed in dopamine-innervated areas of post-mortem PD and control brains, was found to interact with FADD in a cellular study, triggering caspase-8 activation and extrinsic apoptotic cell death (Ratovitski et al., 2007).

Mutations in the Htt protein are a hallmark of HD and evidences support de role of apoptosis in the neurodegeneration that is produced in HD. For instance, caspase-6 proteolytically cleaves Htt (Y. J. Kim et al., 2001), generating toxic Htt fragments (Ratovitski et al., 2007). Furthermore, the activation of caspase-6 has been observed to occur before onset of mobility abnormalities in human and murine HD brains (Milnerwood et al., 2010).

In ALS, MNs from the SOD1 G93A mouse model revealed activation and nuclear translocation of the transcription factor AIF (Apoptosis Inhibitor Factor), which promotes chromatin condensation, DNA fragmentation and caspase-independent apoptosis (Daugas et al., 2000). Other evidences suggest that ER stress observed in ALS can activate the mitochondrial apoptotic pathway provoking the release of cytochrome c (Heath-Engel et al., 2008).

Furthermore, dysregulation of the X-linked IAP has also been described in some neurologic disorders such as AD (Christie et al., 2007), HD (Goffredo et al., 2005), ALS (Guégan et al., 2001), and even in axotomy (Kügler et al., 2000). Additionally, FAIM-L reduction is associated with AD progression (Carriba et al., 2015). Together, these observations suggest common alterations in diverse neurodegenerative pathologies. Hence, these proteins could become targets for developing novel therapies for neurodegenerative diseases.

In SMA, several alterations in apoptotic proteins have been described:

- In the Drosophila S2 cell line (Ilangovan et al., 2003) and in NSC34 cells (Parker et al., 2008), SMN deficiency activated caspase-dependent apoptosis.
- An in vitro model of human differentiated SMA MNs showed an increase in Fas ligand-mediated apoptosis and cleaved caspase-8 and caspase-3 (Sareen et al., 2012). Importantly, treatment with a caspase-3 inhibitor rescued SMA MN population (Sareen et al., 2012).

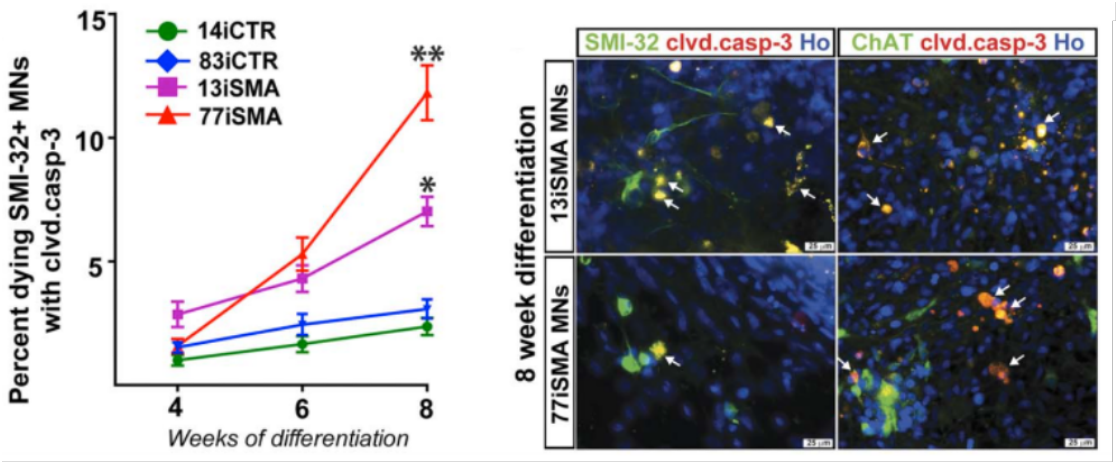

Figure 28 | Detection of apoptosis in SMA-iPSC MN cultures. Sareen and colleagues demonstrated an increase of cleaved in SMA-iPSC lines compared to control iPSC lines over time. Percent dying Caspase-3/SMI-32+ MNs over time (left), and cleaved caspase-3/ChAT/SMI-32 positive SMA-IPSCs at 8 weeks of differentiation. Adapted from (Sareen et al., 2012) with permission from Elsevier.

- Phosphorylated p53 at S18 was increased in L1 and L5 vulnerable (Fast Twitch Fatigable) MNs from the medial motor column of SMNΔ7 mice, and its pharmacological or genetic inhibition prevented MN death (Simon et al., 2017). p53 is a tumor suppressor protein controlling many biological processes, including autophagy, apoptosis, cell cycle arrest, senescence, and DNA repair among others (Hernández Borrero & El-Deiry, 2021).
- Activation of the JNK pathway was described in SMNΔ7 mice and in SMA patients (Genabai et al., 2015). This pathway is linked to a pro-apoptotic role. Its pharmacological inhibition ameliorated morphological features, motor performances and lifespan of SMA mice (Schellino et al., 2018).
- Bcl-2 and Bcl-XL proteins are reduced in MNs of SMA fetuses, suggesting enhanced apoptosis and cell death in early development (Soler-Botija et al., 2003). The Bcl-2 regulating protein WT-1 is expressed at lower amounts in a SMA mouse model (Anderson et al., 2003). Interestingly, Bcl-XL overexpression ameliorated motor functions and life expectancy in a SMA mouse model (L. K. Tsai et al., 2008), and rescued neurite degeneration and cell death in cultured mouse MNs (Garcera et al., 2011).
- Administration of the neuroprotective drug loganin decreased apoptotic cell number and neurite damage in a SMA cell model and stimulated SMN, Gemin2, Akt and Bcl-2 expression (Tseng et al., 2016).

HYPOTHESIS AND OBJECTIVES

HYPOTHESIS

Systemic SMN decrease results in the alteration of tissues and cells among which spinal cord MNs are the cellular type with greatest dysregulations in SMA disease. SMN protein is implicated in multiple house-keeping functions in MNs, including snRNP biogenesis, pre-mRNA splicing, ribosome regulation, and mRNA transport along the axon. Therefore, SMN reduction in these cells may compromise their integrity. In addition to SMN decrease, alterations in survival signaling pathways, autophagy, and apoptosis may contribute to degeneration in SMA tissues and cells. Current SMA therapies are focused on systemically increasing SMN level. Besides, SMN-independent approaches are being designed for combined therapies. Understanding the cellular and molecular mechanisms underlying SMN-reduced MN degeneration, may contribute to develop these new strategies. Here we hypothesize that SMA MNs exhibit alterations in survival signaling pathways, autophagy, and apoptosis processes, and these modifications could provide new targets for SMN-independent drug development.

OBJECTIVES

1. Study of the apoptosis markers FAIM-L, XIAP and cleaved-caspase 3 in mouse and human SMA MNs.
2. Analyze the PI3K/Akt and ERK MAPK survival signaling pathways in SMA cells and their involvement in SMN protein regulation.
3. Analysis of the autophagy process in mouse and human SMA muscle, fibroblasts and MNs.
4. Investigate the implication of ERK MAPK survival signaling pathway in contributing to altered autophagy in SMA MNs.

MATERIALS AND METHODS

1. MOUSE MODELS

CD1 mice and two severe SMA transgenic mouse models were used; the FVB-Cg-Tg (SMN2)^{89Ahmb}Smn1^{tm1Msd}/J and the FVB.Cg-*Grm*$^{Tg(SMN2)89Ahmb}$Smn1^{tm1Msd}Tg(SMN2*delta7) 4299Ahmb/J (*Smn*$^{-/-}$; *SMN2*$^{+/+}$ *SMN*Δ*7*$^{+/+}$). Heterozygous females and males of each mouse strain were crossed to obtain *Smn*$^{-/-}$; *SMN2*$^{+/+}$ (hereafter referred to as mutSMA) or *Smn*$^{-/-}$; *SMN2*$^{+/+}$ *SMN*Δ*7*$^{+/+}$ (hereafter referred to as SMNdelta7). Homozygous mice for the *Smn* gene, *Smn*$^{+/+}$; *SMN2*$^{+/+}$ or *Smn*$^{+/+}$; *SMN2*$^{+/+}$ *SMN*Δ*7*$^{+/+}$ were used as controls (hereafter referred to as WT).

The animals were held in the animal house of the University of Lleida, where all conditions were maintained in accordance to the European Directive Committee Council and the rules established by the Animal Care guidelines of the Generalitat de Catalunya ([DOGC] 2073, 1995). Mice were housed in propylene cages (33 cm x 18 cm x 14 cm) at a constant room temperature of 22±2 ºC, relative humidity of 40%±10% and on a 12/12h light/dark cycle. They were provided ad libitum water and rodent chow (nº 2018, Envigo). All procedures were done in accordance with the Spanish Council on Animal Care guidelines and approved by the University of Lleida Advisory Committee on Animal Services (CEEA02- 01/17).

1.1. CD1 MOUSE MODEL

CD1 mouse line is the most common non-consanguineous mouse in the world, used widely in toxicology, ageing and cancer experiments, transgenic creation and as a surgical model (Chia et al., 2005; Rice and O'Brien, 1980). It was first produced by Charles River Laboratories in 1959, derived from the Lynch's Swiss mice.

In the present work, the CD1 mouse model was used to obtain MNs from embryo's spinal cords due to the large number of pups per pregnancy (≈11.5 animals per litter). The cells obtained were used to analyze the regulation of several molecules related to the pathophysiology of SMA in non-SMA MNs.

1.2. SMA TRANSGENIC MOUSE MODELS

1.2.1. Smn $^{-/-}$; SMN2$^{+/+}$ or SMA

The SMA (The Jackson Laboratory, Sacramento, USA, stock 005024) mouse model is a SMA transgenic mouse obtained through the crossing of a *Smn* knockout mouse (generated by disrupting the exon 2 from the *Smn* gene with a neomycin cassette, in Dr Michael Sendtner laboratory, University of Wurzburg), and a *SMN2* transgenic mouse (created by integrating a genomic fragment with human *SMN2* promoter and gene into the intron 4 of the *Grm7* gene, in Dr Arthur Burghes laboratory, Ohio State University).

Heterozygous animals were crossed for the obtention of WT (*Smn*$^{+/+}$; *SMN2*$^{+/+}$) and mutSMA mice (*Smn*$^{-/-}$; *SMN2*$^{+/+}$), which were used for the experiments. mutSMA mice are homozygous for the mutant *Smn* allele and carriers of the *SMN2* transgene. They are smaller than WT or Heterozygous littermates and die between 4 and 6 days after birth. From postnatal day 2 (P2) they display physical and neurological abnormalities such as decreased movement and lactation, breathing difficulties and limb quaking. At histological level, postnatal day 5 (P5) mutSMA mice exhibit a loss of the 35% of the lower MNs from the spinal cord, atrophy of the quadriceps and gastrocnemius muscles and nearly absent intranuclear aggregates of the Smn protein ('gems') (Monani, Coovert, et al., 2000; Schrank et al., 1997).

Figure 29 | Image of a mutSMA mouse (*Smn*$^{-/-}$; *SMN2*$^{+/+}$) (left) and a WT littermate (*Smn*$^{+/+}$; *SMN2*$^{+/+}$) (right) at postnatal day 4 (P4).

1.2.2. Smn$^{-/-}$; SMN2$^{+/+}$ SMNΔ7$^{+/+}$ or SMNΔ7

The SMNΔ7 (The Jackson Laboratory, Sacramento, USA, stock 005025) is a SMA transgenic mouse model obtained through the crossing of a Δ7*SMN2* transgenic mouse (created by integrating a genomic fragment with human *SMN2* promoter and a fragment of *SMN2* gene lacking the exon 7, in Dr Arthur Burghes laboratory, Ohio State University), and heterozygous animals of the aforementioned SMA model (*Smn*$^{+/-}$; *SMN2*$^{+/+}$), resulting in a triple mutant mouse model which carries two transgenic alleles and a single targeted mutant (*Smn*$^{+/+}$; *SMN2*$^{+/+}$; *SMNΔ7*$^{+/+}$).

Heterozygous animals (*Smn*$^{+/-}$; *SMN2*$^{+/+}$; *SMNΔ7*$^{+/+}$) were crossed for the obtention of WT (*Smn*$^{+/+}$; *SMN2*$^{+/+}$; *SMNΔ7*$^{+/+}$) and SMNdelta7 (*Smn*$^{-/-}$; *SMN2*$^{+/+}$; *SMNΔ7*$^{+/+}$) mice, which were used for the experiments. SMNdelta7 mice are homozygous for the mutant *Smn* allele, carriers of the *SMN2* and the *SMN2Δ7* transgenes. The SMNdelta7 pups originally reported survival is ≈13 days (Le et al., 2005), and they present symptomatology starting at P5, exhibiting progressive muscle weakness and atrophy, resulting in abnormal walk, hind limb shakiness and falling over tendency.

Figure 30 | Image of two SMNdelta7 mice (*Smn*$^{-/-}$; *SMN2*$^{+/+}$; *SMNΔ7*$^{+/+}$) (right) and a WT littermate (*Smn*$^{+/+}$; *SMN2*$^{+/+}$; *SMNΔ7*$^{+/+}$) (left) at postnatal day 10 (P10).

1.3. GENOTYPING SMA MICE

1.3.1. DNA extraction

A piece of the tail from E13 embryos or neonatal offspring was collected for genotyping, and the REDExtract-N-Amp Tissue PCR Kit (Sigma) was used for genomic DNA extraction following manufacturers protocol:

1. Place each sample in separate 1.5 mL polypropylene tubes.
2. Prepare the Extract Solution Mix and vortex gently; for one sample, 75% (v/v) of Extract solution 25% (v/v) plus of Tissue Prep solution.
3. Add 50 μL of Extract Solution Mix to each sample and incubate 10 min at room temperature (RT).
4. Heat the samples up to 95 ºC for 3 min.
5. Add 50 μL of Neutralization Buffer to each sample and mix or vortex them.
6. Centrifuge samples at maximum speed for 10 min and collect the supernatant in a new tube. The DNA extract can be immediately used for PCR analysis or stored at 4 ºC up to 6 months.

1.3.2. Genotyping PCR mutSMA and SMNdelta7 mice

Both SMA mouse models were genotyped by using the same primers, designed by The Jackson Laboratory and ordered at Sigma (**Table 6**).

Table 6 | Primers sequences for SMA mice genotyping.

Primer's Name	Sequence
WT Forward	5'- CTCCGGGATATTGGGATTG-3'
WT Reverse	5'- TTTCTTCTGGCTGTGCCTTT-3'
SMA Reverse (Neomycin R Cassette)	5'- GGTAACGCCAGGGTTTTCC-3'

To amplify genomic DNA, the Phire Tissue Direct PCR Master Mix (Thermo Fisher) was used by following the manufacturers' instructions (**Table 7**). The 2X Phire Tissue Direct PCR Master Mix contains a the dNTPs, $MgCl_2$ and the Phire Hot Start II DNA Polymerase. Besides, it contains a dye that doesn't interfere with PCR performance, allowing direct sample loading on the gel.

Table 7 | Components and volumes for the PCR mix preparation.

Components	15 µL rxn	Final Concentration
H_2O miliQ	Add to 14µL	-
2X Phire Tissue Direct PCR Master Mix	7.5µL	1X
WT Forward (25 µM)	0.3µL	0.5µM
WT Reverse (25 µM)	0.3µL	0.5µM
SMA Reverse (25 µM)	0.3µL	0.5µM
Sample	1µL (1.5-15ng)	0.1-1ng/µL

The PCR cycling parameters are described in the following table:

Table 8 | Cycling parameters for the PCR reaction.

Step	Temperature	Time	Cycle
Initial Denaturation	98ºC	5′	X1
Denaturation	98ºC	5″	X30
Annealing	60ºC	5″	
Extension	72ºC	50″	
Final Extension	72ºC	1′	
Final Hold	4ºC	Infinite hold	

1.3.3. DNA electrophoresis

An agarose gel matrix was prepared diluting 1% of agarose (Sigma) in TAE1X Buffer pH8 (200mM Tris-HCl, 190µM Acetate and 10mM EDTA diluted in miliQ water). SYBR Safe dye (1:10000, Fisher) was added into the gel to stain the amplified DNA.

1. Electrophoresis was run at 90 to 100 V during 40 min.
2. After the electrophoresis, the gel was developed using an ultraviolet tray support on a Gel Doc™ EZ Imager (Bio-Rad).
3. As a result, an amplification of one or two bands was obtained, corresponding to different genotypes (**Figure 31**):
    a. An amplification of 800 kb DNA product corresponding to the endogenous mouse *Smn* gene (WT,+/+).

b. An amplification of 500 kb DNA product corresponding to the neomycin resistance cassette present in the mutSMA and SMNdelta7 mice (mutant, -/-).
c. An amplification of both 500 kb and 800 kb DNA products, indicating the presence of both the *Smn* gene and the cassette gene, corresponding to heterozygous (Ht) samples (+/-).

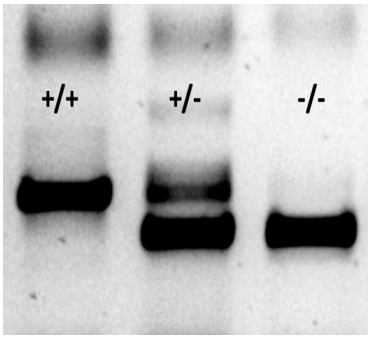

Figure 31 | Representative image of genotype verification for SMA mice. Genotypes obtained, from left to right correspond to WT (+/+), Ht (+/-) and mutSMA or SMNdelta7 (-/-) samples. The upper band corresponds to the 800 kb DNA product (*Smn)* while the lower band corresponds to the 500 kb DNA product (neomycin cassette).

2. MOUSE MN PRIMARY CELL CULTURE

Spinal cord MNs were obtained from day 13 (E13) mouse embryos (either CD1 or SMA transgenic mice) because at E12.5 – E13 developmental stage, MNs are already formed, larger and less dense than the remaining cells of the spinal cord. Embryos were extracted at 13 days after the fecundation (E13). The stage can be identified by looking at the interdigital membranes of anterior and posterior legs, which are still present at E13. These features allow an easier isolation and purification (Arce et al., 1999; Wiese et al., 2010). The technique used for MN isolation was a two-step centrifugation method with density gradients, obtaining a MN culture purity of 97%.

2.1. Polyornithine (P/O)-Laminin plate coating

Culture dishes were pre-coated with a combination of poly-L-ornithine (a positively charged synthetic amino acid chain) with laminin, to promote and enhance cell attachment and adhesion.

1. A 35μg/mL solution of poly-L-ornithine (stock solution of 10mg/mL)(Sigma, Ref. 27378-49-0) was prepared in Boric-Borate solution (**see Table 9**).
2. Tissue culture plates were covered with the polyornithine solution under the hood and incubated for 2 to 4h (alternatively overnight) at room temperature.
    - For cell immunofluorescence, 15mm glass coverslips were placed in M4 plates and the polyornithine solution was placed as a small drop (80μL) onto the glass surface.
3. Plates were then rinsed 3 times with sterile miliQ water and air-dried at room temperature for 10-15 min under the hood. Plates can be stored at 4ºC for 2 weeks or used immediately.
4. After polyornithine coating, plates were treated with Laminin (Sigma, Stock solution 1mg/mL, Ref. L2020) diluted in L-15 medium at a final concentration of 3.5μg/mL.
5. Plates' wells were covered with laminin and incubated at 37ºC for a minimum of 2h into a CO_2 incubator. Laminin-coated plates can be stored in the incubator up to one week.
6. Laminin solution was removed immediately before plating.

2.2. Solutions and culture medium

All the media and solutions used for cell cultures were sterilized under the hood using 0.22μm filters.

Table 9 | Primary cell culture media and solutions.

Media and Solutions	Components
Boric-Borate Solution (pH 8.3 adjusted with HCl)	150mM Sodium Tetraborate (Sigma, Ref. 221732), 150mM Boric Acid (Sigma, Ref. B1934) diluted in miliQ water
GHEBS Solution (pH 7.4 adjusted with NaOH)	173mM NaCl, 2.6mM KCl, 25mM Glucose (Sigma, Ref. G7021), 25mM HEPES (Gibco, Ref. 15630056), 20μg/mL Penicillin-Streptomycin (P/S) (Ref.15140-122, Gibco).
Leibovitz's L-15 Medium Complete (L-15 Complete Medium)	Leibovitz's L-15 Medium (L-15 Medium) (Gibco, Life Technologies, Ref. 11415-049) supplemented with Horse Serum (HS) (2% v/v, Ref.16050-122), N2 (1% v/v, Ref. A13707) (Gibco), 20mM Glucose (Sigma) and 0.1mg/mL P/S
Neurobasal Medium Complete (NBM Complete Medium)	Neurobasal Medium (Gibco, Life Technologies, Ref. 21108-049) supplemented with B27 (2% v/v, Ref. 11530536), HS (2% v/v), 125mM L-Glutamine (Gibco, Ref. 25030) and 25mM 2-mercaptoetanol (Sigma, Ref.M7522)
NBM Complete + Neurotrophic Factors' Cocktail (NTFs Medium)	NBM Complete Medium supplemented with a cocktail of Neurotrophic Factors (NTFs); GDNF (Ref.#450-44), HGF (Ref.#100-39) and CT-1 (Ref.#250-25), all at 10ng/mL (Peprotech) and BDNF (Bio-nova, Ref.450-02) at 1ng/mL
NTFs Medium + Aphidicolin	NTFs Medium supplemented with 2μg/mL aphidicolin (Sigma, Ref. A0781)
Bovine Serum Albumin (BSA) 4%	BSA 7.5% (Sigma, Ref. A8412) diluted in L-15 Medium

2.3. Spinal Cord dissection

First, an adult-pregnant female was sacrificed at 12.5-13 days of gestation by cervical dislocation and the next protocol was followed:

1. Under the dissection microscope, embryos were removed from the uterus and transferred to a Petri dish with GHEBS solution at room temperature.

2. Embryos' heads and tails' were snipped to facilitate manipulation and fixed upside-down with small needles on a plate (base covered with Sylgard™ (Dow Corning) mixed with activated carbon) filled with GHEBS solution.
3. Spinal cords were dissected by opening the dorsal part of the embryo with a longitudinal cut in the middle of the spinal cord area.
4. The dorsal horns of the spinal cord were removed and discarded and the ventral part of the spinal cord was carefully separated from the rest of the embryo's body.

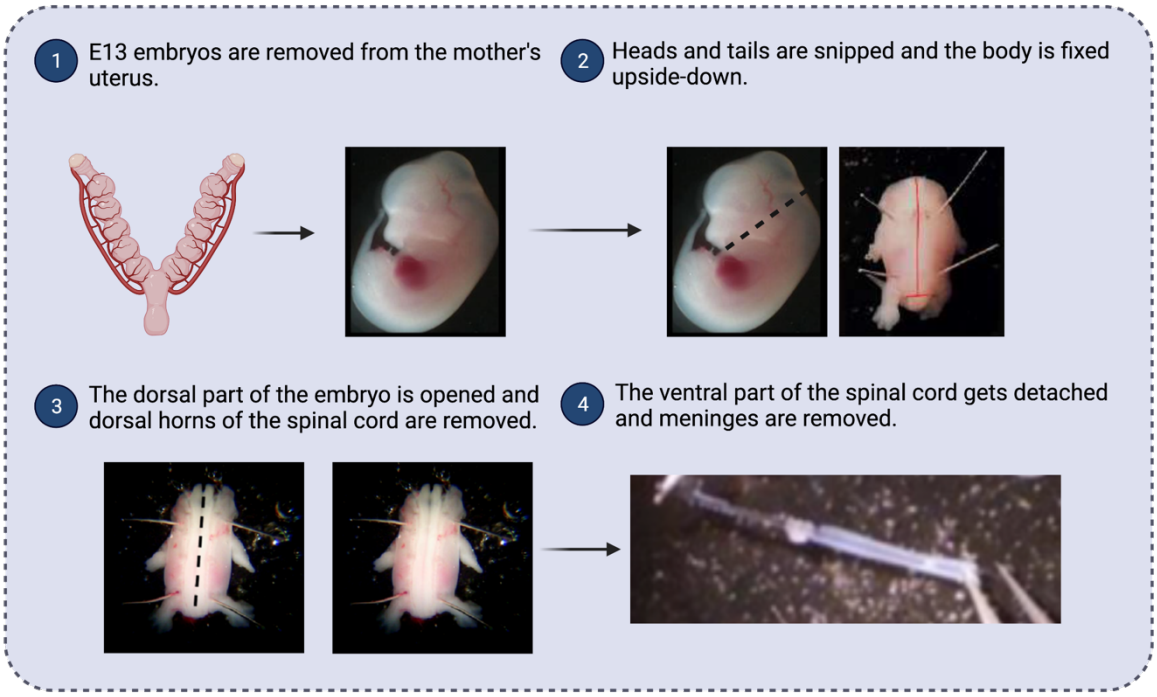

Figure 32 | Representative infographic of the dissection of mouse embryos spinal cord. Based on (de la Fuente Ruiz, 2020). Created with BioRender.com.

The meninges were removed to prevent the presence of other cellular types and the spinal cord was fragmented into 4-5 pieces.

5. Four to five fragmented spinal cords were transferred to polypropylene conic tubes (Fisher, Ref. 11755075) filled with GHEBS solution.

2.4. Mouse MN isolation

The purification process was done under the hood and started with an enzymatic and mechanical dissociation, ending with MNs isolation by a density gradient. The process was done as follows:

1. Once the spinal cord dissection was finished, the pooled fragments were washed 2-3 times with GHEBS solution.
2. Then, they were incubated in 0.025% Trypsin (Sigma, Ref. T4424) diluted in GHEBS solution during 8-10 min at 37ºC. Tubes were gently shacked frequently.
3. Trypsin solution was removed and the spinal cord fragments were transferred into a solution with 88% (v/v) L-15 and 11% (v/v) 4% BSA. Immediately after, tubes were manually shaked during 2 min.
4. Spinal cords where then four times mechanically dissociated in L-15 with 4% BSA solution containing 0.14mg/mL DNase (Ref. 10104159001, Sigma) using a Blue Tip (DdBiolab, Dutcher, Ref. 0351056).
5. The fragments were incubated for 2 min and were let to precipitate. The supernatant containing isolated cells was then collected in a conic polypropylene tube.
6. Spinal cords were subjected to a second mechanical dissociation with the L-15 with 4% BSA solution containing 0.1mg/mL DNase. Tissue fragments were passed through a Blue Tip 9 times and incubated during 2 min.
7. Supernatants with dissociated cells were collected into the conic polypropylene tubes and the remaining tissue was discarded.
8. A 4% BSA solution was slowly added to the tubes containing the dissociated cells, creating a two-phase gradient, which was then centrifuged during 5 min at 1000 rpm (**Figure 33**). Acceleration and deacceleration was adjusted to the minimum. The obtained pellet was resuspended in 1mL of L-15 complete medium.

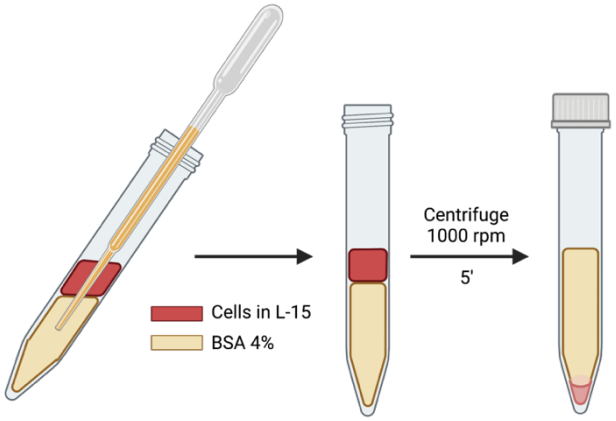

Figure 33 | Graphic representation of the centrifugation step of cells in a 4% BSA gradient. Created with BioRender.com.

9. Cells were subjected to a density gradient to achieve MN isolation by using a freshly prepared 12.5% OptiPrep™ solution (Axis-Shield) diluted in GHEBS solution in a polystyrene round-flat bottom tube (DdBiolab, Ref. 80192).

a. OptiPrep™ was gently mixed with GHEBS solution, added into the tubes and then resuspended cells were slowly added on top, creating two differentiated phases.
b. The mixture was centrifuged during 10 min at 1650rpm without acceleration and deacceleration.

10. After the centrifugation, a pale white band was obtained between the OptiPrep™ and the L-15 complete medium, corresponding to the isolated MNs. Five hundred µL of this pale white band was collected into a polypropylene conic tube (**Figure 34**).

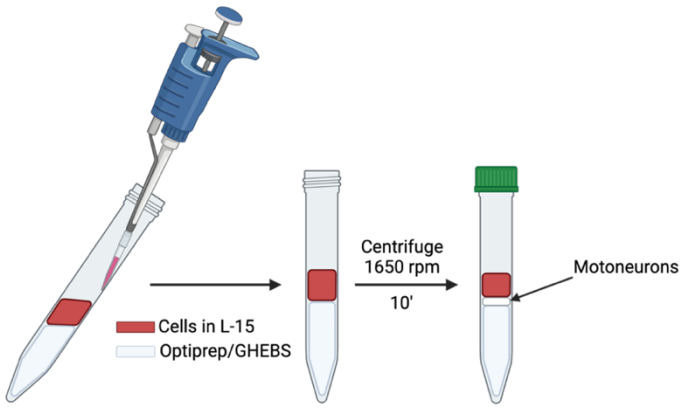

Figure 34 | Graphic representation of the Optiprep™ gradient centrifugation step. Created with BioRender.com.

2.5. Plating and cell culture

Isolated MNs were counted for posterior plating onto laminin-coated plates:

1. Four well tissue culture dishes (Nunc, Thermo Fisher Scientific, Madrid, Spain) were used for survival experiments (8000 cells/cm^2), neurite degeneration evaluation (5000 cells/cm^2), and western blot analysis (26000 cells/cm^2).
2. Four well tissue culture dishes with 15mm glass coverslips were used for immunofluorescence (7000 cells/cm^2).
3. Six well tissue culture dishes (Falcon) were used for total mRNA extraction and qRT-PCR experiments (50000 cells/cm^2).

Cells were directly plated in NTFs medium and kept for up to 12-15 days in a CO_2 incubator. To avoid the potential growth of non-neuronal cells in the culture, aphidicolin (2µg/mL) (Sigma, Ref. A0781) was added to the culture medium 24h after plating.

Six to twelve days after plating cells expressed MN markers such as Islet 1/2, ßIII- tubulin, Hb9 (Homeobox transcription factor B9), and ChAT (Choline Acetyltransferase), as seen in **Figure 35**.

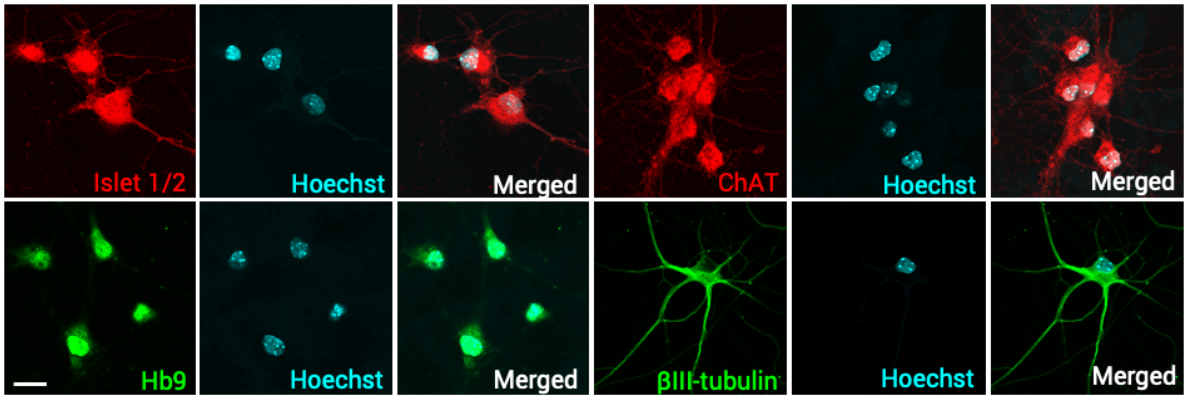

Figure 35 | Immunofluorescence of MN markers in mouse isolated MNs. Isolated MNs were fixed after 6 days *in vitro* and immunofluorescence was performed using different specific MN markers to demonstrate the efficacy of the isolation process. Top photos: Islet 1/2 and ChAT (red). Bottom photos: Hb9 and ßIII-tubulin (green). Scale bar, 15μm.

3. HUMAN FIBROBLAST CELL LINES

Three human fibroblast cell lines from two SMA patients and a healthy Control patient (**Table 10**) were purchased from Coriell Institute for Medical Research (Camden, NJ, USA). All cell lines are untransformed.

Table 10 | Fibroblast cell lines used.

Patient's code	Condition	SMN Copy Number	Age	Sex	Name
GM03814	non-SMA	SMN1: 1 SMN2: 5	No data	Female	Control
GM03813	SMA II	SMN1: 0 SMN2: 3	3 years old	Male	SMAII
GM09677	SMA I	SMN1: 0 SMN2: 3	2 years old	Male	SMAI

GM03814 cells were obtained from a skin biopsy of an American Caucasian female clinically unaffected, and mother of two clinically affected children; 1st child is GM03813 whereas the 2nd child was not in the repository. Copy number analysis revealed that the donor subject was heterozygous for deletion of exons 7 and 8 in de *SMN1* gene and had 5 copies of *SMN2* gene.

GM03813 cells were obtained from a skin biopsy of a 3-year-old American Caucasian male clinically affected with SMA, and son of the GM03814 subject. Clinical affectations described were; rolling over at 6 months, babbling at 9 months and marked muscle atrophy and weakness

by 12 months old. The subject also presented absence of deep tendon reflexes and constipation. Copy number analysis revealed an homozygous deletion of exon 7 and 8 in the *SMN1* gene and 3 copies of the *SMN2* gene. He was first classified as a type I SMA but was lately re-classified as a type II SMA due to onset symptoms and *SMN2* dosage.

GM09677 cells were obtained from an eye lens biopsy of a 2-year-old Polish/German Caucasian male clinically affected with SMA. Donor showed hypotonia, decreased muscle bulk, absence of deep tendon reflexes, possible fasciculations and abnormal electromyography. He expired at 23 months old. Copy number analysis revealed an homozygous deletion of exons 7 and 8 of de *SMN1* gene and 3 copies of the *SMN2* gene. He was categorized as type I SMA, as muscle biopsy was consistent with the diagnosis. No previous cases in the family were reported.

3.1. Thawing and maintenance

1. Cryopreserved cell vials were thawed during <5 min into a water bath at 37ºC and rapidly collected in a 15mL conical bottom centrifuge tube with 5mL of previously added Fibroblast Growth Medium.
2. After 3 min of centrifugation at 1000rpm, cells were resuspended in Fibroblast Growth Medium and cultured in p60 culture dishes for western blot analysis or onto collagen-coated glass coverslips for immunofluorescence technique.
3. Medium was changed every 2 days until the culture reached 80-90% confluence, where cells were either collected for western blot or fixed for immunofluorescence analysis:
    - Western Blot: Cells were washed once with 5mL of Hanks' Balanced Salt Solution (Sigma) and detached using 0.25% (v/v) of Trypsin-EDTA (Sigma) for 3-4 min at 37ºC. DMEM-FBS (10%) was added to block the trypsin reaction (5mL per each 1mL of Trypsin-EDTA). After 3 min of centrifugation at 1000rpm, cells were resuspended in 1mL of Fibroblast Growth Medium and plated at 1:3 or 1:4 dilution.
    - Immunofluorescence: Cells were fixed with 4% paraformaldehyde (PFA) for 10 min (8% PFA was added in a 1:1 ratio directly to the existing volume of culture medium). Following 3 washes with PBS1X, a second fixation with cold methanol (-20ºC) was performed for 10 min. Three final washes with PBS1x were done and cells were kept in PBS1X. For LC3 marker evaluation, the step with PFA was avoided.

3.2. Freezing

Cells were detached from confluent p60 plates and after 3 min centrifugation at 1000 rpm, they were resuspended in 1mL of the Fibroblast Freezing Medium (**Table 11**) and added into a cryogenic vial (Corning, 2mL tube). Cells were stored in a thermo flask at -80ºC for 24-48h and moved into a liquid nitrogen tank to provide a slow freezing process.

Table 11 | Media used for fibroblast maintenance and freezing.

Fibroblast Media	Components
Fibroblast Growth Medium	Minimum Essential Medium Eagle (MEM) (Sigma, Life Science, Ref. M2279) supplemented with 15% (v/v) non-inactivated FBS, 0.5M of L-Glutamine, 1% Non-Essential Amino acids (NEAA)(Ref. 11350912) (v/v) and 20μg/mL of P/S (all from Gibco, Invitrogen)
Fibroblast Freezing Medium	Fibroblast Growth Medium 95% (v/v) supplemented with 5% DMSO (v/v) (Sigma, Ref. D2650)

4. HUMAN INDUCED PLURIPOTENT STEM CELLS (iPSCs)

In the laboratory we have developed the differentiation of human MNs from induced Pluripotent Stem Cells (hiPSCs), purchased from Coriell Institute for Medical Research. The protocol followed was based on (Du et al., 2015) with few modifications. We used the GM23411*B iPSC cell line as a control (**Control**) and the GM23240*B iPSC cell line (**SMA**), derived from an SMA Type 2 patient (**Table 12**).

Table 12 | List of iPS cell lines used.

Cell line	Information
GM23411*B or Control	Cell line derived from the untransformed human fibroblast cell line GM00041. Biopsy obtained from a 3-month-old Puerto Rican female apparently healthy. Cell line was reprogrammed into iPSC using retroviral vectors with OCT4, SOX2, KLF4, CMYC, NANOG and LYN28.
GM23240*B or SMA	Cell line derived from the untransformed human fibroblast cell line GM03813 (**see Table 10**); donor was a type II SMA patient. Cell line was reprogrammed using lentiviral vectors with OCT4, SOX2, NANOG and LIN28.

4.1. Cell culture media and solutions

Table 13 | Media used for iPSC maintenance and freezing.

Stem Cell Media	Components
hES medium	KnockOut Dulbeco's Modified Eagle Medium (KO DMEM) (Ref. 10829018) supplemented with KO Serum Replacement (Ref. A31815-02) (20% v/v) (both from Gibco, Life Technologies), 2-mercaptoetanol (0.1mM)(Sigma), L-glutamine (0.1mM)(Gibco), basic Fibroblast Growth Factor (bFGF)(6 ng/mL)(Peprotech) and NEAA (Gibco)
MEF-conditioned hES medium	hES medium supplemented with additional 4ng/mL of bFGF
Essential 8 medium	Essential 8^{TM} Basal Medium DMEM/F12 (Ref. A15169-01, Gibco)
Freezing Medium	90% of Knock Out Serum Replacement supplemented with 10% DMSO

Table 14 | Media and supplements used for the differentiation of the iPSCs to mature MNs.

Differentiation media	NEPI	MNP1	MNP2	MN Induction	MN Maturation
Neurobasal Plus Gibco, A3582901	1mM	1mM	1mM	1mM	1mM
DMEM/F12 Gibco, 3133038	1mM	1mM	1mM	1mM	1mM
B27 Plus Gibco, A3583601	0.2mM	0.2mM	0.2mM	0.2mM	0.2mM
Ascorbic Acid Sigma, A4403	0.1mM	0.1mM	0.1mM	0.1mM	0.1mM
L- Glutamine Fisher, 25030024	1mM	1mM	1mM	1mM	1mM
NEEA Fisher, 11140050	1mM	1mM	1mM	-	-
CHIR99021 Cayman, 13122	3μM	1μM	3μM	3μM	-
SB43 Cayman, 13031	2μM	2μM	2μM	2μM	-
DMH1 Cayman, 16679	2μM	2μM	2μM	2μM	-
Retinoic Acid Sigma, R2625	-	0.1μM	0.1μM	0.5μM	0.5μM
Purmorphamine Cayman, 10009634	-	0.5μM	0.5μM	0.1μM	0.1μM
Valproic Acid Sigma, P4543	-	0.5μM	0.5μM	-	-
Compound E Cayman, 15579	-	-	-	-	0.1μM
CNTF Peprotech, 450-50	-	-	-	-	20ng/mL
IGF-1 Fisher, 11682069	-	-	-	-	20ng/mL
Y-27632 Stem Cell Technologies, 72302	10μM	10μM	10μM	10μM	10μM

4.2. Human iPSC thawing, maintenance and cryopreservation

1. Cryopreserved cell vials were thawed during <5 min into a water bath at 37ºC and rapidly collected in a 15mL conical bottom centrifuge tube with 9mL of previously added hiPSC Medium (SMA) or Essential 8 medium (Control).
2. After 3 min of centrifugation at 1100rpm (6500g), cells were resuspended in hiPSC medium (SMA) or Essential 8 medium (Control) and cultured in M6 culture plates; on a layer of irradiated mouse embryonic fibroblasts (Gibco) for SMA cell line, and on Geltrex^{TM} coated M6 culture plates for Control cell line. 10μM of Y-27632 (Cayman) was added to provide cell adhesion and survival to the plates.
3. Forty eight h after plating, the Y-27632 inhibitor was removed and fresh medium was added. Medium was changed every day until large colonies of undifferentiated cells were observed, when cells were sub-cultured or frozen.
4. Cells were subcultured for maintenance at a ratio of 1:3 or 1:6, or either cryopreserved ,avoiding the colonies to overgrow and dedifferentiate
    a. Cells were washed with PBS1x free of Mg^{2+} and Ca^{2+} and disaggregated with 1mL of Versene® (Ref. 15040066, Thermo Fisher)(or 0.5M EDTA pH 8) at room temperature, until detaching of colony edges was observed.
    b. Cells were then washed with medium and 1mL of medium was added to detach the cells gently with a StemPro EZ Stem Cell Passaging tool (Ref. 11523127, Thermo Fisher). Cells were collected into 15mL conic tubes using a 2mL pipette.
    c. After, cells were diluted with extra amount of medium and:
        i. Plated at the desired dilution. Then, 10 μM of Y-27632 was added.
        ii. Centrifuged at 1100rpm for 3 min, resuspended with hiPSC Freezing Medium and frozen at -80ºC. After 24-48h, cells were transferred into liquid nitrogen.

4.3. Neuroepithelial Induction of the hIPSCs

When large undifferentiated colonies of hIPSCs were observed, the differentiation process started by generating neuroepithelial cells (**Figure 36**).

1. Once hiPSCs were detached and collected into 15mL conical tubes, cells were centrifuged at 1200rpm during 5 min.

2. Cells were then resuspended with 250μL of cold Accutase™ (Ref. 00-4555-56, Invitrogen) and incubated during 5 min at 37ºC.
3. Colonies were disaggregated with a 1mL tip and Accutase™ was blocked with 5mL of DMEM/F12 medium.
4. A second centrifugation of 5 min and 1200rpm was done and finally cells were resuspended in NEPI Medium with 10μM of Y-27632 and seeded in p35 plates at a density of 200000 cells/plate.
5. Twenty h later medium was changed to remove the Y-27632 inhibitor. Cultures were refilled with fresh medium every 48h, and maintained in this condition for 6 days.
6. If confluence was reached, cells were split as described below:
    a. NEPI Medium was removed, 500μL/p35 of cold Accutase™ was added and cells were incubated at 37ºC during 5-7 min.
    b. Accutase™ reaction was blocked with 6mL of DMEM/F12 medium and cells were centrifuged at 1200rpm for 5 min. Cells were resuspended and plated at a density of 200000 cells/plate.

4.4. MN Progenitor Induction

After six days in NEPI Medium, we generated MN progenitors. Cells were split following the same protocol performed for the neuroepithelial cells. Cultures were refilled with fresh medium every 48h.

Phase 1. MN Progenitors 1 (MNP1): Once neuroepithelial cells were detached and centrifuged, they were resuspended in MNP1 Medium with 10μM of Y-27632 and seeded in p35 plates at a density of 200000 cells/plate. Cells were maintained in MNP1 medium during 6 days and split if necessary.

Phase 2. MN Progenitors 2 (MNP2): When MN progenitors in MNP1 Medium reached 6 days of maturation, were detached, centrifuged and resuspended in MNP2 Medium with 10μM of the Y-27632 inhibitor. Then, they were seeded at 200000 cells/plate and maintained in MNP2 medium during 6 days. At the stage of 6 days *in vitro,* cultured MNP2 cells could be frozen for stockage for additional 5-6 passages, before they lost the potential of forming MNs.

4.5. Neuroespheres / Embryonic bodies Induction or MN Induction

1. Once MNP2 cells were detached with Accutase™ and collected into 15mL conical tubes, cells were centrifuged at 1200rpm during 5 min.

2. Cells were resuspended in MN Induction Medium with 10μM of Y-27632 and plated in suspension into non-treated p35 Petri dishes (to avoid cell attachment), at a density of 1-2000000 cells/plate.
3. Twenty h later medium was changed to remove the Y-27632 inhibitor. Cultures were refilled with fresh medium every 48h, and maintained in this condition for 6 days.
    - As these cells grow in suspension, medium replacement was done by collecting the cells into 15mL conical tubes and allowing them to settle to remove the old medium. Then, cells were resuspended with fresh MN Induction Medium and put back into their culture dish.

4.6. MN Maturation Induction

After six days *in vitro,* cultured neurospheres were ready for the induction of their differentiation into mature MNs.

1. First, neurospheres were collected into 15mL conical tubes, centrifuged at 1200rpm during 5 min and resuspended with 0.5mL of Accumax (Ref. 00-4666-56, Invitrogen).
2. Cells were incubated at 37ºC during 7 min and then disaggregated with 200μL tips.
3. The dissociation was then blocked with 5mL of DMEM/12 followed by a second centrifugation at 1200rpm for 5 min. Finally, cells were resuspended in MN Maturation Medium with 10μM of Y-27632 inhibitor, and plated onto laminin-coated plates at 20000 cells/cm^2.
    - Alternatively, dissociated neuroespheres were resuspended in freezing medium and stored in liquid nitrogen. When thawing, cells were first maintained in MN induction medium for a few days before plating mature MNs.
4. Cells were placed in incubators at 37ºC and 5% CO_2 until the end of the experiment.
5. For western blot or immunofluorescence analysis, cells were collected at 7 days *in vitro,* whereas for survival and neurite degeneration experiments, mature MNs were held in the incubators for up to 28 days *in vitro.*

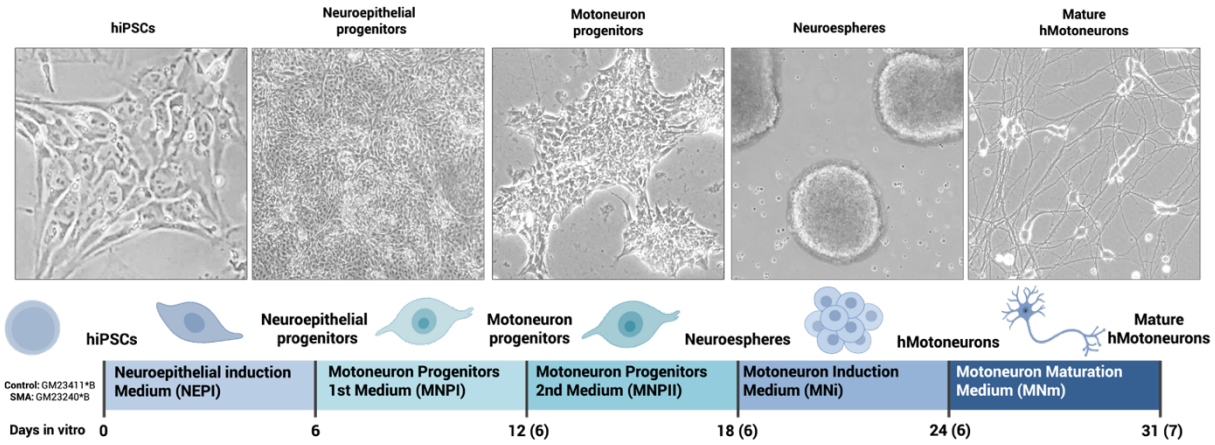

Figure 36 | Differentiation protocol from hiPSCs to mature human MNs. The whole differentiation process takes about 31 days *in vitro* to obtain mature MNs.

4.7. Thawing and freezing of NEP, MNP1 and MNP2

1. Cryopreserved cell vials were thawed during <5 min into a water bath at 37ºC and rapidly collected in a 15mL conical bottom centrifuge tube with 9mL of previously added DMEM/F12 medium.
2. After 3 min of centrifugation at 1100rpm (6500g), cells were resuspended in their media and cultured in p35 culture plates with 10μM of Y-27632.
3. Twenty h after plating, the Y-27632 inhibitor was removed and fresh medium was added. Medium was changed every day until large colonies of undifferentiated cells were observed, when cells were sub-cultured or frozen.
4. Cells were sub-cultured for differentiation as described before, or either cryopreserved:
    a. Cells were disaggregated with 0.5mL of Accutase™ at 37ºC during 5-7 min.
    b. Accutase™ reaction was blocked with 6mL of DMEM/F12 medium and cells were centrifuged at 1200rpm for 5 min. Cells were resuspended in Freezing Medium, and frozen at -80ºC. After 24-48h, cells were transferred into liquid nitrogen.

5. CELL CULTURE DRUGS

All drugs were prepared in the culture hood, diluted as described in their data sheet and filtered with a 0.22μm filter before being added to cell cultures.

Table 15 | Drugs used in cell cultures.

Treatment	Description	In solution	Final concentration	Reference
LY294002	PI3K Inhibitor	DMSO	25μM	Sigma (Ref. 440204)
U0126	MEK1/2 Inhibitor	DMSO	20μM	Calbiochem (Ref. CAS109511-58-2)
BAPTA-AM	Calcium chelator	DMSO	10μM	Invitrogen (Ref. B6769)

6. LENTIVIRAL PRODUCTION, TRANSFECTION AND TRANSDUCTION

6.1. Bacterial transformation

Escherichia Coli (E.Coli) bacteria were transformed in order to amplify the plasmids containing the RNA constructs of interest.

1. To this end, $1 \cdot 10^6$ competent cells from the strain DH5α were thawed on ice. Two hundred ng of plasmid DNA were added for every 200μL of competent cells.
2. After 10 min on ice, cells were subjected to a heat shock, raising the temperature up to 42ºC during 2 min, and finally 1 min on ice.
3. Luria Broth (LB) medium without antibiotic was added to the cells and they were incubated for 1h at 37ºC, following a centrifugation at 5000rpm during 2 min.
4. Supernatant was removed and the pellet obtained was seeded in an LB with ampicillin petri plate (LB medium with 20g/L of agar and 50μg/mL ampicillin).
5. Once colonies were grown, plasmid DNA was obtained using the "Kit Qiagen Plasmid Purification" (Qiagen) and following the instructions given by the manufacturer.

6.2. Human Embryonic Kidney cell line (HEK293T)

The HEK293T cell line was created by transfecting the human kidney 293 epithelium cell line with a gene encoding the Simian Virus 40 (SV40) large T antigen and a neomycin resistance gene. The constitutive expression of this antigen enhances the protein expression and production of many viral vectors. For that, these cells are widely used for transfection, DNA replication and gene expression experiments.

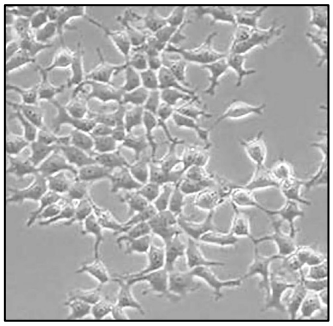

Figure 37 | Representative image of a HEK293T cell culture.

6.2.1. Thawing, freezing and maintenance

1. Cryovials containing the HEK293T cell line were warmed at 37ºC during <5 min into a water bath at 37ºC and rapidly placed in a 15mL conical bottom centrifuge tube with 9mL of previously added DMEM.
2. Then, cells were centrifuged at 1000rpm for 5 min, resuspended in HEK293T Medium (**Table 16**) and plated in p100 culture dishes in a CO_2 incubator.
3. When cells reached 80-90% of confluence, they were detached mechanically, centrifuged at 1000rpm for 5 min and diluted and plated in p100 plates. The culture medium was changed every 2-3 days.
    - For freezing, cells were detached and centrifuged as described above and frozen in 90% Horse Serum with 10% of DMSO.
4. For lentivirus production, cells were plated onto 0.2% gelatin-coated culture dishes.

Table 16 | Media used for HEK293T cell cultures.

Media and Solutions	Components
HEK 293T Medium	Dulbeco's Modified Eagle Medium (DMEM) (Gibco, Life Technologies, Ref. 41966-29) supplemented with 20μg/mL P/S and 10% (v/v) of HI-Fetal Bobine Serum (FBS) (Gibco, Invitrogen)
Freezing Medium	90% Heat Inhibited Fetal Bovine Serum (HI-FBS) supplemented with 10% DMSO

6.3. RNA constructs

In the present work we have used two approaches to regulate SMN expression.

1. Smn protein expression was knocked down using an shRNA construct and introduced it into MNs by lentiviral transduction.
    - The shRNA design was based on an RNAi sequence using the informatics tool siDESIGN® and sDirect, and was mainly performed by Dr. Ana Garcera. Lentiviral shRNA constructs were generated by digesting pSUPER-sh

(OligoEngine, Seattle, WA, USA) with EcoRI and ClaI to replace the H1 promoter with the H1-short hairpin RNA (shRNA) cassette in pLVTHM.

2. The human SMN protein was overexpressed by cloning the sequence into an integrative plasmid.
    - The SMN over-expression was achieved by PCR amplification of the Open Reading Frame (ORF) of the human SMN1 cDNA (NCBI accession number NM000344) from the pDNR-LIB vector (Invitrogen), using the primers listed in (**Table 17**). The PCR product was digested with BamH1 and cloned into FCIV plasmid (kindly provided by Dr Mario Encinas, Universitat de Lleida).

Table 17 | Primers used for the viral constructions.

Protein	Primers	Sequence (5' to 3')
Smn1	Forward	gatccccAGTAAAGCACACAGCAAGTttcaagagaACTTGCTGTGTGCTTTACTttttt
	Reverse	agctaaaaaAGTAAAGCACACAGCAAGTtctcttgaaACTTGCTGTGTGCTTTACTggg
Human SMN1	Forward	cacaggatccatggcgatgagcagcggcggc
	Reverse	tgtgggatccttaatttaaggaatgtgagca

Lentiviruses are designed based on the Human Immunodeficiency Virus-1, which can integrate randomly into the host genome, allowing long term gene expression. To reduce the mutagenic potential during the process of production and manipulation, 2nd and 3rd generation lentiviral systems have been created. These systems have only the essential genes required for transcriptional and post-transcriptional functions, structural utilities and enzymatic components split in 3 plasmids, so the possibility of infection is highly reduced. In our laboratory, a 2nd generation system of lentivirus is produced with the following components:

- **Packaging plasmid.** It is the vector encoding components of the HIV-1 viral capsid, containing all the proteins necessary for the packaging of the virus. For that, we have used the psPAX2 (Dr. Trono laboratory, University of Geneva, Switzerland) plasmid.
- **Envelope plasmid.** It is the vector encoding components of the vesicular stomatitis virus (VSV) protein, responsible for the infection process. For that, we used the pMD2.G (Dr. Trono laboratory, University of Geneva, Switzerland) plasmid.
- **Lentiviral transfer plasmid.** It is the plasmid encoding the genetic material of interest that we will insert. For that, we have used the pLVTHM (Dr. Trono, University of Geneva, Switzerland) and the FCIV (kindly provided by Dr. Mario Encinas, Universitat de Lleida)

vectors. These plasmids have a locus where we can clone our sequences of interest and a sequence for the expression of the Green Fluorescent Protein (GFP) for monitoring the transduction efficiency.

6.4. shRNA interference

The RNA interference technique allows the silencing of targeted genes at the post-transcriptional stage, reducing the expression of specific mRNA sequences in living cells.

Short hairpin RNA (shRNA) is an artificial RNA that has a tight hairpin-like loop with a low rate of degradation, which precedes a small interfering RNA sequence (siRNA). This modification allows a long-term gene silencing in *in vitro* cell cultures.

This shRNA sequence can be introduced inside the cells by lentiviral transduction. It is produced inside the cell nucleus and transported to the cytoplasm via the microRNA (miRNA) export pathway, where it is processed into siRNA by an enzyme that degrades the double-stranded RNA precursors (Dicer). Then, the siRNA is recognized by the RISC complex (RNA-Induced Silencing Complex), which allows the hybridization of the siRNA with the mRNA target, and cleaves it, leading the targeted sequence to its degradation (reviewed in (Hannon & Rossi, 2004).

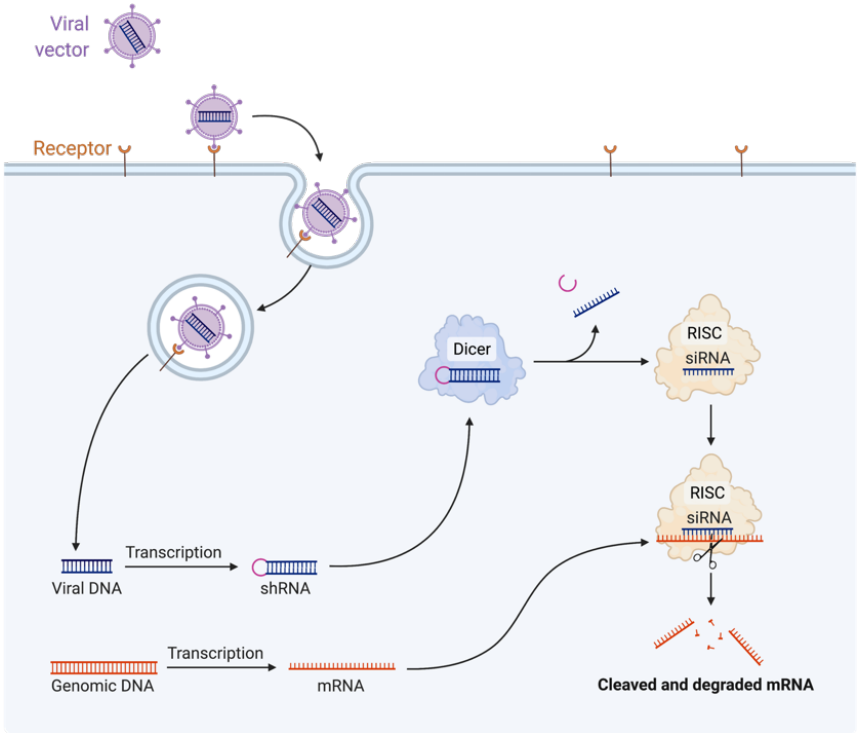

Figure 38 | Mechanism of gene silencing induced by shRNAs. BioRender.com.

6.5. Lentiviral transduction in HEK293T

Lentiviruses were propagated in HEK293T cells. For the transfection, we used polyethylenimine (PEI) (Sigma). Due to its cationic properties, PEI allows the condensation of DNA into positively charged particles, which bind to anionic cell surface residues inducing cell endocytosis.

1. PEI was prepared at an initial concentration of 20% in filtered miliQ water (Final concentration 4.5M), and then re-diluted to a stock concentration of 200mM, pH 5.6. For cell co-transfection, PEI was used at a final concentration of 10μM (stored at -20ºC in aliquots of 1mL). For lentivirus production, HEK293T cells were plated in p100 gelatin-coated dishes 24h before the transfection.
2. A total amount of 40μg of DNA was transfected using a total volume of 240μL PEI 10μM per each p100 plate. The μg of each plasmid are listed in **Table 18**.
3. For each p100, 40μg of DNA was diluted in 1500 μL of OptiMEM™ medium (Ref. 31985047, Thermo Fisher) and vortexed for 2 min.
4. In another tube, 240μL of PEI was diluted drop by drop into 1260μL of OptiMEM.
5. The PEI-OptiMEM™ solution was then slowly added into the DNA mix and rapidly vortexed for 5 to 15 seconds in order to let PEI engulf the DNA plasmids. Then, the solution was incubated at room temperature for 10 min.
6. Plates containing HEK293T cells were washed once with OptiMEM™ medium, 4mL of OptiMEM™ were added and then 3mL/p100 of transfection solution were added drop-wise, while gently swirling the plate.
7. After one to three h of incubation at 37ºC, the medium was changed to 10mL of complete HEK293T medium and the cells were reintroduced into the incubator for virus production.
8. 72 h after, supernatants were collected in 50mL Falcon tubes and stored at 4ºC to precipitate any remaining HEK293T cell. Then, the supernatants were carefully collected and filtered into new tubes using 0.22μm filters. Finally, these solutions were aliquoted in 2mL cryogenic tubes and stored at -80ºC.

Table 18 | Plasmids used for HEK293T transfection

Plasmids	Amount / p100
Lentiviral transfer plasmid	20µg (e.g. pLVTHM)
Packaging plasmid	13µg (psPAX2)
Envelope plasmid	7µg (pM2)

6.6. Virus titration

The lentiviral constructions used in our laboratory contain either the GFP or Yellow Fluorescent Protein (YFP), which allowed the evaluation of transfection efficacy.

1. For that, HEK293T cells were plated at 5000 cells/cm^2. Once attached, 3 different volumes of the virus medium was added.
2. After 72h, the percentage of transduced cells (GFP or YFP positive) was assessed by image acquisition with fluorescence microscopy and the ImageJ software.
3. Biological titles of the viral preparation were expressed as the number of transducing units (TU) per mL (TU/mL) using the following formula:

$$\mathrm{TU}/_{\mathrm{mL}} = \frac{(\text{Initial number of cells} \times \text{Percent of transduced cells})}{\text{Virus volume added (mL)}}$$

4. Viruses at $4{\cdot}10^5$-$1{\cdot}10^6$ TU/mL were used for the experiments.

6.7. Lentiviral transduction of primary cell cultures and human cell lines

For lentiviral transduction, human or mouse MNs were plated in 4-well laminin-coated plates and 3h later the lentivirus enriched medium (2TU/cell) was added.

1. Twenty h later cell culture medium was changed with the respective fresh medium. In primary cell cultures, aphidicolin (2µg/mL) (Ref. A0781, Sigma) was added.
2. After 72h, the transduction efficiency was monitored in each experiment by direct counting GFP-positive cells and lately by western blot analysis using antibodies against the protein to be analyzed.

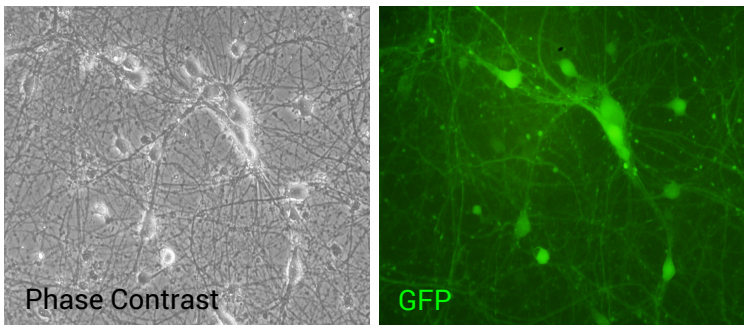

Figure 39 | Representative image of mouse MNs transduced with lentivirus. Isolated mouse MNs were treated with the lentivirus 3 h after plating. GFP signal was observed after 6 *div*.

7. EVALUATION OF NEURONAL VIABILITY IN CULTURE

Survival and neurite degeneration experiments were carried out by analyzing a triplicate of each condition per each experiment, performing a minimum of 3 independent experiments.

7.1. MN survival

To evaluate MN survival, cells were plated onto laminin-coated M4 plates at a low density (5,000 to 8,000 cells/cm^2) to reduce the possible cell-contact signaling, in their culture medium.

1. First, four-well plates were marked on the bottom with a cross to delimitate the microscopic areas to be analyzed.
2. Then, cells were plated and the number of counted cells present in each well on day 0 was considered our initial 100%. Image counting was performed with the Image J software.
3. Counts were performed in the same microscopic areas as the initial count at days 3, 7, 14, 21 and 28 days after plating, and survival was expressed as the percentage of cells counted with respect to the initial value (100%).

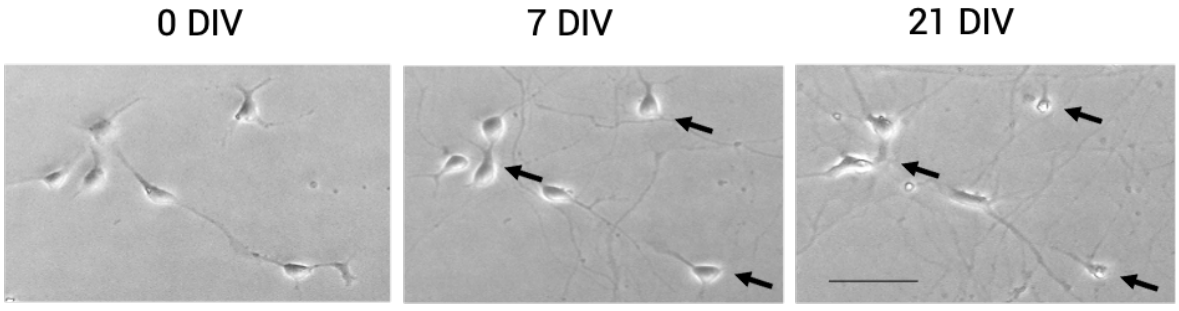

Figure 40 | Representative images of human MN survival analysis. Scale bar, 50μm.

7.2. Neurite degeneration

Morphometric analysis of neurite degeneration was performed as described (Press & Milbrandt, 2008), with modifications.

1. MNs were plated in 4-well laminin-coated plates at a density of 5,000 to 8,000 cells/cm^2.
2. Phase contrast microscopy images were obtained from the same microscopic areas with a 20x lens at 0, 3, 7, 14, 21 and 28 days after plating.
3. To analyze the images, a grid was created over each image with NIH ImageJ (Schindelin et al., 2012) software , using the grid plugin (line area = 50,000), and the cell-counting plugin was used to score each neurite.
4. Degenerating and healthy prolongations were counted in at least 10 high-power fields per image (30–50 neurites) for each well. Four different wells were counted for each condition (with the observer blinded to the condition) and the experiments were repeated at least three times.

Neurite segments were considered degenerated if they showed evidence of swelling and/or blebbing, reflecting interruptions of the neurite cytoskeleton and accumulations of proteins and organelles in the disrupted areas (**Figure 41**).

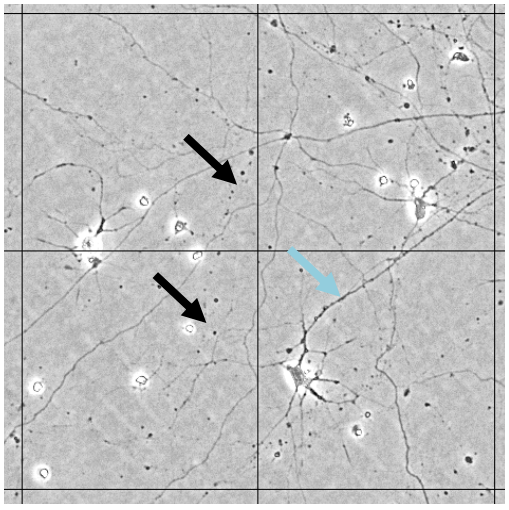

Figure 41 | Representative image of neurite degeneration analysis. Black arrows indicate degenerated neurites. Blue arrows indicate healthy neurites.

8. IMMUNOFLUORESCENCE TECHNIQUE

The immunofluorescence technique is based on the use of specific antibodies conjugated to fluorescent dyes, and allows the analysis of the presence, distribution and pattern of target molecules in individual cells and tissues.

8.1. Cell culture immunofluorescence

8.1.1. Cell fixation

For the fixation of cultured cells, the following protocol was performed:

1. First, cells were fixed with paraformaldehyde (PFA) for 10 min. 8% PFA was added in 1:1 ratio directly to the existing volume of culture medium to avoid alterations in the basal state due to the fixation process (final concentration 4%).
2. Three quick washes were made with PBS1X following a second 10 min fixation with cold methanol (-20ºC) was performed.
    - To evaluate the autophagy marker LC3 by immunofluorescence, the step with PFA was avoided, and cells were incubated with cold methanol only 30 sec.
3. After fixation, cells were washed again 3 times with PBS1X and left with PBS1X for the immunofluorescence protocol or stored at 4ºC until their use.

8.1.2. Immunofluorescence protocol

For the detection of specific molecules in cultured cells, the following protocol was performed:

1. Fixed cells were permeabilized with 0.3% Triton X-100 (Sigma) in PBS1X for 30 min in shake at room temperature.
2. Blocking solution (10% BSA (Sigma) and 0.2% Triton X-100 diluted in PBS1X) was added and incubated for 30 min in shake at room temperature.
3. Primary antibody was diluted in blocking solution and incubated overnight at 4ºC.
4. The following day, 3 washes of 10 min with PBS1X in shake at room temperature were done before secondary antibody was added.
5. Secondary antibody and Hoechst dye were added at the same time and incubated in shake at room temperature and protecting the samples from light during 1h.
6. Four washes of 10 min each with PBS1X in agitation at room temperature were done and glass coverslips containing the samples were ultimately mounted with Mowiol® mounting medium (Abcam) onto glass slides.
7. Samples were let to dry overnight at room temperature and protected from light, and then stored at 4ºC until imaging analysis.

8.2. Apoptotic nuclei quantification

To analyze the presence of nuclear apoptotic morphological features (condensed pyknotic and/or fragmented nuclei), Hoechst (Sigma) dye was used to stain cell nuclei (**Figure 42**). Hoechst is a part of a group of bis-benzamides used to stain DNA due to its capacity of binding to the AT-rich regions of the double stranded DNA.

1. For the experiments, cells were fixed with 4% PFA and cold methanol as described in the 8.1.1. section.
2. Then, MNs were incubated with Hoechst dye at a concentration of 2μg/mL for 30 min, washed 3 times with PBS1X and mounted with Mowiol® mounting medium onto glass slides.
3. The percentage of apoptotic nuclei was assessed by counting cells presenting the nucleus with apoptotic features with respect to the number of counted nuclei.

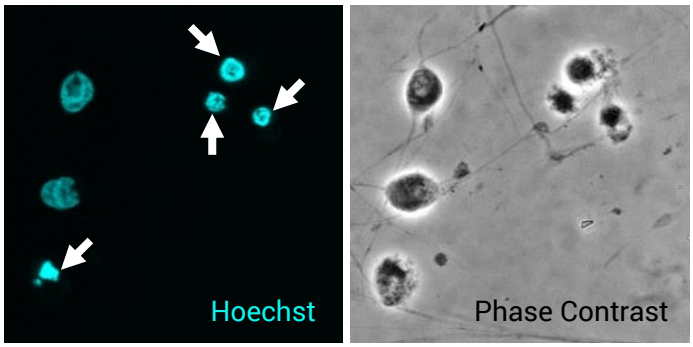

Figure 42 | Representative confocal image of human MN nuclei stained with Hoechst dye. Nucleus was considered apoptotic when showing pyknotic features and/or fragmentation. White arrows indicate apoptotic nuclei.

8.3. Tissue immunofluorescence

For immunodetection of antigens in spinal cord or muscle tissue, the samples must be pre-treated in order to maintain structural and cellular integrity.

8.3.1. Tissue preparation and cryopreservation

Mice were sacrificed at P0, P3 or P5 by decapitation and the following protocols were performed.

For spinal cords:

1. The spinal vertebral column lumbar region 1 and lumbar region 2 (L1 and L2), of mutSMA and WT mice were dissected and fixed in 4% PFA for 24h.

2. Cryopreservation with 30% sucrose solution (30% sucrose (Sigma), 0.1M Phosphate buffer and 0.02% of Sodium Azide)) was done during at least 48h, changing the tissue into fresh sucrose solution every day.
3. Finally, spinal cords were dissected from their bone scaffold and submerged again into new sucrose solution for at least 24h.

For SMNdelta7 spinal cord immunofluorescence analysis, animals were anesthetized and perfused with 4% paraformaldehyde in 0.1 M phosphate buffer (PB), pH 7.4. L1 and L2 spinal cord regions were dissected, cryoprotected in 30% sucrose in 0.1 M PB (pH 7.4), embedded in cryostat medium (Killik; Bio-Optica) and frozen. Sections were cut in the cryostat at a thickness of 40 µm and stored at −20 °C in 96-well plates in a freezing solution (30% ethylene glycol and 25% glycerol in PBS1X). Spinal cord slices were washed in PBS1X and incubated in blocking solution for unspecific binding sites for 30 min at RT with 0.3% Triton X-100 and 10% normal donkey serum (NDS, Sigma-Aldrich) in PBS pH 7.4. Primary antibodies were incubated overnight at 4ºC with 2% NDS and 0.3% Triton X-100. After washing, the secondary antibodies were added and DAPI staining was performed to identify nuclear localization in cell soma. Samples were mounted onto gelatin-coated Superfrost® slides using Mowiol (Calbiochem) medium and microscopy observations were performed in a Leica DM6000CS (Leica Microsystems, Wetzlar, Germany).

For gastrocnemius muscle:

1. The left and right gastrocnemius muscles from mutSMA and WT mice were dissected and fixed in 4% PFA for 2 h.
2. Cryopreservation with 30% sucrose solution was done during at least 48 h, changing the tissue into fresh sucrose solution every day.

Once the tissue was dissected, samples were embedded using Tissue Freezing Medium (TBS, Electron Microscopy Sciences), and cryopreserved at -80ºC.

1. Tissue was sectioned at 16-µm thickness in a cryostat (Leica CM3000) and placed onto glass slides (Superfrost plus EV, Thermo Scientific).
2. Sections were dried overnight before storing them at -80ºC until their use.

8.3.2. Tissue immunofluorescence protocol

For the immunofluorescence protocol of mouse spinal cord and gastrocnemius slices, the following protocol was performed:

1. Samples were thawed and let at room temperature for 15-20 min and then rehydrated with 2 washes of PBS1X.
    - For gastrocnemius samples: to break protein cross-links and unmask the antigens and epitopes, tissue sections were incubated at 450 Watts for 15 min in 10mM Citrate Buffer solution.
2. Sections were permeabilized with a detergent solution (0.3% Triton X-100 in PBS1X) for 30 min.
3. To block unspecific antigen union, samples were treated with blocking solution (5% BSA diluted in PBS1X) for 2 h.
4. Primary antibody was added diluted in blocking solution and incubated overnight at 4ºC.
5. After washing 3 times with PBS1X, secondary antibody was added diluted in blocking solution, and incubated in darkness at room temperature for 1h.
6. Samples were washed 3 times with PBS1X and mounted using Mowiol medium.

Finally, microscopy observations were performed in a FV10i Olympus confocal microscope (Tokyo, Japan).

Table 19 | Antibodies used for Immunofluorescence analysis.

Primary antibody	Host	Dilution	Reference
SMN	Mouse	1:100	BD Biosciences (Cat. No. 610646)
FAIM-L	Rabbit	1:200	Comella J.X.
XIAP	Mouse	1:100	BD Biosciences (Cat. No. 610762)
Cleaved caspase-3 (Asp 175)	Rabbit	1:100	Cell Signaling Technology (Cat. No. 9661)
Hb9	Rabbit	1:100	Abcam (Cat. No. ab92606)
Islet 1/2	Mouse	1:50	Developmental Studies Hybridoma Bank (Cat. No. 39.4D5)
ß-III-Tubulin	Rabbit	1:150	Cell Signaling Technology (Cat. No. 5568)
Choline Acetyltransferase (ChAT)	Sheep	1:100	Abcam (Cat. No. ab18736)
LC3	Rabbit	1:100	Cell Signaling Technology (Cat. No. 2775)
Laminin2	Rat	1:200	Abcam (Cat. No. L0663)
SMI-32	Mouse	1:1000	Covance (Cat. No. #SMI-32R)
Secondary antibody	**Host / Isotype**	**Dilution**	**Reference**
Alexa Fluor 488 goat anti-Rabbit	Goat / IgG	1:400	Invitrogen (Cat. No. A11008)
Alexa Fluor 555 goat anti-Mouse	Goat / IgG	1:400	Invitrogen (Cat. No. A21422)
Cy™3 AffiniPure F(ab')2 Fragment Donkey anti-Sheep	Donkey / IgG (H + L)	1:400	Jackson ImmunoResearch (Cat. No. 713-166-147)
Cy™3 AffiniPure F(ab')2 Fragment Donkey anti-Rat	Rat / IgG (H + L)	1:400	Jackson ImmunoResearch (Cat. No.712-166-153)
Cy2 AffiniPure donkey anti-Mouse IgG (H+L)	Donkey / IgG (H+L)	1:400	Jackson ImmunoResearch (Cat. No. 715-225-150)
Cy3 AffiniPure donkey anti-Rabbit (H+L)	Donkey / IgG (H+L)	1:400	Jackson ImmunoResearch (Cat. No. 711-225-152)

Table 20 | Counterstaining dyes used for Immunofluorescence analysis.

Counterstaining	Dilution	Reference
DAPI	1:100	Sigma (Cat. No. #d9564)
Hoechst	1:500 to 1:1000	Sigma (Cat. No. 23491-45-4)
NeuroTrace 530/615 Red Fluorescent Nissl Stain	1:200	Life Technologies (Cat. No. N21482)

8.4. Quantification analysis

Images were acquired with the immersion oil objective at 60X (Olympus FV10i confocal microscope) with the same microscope settings for each experiment, and then analyzed with the NIH ImageJ software.

- For all morphometric analysis, 80-100 fixed cells per condition were analyzed in different coverslip areas or slice sections.
- The experiments with cells were repeated at least 3 times, and for animal tissue samples, a minimum of 3 animals per condition were included.

8.5. Cell fluorescence measurements

For some experiments, determining the relative levels of proteins in a specific location or cellular structure, like neurites, cytoplasm or nuclei was required. For that, quantification of the immunofluorescence signal in each compartment of the cells was performed.

To quantify the fluorescence intensity, a formula for the obtention of the Corrected Total Cell Fluorescence (CTCF) was used with the analysis obtained using the NIH ImageJ software and by adapting the original protocol from (Gavet & Pines, 2010):

1. Using a Nissl, GFP or phase contrast image, cell perimeter was delimitated.
2. The selected perimeter was transferred to the corresponding image where the fluorescence had to be measured.
3. The Integrated Density (IntDen) was measured in the specified area of the cell, together with three non-fluorescent surrounding regions to be set up as the background (Bck) readings.
4. To calculate the CTCF of the selected area, the following formula was applied:

$$\mathbf{CTCF} = \mathbf{IntDen} - (\mathbf{Area\ of\ selected\ cell} \times \mathbf{Mean\ fluorescence\ of\ Bck\ readings})$$

8.6. Spots number quantification of LC3 immunostaining

Some proteins of interest change their cellular localization and/or morphological pattern depending on their activation state. In this work, the autophagy marker LC3 has been analyzed in MNs and cell lines. When activated, this protein changes its localization, getting recruited into the autophagic vesicles (Mizushima, 2004). The immunolocalization reveals then a dotted pattern. To measure LC3, then, the quantification of the spots ('puncta') in a determinate area is used.

1. For puncta quantification of LC3 immunostaining samples, the threshold level of the LC3 image was adjusted to highlight all the spots.
2. Using the corresponding phase contrast image, cell perimeter was delimited and transferred to the LC3 image.
3. Quantification of the number of spots in the selected area was performed automatically using the ImageJ "Find Maxima Tool" (**Figure 43**). For every experiment, the threshold value was adjusted at the same level for all the analyzed images.

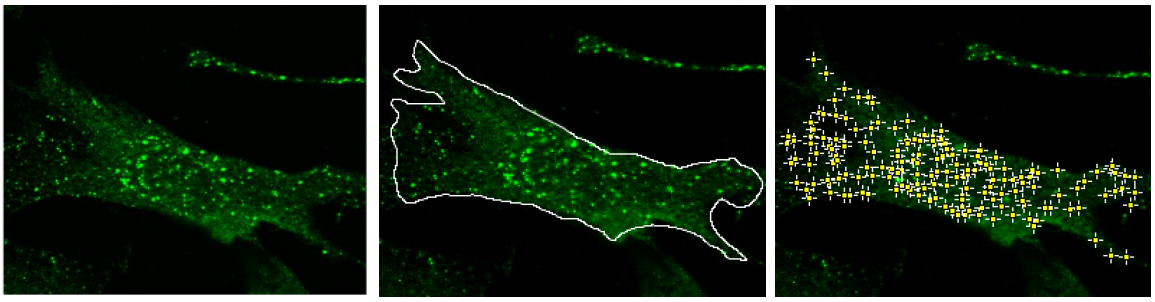

Figure 43 | Representative images of LC3 spots quantification using ImageJ software. Cell perimeter was delimitated and spots were automatically identified and quantified by the 'Find Maxima' tool from the software.

9. PROTEIN ANALYSIS TECHNIQUE – WESTERN BLOT

Western blot analysis is a technique that allows the separation of proteins by molecular weight from a complex mixture of proteins present in cells and/or tissues, and it is based on three steps:

1. Separation by size: The tissue homogenate or cellular extract is separated based on protein molecular weight through gel electrophoresis.
2. Protein transference to a membrane.
3. Targeting specific proteins using specific primary and secondary antibodies and visualized by a chemiluminescent reaction.

9.1. Protein extraction

9.1.1. Cell culture

1. First, cell cultures were rinsed with cold PBS1X to stop intracellular reactions, eliminate cell debris and extracellular floating proteins.
2. PBS1X was removed and cells were collected with Lysis Buffer (2% SDS, 125mM Tris-HCl, pH 6.8).
    - Cells were scraped from the bottom of the plate using a p200 tip for M4 plates (27μL) or a cell scraper for M6 or p35 plates (80-100μL).
3. Protein samples were collected in a sterile Eppendorf tube and boiled during 5 min at 95ºC and finally stored at -20ºC.

9.1.2. Spinal cord and muscle tissue

9.1.2.1. Protein extraction with DireCtQuant 100T

The lumbar region 1 and lumbar region 2 (L1 and L2, respectively) of mutSMA mouse spinal cords at specific days were dissected for protein extraction.

1. Spinal cords and gastrocnemius were rinsed with PBS1X and immediately placed in sterile Eppendorf tubes and frozen with liquid nitrogen. Then, tissue was stored at -80ºC until its use to avoid degradation.
2. Protein extraction of spinal cord and gastrocnemius tissue was done using Direct Quant 100ST Buffer (DireCt Quant) according to the manufacturer's instructions.
3. Thirty μL of DireCt Quant were added for every 1mg of tissue.
4. Samples were homogenized with a G50 Tissue Grinder (Coyote Bioscience) at 3000-4000rpm until the tissue was fragmented.
5. Samples were boiled at 90ºC for 3 min while shaking at 750rpm in a thermal block (Eppendorf).
6. After cooling down in ice, samples were centrifuged at 5000rcf (relative centrifugal force) in an Eppendorf MiniSpin centrifuge for 5 min.
7. The supernatant was collected and stored at -20ºC until its use.
8. Total protein concentration was assayed by using Bradford reagent (Bio-Rad).

9. Protein denaturation was performed with Loading Buffer 5X (LB5X) (10% SDS, 50% Glycerol, 25% 2-mercaptoethanol, 0.015% bromophenol blue (Sigma) and 62.5mM Tris-HCl pH6.8) by heating the samples at 95ºC for 5 min.

9.1.2.2. Protein extraction with RIPA buffer

For cleaved-caspase-3 detection, tissues were homogenized on ice using a pestle homogenizer.

1. SMNdelta7 spinal cords were disaggregated in RIPA lysis buffer (Merck Life Sciences) supplemented with 1mM PMSF (Phenylmethylsulphonyl fluoride), 1mM DTT (dithiothreitol), 2mM sodium orthovanadate (ThermoFisher Scientific) and 1X Complete™ Protease Inhibitor Cocktail (Merck Life Sciences).
2. Sample homogenates were incubated on ice for 20 min before being centrifuged for the insoluble material separation at 14000 rpm for 20 min at 4 °C.
3. Total protein concentration was assayed on supernatants using Bradford reagent (Bio-Rad). Protein denaturation was performed with NuPAGE® LDS Sample Buffer supplemented with NuPAGE® Sample Reducing Agent (ThermoFisher Scientific), by heating at 95 °C for 5 min.

9.2. Protein concentration quantification

1. For primary MN cultures and human cell lines, samples were sonicated if necessary and protein concentration was measured using a NanoDrop Spectrophotometer (NanoDrop). For western blot analysis, 15 to 40μg of total protein was loaded.
2. To measure protein content of tissue protein extracts, the Bradford method was performed, a colorimetric technique used to indirectly measure protein quantity:
   - Bradford Reactive (Bio-Rad) was first diluted 1:5 in miliQ sterile water.
   - Eight hundred μL of sterile miliQ water with 2μL of the sample were placed into a 1cm^2 spectrophotometer cuvette.
   - Two hundred μL of the 1:5 diluted Bradford Reactive was added to each cuvette and posteriorly mixed gently.
   - Absorbance was measured at a wavelength of 595nm and protein concentration was obtained with the numbers of the following standard curve:

$$y = 0.1158x - 0{,}0991 \rightarrow x = (y + 0.0991) / 0.1158$$

9.3. Electrophoresis in SDS-polyacrylamide gel

9.3.1. Polyacrylamide gel preparation

For protein separation, one-dimensional electrophoresis was performed under denaturing conditions. For that, Sodium dodecyl-sulfate (SDS), an anionic surfactant compound used for protein denaturation, was used. This detergent binds to the polypeptide chains, conferring them negative charges and allowing the separation only according to the molecular weight of the proteins.

Two polyacrylamide matrix with 0.1% SDS were prepared using a Mini-PROTEAN® Tetra cell system (Bio-Rad).

1. First, the lower or resolving gel, basic (pH8.8) and with higher polyacrylamide content to allow a better separation of the proteins.
2. Second, the upper or stacking gel, slightly acidic (pH6.8) and with lower polyacrylamide content. This gel allows the protein concentration and distribution as a thin defined band. Thus, all the proteins enter the resolving gel at the same time.

For cleaved-caspase-3 detection in spinal cord tissue, SDS-PAGE was performed on 4-20% Mini-PROTEAN® TGX™ Precast Protein Gels.

Table 21 | Components for staking and resolving SDS-PAGE gels. 0.1% of SDS was added to the acrylamide mix to denature proteins and help isolate protein molecules.

Stacking gel		**Resolving gel**	
Tris-HCl (pH 6.8)	125mM	**Tris-HCl (pH 8.8)**	375mM
Acrylamide	3-5% (v/v)	**Acrylamide**	7-15% (v/v)
SDS	0.1 % (w/v)	**SDS**	0.1 % (w/v)
Ammonium persulfate	0.05% (w/v)	**Ammonium persulfate**	0.05% (w/v)
TEMED	0.025% (v/v)	**TEMED**	0.025% (v/v)

9.3.2. Electrophoresis

1. Boiled samples and the ladder standard (Precision Plus Protein All Blue Standard, Bio Rad) were diluted in LB1X to achieve an equal loading volume.
2. Polymerized gels were equilibrated with an electrophoresis Running Buffer (25 mM pH 8.8 Tris-HCl, 192 mM glycine and 0.1% SDS).
3. All samples were loaded into the gel and run at a constant amperage of 15 mA/gel into a support for SDS-PAGE electrophoresis.

9.4. Protein transference to a PVDF membrane

Once the proteins were separated by molecular weight in the SDS-PAGE gel, gels were transferred onto 0.45μm polyvinylidene difluoride (PVDF) membranes (Millipore) using a Transfer Buffer containing SDS (48mM Tris-HCl, 39mM glycine 0.0375% SDS (w/v) and 10% methanol (v/v)).

1. PVDF membranes were hydrated with methanol for 1-5 min and then immersed in Transfer Buffer until the transfer was performed.
2. Two Blot papers (Albert LabScience) were submerged in Transfer Buffer until the electrophoresis was finished and the gels were ready for the protein transference.
3. The gel transference into (9 x 5.8 cm) PVDF membranes was done in an TE 70 ECL Semi-Dry Transfer Unit (Amersham Biosciences) as follows:
    - Blot papers, the membrane and the gel were assembled in the center of the unit following the order from bottom to top: *anode – Blot paper – Membrane – Gel – Blot paper – cathode.*
4. The transfer was performed at a constant amperage of 0.8mA/cm^2 (45 mA/membrane) for 1h - 1h15 min (for the detection of proteins with high molecular weight).

For cleaved-caspase-3 detection in spinal cord tissue, protein transference was performed on Trans-Blot® Turbo™ mini nitrocellulose membranes using a Trans-Blot® Turbo™ transfer System (Bio-Rad).

9.5. Protein immunodetection

1. Once proteins were transferred to the PVDF membrane, unspecific antigens from the separated proteins were blocked during 2h with Blocking Solution (5% Skim Milk

Powder (Sigma) diluted in TBST (20 mM Tris-HCl pH8, 125 mM NaCl and 0.1% v/v Tween-20®) at room temperature under shaking.

2. After washing the membrane with TBST, membranes were incubated with a specific antibody overnight at 4ºC.
    - Primary antibodies were diluted in TBST with 0.02% of Sodium Aside solution at the concentration described in **Table 22**.
3. Membrane was washed 3 times with TBST for 5 min each and then secondary antibody incubation was performed.
    - The secondary antibody used was conjugated to the horseradish peroxidase (HRP) enzyme and was incubated at indicated concentrations (**Table 23**) diluted into Blocking Solution during 1 h at room temperature.
4. Membranes were washed to remove the excess of secondary antibody.
5. The detection of proteins was achieved by producing a chemical reaction between the HRP (Horse Radish Peroxidase) enzyme of the secondary antibody and an HRP substrate (Millipore Immobilon Western Chemiluminescent HRP substrates, Cat. No. WBKLS0100, Merck).
    - Membranes were incubated for 5 min at room temperature with the HRP substrate solution with the exception of tubulin, that was incubated for only 1-2 min.
6. Image acquisition was made in a ChemiDoc XRS (Bio-Rad) CCD Chamber.

For cleaved-caspase-3 immunodetection in SMNdelta7 spinal cord tissue, the subsequent protocol was followed:

1. Once proteins were transferred to nitrocellulose membranes, nonspecific binding sites were blocked using 5% nonfat dried milk in PBS-0.2% Tween-20® (PBS-T) for 1h at room temperature under shaking.
2. After washing the membrane with TBST, membranes were incubated under shaking overnight at 4ºC with a specific antibody diluted in 2% nonfat dried milk in TBST.
3. Membrane was washed 3 times with TBST and secondary antibody incubation was performed.
    - HRP-conjugated secondary antibody was diluted in 2% nonfat dried milk in TBST and incubated for 1h at room temperature under shaking.
4. Immunolabeling was detected with Clarity™ Western ECL Blotting Substrates (Bio-Rad) using the ChemiDoc™ imaging system (Bio-Rad).

For p-Akt and p62 immunodetection in human MNs:

1. Unspecific antigens from the PVDF membranes were blocked during 2h with BSA blocking Solution (10% BSA diluted in TBST) at room temperature under shaking.
2. After washing the membrane with TBST, membranes were incubated with the primary antibody overnight at 4ºC in BSA blocking solution with 0.02% of Sodium Aside (**Table 22**).
3. Membrane was washed 3 times with TBST for 5 min each and then secondary antibody (**Table 23**) incubation was performed with Blocking solution during 1h at room temperature.
4. Membranes were washed to remove the excess of secondary antibody and protein detection was achieved with an HRP substrate and a ChemiDoc XRS (Bio-Rad) CCD Chamber.

Table 22 | Primary antibodies used for Western Blot analysis.

Primary antibody	Host	Dilutiion	Molecular Weight (kDa)	Reference
Beclin-1	Rabbit	1:1000	60	Cell Signaling Technology (Cat. No. 3738)
Cleaved caspase-3 (Asp 175)	Rabbit	1:1000	17	Cell Signaling Technology (Cat. No. 9661)
CREB	Mouse	1:1000	43	Cell Signaling Technology (Cat. No. 9104S)
FAIM-L	Rabbit	1:1000	15	Comella J.X.
LAMP-1	Rabbit	1:1000	42-90-120	Cell Signaling Technology (Cat. No. 3243)
LC3	Rabbit	1:1000	15	Cell Signaling Technology (Cat. No. 2775)
SMN	Mouse	1:5000	37	BD Biosciences (Cat. No. 610646)
p62	Rabbit	1:1000	62	Cell Signaling (Cat. No. 5114)
p-AKT (Thr308)	Rabbit	1:1000	60	Cell Signaling Technology (Cat. No. 9275)
p-ERK (p42/p44)	Rabbit	1:5000	42-44	Cell Signaling Technology (Cat. No. 9101)
p-CREB (Ser133)	Rabbit	1:1000	43	Cell Signaling Technology (Cat. No. 9198)
p-mTOR (Ser2448)	Rabbit	1:1000	289	Cell Signaling Technology (Cat. No. 5536)
pan-AKT	Mouse	1:100	60	Santa Cruz (Cat. No. sc-5298)
pan-ERK	Mouse	1:15000	42	BD Biosciences (Cat. No. 612641)
mTOR	Rabbit	1:1000	289	Cell Signaling Technology (Cat. No. 2972S)
α-Tubulin	Mouse	1:50000	50	Sigma (Cat. No. T5168)
Vinculin	Mouse	1:2000	130	Merck Life Sciences
XIAP	Mouse	1:1000	55	BD Biosciences (Cat. No. 610762)

Table 23 | Secondary antibodies used for Western Blot analysis.

Secondary antibody	Host	Dilution	Reference
ImmunoPure Goat anti-mouse IgG (H+L) HRP conjugate	Goat	1:10000	Thermo Fisher (Cat. No. 31430)
ImmunoPure Goat anti-rabbit IgG (H+L) HRP conjugate	Goat	1:10000	Thermo Fisher (Cat. No. 31460)
Immunopure Rabbit anti-goat IgG (H+L) HRP conjugate	Rabbit	1:10000	Pierce (Cat. No. 31402)

9.6. Stripping conditions

To immunodetect proteins with similar molecular weight in the same membrane, Restore™ Western Blot stripping buffer (Cat. No. UK290782) was used to remove the previous attached antibodies.

1. The membrane was washed with TBST and immersed in the stripping buffer during 15-30 min at room temperature.
2. Membrane was washed with TBST, blocked for 1h with Blocking Solution (5% Skim Milk Powder in TBST) and finally incubated overnight with the desired primary antibody.

10. REVERSE TRANSCRIPTASE QUANTITATIVE PCR

The Reverse Transcriptase quantitative Polymerase Chain Reaction (RT-qPCR) is a molecular biology technique frequently used to analyze gene expression. The amplification of a targeted DNA sequence is monitored as the PCR progresses by using a fluorescent reporter, being the fluorescent signal intensity directly proportional to the number of amplified DNA molecules.

10.1. RNA extraction and purification

For the obtention of enough quantity of RNA, a minimum of 400000 MNs were cultured in M6 (Falcon, Corning) laminin-coated cell culture plates. RNA was extracted and purified with the RNeasy Mini Kit (Qiagen) according to the manufacturer's instructions:

1. Cultured human or mouse MNs were cultured for 6 to 7 days *in vitro* in their respective growth media.

2. Cells were washed with sterile cold PBS1X and lysed with 350μL of RLT Buffer with 1% 2-mercaptoethanol and a sterile cell scraper.
3. Cell lysates were collected into a microcentrifuge tube and frozen at -80ºC until RNA purification or immediately used.
4. After thawing, samples were centrifuged at 4ºC for 3 min at 14000-15000rpm. Then, the supernatant was collected in a new tube.
5. An equal volume of 70% ethanol solution was added to the collected supernatant and mixed gently.
6. The mixed solution was transferred to an RNeasy spin column placed in a 2mL collection tube and centrifuged 15 sec at 15000rpm to load the RNA into the column. Flowthrough was discarded.
7. Seven hundred μL of RW1 Buffer was added to the RNeasy spin column and centrifuged for 15 sec at 15000rpm.
8. Flowthrough was discarded and 500μL of RPE Buffer was added. After 15 sec of centrifugation at 15000rpm, flowthrough was discarded.
9. A second RPE Buffer wash with 500μL of RPE Buffer was done. Following a 2 min centrifugation at 15000rpm, flowthrough was discarded.
10. Samples were centrifuged for an additional min, ensuring the total elution of ethanol, which may interfere with downstream reactions.
11. The RNeasy spin column was finally placed in new 1.5mL Eppendorf tubes and 30μL of RNase-free water was added to the spin column. After 1 min of centrifugation at 15000rpm, the RNA was eluted and stored at -80ºC.

10.2. ONE- STEP RT-qPCR – SYBR Green approach

Using this method, the reverse transcriptase reaction is performed in the same reaction vessel as the quantitative PCR reaction, in a common buffer (**Figure 44**). First, the gene-specific primers direct complementary DNA (cDNA) synthesis of a specific target. Then, cDNA starts its denaturation at 95ºC, following the start of specific primer annealing (at 60ºC). Once the DNA polymerase starts generating double stranded DNA (dsDNA), the SYBR Green fluorophore starts binding to the dsDNA, releasing a fluorescent signal. The reaction is monitored continuously and an increase in fluorescence is viewed in real-time. Fluorescence measurement at the end of the elongation step of every PCR cycle is performed to monitor the increasing amount of amplified DNA. A melting curve analysis performed subsequently to the PCR, to determine the relative amount and expression of the specific targeted gene.

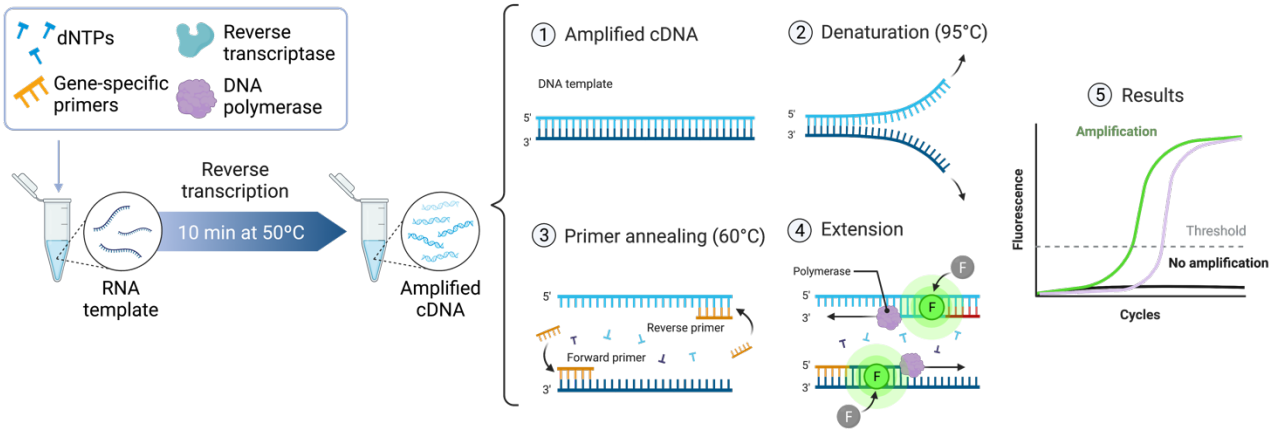

Figure 44 | Schematic representation of ONE-STEP RT-qPCR. cDNA synthesis and quantitative PCR are carried out in the same reaction vessel. The gene-specific primers direct cDNA synthesis of a specific target. (4) Then, with the amplification of that cDNA, SYBR Green dye binds to the amplified dsDNA emitting fluorescence. (5) Fluorescence measurement at the end of the elongation step of every PCR cycle is performed to monitor the increasing amount of amplified DNA. Created with BioRender.com.

The iTaq™ Universal SYBR® Green One-Step Kit (Bio-Rad) was used for the experiments. Sixty to 80 ng of total RNA from each condition were used for each individual qRT-PCR reaction. The following mix was prepared for each sample per triplicate (**Table 24**), plus another triplicate for the housekeeping control.

- Twelve µL of the SYBR Green-Primer Mix were added in each well in 96-well plates.
- Finally, 60 to 80 ng of RNA sample diluted in sterile RNase-free water (reaching a final volume of 8µL) were added in the 96-well plates.
    - Six replicates of the same sample were added in the plates; a triplicate for the targeted gene and a triplicate for the housekeeping gene (*GAPDH* or *Gapdh*) (**Table 25**).

Table 24 | Quantitative PCR Mix Preparation

Reagents	Volume per 20µL reaction	Concentration
iTaq Universal SYBR Green Supermix	10µL	1X
Forward primer	0.875µL (6857nM)	300nM
Reverse primer	0.875µL (6857nM)	300nM
iScript Reverse Transcriptase	0.25µL	1X
Sterile RNase-free water	Variable	-
RNA sample	Variable	up to 500ng (60-80ng)

Table 25 | Primers used for RT-qPCR analysis. The genes written in capital letters belong to human primers while the genes written in lowercase letters belong to mouse primers.

Gene	Primers	Sequence
SMN	Forward	5′-CCGCCACCCCCTCCCATCTCT-3′
	Reverse	5′-CATCTCCTGAGACAGAGCTGA-3′
Smn	Forward	5′-GATGATTCTGACATTTGGGATG-3′
	Reverse	5′-TGGCTTATCTGGAGTTTCAGAA-3′
GEMIN2	Forward	5′-GGGTGAAAAGTTATGTGCTG-3′
	Reverse	5′-GACACTAGTTACTGTTGCCTGA-3′
Gemin2	Forward	5′-GGGTGAAAGGTTATGTGCTG-3′
	Reverse	5′-GTCGGATTCGTGAATGAGCC-3′
mFaim-L	Forward	5′-TCCAGGCTATAGAGAGGGCTT-3′
	Reverse	5′-GCGCGGAGCAGACTGT-3′
GAPDH	Forward	5′-TGCACCACCAACTGCTTAG-3′
	Reverse	5′-AGAGGCAGGGATGATGTTG-3′
Gapdh	Forward	5′-TGCACCACCAACTGCTTAG-3′
	Reverse	5′-GGATGCAGGGATGATGTTC-3′

The qPCR was performed in a CFX96 Real-Time System (Bio-Rad) with the following protocol:

Table 26 | Cycling parameters for the RT-qPCR.

Step	Temperature	Time	Cycles
Reverse Transcription	50ºC	10 min	1
Polymerase activation / DNA denaturation	95ºC	1 min	1
DNA denaturation	95ºC	10 sec	40
Annealing / Extension	60ºC	30 sec	
Melt curve analysis	Instrument default settings		

Quantification was completed using Bio-Rad CFX Manager real-time detection system software (version 3.1, Bio-Rad). Relative expression ratios were calculated on the basis of ΔCq values with efficiency correction based on multiple samples.

11. STATISTICS

All the experiments were done a minimum of three independent times. For animal tissue analysis experiments, a minimum of 2-3 animals per condition were analyzed.

Raw data was analyzed with Microsoft Excel 2020. Graph design and statistical analysis were performed with the GraphPad Prism 9 software. Values in the graphs are shown as the mean±SEM (Standard Error of the Mean), and the results were considered significant when the p-value was $p<0.05$.

The differences between groups were analyzed with the following tests:

- **Student *t*-test** was used to analyze differences in a variable between two conditions. Values were analyzed assuming that they followed a Gaussian distribution without an equal standard deviation (SD).
- **One-way ANOVA** test was used to compare differences in a variable between more than two conditions. Gaussian distribution was assumed for all the values. Posterior tests were used to compare means of pairs of groups. The Dunnett's test was used to compare all columns with one control column, and Tukey's test was used to compare all pairs of columns.
- **Multiple *t*-test** was used to analyze differences in a variable between two conditions through time, such as survival or neurite degeneration analyses. Statistical significance in these analyses was determined using the Holm-Sidak method, with an alpha=0.05 and without assuming equal SD.

RESULTS

CHAPTER 1. APOPTOSIS-RELATED PROTEINS ARE DEREGULATED IN MOUSE AND HUMAN SPINAL MUSCULAR ATROPHY MODELS

SUMMARY

The implication of the apoptotic pathway in SMA disease is still under investigation. Nonetheless, studies suggest that MN degeneration in SMA disease may be related to increased apoptosis, and several apoptosis-related proteins have been reported to be altered in SMA models (Garcera et al., 2011; Jablonka et al., 2000; Maretina et al., 2018; Sareen et al., 2012; L. K. Tsai et al., 2008; M. S. Tsai et al., 2006).

FAIM-L is an antiapoptotic protein expressed exclusively in the nervous system (Micheau et al., 2003; Segura et al., 2007; Sole et al., 2004) that is implicated in the regulation of apoptosis, preventing its activation through both the extrinsic and intrinsic pathways (**Figure 45**) (Carriba et al., 2015; Carriba & Comella, 2014, 2015). FAIM-L is decreased in AD patients with beta-amyloid peptide accumulation and is able to protect neurons from Fas-induced apoptosis through regulating XIAP, a caspase inhibitor (Moubarak et al., 2013; Obexer et al., 2014), capable to block both pro-caspases and active caspases.

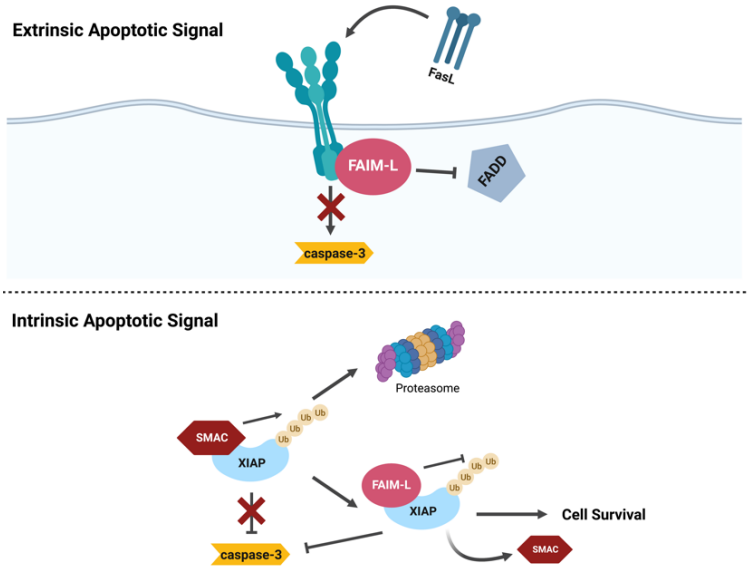

Figure 45 | FAIM-L inhibition of apoptosis. FAIM-L prevents FADD binding to death receptors and stabilizes XIAP protein to prevent its degradation in the proteasome. Based on (Planells-Ferrer et al., 2016). Created with BioRender.com.

Alteration of apoptosis-related proteins in AD and SMA diseases suggest that these proteins may play important roles in neuronal viability. Hence, investigating the intracellular pathways that lead to MN degeneration in SMN-reduced models could be relevant to therapeutically prevent or delay SMA disease progression. To this end, the objective of this chapter is to analyze the degeneration of MNs in SMN-reduced models, including mouse spinal cord tissue, mouse and human differentiated MNs, and human fibroblasts, and the role of apoptosis and the antiapoptotic proteins FAIM-L and XIAP in the development of SMA disease.

1. Evaluation of cell survival in mutSMA MNs

Previous results in our group revealed that neurite degeneration was increased in primary MNs from the mutSMA mouse model when compared to the WT condition (de la Fuente Ruiz, 2020). Hence, we hypothesized that cellular survival could also be affected in these cells.

To this end, embryonic day 13 (E13) mutSMA and WT MNs were isolated and cultured during 12 days in vitro (DIV), and cell survival was evaluated at 6 and 12 DIV. The percentage of the surviving cells was measured starting from 100% at day 0 of differentiation by taking pictures of the same microscope field (**see Materials and Methods section 7.1**). The analysis of cell survival in mutSMA MNs revealed a significant reduction of cell viability after 12 DIV (21.004±1.16, p=0.0026) compared to WT condition (33.95±1.55) (**Figure 46**).

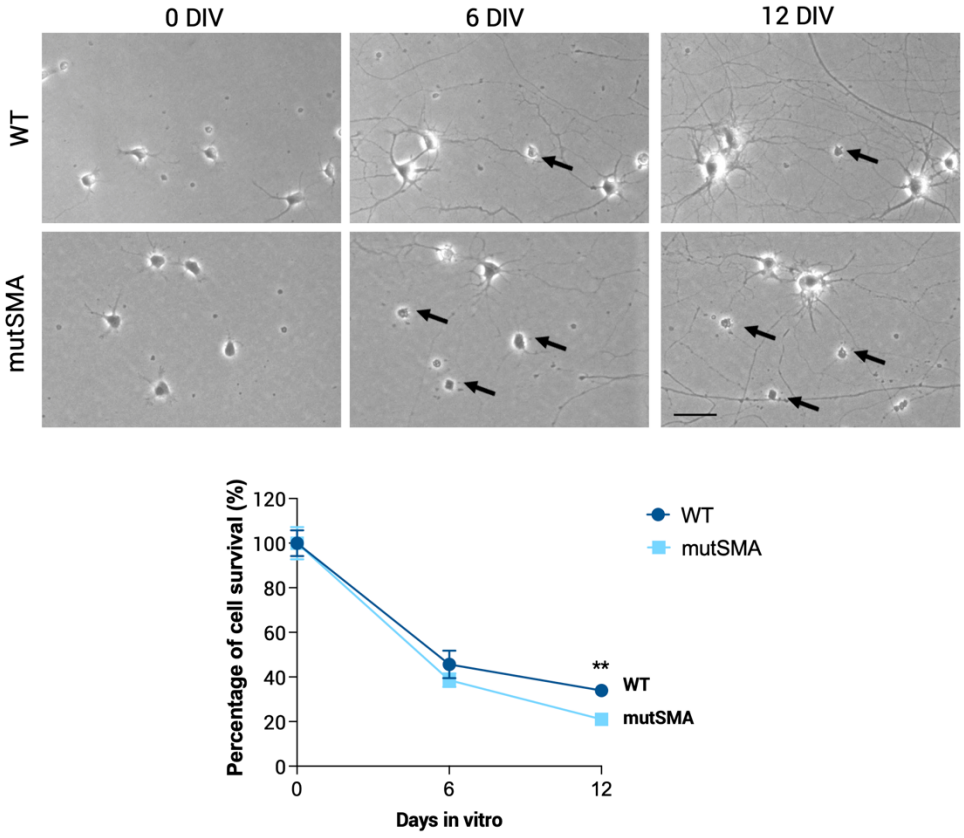

Figure 46 | Survival is reduced in 12DIV mutSMA MNs. Representative images of the same microscopic area of WT and mutSMA primary MNs at day 0, 6, and 12 in vitro (0DIV, 6DIV, 12DIV, respectively). Arrows point out degenerated somas of MNs. Graph values are the mean of the percentage of cell survival for each condition of 12 wells from 3 independent experiments ± SEM. Scale bar, 50µm. Asterisks indicate differences using Multiple *t*-test (**p<0.01).

2. Characterization of *in vitro* differentiated human MNs

To evaluate the levels of FAIM-L and XIAP protein levels in other MN models of SMA disease, we differentiated SMA and non-affected control human iPS cells (hiPSC) (Coriell Institute) (**see Materials and Methods section 4**).

First, cells were characterized to confirm that they properly differentiated into MNs. Cells were plated onto laminin-coated glass coverslips and cultured in MN maturation medium. Seven days after differentiation, cells were fixed with 4% PFA and cold methanol. After fixation, immunostaining against the following MN markers was performed: Islet 1/2 (Insulin related protein 1 and 2, expressed in all islet cells in the pancreas and in spinal cord MNs), HB9 (a transcription factor described as a spinal cord MN-specific marker and critical for the postmitotic specification of these cells), ChAT (an enzyme responsible of acetylcholine synthesis and specific indicator of cholinergic cells), and βIII Tubulin (component of the microtubule chain in neurons). Images were acquired with an FV10i confocal microscope (Olympus) using the x60 objective and the same microscopic settings. Immunofluorescence images showed that the differentiated MNs expressed all these aforementioned MN markers indicating that SMA and Control human iPS cells were properly differentiated to MNs (**Figure 47**).

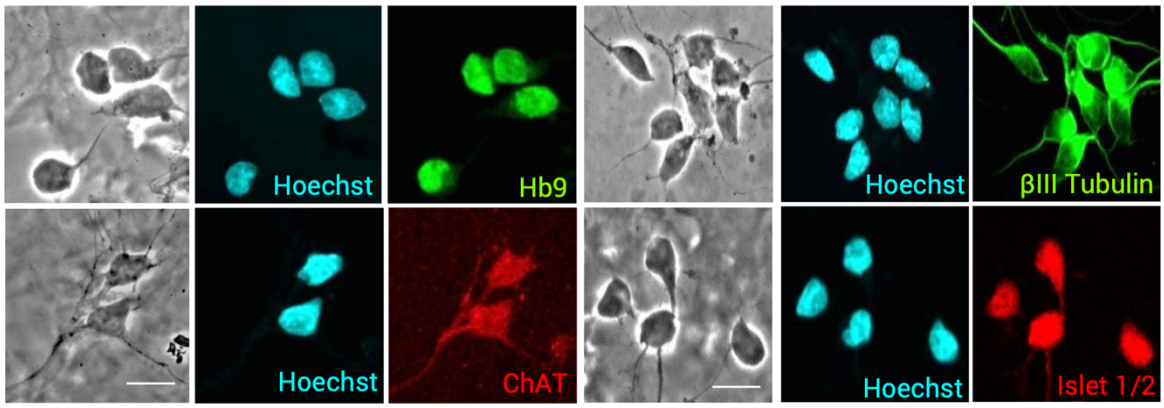

Figure 47 | Characterization of differentiated human MNs using immunofluorescence. Representative phase contrast and immunofluorescence images of 7-day differentiated human MNs, showing the MN markers HB9 (green left section), ChAT (red left section), ßIII-tubulin (green right section), and Islet 1/2 (red right section). Hoechst (blue) staining was used to identify MN nuclei. Scale bars, 15µm.

Next, we measured SMN levels by immunofluorescence, western bot analysis and RT-qPCR. SMN fluorescence intensity was analyzed using NIH ImageJ software in differentiated Control and SMA human MNs, revealing a reduced intensity in differentiated SMA MNs (CTCF: 54.1±1.9, $p<0.001$) compared to the Control MNs (CTCF: 113.3±5.7) (**Figure 48a**). As expected,

SMN levels were also significantly reduced in SMA human MNs in both western blot (0.36 ± 0.04, $p<0.0001$) (**Figure 48b**) and RT-qPCR (0.5 ± 0.063, $p<0.01$)(**Figure 48c**) experiments when compared to their respective controls.

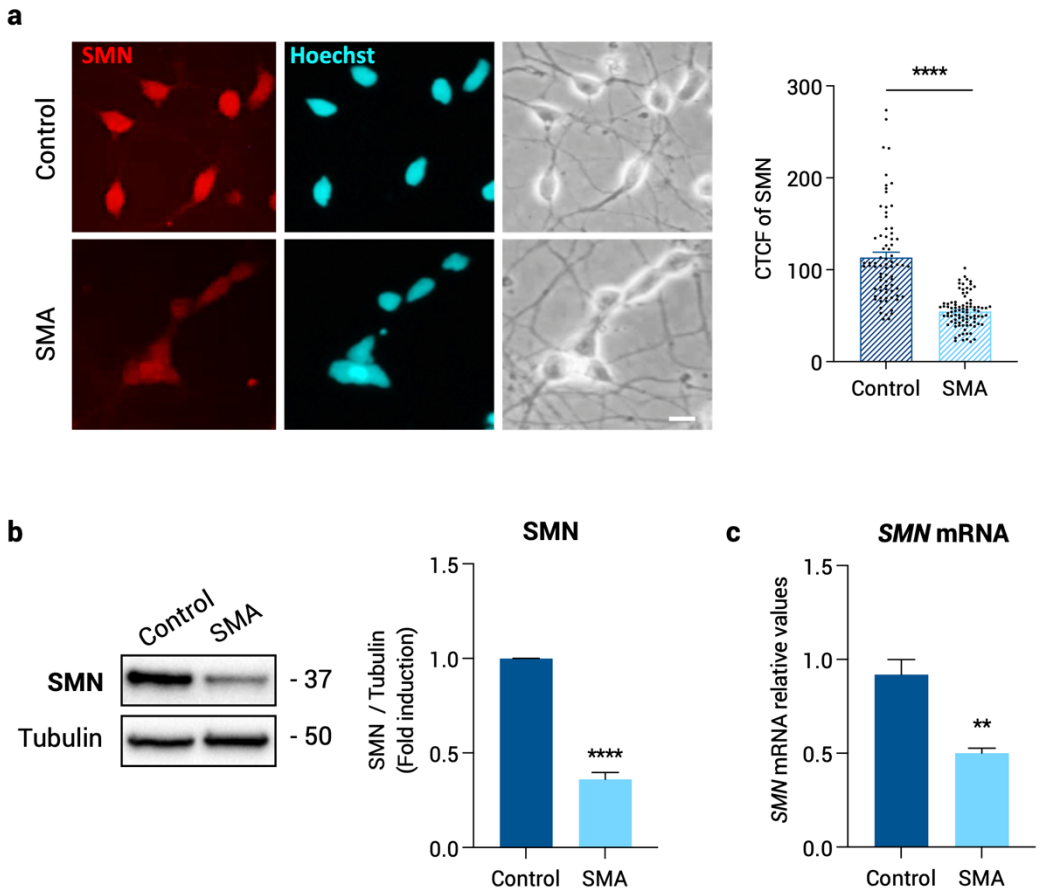

Figure 48 | SMN levels in differentiated SMA and Control human MNs. Seven-day differentiated SMA and Control human MNs were cultured and fixed for immunofluorescence analysis or collected for western blot analysis. (**a**) Immunofluorescence was done using an anti-SMN antibody (red). Hoechst dye (blue) was used to localize MN nuclei. Graph shows mean ± SEM of relative SMN fluorescence levels measured in cells using Student *t*-test (****$p<0.001$). Scale bar 15μm. (**b**) Western Blot analysis using anti-SMN antibody. Anti- α-tubulin was used as a loading control. (**c**) Total RNA was extracted from differentiated Control and SMA human MNs. RNA was reverse transcribed to cDNA and SMN was amplified through RT-qPCR. GAPDH was used as control. Graph values represent the expression of SMN vs α-tubulin (**b**) or vs GAPDH (**c**) and correspond to the quantification of at least 3 independent experiments ± SEM. Asterisks indicate significant differences using Student *t*-test (**$p<0.01$; ****$p<0.0001$).

Phase contrast images of these cells were used to evaluate morphological features. Soma, cytoplasm and nucleus size was measured using ImageJ software. Results in **Figure 49** show that SMA differentiated MNs are significantly smaller compared to the Control in the soma (Control: 106.3±1.8 μm^2; SMA: 88.74±1.6 μm^2, $p<0.0001$), the cytoplasm (Control:

45.9±1.3 μm^2; SMA: 29.94 ± 0.77 μm^2, p<0.0001) and the nucleus (Control: 63.4±1.3 μm^2; SMA: 59.07±1.16 μm^2, p=0.015).

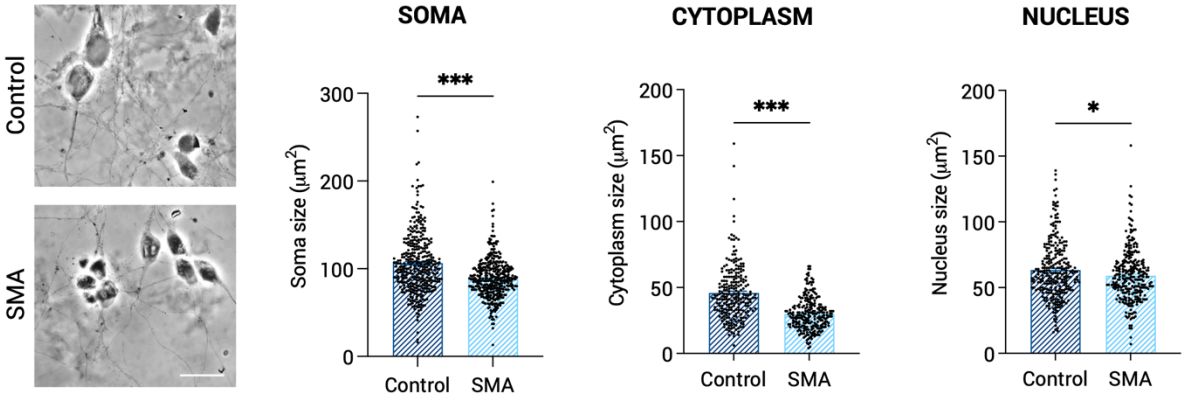

Figure 49 | Cell size characterization of differentiated Control and SMA human MNs. Representative phase contrast images of 7-day differentiated Control and SMA MNs. Scale bar, 30μm. Graph values represent the soma, cytoplasm or nucleus size expressed in μm^2 and correspond to the quantification of 4 independent experiments ± SEM. Asterisks indicate significant differences using Student *t*-test (*p<0.05; ***p<0.0001).

3. Evaluation of cell survival and neurite degeneration in differentiated SMA human MNs

Next, we evaluated the survival rate and the neurodegeneration process occurring in these human SMN-reduced MNs. We analyzed cell survival at 3, 7, 14, 21 and 28 days after differentiation. The percentage of the surviving cells was measured starting from 100% at day 0 of differentiation by taking pictures of the same microscope field (**see Materials and Methods section 7.1**). The analysis of the cell survival in the SMA condition revealed a significant reduction of cell viability after 14, 21 and 28 days of differentiation compared to Control (3 days: Control 100.03±3.6, SMA 84.24±4.58, p=0.053; 7 days: Control 91.83 ± 4.23, SMA 74.3±5.7, p=0.068; 14 days: Control 81.16±5.2, SMA 43.4±11.9, p=0.043; 21 days: Control 73.56±4.9, SMA 30.86±13.5, p=0.041; and 28 days: Control 67.3±4.1, SMA 26.2±7.9, p=0.0098) (**Figure 50a**).

Neurite degeneration was studied in these cells at 3, 7, 14, 21 and 28 days after differentiation. We considered degenerating neurites those that presented morphologic evidences of swelling and/or blebbing, showing interruptions of the cytoskeleton. The percentage of degenerating neurites was obtained by counting the degenerating neurites with respect to the total number of neurites in the microscope field (**see Materials and Methods section 7.2**). We observed a significant increase of the percentage of degenerated neurites in

differentiated SMA MNs at 7, 14, 21, and 28 days, compared to the Control (3 days: Control 2.65±1.41, SMA 9.29±6.52, p=0.37; 7 days: Control 8.3±3.4, SMA 30.25±6.2, p=0.036; 14 days: Control 13.77±3.6, SMA 51.6±7.0, p=0.0086; 21 days: Control 18.4±4.2, SMA 60.48±7.0, p=0.0067; and 28 days: Control 21.04±5.7, SMA 66.02±8.0, p=0.010) (**Figure 50b**).

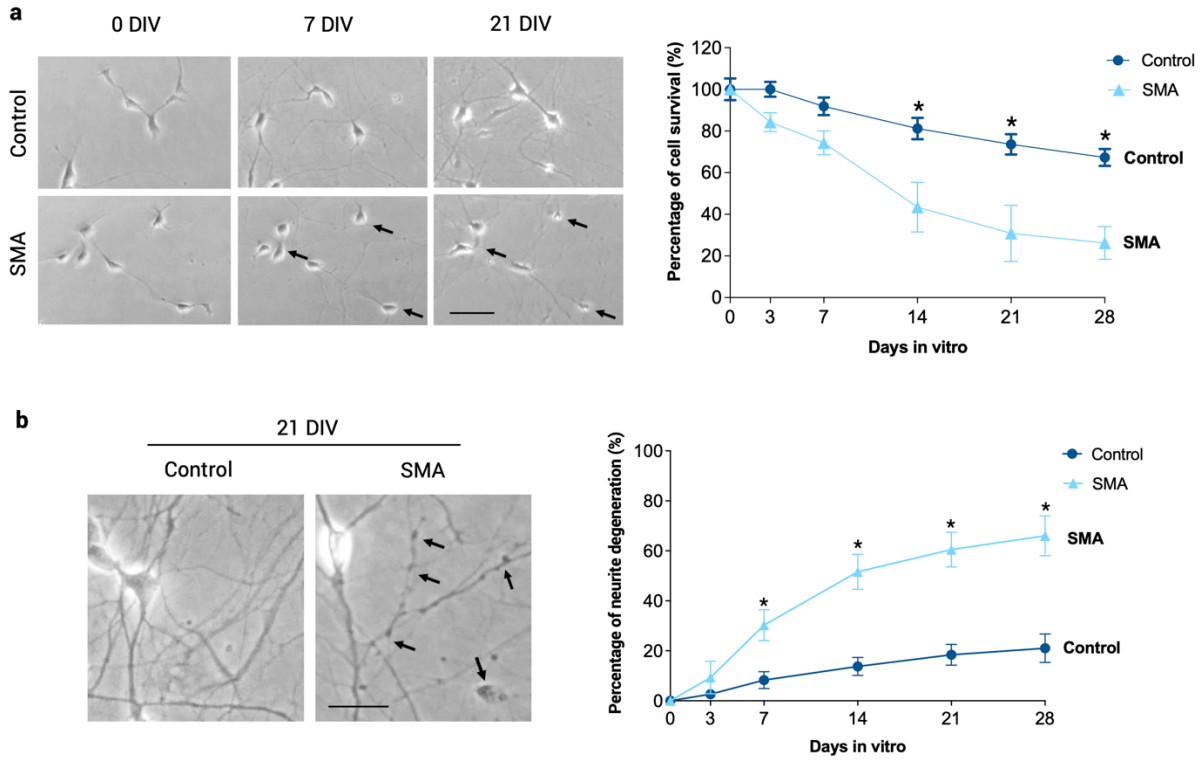

Figure 50 | Cell death and neurite degeneration is increased in differentiated SMA human MNs. (**a**) Representative images of the same microscopic area of differentiated Control and SMA human MNs at day 0, 7, and 21 in vitro (0DIV, 7DIV, 21DIV, respectively). Arrows point out degenerated somas of MNs. Graph values are the mean of the percentage of cell survival for each condition of 12 wells from 3 independent experiments ± SEM. Scale bar, 50µm. (**b**) Representative images of Control and SMA human MNs differentiated for 21 days (21DIV). Arrows indicate degeneration of neurites. Graph values are the mean of the percentage of degenerating neurites for each condition of 12 wells from 3 independent experiments ± SEM. Asterisks indicate differences using Multiple *t*-test (*p<0.05). Scale bar 30µm.

4. Cleaved caspase-3 and apoptotic nuclei are increased in Smn-reduced mouse models

Neurite degeneration and cell survival were compromised in SMA mouse and differentiated human MNs (**Figures 46 and 50**). Thus, we wanted to evaluate if there were additional alterations in the apoptotic pathway.

We examined the level of cleaved-caspase-3 and the number of caspase-3 positive cells and apoptotic nuclei in mouse spinal cord MNs in vitro. E13 isolated MNs from WT and mutSMA mice were cultured in the presence of NTFs, and 6 or 12 days after plating protein extracts were submitted to western blot analysis using anti-cleaved-caspase-3 antibody. Results showed that the level of cleaved-caspase-3 was increased in mutSMA MNs (6DIV: 1.57±0.18, p=0.0031; 12DIV: 1.21±0.1, p=0.039) compared to the WT control (**Figure 51a**). We next performed an immunofluorescence of anti-cleaved caspase-3 in 6 and 12 DIV cultured MNs. Cells were plated onto laminin-coated glass coverslips and fixed with 4% PFA and cold methanol. Immunofluorescence protocol was performed using the anti-cleaved caspase-3 antibody and Hoechst dye was used to stain cell nuclei. The percentage of positive cleaved-caspase-3 cells was increased in mutSMA cultured MNs at 6DIV (32.62±4.35) and at 12DIV (69.83±6.48) compared to the WT control (6DIV: 14.41±0.71, p=0.0033; 12DIV: 49.71±4.68, p=0.0217, respectively), as shown in **Figure 51b**. The percentage of nuclei presenting apoptotic morphology was evaluated using Hoechst dye. Apoptotic nuclei were significantly increased in 6DIV (26.12±5.0) and 12DIV (67.45 ± 6.09) mutSMA cells compared to WT at 6DIV (7.99±0.64, p=0.0049) and 12DIV (41.42±4.66, p=0.0033), respectively.

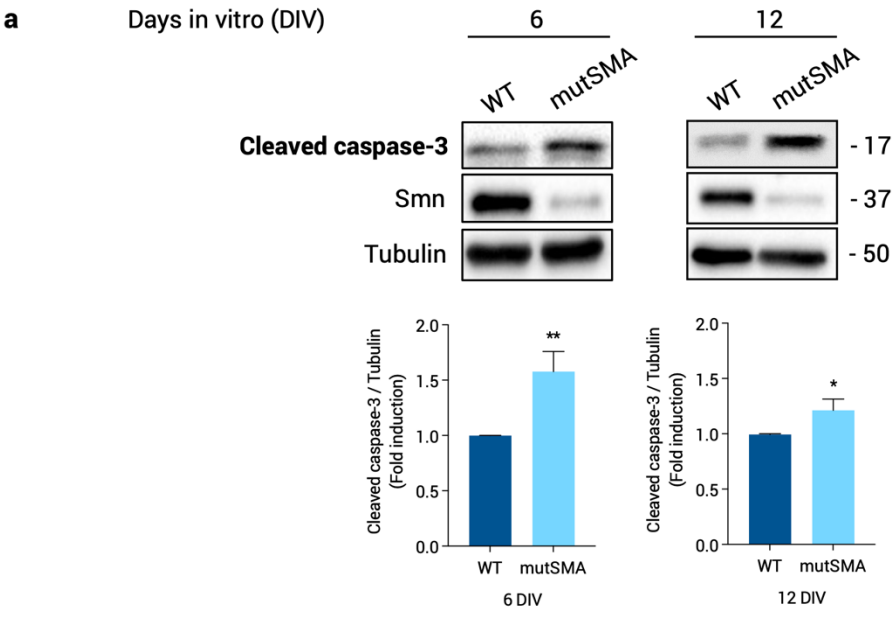

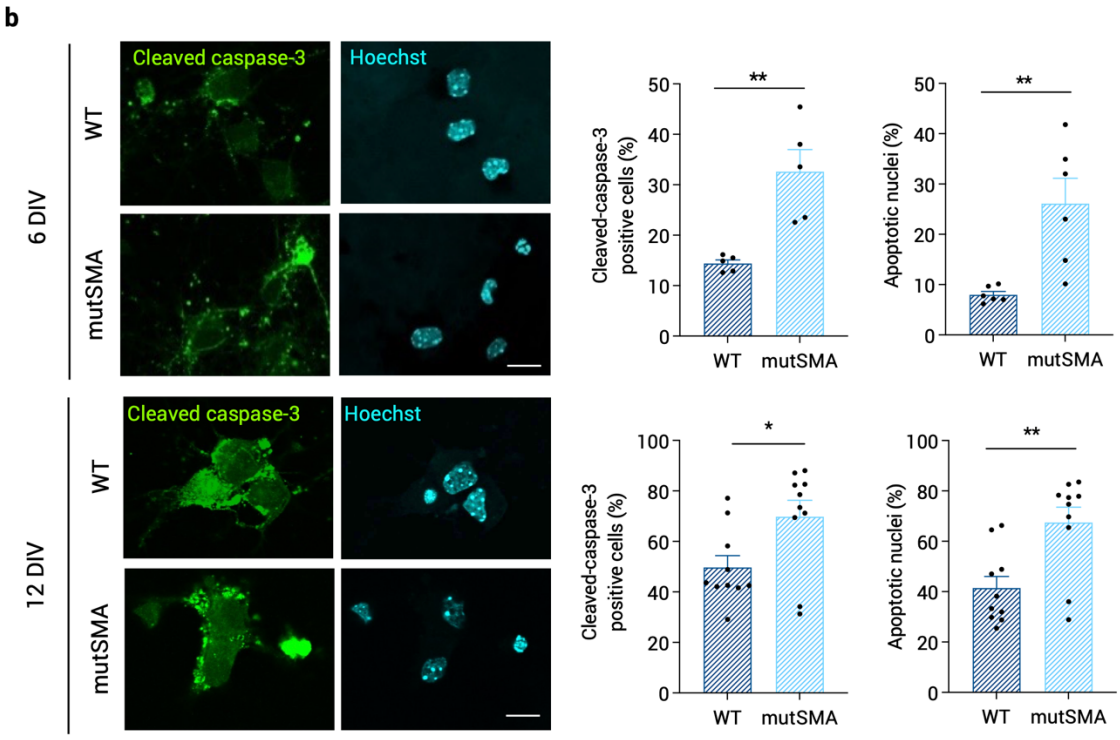

Figure 51 | Cleaved-caspase-3 level and apoptotic nuclei are increased in SMA MNs. (a) Six-day and 12-day (6DIV and 12DIV, respectively) cultured WT and mutSMA spinal cord MNs were submitted to western blot analysis using anti-cleaved-caspase-3 or anti-Smn antibodies. Membranes were reprobed with an anti-α-tubulin antibody, used as a loading control. Graphs represent the expression of cleaved-caspase-3 corresponding to the quantification of at least 6 independent experiments ± SEM. Asterisks indicate differences using Student *t*-test (*p<0.05; **p<0.005). (**b**) Representative confocal images of immunostained 6DIV and 12DIV MNs using an anti-cleaved-caspase-3 antibody. Hoechst (blue) dye was used to identify apoptotic and non-apoptotic nuclei. Graphs represent the percentage of cleaved-caspase-3 positive cells or the percentage of nuclei showing apoptotic morphology, corresponding to the quantification of at least 4 independent experiments (~200 cells/well, 1–2 well/experiment) ± SEM. Asterisks indicate differences using Student *t*-test (**p*<0.05; ***p*<0.01). Scale bar, 15µm.

Further validation of cleaved-caspase-3 presence in spinal cords of Smn-reduced models was assessed in the SMNdelta7 mouse model. For western blot analysis, L1 and L2 spinal cords of P12 wild type (WT) and SMNdelta7 genotyped mice were dissected, tissue was disaggregated and 40µg of protein extracts were submitted to western blot using anti-cleaved-caspase-3 and anti-SMN antibodies. Anti-vinculin antibody was used as a loading control. Results show that Cleaved-caspase-3 protein levels were significantly increased at postnatal day 12 in SMNdelta7 samples (1.26±0.098, p=0.024) compared to the WT control (**Figure 52a**). The percentage of positive cleaved-caspase-3 cells was analyzed in the ventral horn of the spinal cords sections. Results showed a significative increase in the percentage of cleaved caspase-3 positive SMI-32^{+} MNs in SMNdelta7 (59.8±1.57, p<0.0001) spinal cord sections at

P12 (red arrows) compared to the WT control (17.3±2.87), as shown in **Figure 52b**. Altogether, the results obtained in the mutSMA and the SMNdelta7 mice indicate that cleaved-caspase-3 is increased in cultured SMA mouse MNs.

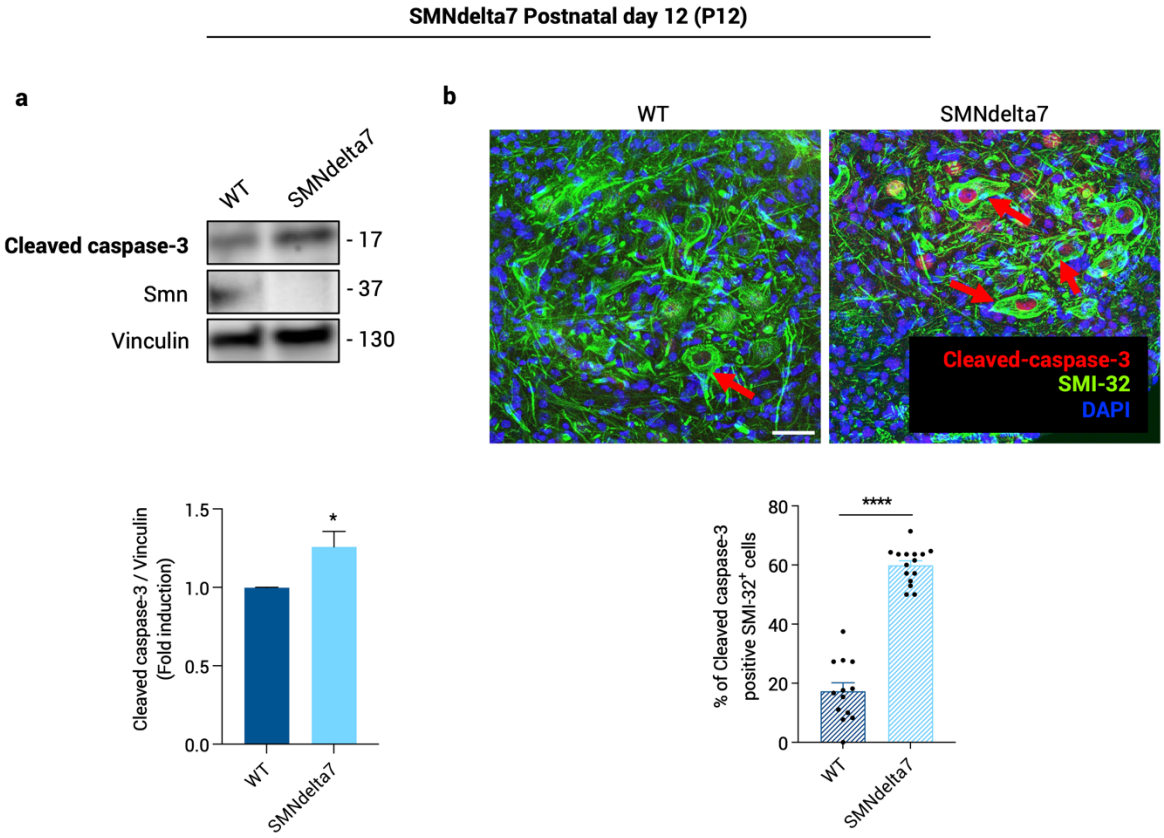

Figure 52 | Cleaved-caspase-3 level is increased in SMNdelta7 spinal cords. Spinal Cords from WT and SMNdelta7 P12 mice were dissected and protein extracts were submitted to western blot analysis (**a**), or fixated with 4% PFA for immunofluorescence analysis (**b**). (**a**) Membranes were blotted with anti-cleaved-caspase-3 antibody or anti-SMN antibody, and reprobed with anti-vinculin antibody as a loading control. Graph values represent the expression of Cleaved-caspase-3 vs vinculin and correspond to the quantification of six independent experiments ± SEM. (**b**) Fixed lumbar spinal cords were cryopreserved and sectioned in a cryostat. Immunofluorescence against cleaved caspase-3 (red) and SMI-32 was performed (green). DAPI (blue) counterstaining was used to identify nuclei. Scale bar, 35µm. Graph represents the percentage of cleaved-caspase-3 and SMI-32 positive cells, corresponding to the quantification of 2 animals per condition (~8 images/animal) ± SEM. Asterisks indicate differences using Student *t*-test (*p<0.05; ****p<0.0001). Scale bar, 15µm.

5. Cleaved caspase-3 protein levels are increased in SMA human MNs

After analyzing cleaved caspase-3 in SMA mouse models, we measured its levels in 7-day differentiated Control and SMA human MNs. Cells were lysed and protein extracts were submitted to western blot analysis using anti-cleaved caspase-3 antibody. Results revealed a significant increase of Cleaved-caspase-3 protein in SMA-differentiated cells (1.19±0.29, p=0.024), compared to the Control **(Figure 53a).** Cleaved-caspase-3 presence was also measured by immunofluorescence, measuring the percentage of stained cells, which was significantly increased in 7-day differentiated SMA human MNs (27.44±2.6, p=0.012) compared to Control (17.3±2.05). Hoechst staining was used to evaluate the percentage of MNs displaying apoptotic features in the nuclei. SMA differentiated MNs presented an increase of apoptotic nuclei (34.22±5.73, p=0.036) compared to Control (18.86±2.72) **(Figure 53b).** These results suggest that apoptosis pathway is deregulated in differentiated SMA human MNs.

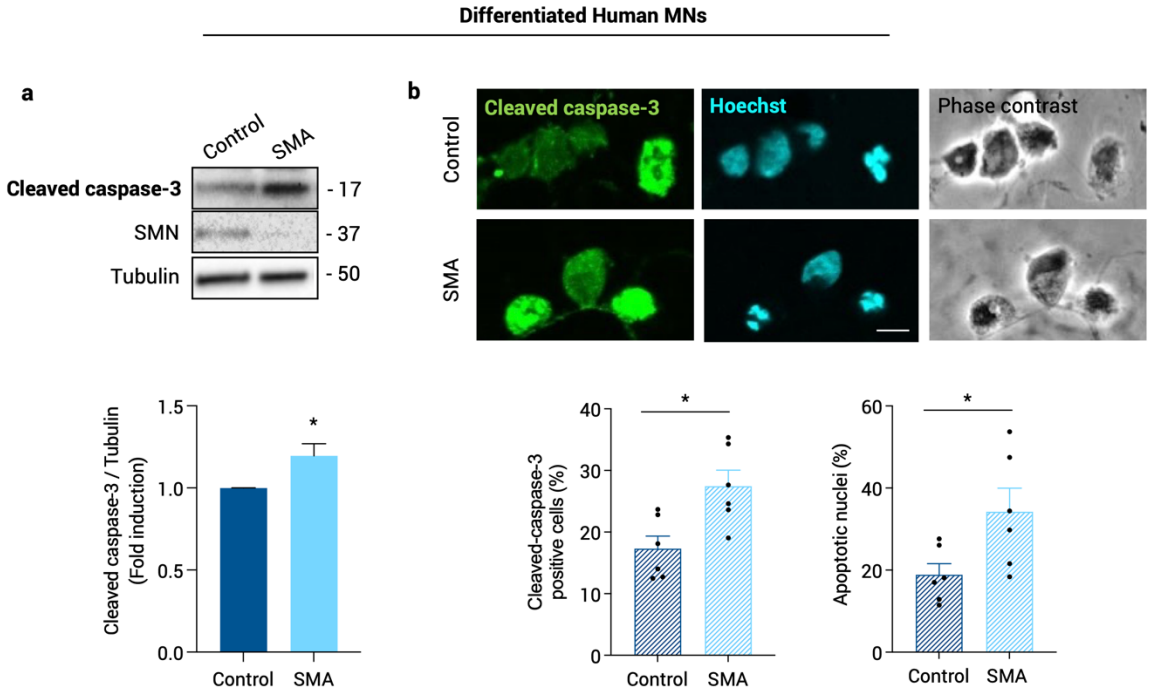

Figure 53 | Cleaved-caspase-3 protein level is increased in differentiated SMA human MNs. (**a**) Protein extracts of 7-day differentiated Control and SMA human MNs were submitted to western blot analysis using anti-cleaved-caspase-3 or anti-SMN antibodies. Membranes were reprobed with an anti-α-tubulin antibody as loading control. Graphs represent the expression of cleaved-caspase-3, corresponding to the quantification of at least 4 independent experiments ± SEM. (**b**) Representative immunofluorescence confocal images of 7-day differentiated human MNs using an anti-cleaved-caspase-3 antibody. Hoechst dye was used to identify apoptotic and non-apoptotic nuclei. Scale bar, 15µm. Graphs represent the percentage of cleaved-caspase-3 positive MNs or the percentage of nuclei with apoptotic morphology, corresponding to the quantification of 3 independent experiments ± SEM. Asterisks indicate differences using Student t-test (*p<0.05).

6. FAIM-L and XIAP protein levels are reduced in spinal cords of mutSMA mice

Next, we studied the antiapoptotic proteins FAIM-L and XIAP in SMA disease models. We measured their levels in protein extracts obtained from embryonic (E) and postnatal (P) spinal cords of SMA mice. Wild type (**WT**) and mutant (**mutSMA**) mice were genotyped and lumbar regions 1 and 2 (L1 and L2, respectively) of the spinal cords were dissected at the following ages: **E13**, **E18**, postnatal days **P0**, **P3** and **P5**. After dissection, tissue was disaggregated and 15μg of protein extracts were submitted to western blot analysis using anti-FAIM-L or anti-XIAP antibodies. Anti-SMN antibody was used to verify the genotype (**Figure 54**).

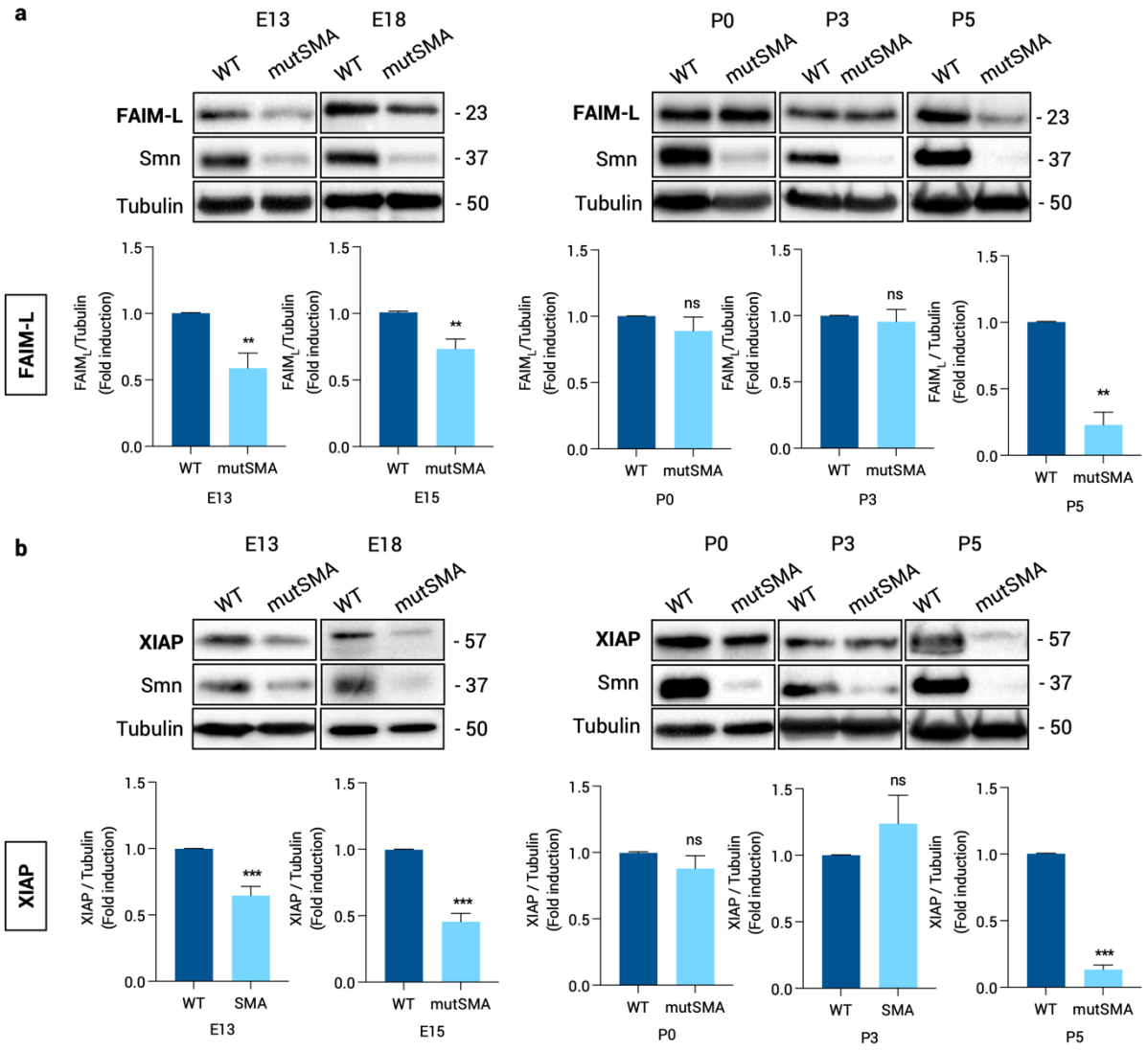

Figure 54 | Antiapoptotic proteins FAIM-L and XIAP levels are reduced in total cell extracts from SMA mice spinal cords. (**a and b**) Spinal Cords from WT and mutSMA E13, E18, P0, P3 and P5 mice were dissected. Protein extracts were submitted to western blot analysis using anti-FAIM-L (**a**), anti-XIAP (**b**) or anti-SMN antibodies (**a and b**). Membranes were reprobed with anti-α-tubulin antibody. Graph values represent the expression of FAIM-L (**a**) or XIAP (**b**) vs α-tubulin and correspond to the quantification of at least 3 independent experiments ± SEM. Asterisks indicate significant differences using Student *t*-test (**p<0.01; ***p<0.0001, no significant differences, ns, p>0.05).

Results showed that both FAIM-L and XIAP protein levels were significantly reduced in E13, E18, and P5 SMA samples (**Figure 54 and Table 27**) compared to the WT control. However, no changes were observed in the levels of these two proteins in SMA P0 and P3 samples compared to WT.

Table 27 | FAIM-L and XIAP levels in protein extracts of lumbar spinal cords fragments from mutSMA compared to the WT controls; ¶ indicate significant differences using Student *t*-test.

	Spinal cord			
	$FAIM_L$		XIAP	
Age	***Mean ± SEM***	***p-value***	***Mean ± SEM***	***p-value***
E13	0.59 ± 0.11	0.0067 ¶	0.65 ± 0.07	0.0004 ¶
E18	0.73 ± 0.07	0.0064 ¶	0.45 ± 0.06	0.0007 ¶
P0	0.89 ± 0.10	0.3289	0.88 ± 0.09	0.1474
P3	0.95 ± 0.09	0.6312	1.24 ± 0.21	0.2510
P5	0.23 ± 0.09	0.0013 ¶	0.13 ± 0.03	< 0.0001 ¶

Next, we wanted to study the localization of FAIM-L protein in the spinal cord of the mutSMA mice. For that, E13 and P3 L1 and L2 segment of the spinal cords of mutSMA and WT mice were dissected, fixed and sectioned at 16μm thickness in a cryostat. Immunofluorescence was performed using a specific antibody against FAIM-L. Nissl staining was used to identify MNs in the spinal cord tissue, and Hoechst dye to localize the nuclei (**Figure 55**). Images revealed a predominant expression of FAIM-L protein specifically in ventral horn MNs of L1 and L2 spinal cord segments. White circles show the localization of the MNs pool in the ventral horns of the spinal cord sections. Bold arrows show both Nissl and FAIM-L positive cells, while thin arrows indicate Nissl and FAIM-L negative cells.

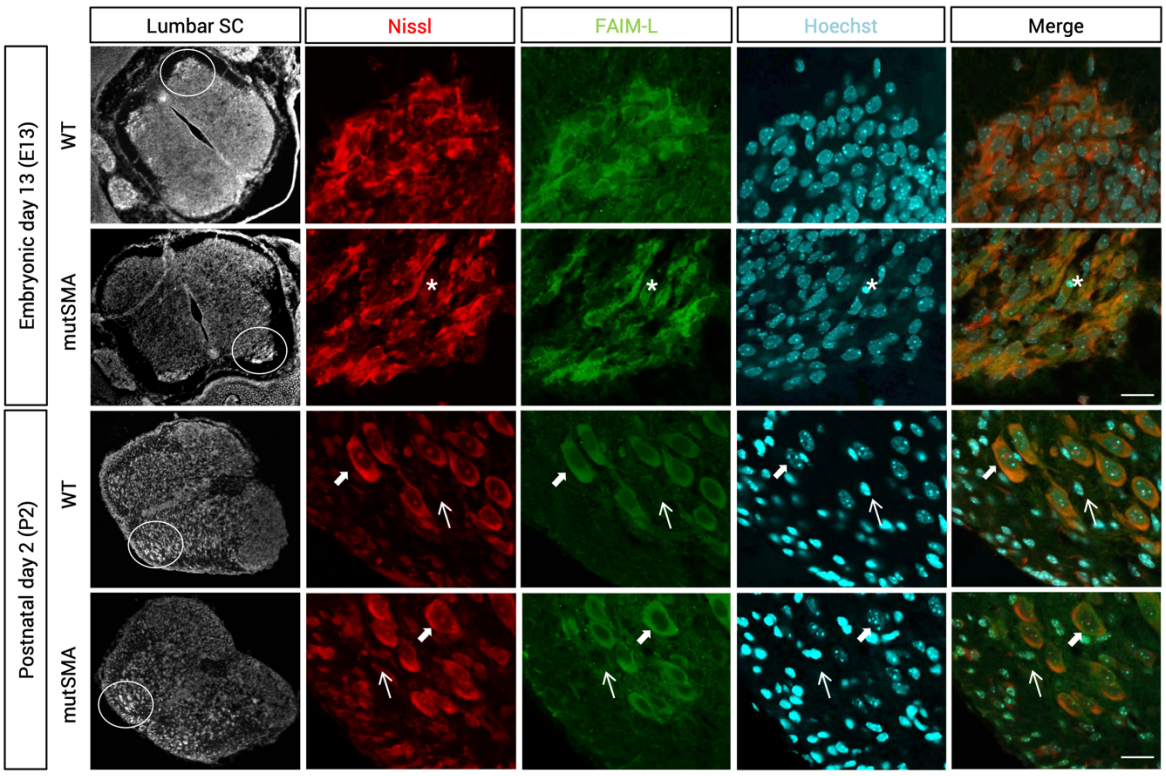

Figure 55 | Representative immunofluorescence images of ventral horn spinal cord sections of embryonic 13-day (E13) and postnatal 3-day (P3) from WT and mutSMA mice. We used an anti-FAIM-L antibody (green) and Nissl staining (red). Nissl and Hoechst (blue) staining were used to identify MNs soma and nucleus, respectively. Scale bar, 20μm. White circles indicate ventral MNs pool localization. Bold arrows indicate Nissl and FAIM-L positive cells and thin arrows indicate Nissl and FAIM-L negative cells. Asterisk indicates the localization of a cell that appears to be undergoing an apoptotic process.

7. In vitro analysis of FAIM-L and XIAP protein levels in cultured spinal cord MNs of SMA mice

We wanted to elucidate whether the alteration of FAIM-L and XIAP levels occurred specifically in MNs. For that, we isolated and cultured MNs from WT and mutSMA genotyped E13 mice. Cultures were maintained during 12 days in vitro (DIV), and cells were collected at 6, 9 and 12 DIV, as indicated in **Figure 56.** These cultured MNs, altogether with isolated non-cultured E13 MNs (0DIV) from the same mouse model, were submitted to protein extraction. Western blot analysis using anti-FAIM-L or anti-XIAP antibodies revealed significant increases in mutSMA MNs, compared to the WT control. FAIM-L was increased at 6DIV, 9DIV and 12DIV and in non-cultured cells (0DIV), and in XIAP protein was increased at 12 DIV and in 0DIV cells, as shown in **Table 28** and in **Figure 56** (**a and b**, respectively). No significant differences in XIAP level were observed in 6DIV and 9DIV WT and mutSMA conditions. Together, these results

indicated that levels of FAIM-L and XIAP proteins are increased in *in vitro* cultured SMA spinal cord MNs, compared to WT control.

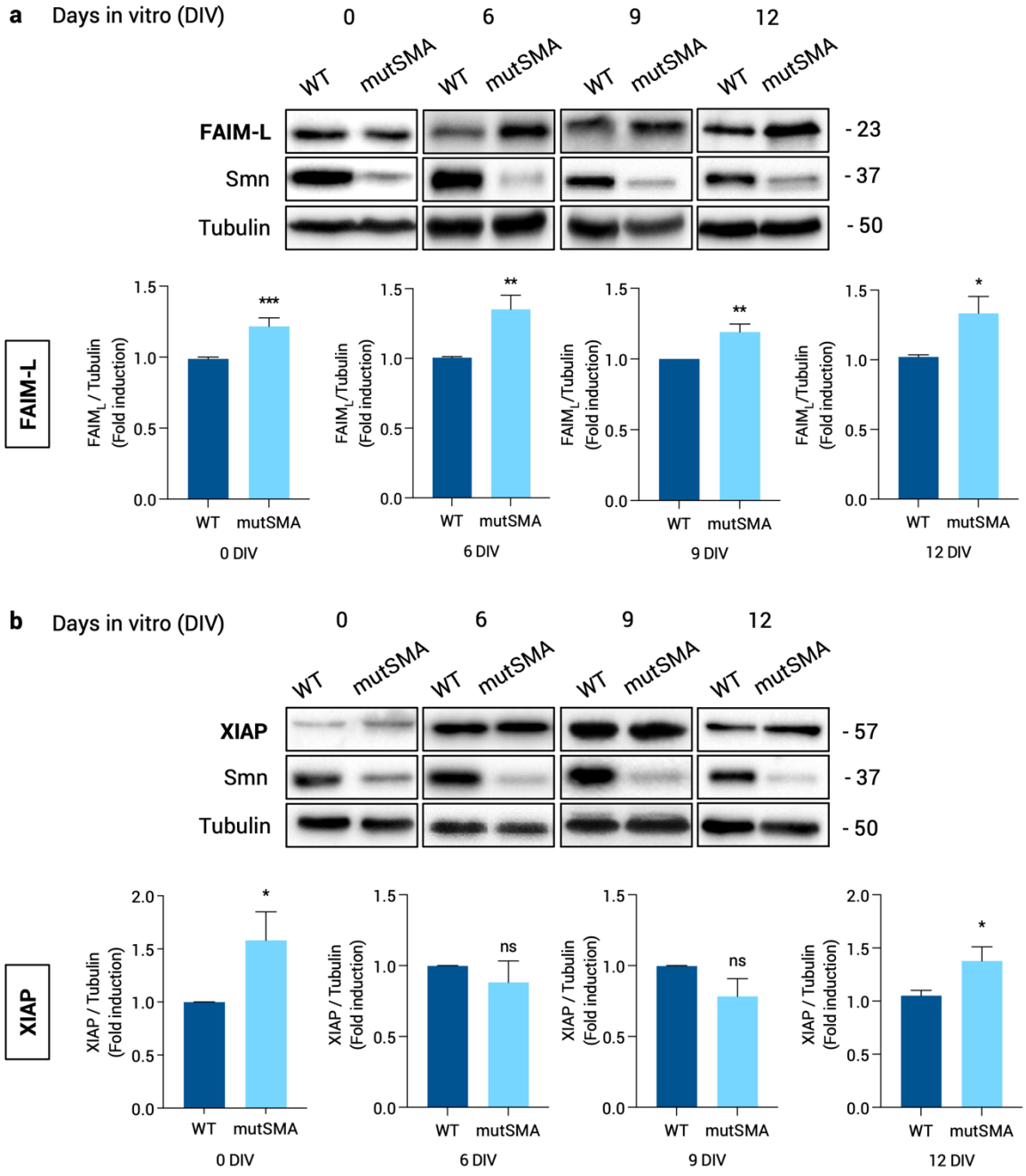

Figure 56 | Antiapoptotic proteins FAIM-L and XIAP levels are increased in cultured SMA spinal cord MNs. Embryonic mouse MNs were isolated from WT and mutSMA spinal cords and cultured in the presence of NTFs. After isolation, 0DIV, 6DIV, 9DIV, and 12DIV total protein extracts were obtained and submitted to western blot analysis. Membranes were probed with anti-FAIM-L antibody (**a**), anti-XIAP antibody (**b**) or anti-SMN antibody (**a and b**). Anti-α-tubulin antibody was used as a loading control. Graph values represent the expression of FAIM-L or XIAP vs α-tubulin and correspond to the quantification of at least 4 independent experiments ± SEM. Asterisks indicate significant differences using Student *t*-test (*p<0.05; **p<0.01; ***p<0.001).

Table 28 | FAIM-L and XIAP levels in protein extracts of cultured spinal cord SMA MNs compared to the WT controls; ¶ indicate significant differences using Student *t*-test.

	Cultured MNs			
	$FAIM_L$		XIAP	
DIV	*Mean ± SEM*	*p-value*	*Mean ± SEM*	*p-value*
0	1.22 ± 0.06	0.0007 ¶	1.5819 ± 0.26	0.0253 ¶
6	1.35 ± 0.10	0.0022 ¶	0.88 ± 0.15	0.4720
9	1.20 ± 0.05	0.0062 ¶	0.78 ± 0.12	0.1620
12	1.34 ± 0.14	0.0293 ¶	1.38 ± 0.13	0.0200 ¶

8. FAIM-L and XIAP dysregulation in differentiated SMA human MNs

Once the differentiated Control and SMA human MNs were characterized, cells were used for western blot analysis experiments to evaluate FAIM-L and XIAP protein levels. For that, protein extracts from 7-day differentiated Control and SMA human MN cells were obtained and submitted to western blot analysis using anti-FAIM-L and anti-XIAP antibodies. Anti-SMN antibody was used to validate the SMA phenotype of the cells. When levels of FAIM-L and XIAP were analyzed, a significant increase of these proteins was observed in SMA-differentiated cells (FAIM-L: 1.33±0.38, p=0.019; XIAP: 1.37±0.73, p=0.034), compared to the Control cells (**Figure 57**). Together, these results indicated that levels of FAIM-L and XIAP proteins are increased in differentiated SMA human MNs compared to Control.

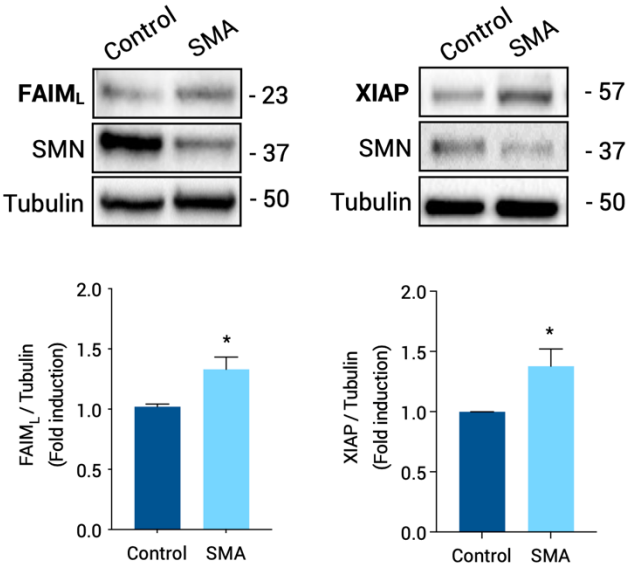

Figure 57 | FAIM-L and XIAP protein levels are increased in differentiated SMA and Control human MNs. Protein extracts of 7-day differentiated Control and SMA human MNs were submitted to western blot analysis using anti-FAIM-L antibody or anti-XIAP antibody or anti-SMN antibody. Membranes were reprobed with anti α-tubulin antibody as a loading control. Graphs represent the expression of FAIM-L or XIAP vs α-tubulin, corresponding to the quantification of at least 4 independent experiments ± SEM. Asterisks indicate differences using Student *t*-test (*p<0.05).

9. XIAP protein level is reduced in SMA human fibroblasts

The differential results in the level of FAIM-L and XIAP proteins observed between spinal cord tissue and cultured MNs led us to evaluate other SMN-reduced cell types. Human SMA (SMAII and SMAI) and one unaffected control fibroblast cell line (Control) (Coriell Institute) were analyzed using western blot and immunofluorescence analysis.

For western blot analysis, 2-day cultured cells were lysed and protein extracts were submitted to western blot and probed against anti-XIAP antibody. Anti-SMN antibody was used to verify SMN reduction in these cells. As expected, SMN protein level was significantly reduced in cell lysates from SMA fibroblasts (SMAII: 0.31±0.03; SMAI: 0.26±0.04, p<0.0001) compared to the clinically unaffected control (**Figure 58a**). These SMN-reduced fibroblasts presented significantly reduced XIAP protein level (SMAII: 0.69±0.06, p=0.0025; and SMAI: 0.75±0.07, p=0.07) compared to the control condition (**Figure 58a**).

For immunofluorescence analysis, fibroblasts were cultured onto collagen-coated glass coverslips, fixed and submitted to immunofluorescence protocol using the anti-XIAP antibody. Images were acquired with an FV10I confocal microscope (Olympus) using the x60 objective and the same microscopic settings. Relative fluorescence level of XIAP was

measured (**see Materials and Methods section 8.5**) and expressed as the Corrected Total Cell Fluorescence (CTCF). As observed in **Figure 58b**, XIAP fluorescence levels were significantly reduced in SMA fibroblasts (SMAII: 8.43±0.68, and SMAI: 11.75±0.67, $p<0.0001$) compared to the Control (20.56±1.51). These results indicated that cultured human SMA fibroblasts show reduced levels of the antiapoptotic protein XIAP.

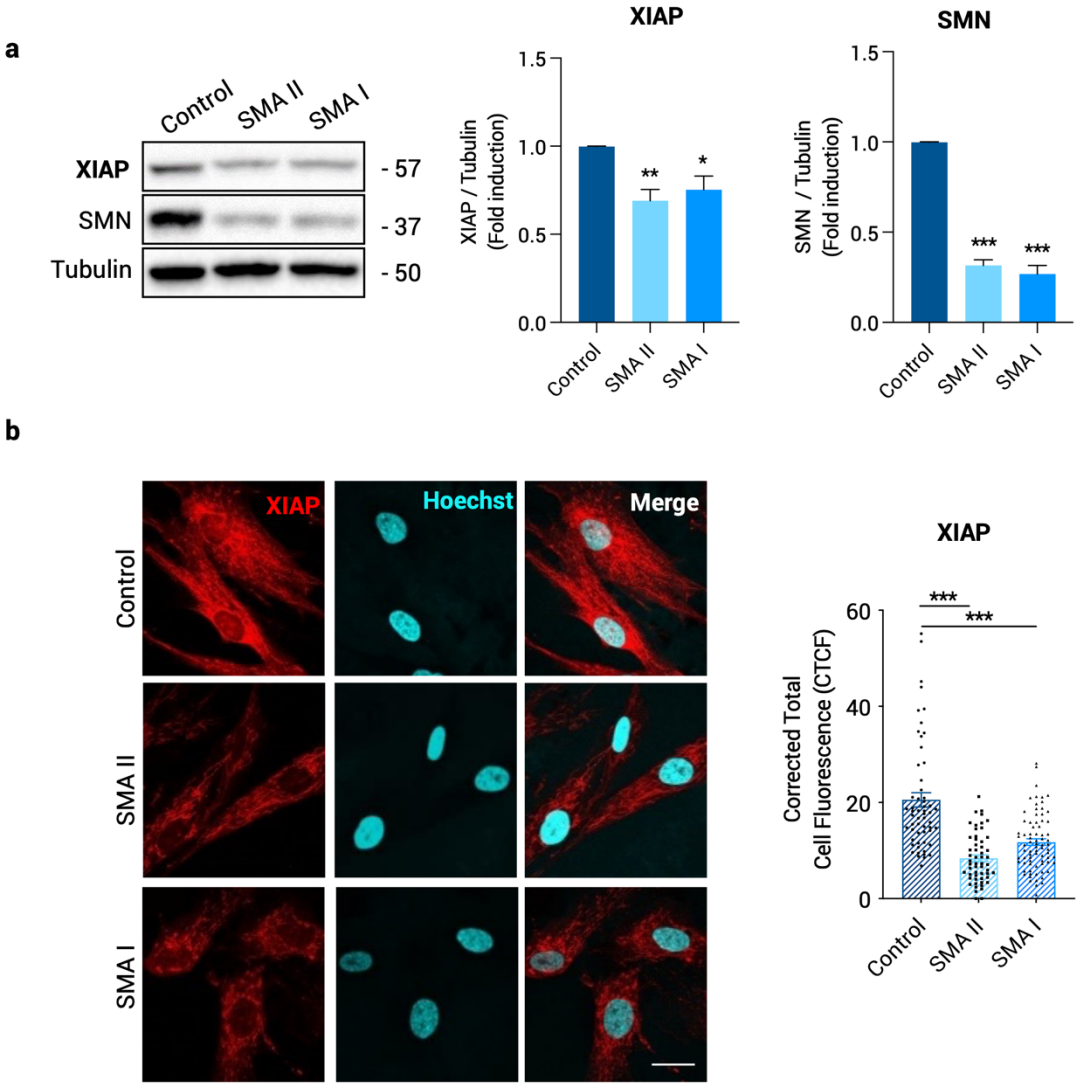

Figure 58 | XIAP protein level is reduced in cultured SMA human fibroblasts. Control, SMAII and SMAI patient fibroblast cell lines were plated and maintained in the presence of supplemented MEM. Two days after, cells were submitted to western blot **(a)** or fixed and prepared for immunofluorescence analysis (**b**). **(a)** Membranes were probed with anti-SMN or anti-XIAP antibodies. Anti- α-tubulin antibody was used as loading control. Graph values represent the expression of XIAP or SMN vs α-tubulin and correspond to the quantification of 4 independent experiments ± SEM. **(b)** Representative immunofluorescence images of 2-day cultured fibroblasts in Control, SMAII and SMAI, showing XIAP (red) and Hoechst (blue), to identify fibroblast nuclei. Scale bar, 25µm. Graph represents the mean of relative XIAP fluorescence measured in fibroblasts soma, corresponding to the quantification of at least 25-30 cells per condition from 3 independent experiments ± SEM. Asterisks indicate significant differences using Student *t*-test (*$p<0.01$; **$p<0.001$; ***$p<0.0001$).

CHAPTER 2. INTRACELLULAR PATHWAYS INVOLVED IN CELL SURVIVAL ARE DEREGULATED IN MOUSE AND HUMAN SPINAL MUSCULAR ATROPHY MOTONEURONS

SUMMARY

MN development and physiology relies on a continuous and regulated trophic support induced by NTFs that trigger the activation of several signaling pathways by binding to their membrane receptors (Tovar-y-Romo et al., 2014).

The PI3K/Akt and the ERK MAPK signaling pathways are two of the most crucial for survival and maintenance amongst the pathways activated by this trophic support, and can induce cell survival on spinal cord MNs (M. V. Chao, 2003). Akt activation can lead to the phosphorylation of transcription factors and other cytosolic proteins, controlling apoptosis through BAD inhibition, or the transcription and translation of pro-survival molecules (LoPiccolo et al., 2008). ERK MAPK pathway activation can lead to the nuclear translocation of phosphorylated ERK protein, activating transcription factors such as c-Myc, c-Jun, Ets1, and Elk-1, and controlling processes like cell cycle, migration, differentiation, survival and apoptosis (Bodart, 2010; LoPiccolo et al., 2008). Therefore, both signaling pathways converge in the regulation of physiological functions of the cells by activating transcription factors that promote cell survival and prevent cell death (**Figure 59**).

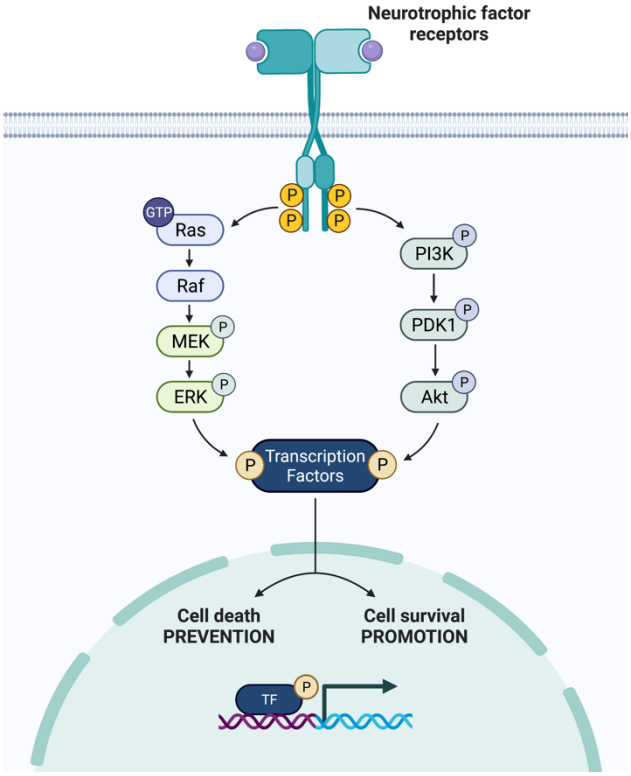

Figure 59 | Schematic simplified representation of PI3K/Akt and ERK MAPK signaling pathways. Created with BioRender.com.

Given the implication of both signaling pathways in MN survival, we wanted to explore whether they are altered in SMN-reduced cells. To this aim, in this chapter we have studied PI3K/Akt and ERK MAPK intracellular survival pathways in mouse and human SMA MNs and their role on the modulation of SMN protein.

1. PI3K/Akt and ERK MAPK intracellular pathways are altered in mouse and human SMA MNs in vitro

To explore whether PI3K/Akt and ERK MAPK pathways are modified in SMN-reduced cells, WT and mutSMA mouse MNs or differentiated Control and SMA human MNs were used for the experiments.

First, WT and mutSMA MNs were isolated from genotyped E13 embryos. Cells were maintained in the presence of NTFs during 6 days and protein extracts were obtained and submitted to western blot analysis using an anti-phospho-Akt (Thr308) (p-Akt) and anti-pan-Akt antibodies. Akt phosphorylation in Thr308 was significantly reduced in mutSMA cells (0.58±0.02, $p<0.0001$) compared to the WT control, whereas no significant differences of Akt protein level were observed in WT and mutSMA (0.9±0.06, $p=0.1$) conditions (**Figure 60a**). On the other hand, human SMA and Control iPSC were in vitro differentiated to MNs, and 7 days after differentiation total cells lysates were collected and analyzed by western blot. Anti-phospho-Akt (Thr308) and anti-Akt antibodies were blotted. Thr308 phosphorylation (0.64±0.09, $p=0.0058$) and Akt protein level (0.82±0.04, $p=0.0003$) were significantly reduced in SMA human MNs compared to the Control condition (**Figure 60b**).

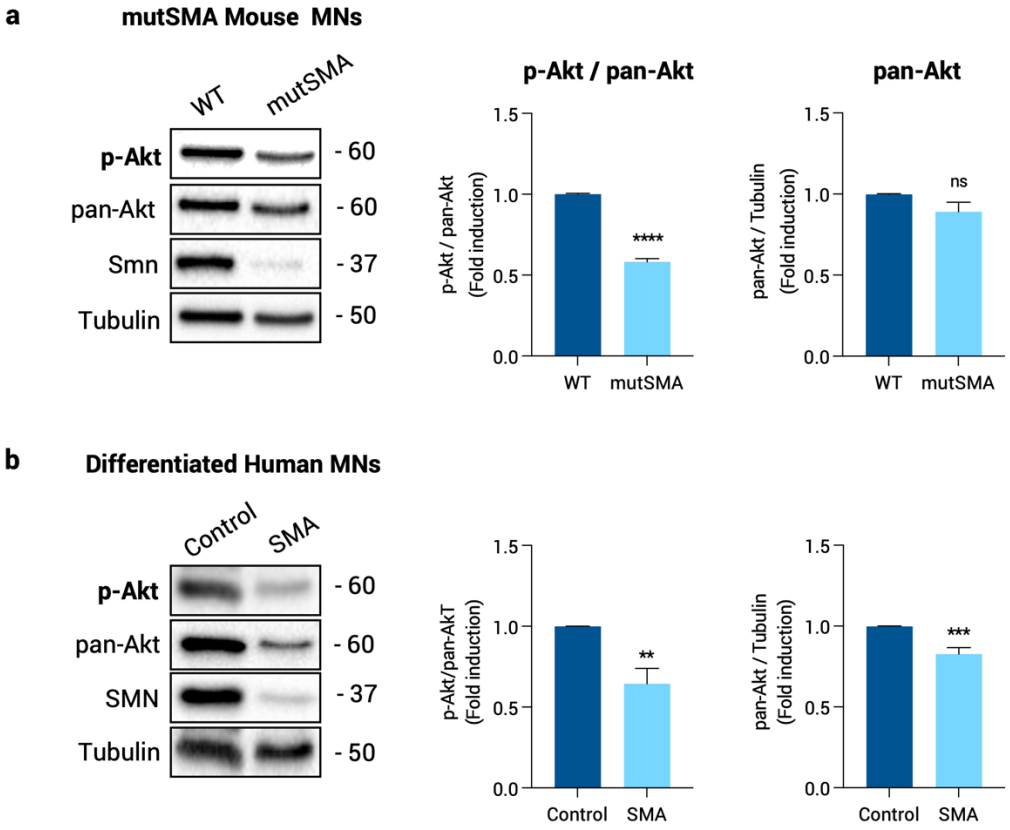

Figure 60 | Changes of Akt phosphorylation in protein extracts of SMN-reduced cells. (**a**) WT and mutSMA spinal cord MNs were isolated and cultured in the presence of NTFs, and (**b**) Control and SMA human MNs were cultured in MN maturation medium. Six (**a**) or seven (**b**) days after plating, protein extracts were obtained and submitted to western blot analysis using anti-phospho-Akt (Thr308) and anti-SMN antibodies. Membranes were stripped and reprobed with an anti-Akt antibody, or reprobed with an anti-α-tubulin antibody. Graphs represent the expression of pan-Akt or the expression of p-Akt versus pan-Akt and indicate fold-reduction contrasted with WT (**a**) or Control (**b**) condition from at least 3 independent experiments ± SEM. Asterisks indicate differences using Student *t*-test (**p<0.01; ***p<0.001;****p<0.0001; no significant differences, ns, p>0.05).

Next, we evaluated the activation and levels of ERK protein in both mouse and human SMN-reduced models. In western blot experiments, phosphorylated ERK was significantly increased in mutSMA mouse cultures (2.15±0.31, p=0.0024) compared to the WT control. No changes in total ERK protein level were found in mutSMA samples (0.9±0.08, ns p=0.27) compared to the WT controls (**Figure 61a**). A similar profile of ERK protein level and phosphorylation was observed in differentiated SMA human MNs; no changes in total ERK protein level in SMA cells (1.06±0.08, ns p=0.72), and increased ERK phosphorylation in SMA cells (4.16±1.36, p=0.043) compared to the control condition (**Figure 61b**).

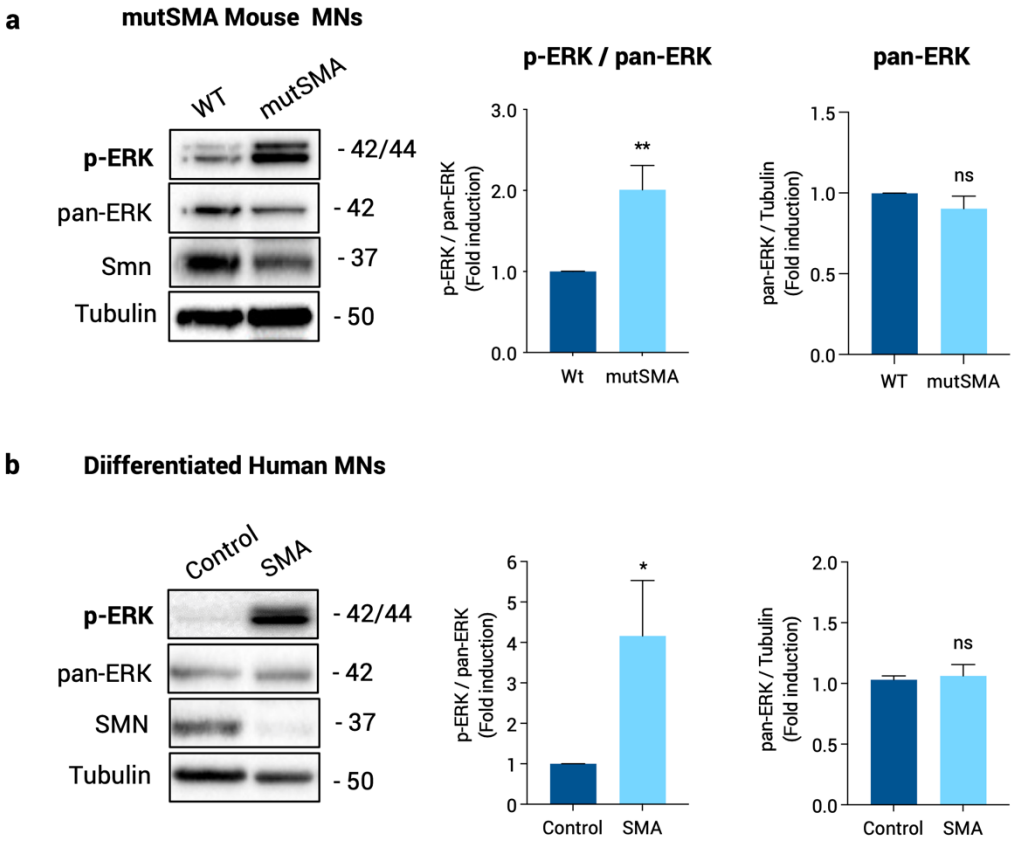

Figure 61 | ERK phosphorylation is increased in protein extracts of SMN-reduced cells. (**a**) WT and mutSMA spinal cord MNs were isolated and cultured in the presence of NTFs, and (**b**) Human Control and SMA MNs were cultured and differentiated in MN maturation medium. Six (**a**) or seven (**b**) days after plating, protein extracts were obtained and submitted to western blot analysis using anti-phospho-44/42 MAPK (ERK1/2) (Thr202/Tyr204) and anti-SMN antibodies. Membranes were stripped and reprobed with an anti-ERK antibody, or reprobed with an anti-α-tubulin antibody. Graphs represent the expression of ERK or the expression of phospho-ERK versus ERK and indicate fold-induction contrasted with WT (**a**) or Control (**b**) condition from at least 3 independent experiments ± SEM. Asterisks indicate differences using Student *t*-test (*p<0.05;**p<0.01; no significant differences, ns, p>0.05).

2. PI3K/Akt pathway regulates SMN at protein level in SMA MNs

Since Akt phosphorylation was decreased in SMN-reduced MNs, we hypothesized that PI3K/Akt pathway inhibition may be likely to modulating Smn levels. For that, we evaluated whether this pathway could have a role in the regulation of Smn using CD1 MNs, where Akt is not altered.

To this end, 6-day CD1 cultured MNs were treated with or without 25μM of the PI3K inhibitor LY294002 during 24 h. Cell lysates were obtained and submitted to western blot analysis. Anti-phospho-Akt (Thr308) (p-Akt), anti-Akt (pan-Akt) and anti-SMN antibodies were

probed in the immunoblot. Results showed that the addition of LY294002 caused a significant reduction in Akt phosphorylation (+LY: 0.068±0.015, p<0.0001) compared to the non-treated control (-LY), while pan-Akt protein levels did not change (+LY: 0.83±0.11, p=0.18) compared to the non-treated control (-LY). Additionally, when Smn level was analyzed, we observed a significant reduction of this protein in LY294002-treated condition (+LY: 0.58±0.078, p=0.0007) compared to the non-treated control (-LY) (**Figure 62**), suggesting that PI3K inhibition regulates Smn level in MNs.

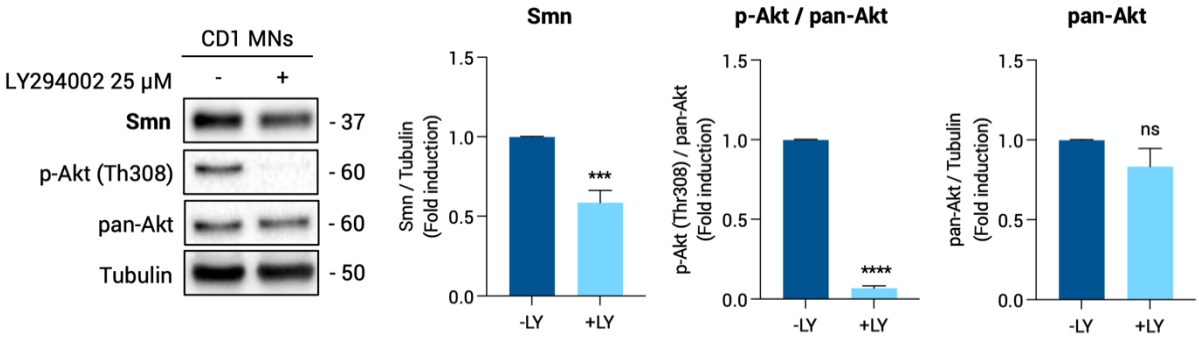

Figure 62 | PI3K/Akt pathway regulates Smn protein level in CD1 MNs. CD1 spinal cord MNs were isolated and cultured in the presence of NTFs. Six days after plating, cells were treated with 25µM LY294002 or left untreated. Twenty-four h later, protein extracts were obtained and submitted to western blot analysis using anti-phospho-Akt (Thr308) and anti- SMN antibodies. Membranes were stripped and reprobed with an anti-Akt antibody or reprobed with an anti-α-tubulin antibody. Graphs represent the expression of Smn vs α-tubulin, phospho-Akt vs Akt and total Akt vs α-tubulin, and correspond to the quantification of at least 3 independent experiments ± SEM. Asterisks indicate differences using Student t-test (***p<0.001;****p<0.0001; no significant differences, ns, p>0.05).

Next, we evaluated the effect of the inhibition of PI3K/Akt pathway in Smn-reduced MNs. To this end, six-day cultured WT and mutSMA MNs were treated or not with the PI3K inhibitor LY294002 (25µM). Twenty-four h later, protein extracts were obtained and submitted to western blot analysis using anti-phospho-Akt (Thr308), anti-Akt and anti-SMN antibodies. When the LY294002 inhibitor was added to the culture medium, Akt phosphorylation was significantly decreased in LY-treated conditions (+LY WT: 0.42±0.10, p=0.0002; +LY mutSMA: 0.43 ± 0.11, p=0.0002) compared to their respective WT and mutSMA untreated controls (-LY). In contrast, pan-Akt levels did not change (+LY WT: 0.83±0.04, p=0.2; +LY mutSMA: 0.79±0.12, p=0.1) compared to the WT and mutSMA untreated controls (-LY). When Smn level was analyzed, we observed a significant reduction of this protein in LY294002-treated WT (+LY: 0.57±0.09, p=0.0005) and mutSMA (+LY: 0.42 ± 0.06, p<0.0001) conditions compared to their respective non-treated controls (-LY) (**Figure 63**).

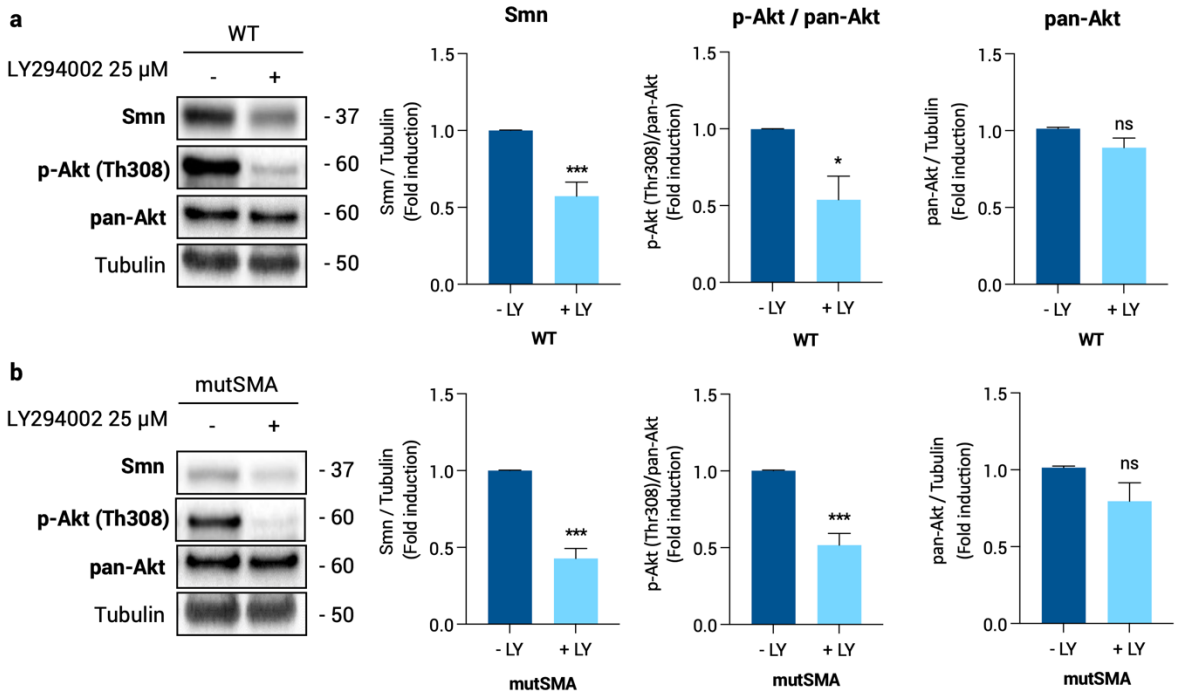

Figure 63 | PI3K/Akt pathway regulates Smn protein level in mutSMA MNs. Six-day WT and mutSMA cultured MNs were treated or not with 25µM of LY294002 during 24 h. Cell lysates were obtained and submitted to western blot analysis using anti-phospho-Akt (Thr308) and anti-SMN antibodies. Membranes were stripped and reprobed with an anti-Akt antibody or reprobed with an anti-α-tubulin antibody. Graphs represent the expression of Smn vs α-tubulin, and correspond to the quantification of at least 3 independent experiments ± SEM. Asterisks indicate differences using Student *t*-test (***p<0.001; no significant differences, ns, p>0.05).

To validate the results obtained with the PI3K/Akt inhibition in the CD1 and the mutSMA mouse model, we treated 7-day differentiated Control and SMA human MNs with the LY294002 inhibitor (25µM for 24 h). Cell lysates were submitted to western blot analysis using anti-phospho-Akt (Thr308), anti-Akt and anti-SMN antibodies. When the LY294002 inhibitor was added to the culture medium, Akt phosphorylation was significantly decreased in LY-treated cells (+LY Control: 0.691±0.075, p=0.001; +LY SMA: 0.72±0.094, p=0.014) compared to the WT and SMA untreated respective controls (-LY), whereas total Akt didn't change in LY-treated cells neither in Control nor in SMA condition (+LY Control: 0.93±0.03, p=0.09; +LY SMA: 0.96±0.05, p=0.52). When SMN level was analyzed, we observed a significant reduction of this protein in LY294002-treated Control (+LY Control: 0.67 ± 0.079, p=0.0024) and SMA (+LY SMA: 0.57±0.108, p=0.0033) conditions compared to the non-treated controls (-LY Control and -LY SMA, respectively) (**Figure 64**). Together, these results suggest that PI3K/Akt signaling pathway regulates SMN protein level in SMA and non-SMA mouse and human MNs.

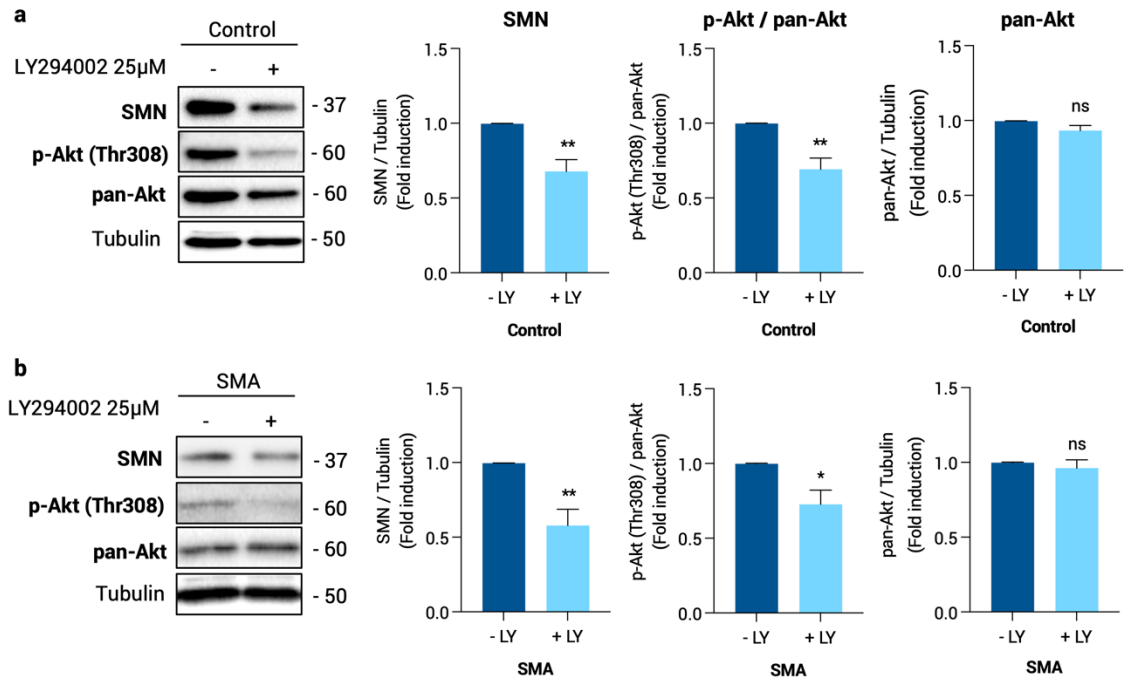

Figure 64 | PI3K/AKTpathway regulates Smn protein level in Control and SMA human MNs. Seven-day Control and SMA human differentiated MNs were treated or not with 25μM of LY294002 during 24 h. Cell lysates were obtained and submitted to western blot analysis using anti-phospho-Akt (Thr308) and anti-SMN antibodies. Membranes were stripped and reprobed with an anti-Akt antibody or reprobed with an anti-α-tubulin antibody. Graphs represent the expression of SMN vs α-tubulin, and phospho-Akt vs Akt, and correspond to the quantification of at least 3 independent experiments ± SEM. Asterisks indicate differences using Student *t*-test (*p<0.05;**p<0.01; no significant differences, ns, p>0.05).

3. ERK MAPK intracellular pathway regulates SMN at protein level in SMA MNs

Previous results in the literature have described an increased phosphorylation of ERK (p-ERK) protein in several murine and human SMA models (Hensel et al., 2017). Moreover, its association in SMN transcription has been postulated (Biondi et al., 2015; Demir et al., 2011). Here we wanted to validate these findings in our mouse and human SMA models. To this end, we examined the levels of Smn protein in mouse CD1, WT and mutSMA MNs, and differentiated Control and SMA human MNs, when the ERK MAPK pathway was inhibited by the addition of 20μM of U0126 (U0), a well-known inhibitor of the ERK MAPK pathway.

Six-day cultured CD1, or WT and mutSMA MNs were treated or not with the ERK inhibitor U0126 (20μM). Twenty-four h later, cell lysates were obtained and submitted to western blot using anti-phospho-ERK, anti-ERK and anti-SMN antibodies. Results showed that 6-day CD1 U0126-treated cells presented a significant reduction of ERK phosphorylation (+U0: 0.116±0.074, p<0.0001) while the total ERK levels (+U0: 1.411±0.363, p=0.3) did not change.

Smn protein level analysis revealed a significant decrease in U0126-treated cells (+U0: 0.675±0.076, p=0.0053) compared to the non-treated control (**Figure 65**).

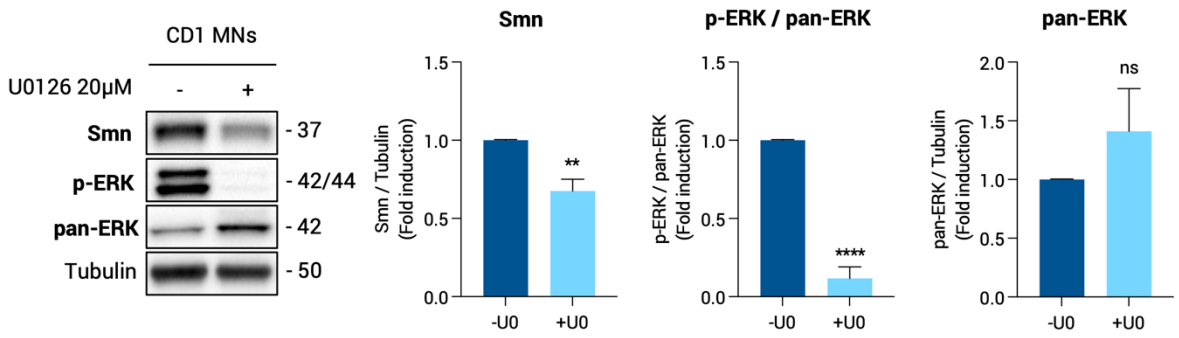

Figure 65 | ERK MAPK pathway regulates Smn protein level in CD1 MNs. Six-day CD1 cultured MNs were treated or not with 20µM of U0126 during 24 h. Cell lysates were then obtained and submitted to western blot analysis using anti-phospho-42/44 MAPK (ERK1/2)(Thr202/Tyr204) and anti-SMN antibodies. Membranes were stripped and reprobed with an anti-ERK antibody or reprobed with an anti-α-tubulin antibody. Graphs represent the expression of Smn vs α-tubulin, phospho-ERK vs ERK and total ERK vs α-tubulin, and correspond to the quantification of 4 independent experiments ± SEM. Asterisks indicate differences using Student *t*-test (**p<0.01;****p<0.0001; no significant differences, ns, p>0.05).

Similar results were observed when the U0126 inhibitor was added to the medium of cultured WT and mutSMA MNs; the ratio of p-ERK versus total ERK protein was significantly decreased (+U0 WT: 0.122±0.040, p<0.0001; +U0 mutSMA: 0.104±0.318, p=0.0005) compared to the WT and mutSMA untreated respective controls (-U0) (**Figure 66**), whereas total ERK protein levels didn't change (+U0 WT: 1.14±0.18, p=0.46; +U0 mutSMA: 1.3±0.21, p=0.09). When analyzing Smn protein levels, we observed a significant reduction in U0126-treated (+U0 WT: 0.385±0.081, p<0,0001; +U0 mutSMA: 0.055±0.054, p=0.018) conditions compared to the non-treated controls (-U0 WT and -U0 mutSMA, respectively) (**Figure 66**).

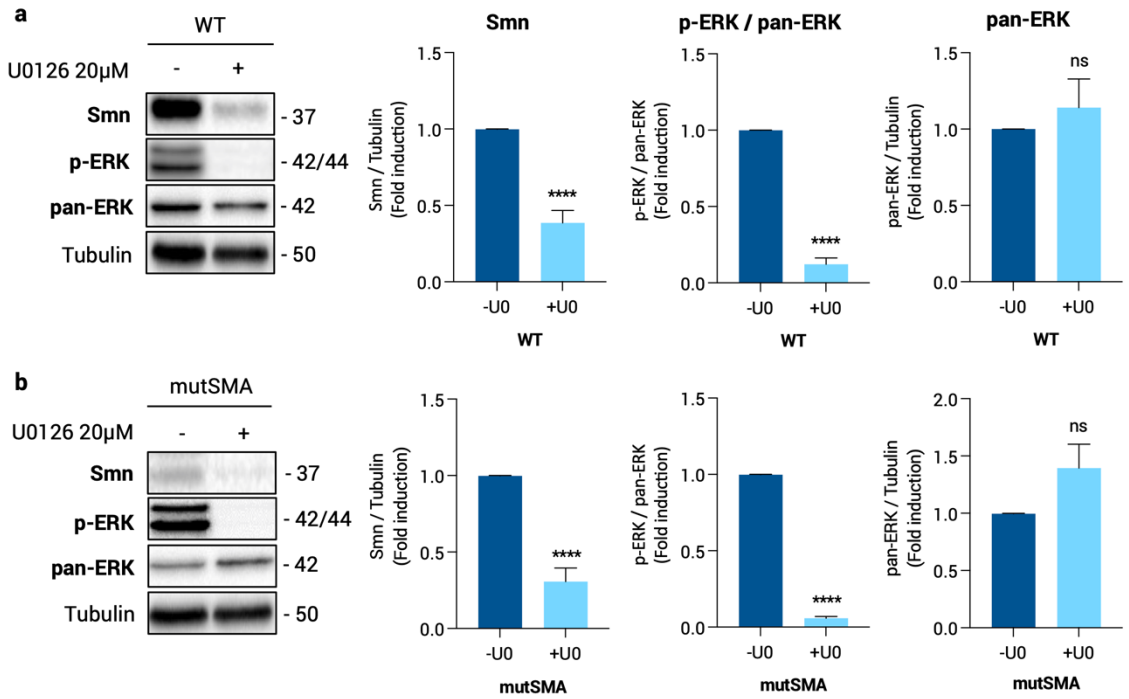

Figure 66 | ERK MAPK pathway regulates Smn protein level in WT and mutSMA MNs. Six-day WT and mutSMA cultured MNs were treated or not with 20μM of U0126 during 24 h. Cell lysates were submitted to western blot analysis using anti-phospho-42/44 MAPK (ERK1/2)(Thr202/Tyr204) and anti-SMN antibodies. Membranes were stripped and reprobed with an anti-ERK antibody or reprobed with an anti-α-tubulin antibody. Graphs represent the expression of Smn vs α-tubulin and phosphor-ERK vs ERK, and correspond to the quantification of at least 3 independent experiments ± SEM. Asterisks indicate differences using Student *t*-test (****p<0.0001; no significant differences, ns, p>0.05).

Next, we explored the effect of U0126-mediated ERK inhibition on SMN levels in differentiated Control and SMA human MNs. Seven day-differentiated Control and SMA human MNs were treated with or without 20μM U0126. After 24 h protein extracts were obtained and submitted to western blot analysis. Anti-phospho-ERK, anti-ERK and anti-SMN antibodies were probed, using tubulin as a loading control. Results indicated that the addition of the ERK inhibitor U0126 to the culture medium reduced significantly the ratio of p-ERK versus total ERK (+U0 Control: 0.29±0.076, p<0.0001; +U0 SMA: 0.36±0.100, p<0.0001) compared to the Control and SMA untreated respective conditions (-U0) (**Figure 67**). No changes in total ERK protein levels (+U0 Control: 1.23±0.23, p=0.32; +U0 SMA: 0.8±0.1, p=0.07) were observed when compared the U0126-treated cells with their respective controls (-U0) (**Figure 67 a and b**). Moreover, SMN protein level was significantly decreased in both Control and SMA conditions when treated with the U0126 inhibitor (+U0 Control: 0.80±0.065, p=0.0096; +U0 SMA: 0.47±0.054, p<0.0001), compared to their respective non-treated controls (**Figure 67**).

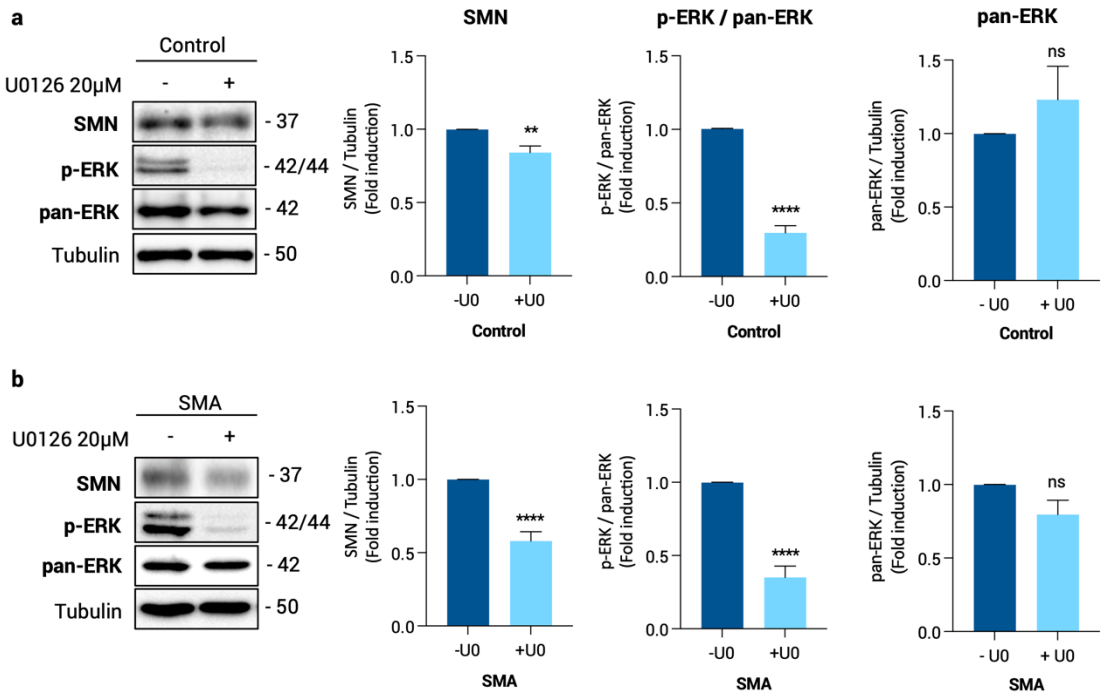

Figure 67 | ERK MAPK pathway regulates SMN protein level in differentiated Control and SMA human MNs. Seven-day Control (**a**) and SMA (**b**) human differentiated MNs were treated or not with 20µM of U0126 during 24 h. Cell lysates were obtained and submitted to western blot analysis using anti-phospho-42/44 MAPK (ERK1/2)(Thr202/Tyr204) and anti-SMN antibodies. Membranes were stripped and reprobed with an anti-ERK antibody or reprobed with an anti-α-tubulin antibody. Graphs represent the expression of SMN vs α-tubulin and phospho-ERK vs ERK, and correspond to the quantification of at least 3 independent experiments ± SEM. Asterisks indicate differences using Student *t*-test (**p<0.01;****p<0.0001; no significant differences, ns, p>0.05).

4. PI3K/Akt pathway regulates SMN at transcriptional level in mouse and human MNs

To determine whether Smn reduction caused by LY294002 treatment was associated with decreased activity of *Smn* gene expression, we quantified *Smn* (mouse) or *SMN* (human) messenger RNA (mRNA) by quantitative RT-PCR (qRT-PCR) in both CD1 and human differentiated MNs. *Gapdh* (mouse) or *GAPDH* (human) genes were used as a control. Embryonic (E13) spinal cord isolated CD1 mice MNs and differentiated Control and SMA human MNs were cultured during 6 or 7 days, respectively, and then treated with or without 25µM LY294002. After 24 h, total RNA was extracted and reverse-transcribed to cDNA, used as a template to quantify *Smn* or *SMN* transcript level. LY294002 addition was related to a reduction in *Smn* mRNA expression in CD1 MNs (+LY: 0.58±0.034, p<0.0001) compared with control non-treated condition (**Figure 68a**). When analyzing *SMN* mRNA expression in differentiated Control and SMA human MNs, we observed that LY-treated Control and SMA

cells presented significantly reduced levels of *SMN* mRNA (+LY Control: 0.79±0.06, p=0.029; + LY SMA: 0.80±0.048, p=0.004) when compared to their control condition (-LY Control and -LY SMA, respectively) (**Figure 68b**). Together, these results showed that PI3K/Akt inhibition regulates Smn at transcriptional level in SMA and non-SMA mouse and human MNs.

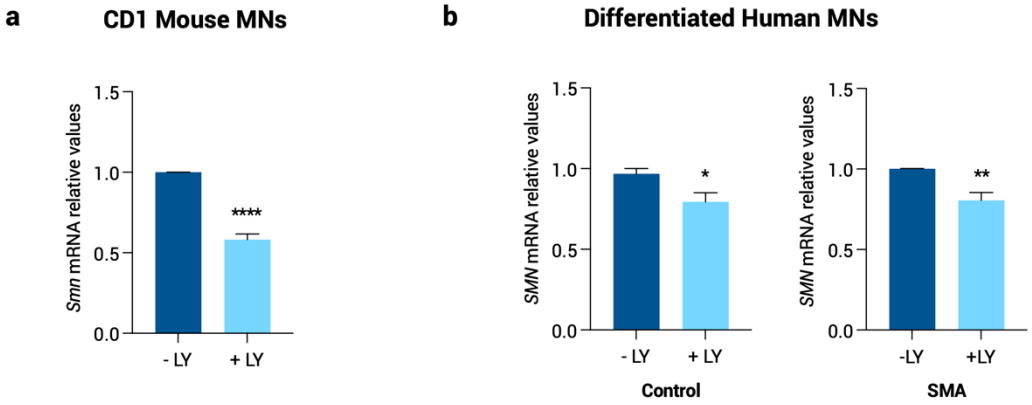

Figure 68 | PI3K/AKT pathway regulates SMN at transcriptional level. Total RNA was extracted from 25µM LY294002-treated (+LY) or non-treated (-LY) 6-day CD1 MN cultures (**a**) and seven-day differentiated Control and SMA human MN cultures (**b**). Reverse transcription to cDNA and *Smn* (**a**) or *SMN* (**b**) amplification was done. *Gapdh* (**a**) or *GAPDH* (**b**) gene was used as control. Graph values are the mean of *Smn* (**a**) or *SMN* (**b**) gene expression from 3 independent experiments ± SEM. Asterisks indicate significant differences using Student *t*-test (*p<0.05;**p<0.01;****p<0.0001).

Next, we evaluated *Gemin2* mRNA regulation in these two MN models. Gemin2 is part of a protein complex formed by SMN protein, Unrip, and other Gemins, and has specific functions such as vesicle trafficking in the axonal compartment (H. Zhang et al., 2006). Gemin2 protein regulation is associated with SMN; for instance, SMN-deficient ES cells presented reduced SMN and Gemin2 levels (C. Y. Wu et al., 2011), and SMN reduction by RNA interference caused Gemin2 and other Gemins decrease (W. Feng et al., 2005). Moreover, Gemin2 reduction strongly decreased SMN complex activity (W. Feng et al., 2005). Together, these observations suggested that SMN and Gemin2 regulation is linked. Thereby, we hypothesized that PI3K/Akt pathway inhibition could be regulating not only SMN expression but also other Gemins, such as Gemin2. To this aim, 6-day cultured CD1 MNs or 7-day differentiated Control and SMA human MNs were treated or not during 24 h with 25µM of the PI3K/AKT inhibitor LY294002 (+LY). Results indicated that *Gemin2* mRNA expression (+LY: 0.65±0.029, p<0.0001) was reduced in LY294002 treated CD1 MNs compared to the non-treated cells (**Figure 69a**). However, when analyzing the mRNA levels of human *GEMIN2* in 7-day differentiated Control and SMA human MNs, no significant differences were observed in LY294002 treated cells, neither in the Control (+LY: 1.105±0.091, p=0.33) nor in the SMA

condition (+LY: 1.03±0.087, *p*=0.72) (**Figure 69b**) when compared to their non-treated control (-LY Control and -LY SMA, respectively). We also analyzed the basal mRNA levels of *GEMIN2* in differentiated Control and SMA human MNs. However, no differences were observed between Control (0.85±0.07) and SMA (0.86±0.024, *p*=0.85) cells (**Figure 69c**).

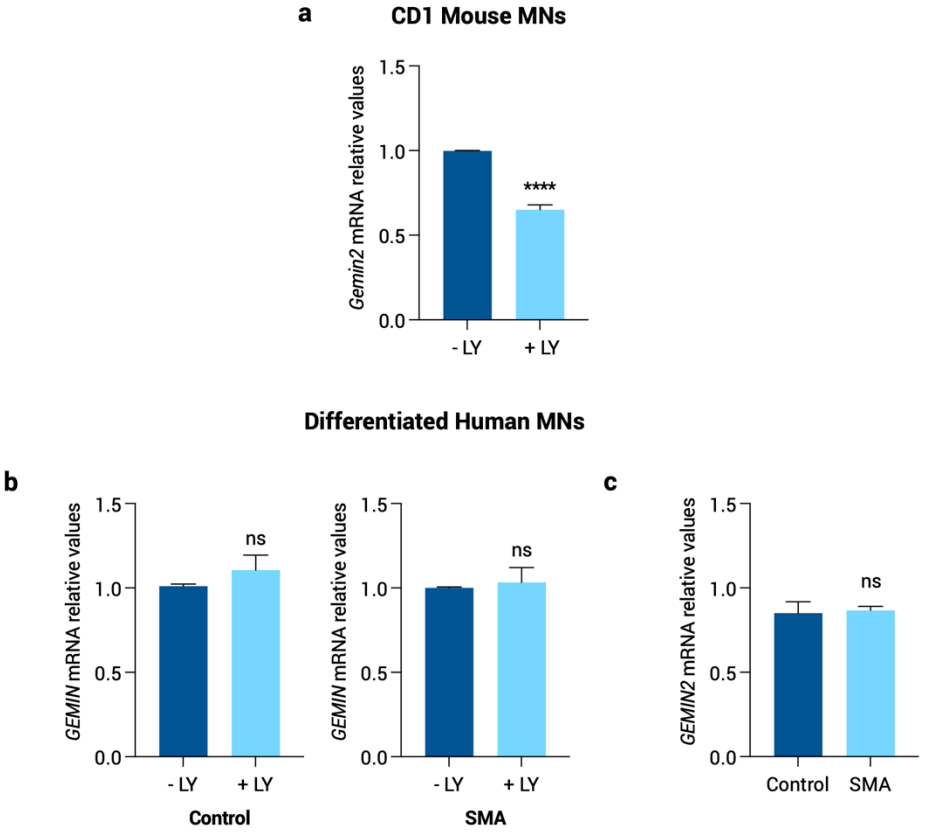

Figure 69 | PI3K/AKT pathway regulates Gemin2 at transcriptional level in CD1 MNs but not in differentiated human MNs. Total RNA was extracted from 25µM LY294002-treated (+LY) or non-treated (-LY) 6-day CD1 MN cultures (**a**) and 7-day differentiated Control and SMA human MN cultures (**b and c**). Reverse transcription to cDNA and *Gemin2* (**a**) or *GEMIN2* (**b and c**) amplification was done. *Gapdh* (**a**) or *GAPDH* (**b**) gene was used as control. Graph values are the mean of *Gemin2* (**a**) or *GEMIN2* (**b and c**) gene expression from 3 independent experiments ± SEM. Asterisks indicate significant differences using Student *t*-test (****$p<0.0001$; no significant differences, ns, $p>0.05$).

5. ERK MAPK pathway regulates SMN at transcriptional level in mouse and human MNs

To determine whether Smn reduction caused by U0126 treatment was associated with decreased activity of *Smn* gene expression, we quantified *Smn* (mouse) or *SMN* (human) messenger RNA (mRNA) by quantitative RT-PCR (qRT-PCR) in ERK-inhibited CD1 and differentiated Control and SMA human MNs.

Six-days cultured CD1 MNs were treated with or without 20μM U0126 and after 24 h, total RNA was extracted and reverse transcription and amplification of *Smn* transcript was done. The results showed that the inhibitor U0126 caused a significant reduction in *Smn* mRNA expression (0.71±0.042, p=0.0024) in CD1 MNs compared with the non-treated control (**Figure 70a**). Next, we extracted and quantified *SMN* mRNA by qRT-PCR of 7-day differentiated Control and SMA human MNs treated with or without 20μM U0126 for 24 h. Results indicated a significant reduction in *SMN* mRNA expression (+UO Control: 0.69±0.107, p=0.045; +UO SMA: 0.43±0.18, p=0.023) compared with control non-treated conditions (**Figure 70b**). Together, these results showed that ERK MAPK inhibition regulates Smn at transcriptional level in SMA and non-SMA mouse and human MNs.

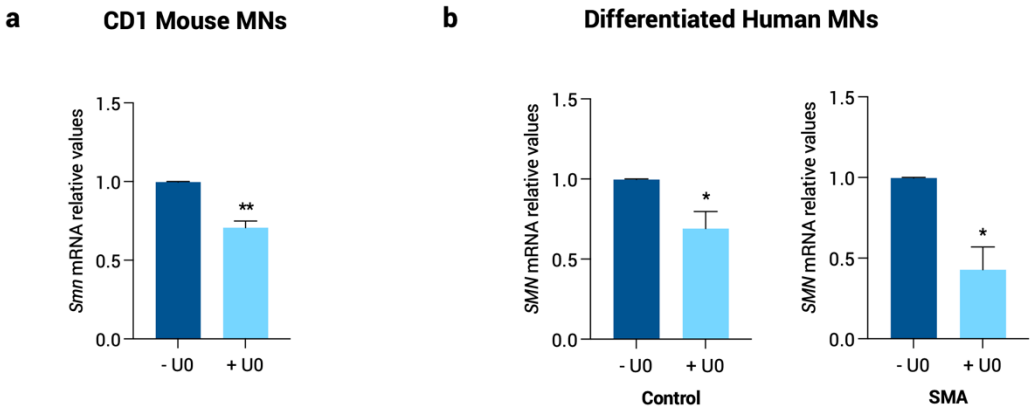

Figure 70 | ERK MAPK pathway regulates Smn at transcriptional level in CD1 MNs. Total RNA was extracted from 20μM U0126-treated (+U0) or non-treated (-U0) 6-day cultured CD1 MNs (**a**) or 7-day differentiated Control and SMA human MNs (**b**). Reverse transcription to cDNA and *Smn* or *SMN* amplification was done. *Gapdh* or *GAPDH* gene was used as control. Graph values are the mean of *SMN* gene expression from 3 independent experiments ± SEM. Asterisks indicate significant differences using Student *t*-test (*p<0.05; **p<0.01).

6. ERK MAPK pathway regulates FAIM-L at transcriptional level in mouse MNs in vitro

Based on the literature, ERK activation by NTFs may be regulating FAIM-L expression (Sole et al., 2004); FAIM-L promotion of neurite outgrowth in the PC12 cell line was counteracted by inhibition of the Ras-ERK pathway (Sole et al., 2004). Moreover, FAIM-L increase in these PC12 cells prevented Fas-induced apoptosis by regulating XIAP (Moubarak et al., 2013; Segura et al., 2007). We had observed an over-activation of ERK protein in SMN-reduced MNs, which also presented elevated levels of FAIM-L. Thereby, we wanted to confirm the relationship between ERK activation and increased FAIM-L levels in MNs. To that end, we blocked the phosphorylation of ERK protein with 20μM U0126 in 6-day CD1 cultured MNs for 24h. Total RNA was extracted and reverse-transcribed to cDNA, used as a template to quantify *FAIM-L* transcript level. U0126 addition was related to a reduction in *FAIM-L* mRNA expression (+U0: 0.58±0.11, p=0.023) compared to control non-treated condition (-U0), showing that ERK inhibition regulates *FAIM-L* at transcriptional level in these cells (**Figure 71**).

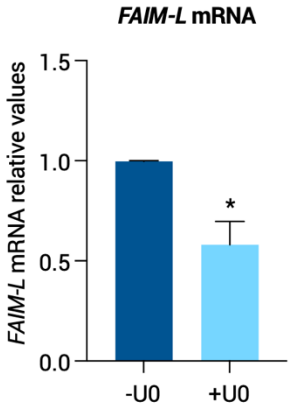

Figure 71 | ERK inhibition regulates FAIM-L at transcriptional level. Total RNA was extracted from 20μM U0126-treated (+U0) or non-treated (-U0) 6-day cultured CD1 MNs. Reverse transcription to cDNA and amplification of *FAIM-L* gene was done. *Gapdh* gene was used as an internal control. Graph values are the mean of *FAIM-L* gene expression from 3 independent experiments ± SEM. Asterisk indicates significant differences using Student *t*-test (*p<0.05).

7. SMN modulation does not regulate Akt or ERK phosphorylation in CD1 mouse MNs and differentiated human MNs

We observed a dysregulation in the Akt and ERK pathways in SMA conditions, and the inhibition of these pathways caused a reduction of SMN levels in non-SMA and SMA cultured mouse and differentiated human MNs.

To explore SMN modulation influence on regulating either PI3K/Akt or ERK MAPK pathway in spinal cord MNs, we used lentiviral RNA vectors to reduce or over-express the SMN protein. E13 spinal cord MNs were isolated and plated in laminin-coated M4 multi-well culture dishes. Three h later, we transduced the cells with lentivirus containing; empty vector (EV), short hairpin RNA (shRNA) sequences targeting specific sites of mouse Smn1 (shSmn), or an expression construct carrying the human SMN gene (ovSMN). Medium was changed after 24 h and cells were maintained for 6 days *in vitro.* Efficacy of transduction was assessed by observing GFP-positive cells and by blotting SMN antibody (**Figure 72a**). Cell lysates were obtained and submitted to immunoblot analysis using: anti-p-Akt(Thr308) and anti-pan-Akt (**Figure 72b**), or anti-p-ERK and anti-pan-ERK (**Figure 72c**). Smn protein level was significantly reduced in shSmn-transduced CD1 cells (shSmn: 0.41±0.12, p=0.0006) and increased in ovSMN-transduced cells (ovSMN: 6.18±1.01, p=0.0002) when compared with the EV condition, respectively (**Figure 72a**).

Regarding the PI3K/Akt pathway, results showed that neither the knockdown of Smn protein (p-Akt vs pan-Akt ShSmn: 1.148±0.57, p=0.93) nor the SMN overexpression (p-Akt vs pan-Akt ovSMN: 0.92±0.37, p=0.98) showed a modulation on the ratio of p-Akt versus total Akt or on the total Akt protein levels (pan-Akt shSmn: 0.95±0.18, p=0.99; pan-Akt ovSMN: 1.16±0.39, p=0.88) compared with the control condition (EV) (**Figure 72b**). When analyzing ERK MAPK pathway, results showed that neither the knockdown (p-ERK vs pan-ERK shSmn: 0.86±0.18, p=0.43) nor the overexpression (p-ERK vs pan-ERK ovSMN: 1.0±0.13, p=0.95) of Smn protein showed a modulation on the ratio of p-ERK versus total ERK or on the total ERK protein levels (pan-ERK shSmn: 1.19±0.38, p=0.65; pan-ERK ovSMN: 1.1±0.17, p=0.61) compared with the control condition (EV) (**Figure 72c**).

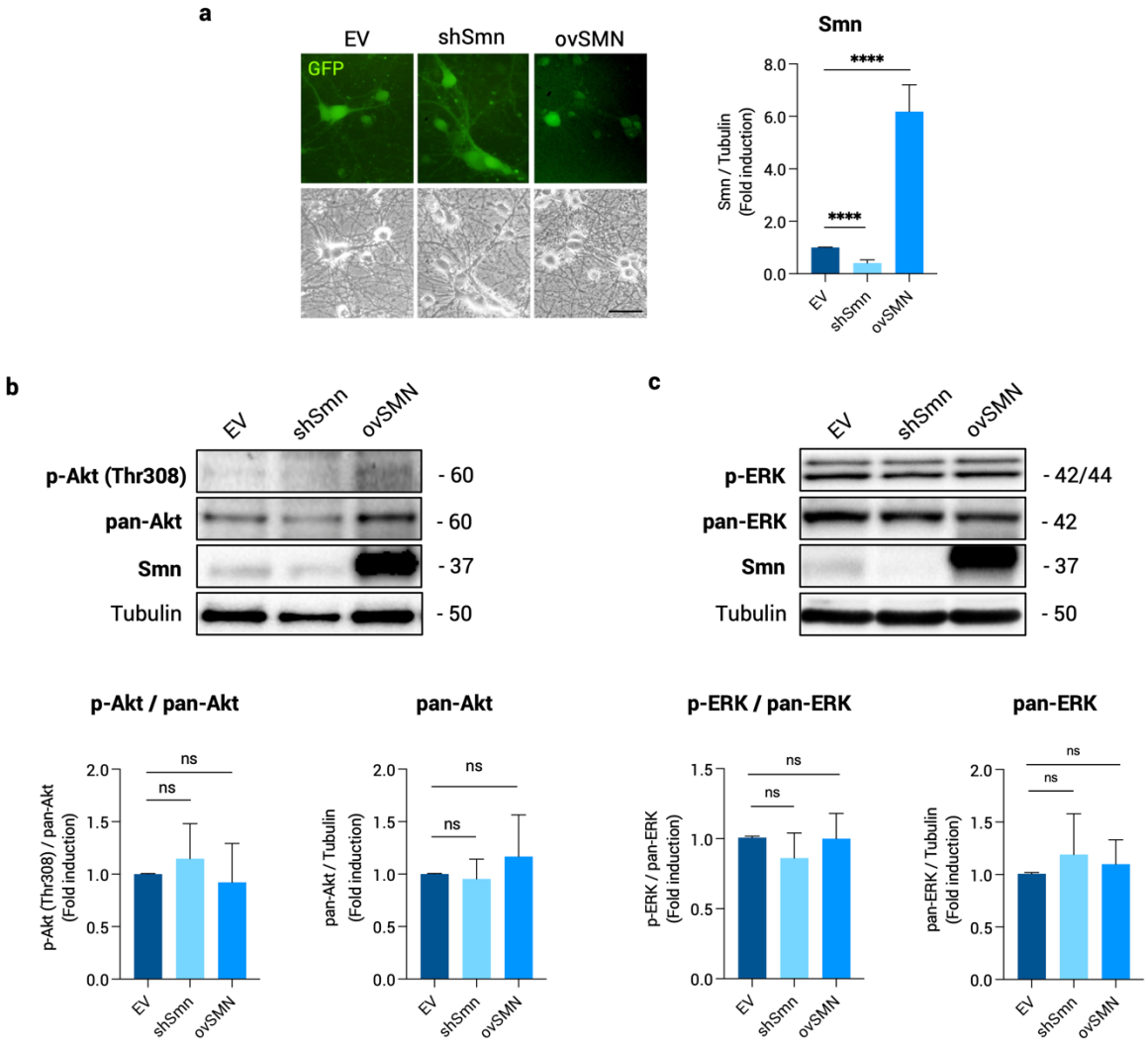

Figure 72 | SMN modulation does not regulate Akt or ERK phosphorylation in CD1 mouse MNs. CD1 mouse MNs were plated and transduced with lentivirus containing the empty vector (EV) and the shSmn or the ovSMN constructs and cultured for 6 days. Representative microscopy images of 6-day CD1 MNs cultures. GFP shows the effective transduction of lentivirus. Scale bar, 15µm (**a, left**). Protein extracts were probed with anti-p-ERK or anti-SMN antibodies by western blot analysis. Membranes were stripped and reprobed with an anti-pan-ERK antibody or reprobed with an anti-α-tubulin antibody. Graphs represent the expression of p-Akt (Thr308) vs pan-Akt or total Akt (**b**), p-ERK vs pan-ERK or total ERK (**c**), and of SMN vs α-tubulin (**a, right**), and correspond to the quantification of 3 (**b**) and 4 (**c**) independent experiments ± SEM. Asterisks indicate significant differences using one-way Anova with Tukey's multiple comparisons post-test (no significant differences, ns, $p>0.05$).

To explore whether SMN modulation could influence on the activation of the PI3K/Akt or ERK MAPK signaling pathways in differentiated Control and SMA human MNs, we used lentiviral RNA vectors over-express the SMN protein in these cells. Embryonic bodies were disaggregated and plated in laminin-coated M4 multi-well culture dishes. Three h later, we cells were transduced with lentivirus containing; EV or ovSMN. Medium was changed after 24 h and MNs were maintained for 7 days *in vitro.* Cell lysates were obtained and submitted to immunoblot analysis using: anti-p-Akt(Thr308) and anti-pan-Akt (**Figure 73b**), or anti-p-ERK and anti-pan-ERK (**Figure 73c**). The efficacy of transduction was assessed by observing GFP-positive cells (**Figure 73a**) and by blotting SMN antibody.

As expected, SMN protein level was significantly increased in both Control (5.79 ± 0.69, $p<0.0001$) and SMA (3.6±0.39, $p<0.0001$) ovSMN-transduced cells when compared to the EV condition, respectively. Results showed that both Control (p-Akt: 0.76±0.13, $p=0.73$) and SMA (p-Akt: 0.64±0.16, $p=0.77$) MNs overexpressing SMN protein showed no increase on Akt phosphorylation compared with each control (EV) condition (**Figure 73b**). Likewise, no statistical differences were observed in pan-Akt levels in transduced Control (1.65±0.37, $p=0.53$) or SMA (1.59±0.52, $p=0.63$) conditions compared with their respective control (EV) (**Figure 73b**). On the other hand, we checked the modulation of ERK protein in differentiated SMA MNs when SMN was overexpressed. ERK phosphorylation was confirmed by blotting p-ERK and pan-ERK antibodies. ERK phosphorylation was observed to be significantly increased in EV-transduced SMA cells (1.7±0.25, $p=0.029$) when compared to EV-transduced Control cells (**Figure 73c**). Results showed that both Control (0.92±0.14, $p=0.58$) and SMA (2.25±0.51, $p=0.28$) MNs overexpressing SMN protein showed no increase neither on ERK phosphorylation nor in pan-ERK (pan-ERK Control ovSMN: 1.01±0.01, $p=0.98$; pan-ERK SMA ovSMN: 0.89±0.14, $p=0.78$) levels compared with each control (EV) condition (**Figure 73c**).

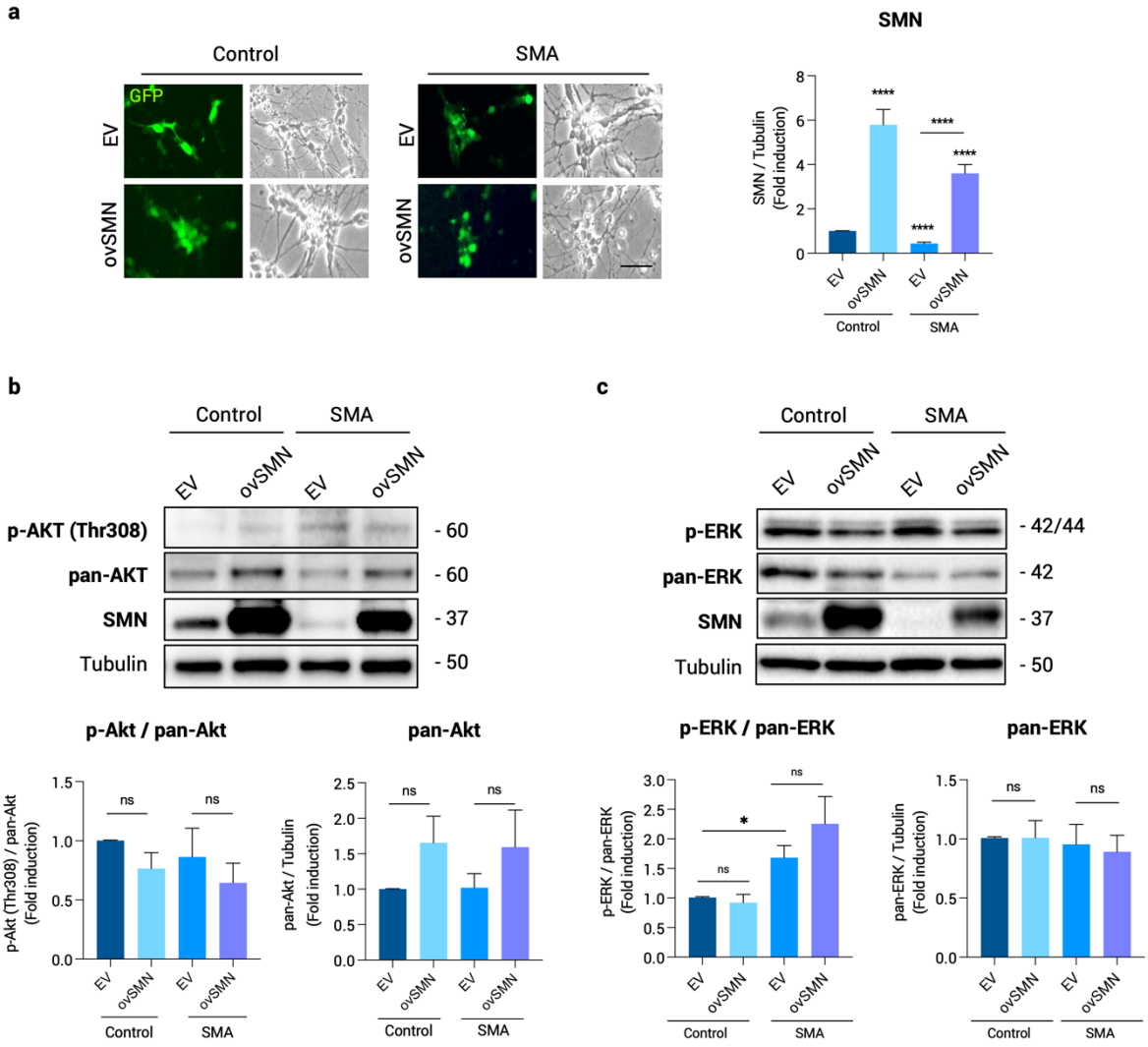

Figure 73 | SMN overexpression does not regulate Akt or ERK phosphorylation in differentiated Control and SMA human MNs. Control and SMA human MNs were plated and transduced with lentivirus containing the empty vector (EV) or the ovSMN construct and cultured for 7 days. **(a)** Representative microscopy images of 7-day human MN cultures. GFP shows the effective transduction of lentivirus. Scale bar, 15µm. Protein extracts of transduced hMN cultures were probed with anti-SMN (**a**), anti-p-Akt(Thr308) (**b**) or anti-p-ERK (**c**) antibodies by western blot analysis. Membranes were stripped and reprobed with an anti-pan-Akt or an anti-pan-ERK antibody, or reprobed with an anti-α-tubulin antibody. Graphs represent the expression of SMN vs α-tubulin (**a**), p-Akt vs pan-Akt or pan-Akt vs α-tubulin (**b**), and p-ERK vs pan-ERK or pan-ERK vs α-tubulin (**c**), and correspond to the quantification of at least 4 independent experiments ± SEM. Asterisks indicate significant differences using Student *t*-test or one-way Anova with Tukey's multiple comparisons post-test (*p<0.05; no significant differences, ns, p>0.05).

CHAPTER 3. SPINAL MUSCULAR ATROPHY AUTOPHAGY PROFILE IS TISSUE-DEPENDENT: DIFFERENTIAL REGULATION BETWEEN MUSCLE AND MOTONEURONS

SUMMARY

The autophagic process is crucial for cell differentiation, homeostasis and survival (Mizushima et al., 2008), and its alteration has been described in several neurodegenerative disorders like HD and AD (Boland et al., 2008; Ravikumar et al., 2004). Additionally, several experimental models have described the participation of autophagy during muscle (Dobrowolny et al., 2008) and MN atrophy (Custer & Androphy, 2014; Garcera et al., 2013), and recently, autophagy changes have been related to SMA disease (Custer & Androphy, 2014; de la Fuente et al., 2020; Garcera et al., 2013; Piras et al., 2017). Regarding SMA MNs, previous results in our laboratory showed that LC3-II and p62 autophagy markers are deregulated in these cells. Moreover, the modulation of this process can increase or decrease SMN protein levels (de la Fuente et al., 2018; Periyakaruppiah et al., 2016). However, the alterations of autophagy markers amongst diverse SMA tissues have not been fully described. In this chapter we have studied the expression of several autophagy markers in different SMA-affected tissues and cell types (**Figure 74**).

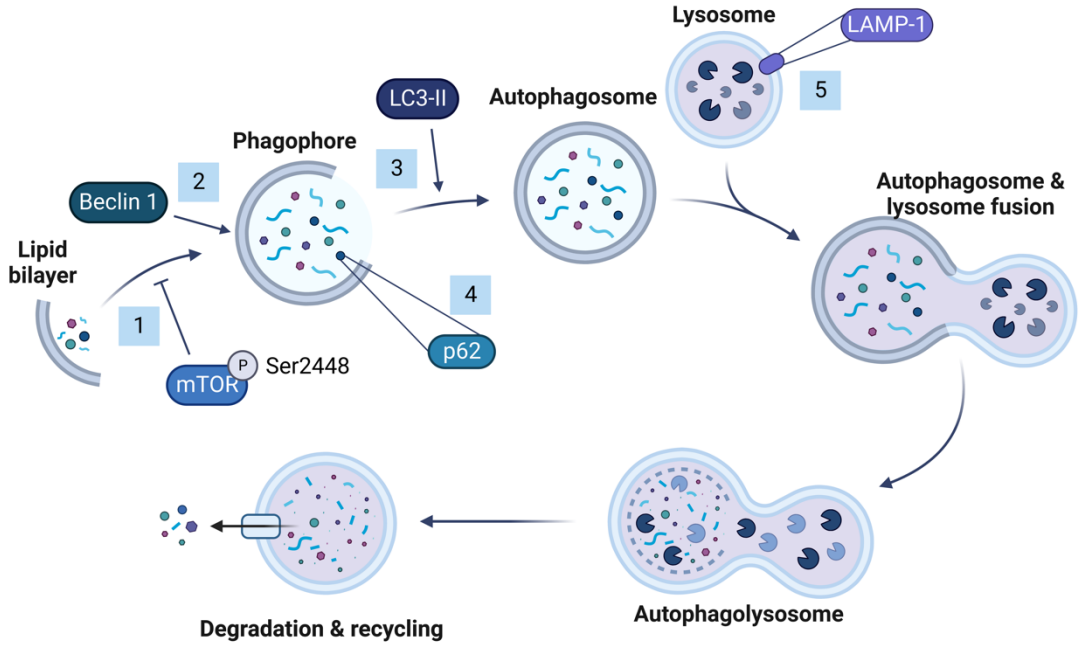

1 Inactivated mTOR allows the initiation of the autophagy process. When it is phosphorylated, mTOR blocks the initiation of the autophagosome formation.

2 Beclin 1 is responsible for the nucleation of the autophagosome.

3 LC3-II is a protein anchored to the membrane of the autophagosome. It is degraded through autophagy and serves as an indicator of autophagosome amount.

4 p62/SQSTM1 is a cargo protein degraded through autophagy and an indicator of the autophagic flux.

5 LAMP-1 is a protein anchored to the lysosomal membrane that serves as an indicator of the amount of lysosomes.

Figure 74 | Schematic representation of the autophagy process and the proteins analyzed. Created with BioRender.com.

1. LC3-II autophagosome marker is decreased in SMA muscle, lymphoblasts and fibroblasts

The levels of LC3-II isoform gives important information about the number of autophagosomes present in the cells (Klionsky, Abdel-Aziz, et al., 2021; Parzych & Klionsky, 2014). To assess possible alterations in the autophagy pathway in several SMA models, we analyzed the level of LC3-II protein in human and mouse muscle SMA samples, and in SMA human lymphoblasts and fibroblasts.

First, western blot analysis of protein extracts obtained from SMA patients muscle biopsies were done. Human muscle samples were from the Pediatric Neurology laboratory collection at Vall d'Hebron Hospital (Spanish Biobank Registry, reference C.0003146). Two non-SMA muscle samples were used for the experiments: one from a 2-month-old girl undergoing surgery (Control) and the other from a 4-month-old girl diagnosed with Pompe disease (Pompe), a lysosomal storage disorder that causes massive accumulation of autophagosomes (Fukuda et al., 2006). The SMA muscle biopsies were obtained from type I (SMAI) and type II (SMAII) patients, quadriceps muscle (4-month-old female, two copies of *SMN2*) and paraspinal muscle (12-year-old male, two copies *SMN2*), respectively. LC3-II protein level Pompe sample was used as an internal control. Results showed that both SMAI and SMAII samples presented reduced levels of LC3-II (SMAI: 0.34; SMAII: 0.41) compared to the Control (**Figure 75**).

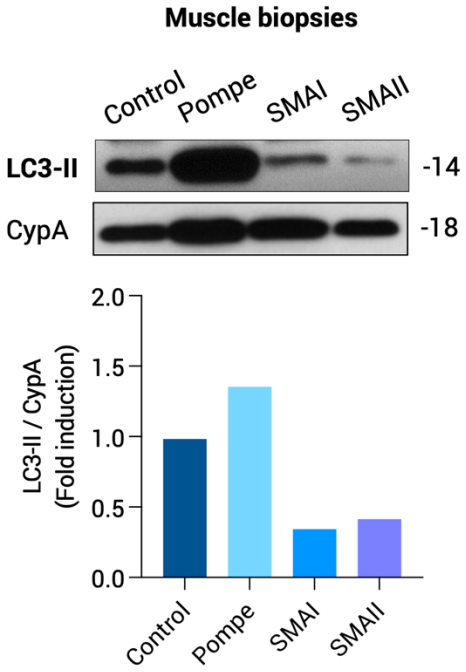

Figure 75 | LC3-II protein level in human samples from SMA muscle biopsies. Muscle biopsies from Control, Pompe and SMA and SMA patients were disaggregated and protein extracts submitted to western blot analysis using anti-LC3 antibody. Membranes were reprobed with anti-CypA antibody, used as a loading control. Graph values represent the expression of LC3-II vs CypA.

To further analyze LC3 alterations in SMA muscle tissue, we dissected gastrocnemius muscles from genotyped Wild-type (WT) and mutant (mutSMA) P2 and P5 mice from the severe mouse model (**see Materials and Methods section 1.2.1**). Protein extracts were obtained and submitted to western blot analysis using anti-LC3 antibody. LC3-II level was significantly reduced in mutSMA (0.46±0.07, p=0.0034) condition compared to WT control at P2 stage. Contrarily, LC3-II protein was significantly increased in P5 extracts from mutSMA (2.03±0.25, p=0.0051) compared to the WT control (**Figure 76a**). To validate our observations in P2 mutSMA animals, the number of LC3 puncta per myotube area of WT and mutSMA P2 gastrocnemius was explored by immunofluorescence using an anti-LC3 antibody. The number of LC3 puncta per myotube area was significantly reduced in mutSMA (35.43±4.63, p<0.0001) compared to the WT control (77.67±7.84) (**Figure 76b**).

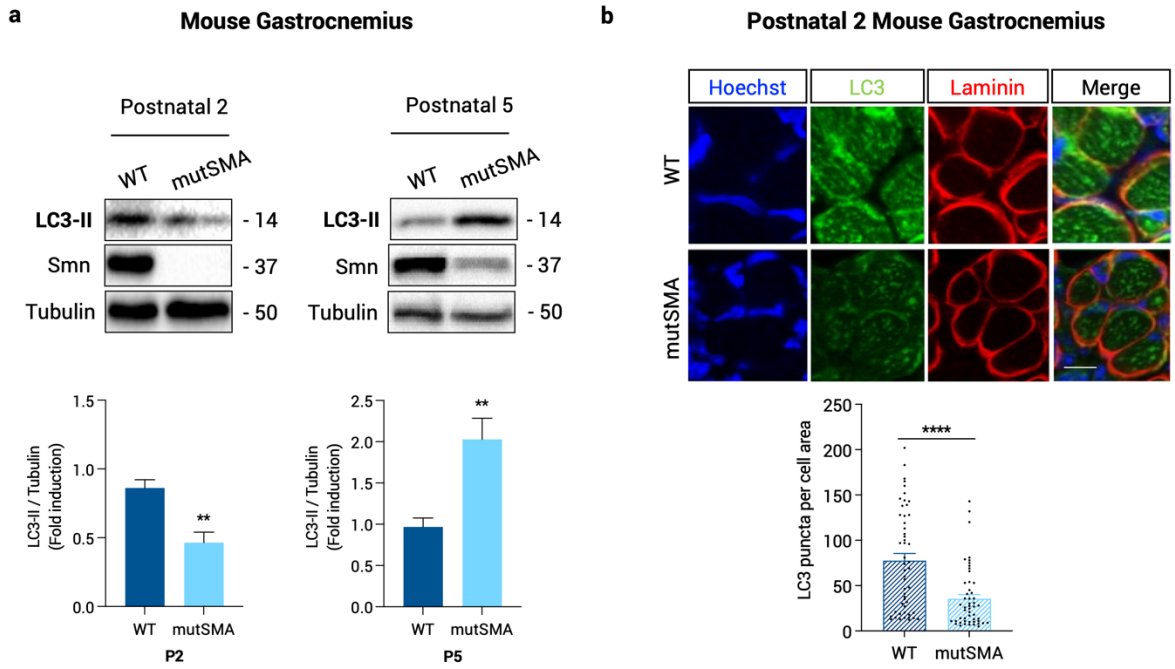

Figure 76 | LC3-II protein level in murine samples from SMA muscle biopsies. (**a**) Protein extracts of gastrocnemius from WT and mutSMA P2 (**a, left**) and P5 (**a, right**) mice were submitted to western blot analysis using anti-LC3 and anti-SMN antibodies. Membranes were reprobed using an antibody against α-tubulin. Graph values represent the expression of LC3-II vs α-tubulin at P2 and P5. (**b**) Representative immunofluorescence images of gastrocnemius sections of P2 WT and P2 mutSMA mice using an anti-LC3 (green) and an anti-Laminin (red) antibodies. Hoechst dye (blue) was used to identify nuclei. Scale bar, 20 µm. Graphs represent the mean of LC3 positive puncta measured in WT and mutSMA myofibers. (**a and b**) Graphs correspond to the quantification of 3 independent experiments ± SEM. Asterisks indicate significant differences using Student t-test (**p<0.01; ****p<0.0001).

To explore autophagy alterations in other SMA-affected tissues, we analyzed by western blot the levels of LC3-II protein in lymphoblast and fibroblast SMA patient cell lines. Protein extracts were obtained from 2-day cultured SMA lymphoblast (**Figure 77a**) or fibroblast samples (**Figure 77b**) (kindly provided by Dr. Eduardo Tizzano, Hospital Santa Creu i Sant Pau, Barcelona). Results showed that LC3-II protein level was markedly reduced in both cellular types (SMAI Lymphocytes: 0.73; SMAI Fibroblasts: 0.63) when compared to their respective controls (**Figure 77 a and b**).

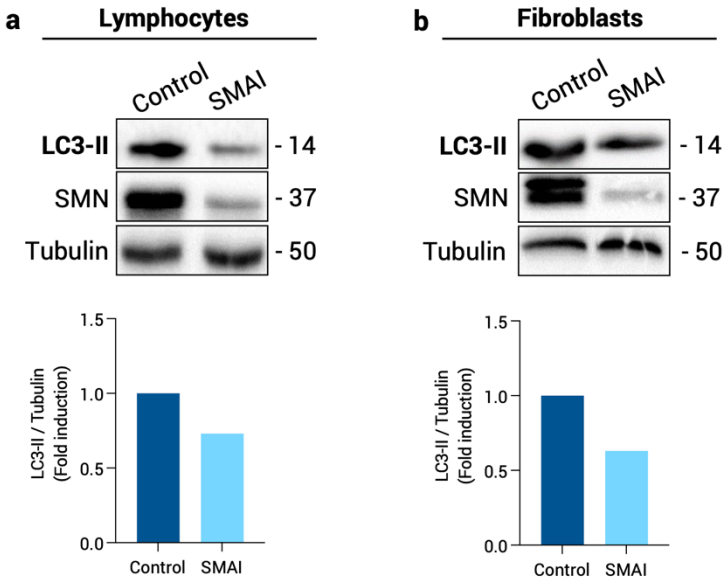

Figure 77 | LC3-II protein level in SMA patient lymphocytes and fibroblasts cells. Protein extracts from lymphoblast (**a**) and fibroblast (**b**) cell lines were submitted to western blot analysis using anti-LC3 and anti-SMN antibodies. Membranes were reprobed with anti-α-tubulin antibody, used as a loading control. Graph values represent the expression of LC3-II versus α-tubulin.

Another set of human fibroblast samples, purchased from Coriell Institute, was included in the analysis of LC3-II protein level. SMAII, SMAI and a clinically unaffected Control were cultured during 2 days and cell lysates were submitted to western blot analysis against LC3. Results revealed a significant reduction of LC3-II protein level in SMA fibroblasts (SMAII: 0.65±0.06, p=0.0006; and SMAI: 0.73±0.08, p=0.004) compared to the clinically unaffected control (**Figure 78a**). We also measured the number of autophagosomes in these SMA fibroblasts by assessing the LC3 puncta number per cell. Five thousand cells per condition were plated onto collagen-coated glass coverslips during 24 h. Cells were then fixed and LC3 immunostaining was performed with anti-LC3 antibody. LC3 fluorescent puncta in SMA fibroblasts (SMAII 32.76±3.01, p=0.0104; and SMAI 24.97±2.96, p<0.0001) were significantly reduced compared to the control (46.37±3.76) (**Figure 78b**). Taken together, these results

indicate an overall marked decrease of the autophagic marker LC3 in SMA muscle tissue, lymphocytes and fibroblasts.

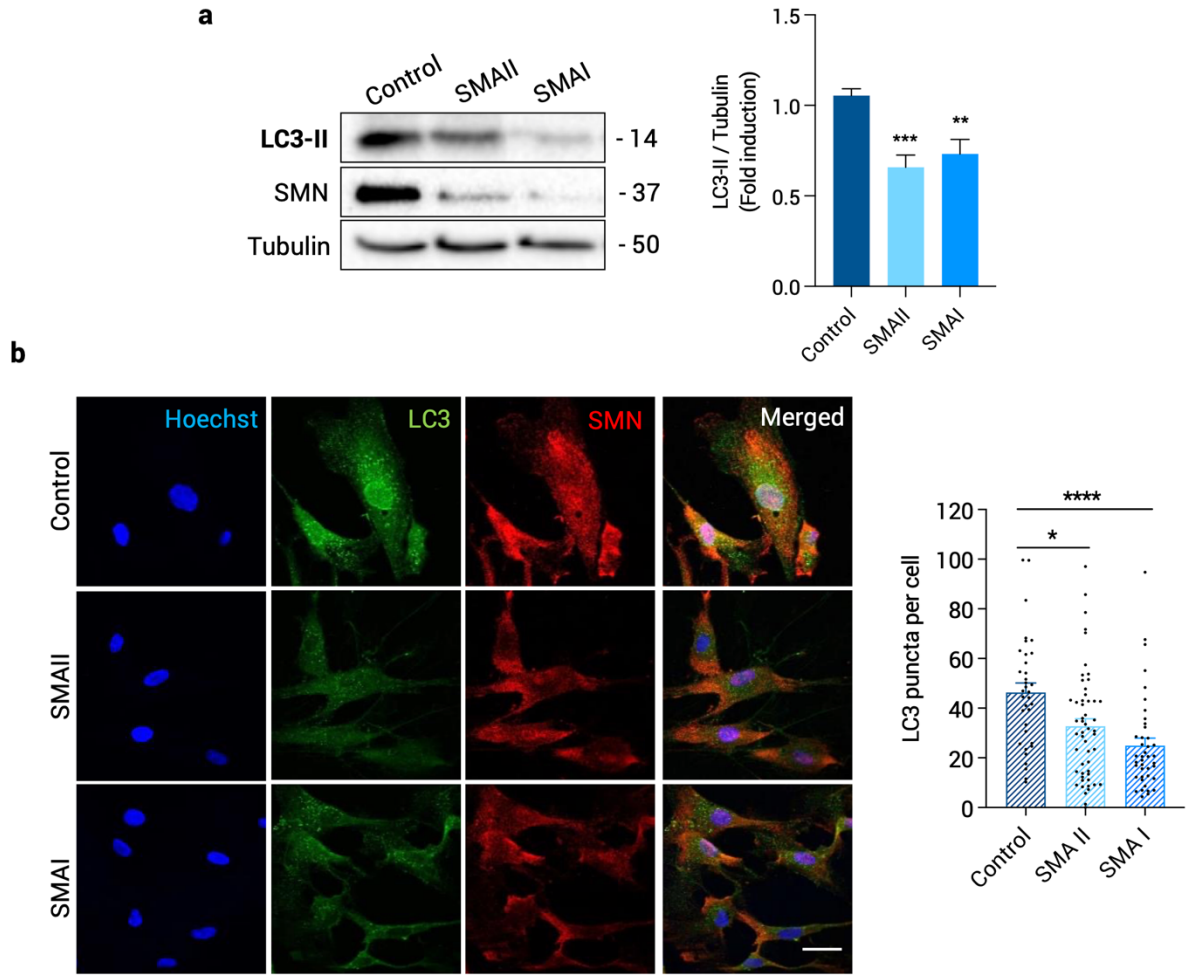

Figure 78 | LC3-II protein level in human SMA fibroblast cell lines. (**a**) Control (unaffected), SMAII and SMAI patient fibroblast cell lines were plated and maintained in supplemented MEM. Two days after plating, cell lysates were obtained and submitted to western blot using anti-LC3 and anti-SMN antibodies. Membranes were reprobed with an anti-α-tubulin antibody. Graph values represent the expression of LC3-II versus α-tubulin and correspond to the quantification of 6 independent experiments. (**b**) Representative immunofluorescence images of 2-day cultured Control, SMAII, and SMAI fibroblasts using anti-LC3 (green), anti-SMN (red) antibodies and Hoechst staining (blue). Hoechst was used to identify fibroblast nuclei. Scale bar, 25µm. Graph represents the mean of LC3 positive puncta per cell and corresponds to the quantification of 3 independent experiments ± SEM. Asterisks indicate significant differences using one-way Anova with Tukey's multiple comparisons post-test (*p<0.05; **p<0.01; ****p<0.0001).

2. LC3-II and p62/SQTM1 autophagy markers are increased in differentiated SMA human MNs

To analyze autophagy alterations in differentiated SMA human MNs, we examined LC3 and p62/SQTM1 (p62) (specifically degraded by autophagy and links ubiquitinated proteins to the autophagic machinery to enable their degradation in the lysosome) level in differentiated SMA and Control human MNs.

Protein extracts of 7-day differentiated SMA and Control human MNs were submitted to western blot analysis using an anti-LC3 antibody. Results showed that LC3-II level was increased in human SMA (3.33±0.96, p=0.035) MNs compared to control condition (**Figure 79a**). To further explore autophagy process changes in differentiated SMA MNs, we then analyzed the levels of p62 protein. Accumulation of p62 indicates reduced autophagic flux. Protein extracts of 7-day differentiated SMA and control human MNs were submitted to western blot analysis using an anti-p62/SQTM1 antibody. Results showed that p62 level was increased in human SMA (1.38±0.12, p=0.005) MNs compared to Control cells (**Figure 79b**).

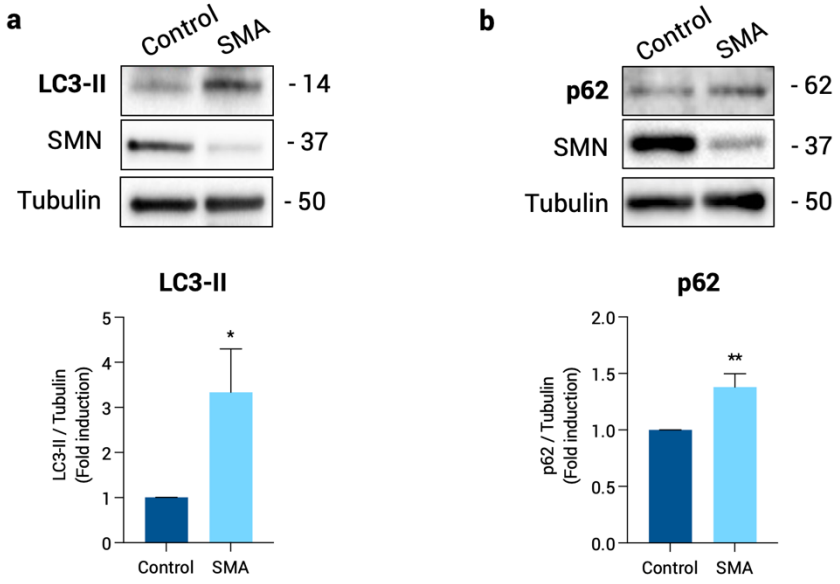

Figure 79 | Increased levels of LC3-II and p62 in differentiated SMA human MNs. Protein extracts of 7-day differentiated control and SMA human MNs were submitted to western blot using anti-LC3, anti-p62 or anti-SMN antibodies (**a and b**). Membranes were reprobed with anti-α-tubulin antibody. Graph values represent the expression of (**a**) LC3-II or (**b**) p62 versus α-tubulin and correspond to the quantification of 6 independent experiments ± SEM. Asterisks indicate significant differences using Student t-test (*p<0.05; **p<0.01).

To validate our observations regarding LC3 protein accumulation in differentiated SMA human MNs, we analyzed by immunofluorescence LC3 protein in cell soma and neurites of these cells. Seven days after differentiation, cultures were fixed and processed using an anti-LC3 antibody. Results showed a significant increase of LC3 in soma and neurites of differentiated SMA MNs (SOMA: 21.72±1.67 puncta per soma, p<0.0001; NEURITES: 0.22±0.018 puncta per µm, p<0.0001) compared to the Control (SOMA: 4.87±0.47 puncta per soma; NEURITES: 0.06±0.012 puncta per µm) (**Figure 80 a and b**). Together these results indicated an increase of LC3-II and p62 autophagosome markers in differentiated SMA human MNs, suggesting that SMA MNs exhibit a reduction in the autophagic flux.

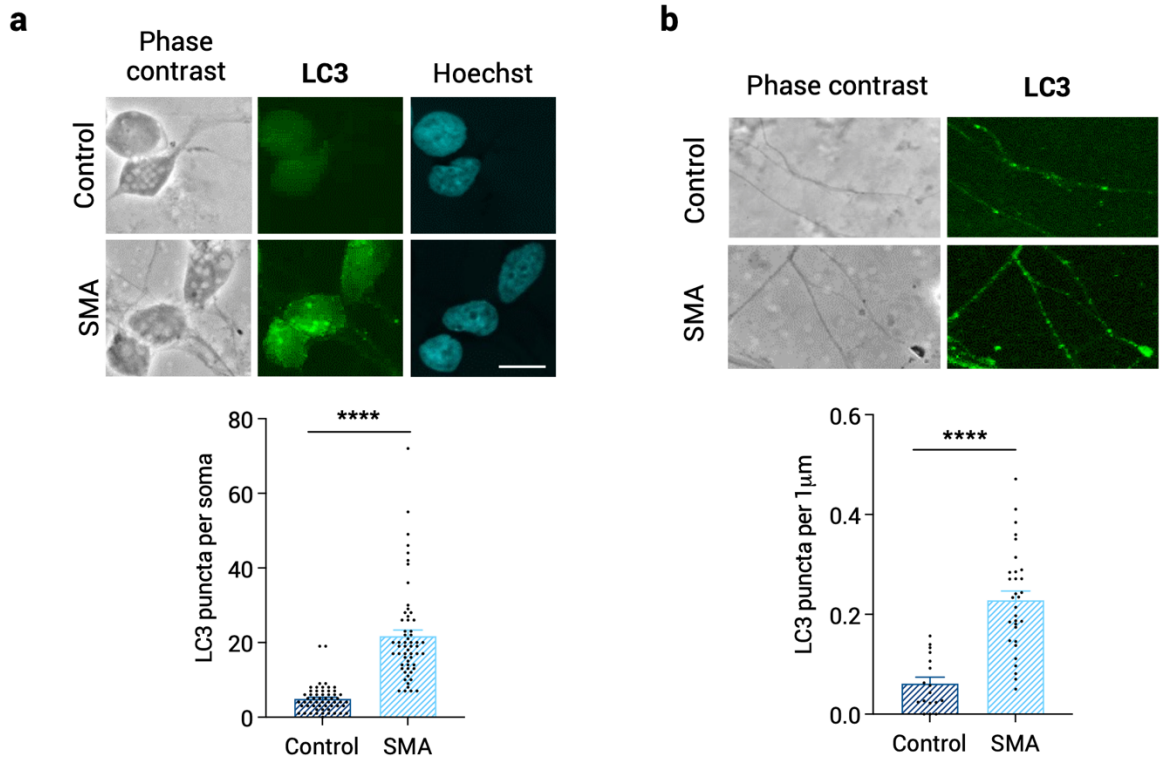

Figure 80 | LC3 puncta is increased in soma and neurites of differentiated SMA human MNs. Representative immunofluorescence confocal images of 7-day differentiated human MNs using an anti-LC3 (green) antibody. Hoechst (blue) dye was used to identify nuclei (**a and b**). Graphs represent the mean of LC3 positive puncta per soma (above) or per neurite (1µm) (**b**) and correspond to the quantification of 3 independent experiments ± SEM. Asterisks indicate significant differences using Student *t*-test (****p<0.0001). Scale bar, 15µm.

3. Beclin 1, p62/SQTM1 and LAMP-1 protein level are altered in SMA mouse gastrocnemius and SMA human fibroblasts

To further explore changes in SMA muscle and fibroblasts autophagy pathway, we next analyzed the levels of Beclin 1, p62 and the Lysosome Associated Membrane Protein-1 LAMP-1 proteins. Beclin 1 activity controls the assembly of the double-membrane autophagosome and regulates the number of these structures and LC3-II level. LAMP-1 is one of the major protein components of the lysosomal membrane, and a good indicator of changes in the lysosomal compartment.

WT and mutSMA P2 and P5 gastrocnemius protein extracts were obtained and western blot analysis using anti-Beclin1 antibody and anti-p62 antibody revealed that both Beclin1 and p62 levels were significantly reduced in mutSMA P2 (Beclin1: 0.49±0.028, $p<0.0001$; p62: 0.73±0.078, $p=0.022$) and P5 (Beclin1: 0.65±0.098, $p=0.022$; p62: 0.62±0.14, $p=0.049$) compared to their respective WT controls (**Figure 81 a and b**). To evaluate whether alteration of the autophagic flux in muscle cells was associated to changes in the lysosomal compartment, we analyzed LAMP-1 protein level. LAMP-1 was not statistically different in mutSMA P2 (1.04±0.24, $p=0.75$) and P5 (0.805±0.19, $p=0.43$) mouse gastrocnemius compared to the respective WT control conditions (**Figure 81 a and b**). These results suggested an increased autophagic flux in mutSMA gastrocnemius, whithout autophagolysosome accumulation in mutSMA muscle tissue.

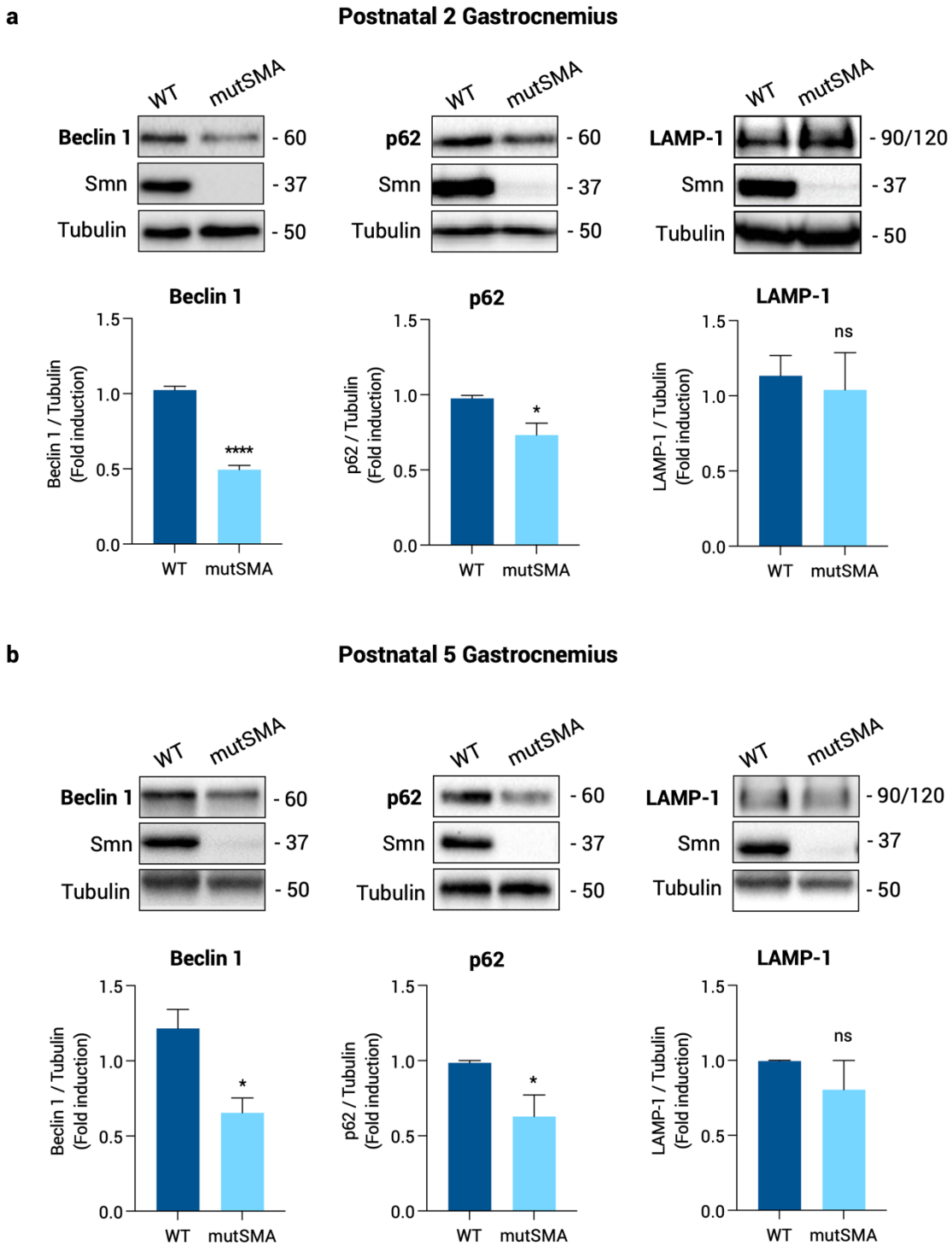

Figure 81 | Beclin 1, p62/SQTM1 and LAMP-1 protein levels in mutSMA gastrocnemius. Total cell lysates of gastrocnemius from P2 (**a**) and P5 (**b**) genotyped WT and mutSMA mice were submitted to western blot analysis using anti-Beclin 1, anti-p62/ SQSTM1, anti-LAMP-1, and anti-SMN antibodies. Membranes were reprobed using an antibody against α-tubulin. Graph values represent the expression of the targeted proteins vs α-tubulin at P2 and P5, and correspond to the quantification of 4 and 3 independent experiments ± SEM, respectively. Asterisks indicate significant differences using Student *t*-test (*p<0.05, ****p<0.0001, no significant differences, ns, p>0.05).

Next, we evaluated the levels of these three aforementioned proteins involved in the autophagic flux in human SMA fibroblast cell lines (Coriell Institute). Protein extracts of 2-day cultured Control, SMAII and SMAI fibroblasts were submitted to western blot analysis using anti-Beclin1, anti-p62 or anti-LAMP-1 antibodies. No significant differences between control and SMA Beclin 1 protein levels were observed, although the level was slightly reduced in SMA conditions (SMAII: 0.87±0.047 p=0.31; and SMAI: 0.81±0.097, p=0.095) (**Figure 82**). Conversely, western blot analysis of p62 protein revealed significantly increased level in SMA fibroblasts (SMAII: 1.43±0.17, p=0.014; and SMAI 2.04±0.33, p=0.01) compared to Control (**Figure 82**). Finally, LAMP-1 was significantly reduced in human SMA fibroblasts (SMAII: 0.85±0.02, p=0.03; SMAI: 0.64±0.04, p=0.0004) compared to non-affected control (**Figure 82**). Together, these results suggested that autophagy flux is reduced and the lysosomal compartment is altered in human SMA fibroblasts.

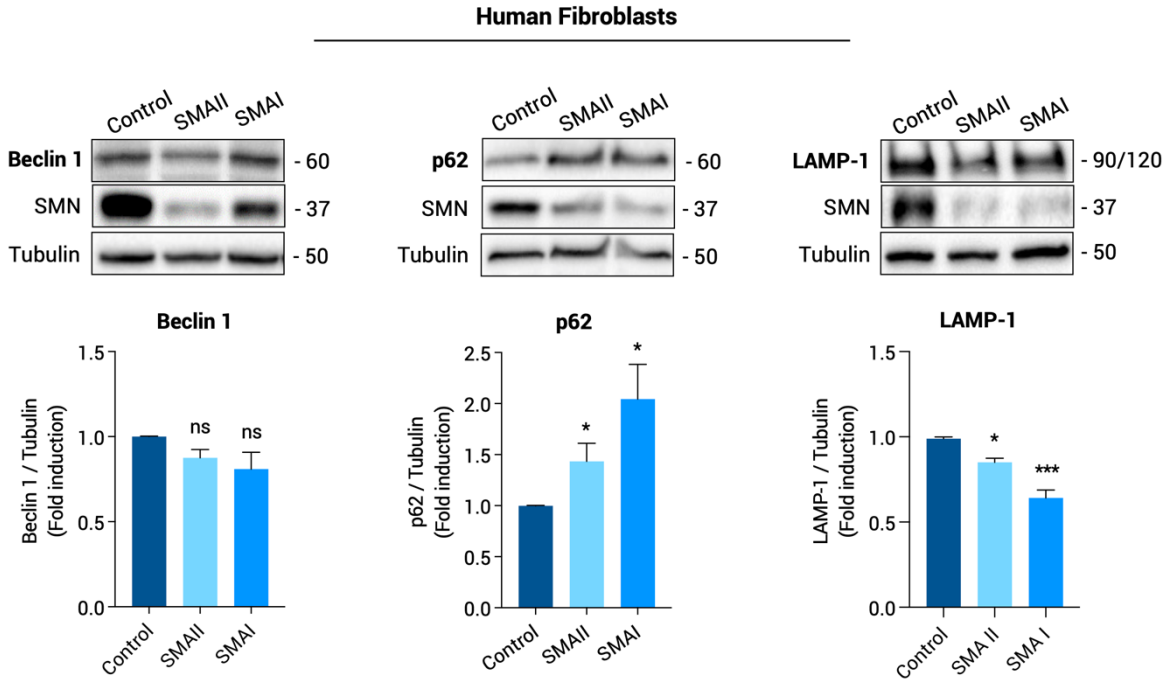

Figure 82 | Beclin 1, p62/SQTM1 and LAMP-1 protein levels in SMA fibroblast cell lines. Two-day cultured Control, SMAII and SMAI patient fibroblast cell lines protein extracts were obtained and submitted to western blot analysis using anti-Beclin 1, anti-p62/SQSTM1 or anti-LAMP-1, and anti-SMN antibodies. Membranes were reprobed with an anti-α-tubulin antibody. Graph values represent the expression of the targeted proteins versus α-tubulin and correspond to the quantification of 3 independents experiments ± SEM. Asterisks indicate significant differences using one-way Anova with Tukey's multiple comparisons post-test (*p<0.05, ***p<0.0005, no significant differences, ns, p>0.05).

4. Beclin 1 and LAMP-1 protein level are altered in differentiated SMA human MNs

To analyze autophagy nucleation and autophagosome fusion with the lysosome in SMA human MNs, we examined Beclin 1 and LAMP-1 level in differentiated SMA and Control human MNs.

Western blot analysis of 7-day differentiated Control and SMA human MNs protein extracts revealed that Beclin 1 level was increased in human SMA (1.99±0.33, p=0.039) MNs compared to Control cells. (**Figure 83a**). To explore changes associated in the lysosomal compartment, LAMP-1 protein level was analyzed. LAMP-1 was significantly reduced in human SMA (0.44±0.04, p=0.0002) MNs compared to control condition (**Figure 83b**). These results indicated Beclin 1 accumulation whith autophagolysosome reduction in differentiated SMA human MNs.

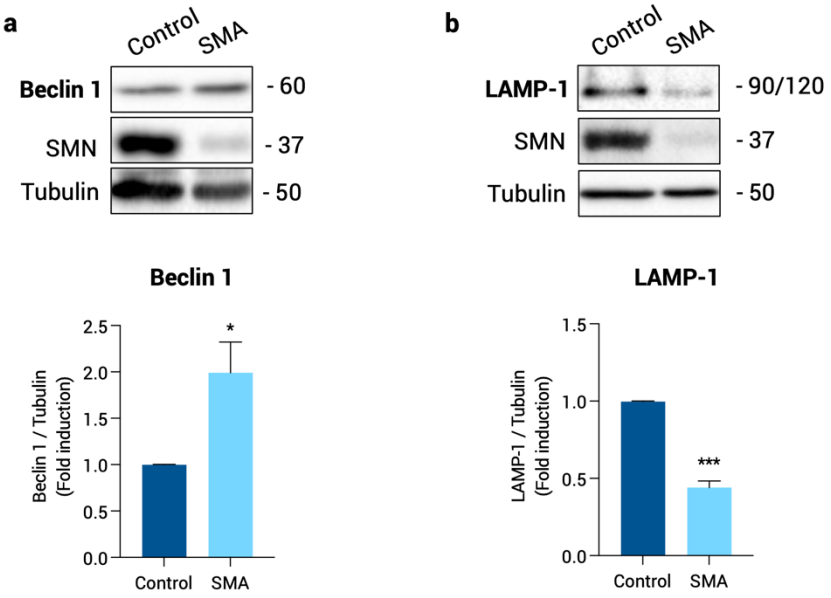

Figure 83 | Beclin 1 and LAMP-1 protein levels in differentiated SMA human MNs. Protein extracts of 7-day differentiated Control and SMA human MNs were submitted to western blot using anti-Beclin 1, anti-LAMP-1 or anti-SMN antibodies (**a and b**). Membranes were reprobed with anti-α-tubulin antibody. Graph values represent the expression of (**a**) Beclin 1 or (**b**) LAMP-1 versus α-tubulin and correspond to the quantification of 3 independent experiments ± SEM. Asterisks indicate significant differences using Student t-test (*p<0.05; ***p<0.001).

5. mTOR phosphorylation at Ser2448 is reduced in SMA mouse gastrocnemius and SMA human fibroblasts

mTORC1 signaling is a well-known negative regulator of the autophagy pathway. The specific elimination of mTOR in skeletal muscle leads to severe myopathy and muscle atrophy has been related to the reduction of mTOR phosphorylation at Ser2448 (Risson et al., 2009). Therefore, we decided to examine mTOR protein level and Ser2448 phosphorylation in SMA muscle tissue. To this aim, protein extracts from genotyped WT and mutSMA P2 and P5 mouse gastrocnemius were submitted to western blot analysis using anti-mTOR or anti-mTOR (phospho Ser2448) antibodies. Results showed that mTOR Ser2448 (p-mTOR) phosphorylation level was significantly reduced in P2 and P5 mutSMA (P2: 0.52±0.06, $p<0.0001$; P5: 0.504±0.13, $p=0.037$), compared to WT controls. No differences of mTOR protein level were observed in WT and mutSMA samples at P2 and P5 (**Figure 84 a and b**).

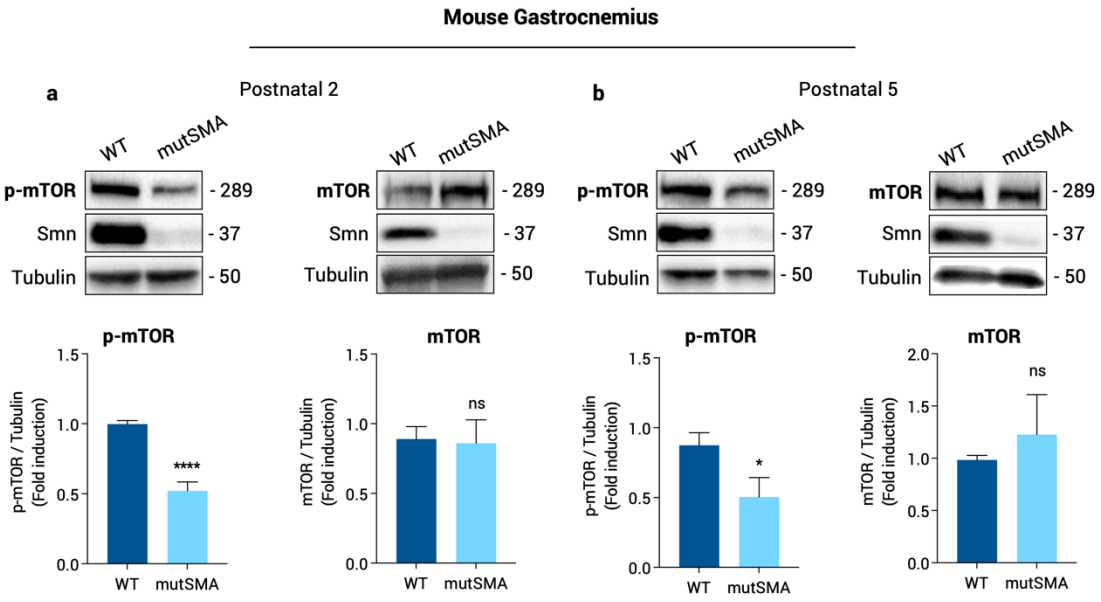

Figure 84 | Changes of mTOR protein level and phosphorylation at Ser2448 in protein extracts of SMA muscle tissue. Total cell lysates of P2 and P5 gastrocnemius from WT and mutSMA genotyped mice were submitted to western blot analysis using anti-mTOR, anti-phospho-mTOR(Ser2448)(p-mTOR) and anti-SMN antibodies. Membranes were reprobed using an anti-α-tubulin antibody. Graph values represent the expression of mTOR or p-mTOR versus α-tubulin and correspond to the quantification of at least 5 independent experiments ± SEM. Asterisks indicate significant differences using Student *t*-test (*$p<0.05$; ****$p<0.0001$; no significant differences, ns, $p>0.05$).

To further investigate mTOR protein in SMA cell types, we next analyzed human SMA cultured fibroblasts. Total protein cell lysates of Control, SMAII and SMAI 2-day cultured fibroblasts were submitted to western blot analysis. As seen in muscle and spinal cord tissue, the level of mTOR Ser2448 phosphorylation was reduced in SMA fibroblasts (SMAII 0.59±0.13, p=0.0114; SMAI 0.41±0.077, p=0.0009) compared to the clinically unaffected control (**Figure 85**). mTOR total protein level was also significantly reduced in cell lysates from SMA fibroblasts (SMAII 0.41±0.096, p=0.0002; SMAI 0.32±0.10, p<0.0001) (**Figure 85**). These results together suggest that mTOR phosphorylation at Ser2448 is reduced in SMA muscle and fibroblasts.

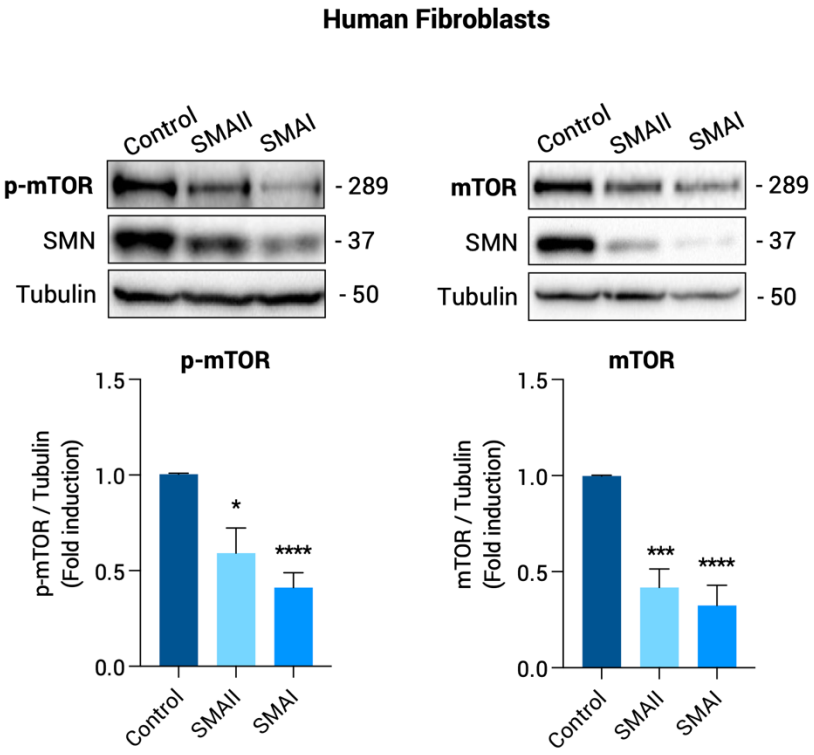

Figure 85 | Changes of mTOR protein level and phosphorylation at Ser2448 in protein extracts of SMA fibroblast cell lines. Protein extracts from 48 h cultured Control, SMAII and SMAI patient fibroblast cell lines were submitted to western blot using anti-mTOR or anti-phospho-mTOR(Ser2448) and anti-SMN antibodies. Membranes were reprobed with an anti-α-tubulin antibody. Graph values represent the expression of mTOR or p-mTOR versus α-tubulin and correspond to the quantification of 5 independent experiments ± SEM. Asterisks indicate significant differences using one-way Anova with Dunnett's multiple comparisons post-test (*p<0.05; ***p<0.001; ****p<0.0001).

6. mTOR phosphorylation at Ser2448 is reduced in SMA mouse spinal cords and increased in mouse and SMA human MNs

As we had seen autophagy pathway alterations in several tissues and cell types, and since an increase in LC3 puncta of mutSMA spinal cord MNs had been previously observed in our laboratory (Periyakaruppiah et al., 2016), we wondered if there could be further alterations in mTOR phosphorylation at Ser2448 and in mTOR total protein levels in spinal cords from the mutSMA mouse model.

To this aim, total protein extracts from P2 and P5 spinal cord lumbar fragments of genotyped WT and mutSMA mouse were submitted to western blot to analyze mTOR and phospho-mTOR. Results showed that phospho-mTOR at Ser2448 was significantly reduced in P2 and P5 mutSMA (P2: 0.58±0.054, p=0.006; P5: 0.67±0.11, p=0.026) conditions compared to P2 and P5 WT controls, respectively (**Figure 86 a and b**), while mTOR protein level was not significantly modified neither in WT and mutSMA conditions (P2: 0.79±0.13, p=0.08; P5: 1.08±0.14, p=0.46) (**Figure 86 a and b**). These results together suggest that mTOR phosphorylation at Ser2448 is reduced in SMA spinal cord, and could be contributing to increasing the autophagic flux in these tissues due to a lack of inhibition of the process.

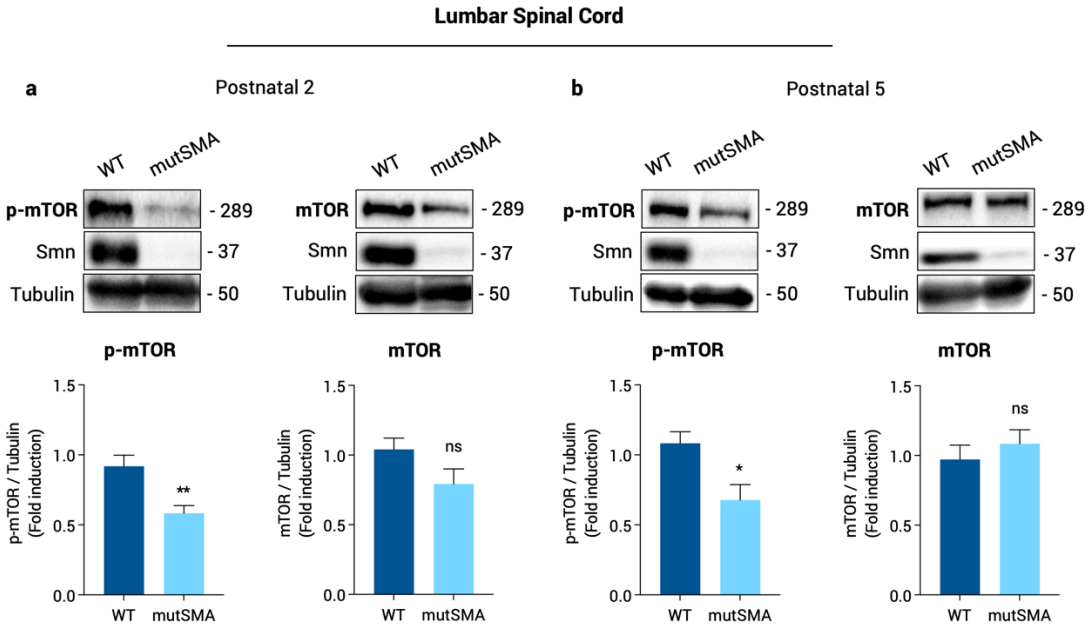

Figure 86 | mTOR phosphorylation at Ser2448 is reduced in spinal cord protein extracts of SMA mice. Spinal Cords from P2 and P5 genotyped WT and mutSMA mice were dissected and protein extracts were submitted to western blot analysis using anti-mTOR or anti-phospho-mTOR (Ser2448) antibodies. Membranes were reprobed with anti-α-tubulin antibody. Graph values represent the expression of mTOR or p-mTOR versus α-tubulin and correspond to the quantification of at least 5 independents experiments ± SEM. Asterisks indicate significant differences using Student t-test (*p<0.05; **p<0.01; no significant differences, ns, p>0.05).

Next, we examined by western blot the level of mTOR protein and phospho-Ser2448-mTOR in cell lysates from mouse and human cultured MNs. First, we isolated MNs from spinal cords of genotyped WT and mutSMA mouse embryos (E13). After 6 days in vitro, total cell lysates were collected and submitted to western blot using anti-mTOR (phospho-Ser2448) or anti-mTOR antibodies. Protein level of p-mTOR analysis revealed a significant increase of Ser2448 phosphorylation in mutSMA (2.39±0.33, p=0.0125) cultures compared to WT controls, while mTOR was not significantly modified in mutSMA MNs compared to the WT condition (0.97±0.14, p=0.86) (**Figure 87a**). To confirm this result in human MNs, SMA and Control iPSCs were differentiated to MNs. Seven days after differentiation, protein extracts were obtained and submitted to western blot analysis. mTOR phosphorylation at Ser2448 was increased in SMA (1.38±0.13, p=0.0198) condition compared to the Control, while the mTOR protein level did not show significant differences between SMA and Control human MNs (1.14±0.08, p=0.14) (**Figure 87b**). These results together indicate that the phosphorylation of Ser2448 mTOR is increased in mouse and human SMA MNs.

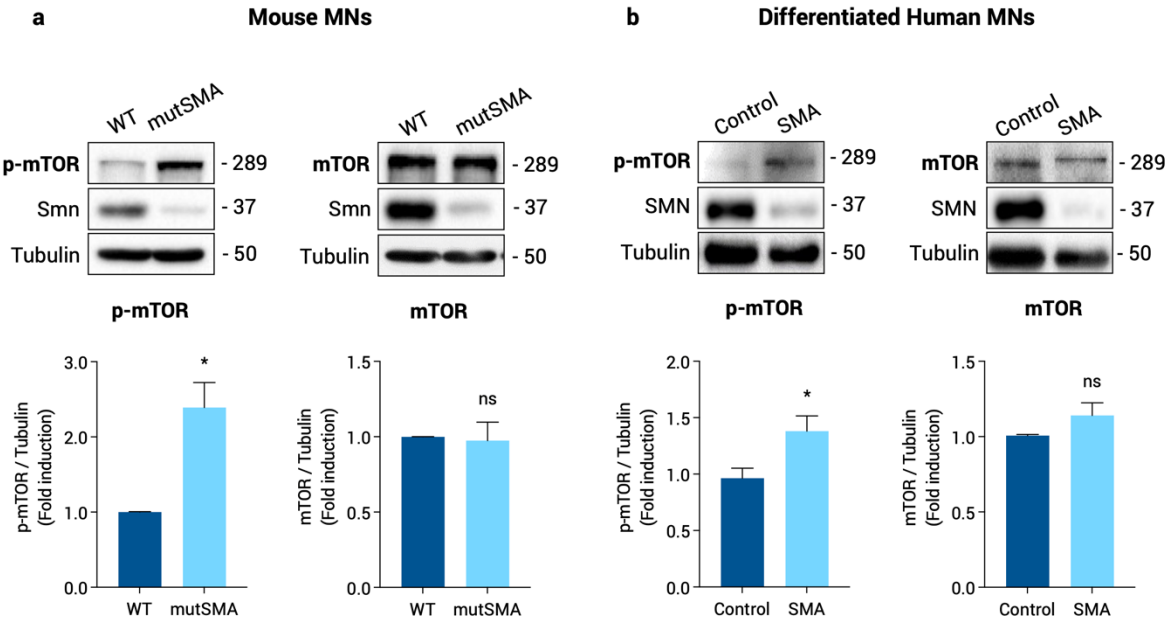

Figure 87 | mTOR phosphorylation at Ser2448 is increased in mouse and human SMA MNs. Protein extracts of 6-day cultured WT and mutSMA mice MNs (**a**) or 7-day differentiated Control and SMA human MNs (**b**) were submitted to western blot analysis using anti anti-phospho-mTOR(Ser2448) or anti-mTOR antibodies. Membranes were reprobed with anti-α-tubulin antibody. Graph values represent the expression of mTOR or p-mTOR versus α-tubulin (**a and b**) and correspond to the quantification of at least 4 independent experiments ± SEM. Asterisks indicate significant differences using Student t-test (*p<0.05; no significant differences, ns, p>0.05).

CHAPTER 4. AUTOPHAGY IS MODULATED BY ERK PATHWAY IN SPINAL MUSCULAR ATROPHY PATIENT MOTONEURONS

SUMMARY

mTOR activation can be controlled by growth factors, nutrient availability and stress stimuli (Melick & Jewell, 2020), and also by PI3K/Akt, ERK MAPK and NFkappaB signaling pathways (D. F. Lee et al., 2007; Ma et al., 2005; Melick & Jewell, 2020; Roux et al., 2004). Previous (Garcera et al., 2013; Periyakaruppiah et al., 2016) and present results from our laboratory revealed a dysregulation on autophagy markers in mouse and human SMA MNs altogether with an increased phosphorylation of mTOR (Ser2448). These results suggested a specific reduction of the autophagic flux in SMA MNs, that could potentially be due to mTOR overactivation. Moreover, ERK phosphorylation was also increased in these SMN-reduced cells. The mechanisms undergoing the overactivation of ERK protein are still under study. There is evidence that ERK can be activated due to high intracellular Ca^{2+} concentrations, which may promote a reduction of phosphorylated ERK nuclear translocation, preventing its action as a transcription factor and favoring its cytoplasmic activity (Chuderland et al., 2020; Chuderland & Seger, 2008). These observations led us to hypothesize that ERK phosphorylation increase in these cells may be due to an intracellular Ca^{2+} dysregulation. Increased phosphorylated ERK could over-activate mTOR protein in these cells, leading to the inhibition of autophagy and potentially producing an accumulation of LC3-II and p62 proteins (**Figure 88**). To this end, in this chapter we have studied the effects of ERK MAPK inhibition on mTOR and autophagy markers protein levels, and the effects of intracellular calcium chelation with BAPTA-AM on autophagy markers and SMN protein levels in differentiated Control and SMA human MNs.

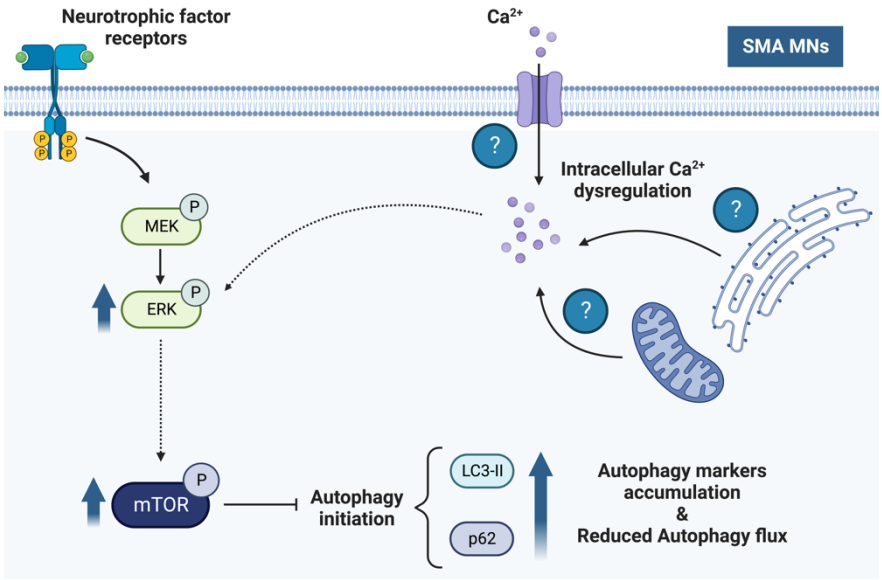

Figure 88 | Proposed mechanism by which ERK overactivation due to Ca^{2+} dysregulation would cause an increase of autophagy markers accumulation and a reduction of the autophagy flux in SMA MNs. Created with BioRender.com.

1. ERK MAPK inhibition regulates autophagy through mTOR inhibition in SMA human MNs

ERK protein participates in the activation of mTOR protein (S. G. Kim et al., 2013; Saxton & Sabatini, 2017; Winter et al., 2011). mTOR is a well-known autophagy inhibitor (Jung et al., 2009; Klionsky, Abdel-Aziz, et al., 2021), therefore increased ERK phosphorylation in SMA cells (**Figure 61**) may be contributing mTOR protein activation, leading to autophagy inhibition and potentially producing LC3-II and p62 proteins accumulation.

To validate this hypothesis, 7-day differentiated Control and SMA human MNs were treated with the MEK inhibitor U0126 (U0) (20µM) to reduce ERK phosphorylation. After 24 h, protein extracts were submitted to western blot analysis using anti-phospho(Ser2448)-mTOR and anti-mTOR antibodies. Inhibition of ERK phosphorylation was confirmed by blotting p-ERK and pan-ERK antibodies. As expected (**see Chapter 3**), untreated SMA cells presented increased p-mTOR level (SMA -U0: 1.81±0.2, p=0.0012) and no changes in mTOR (SMA -U0: 1.6±0.45, p=0.19) levels when compared with the untreated Control human MNs (Control -U0). Results showed no variation of p-mTOR (Control +U0: 0.86±0.36) or mTOR (Control +U0: 0.99±0.16) protein levels when treating the Control cells with the U0126 inhibitor (**Figure 89a**). Nevertheless, U0126-treated SMA cells showed a significant reduction of p-mTOR (SMA +U0: 0.77±0.007, p<0.0001) and mTOR (SMA +U0: 0.69±0.06, p<0.0001) protein levels, compared with the non-treated condition (SMA -U0) (**Figure 89b**). These results indicated that ERK MAPK inhibition with U0126 regulate mTOR protein levels and phosphorylation in differentiated SMA human MNs.

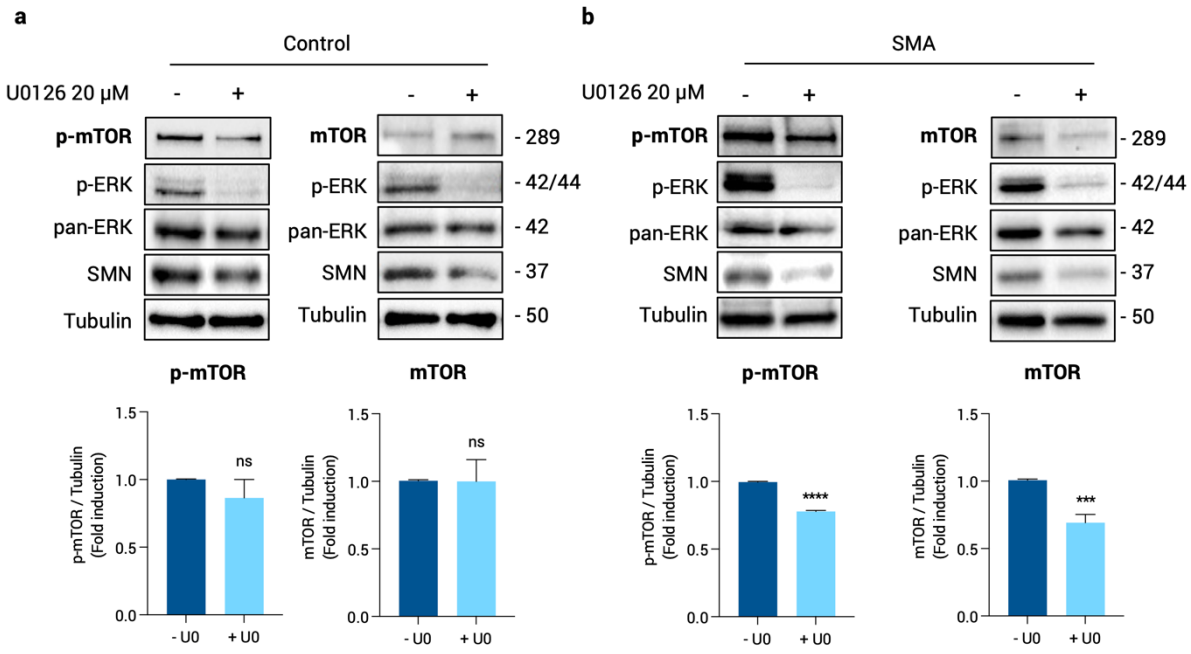

Figure 89 | ERK MAPK inhibition regulates mTOR in SMA human MNs. Seven day differentiated Control and SMA human MNs were treated with 20µM U0126 (U0) during 24 h or left untreated. Cell lysates were then obtained and submitted to western blot analysis. Anti-p-mTOR, anti-mTOR, anti-p-ERK and anti-SMN antibodies were probed in the blot membranes. Membranes were stripped and reprobed with an anti-pan-ERK antibody or reprobed with an anti-α-tubulin antibody. Graphs represent the expression of p-mTOR and mTOR vs α-tubulin, and correspond to the quantification of at least 4 independent experiments ± SEM. Asterisks indicate differences using Student *t*-test (***p<0.001; ****p<0.0001; no significant differences, ns, p>0.05).

The autophagy markers LC3-II and p62 proteins are increased in mouse and human SMA MNs (Chapter 3), therefore, we then analyzed the levels of these proteins in inhibited ERK pathway condition. Seven-day differentiated human Control and SMA MNs were treated with 20µM of U0126 during 24 h. Protein extracts were obtained and submitted to western blot analysis using anti-LC3 or anti-p62 antibodies (**Figure 90**). As expected, both p62 (SMA -U0: 1.42±0.12, p=0.0018) and LC3-II (SMA -U0: 2.53±0.6, p=0.025) levels were increased in non-treated SMA cells (-U0 SMA) when compared to the non-treated control (-U0 Control). No differences on p62 (Control +U0: 1.06±0.08, p=0.96) or LC3-II (Control +U0: 1.15±0.23, p=0.98) protein level were observed in Control U0126 treated cells compared to their respective non-treated controls (-U0 Control) (**Figure 90**). However, in SMA condition U0126 treatment significantly reduced p62 (SMA +U0: 0.94±0.04, p=0.019) and LC3-II (SMA +U0: 0.6±0.09, p=0.009) protein level compared to the non-treated SMA controls (p62 SMA -U0: 1.42±0.12; LC3-II SMA -U0: 2.53±0.6) (**Figure 90**), suggesting that ERK activation can regulate the autophagy flux in SMN-reduced MNs.

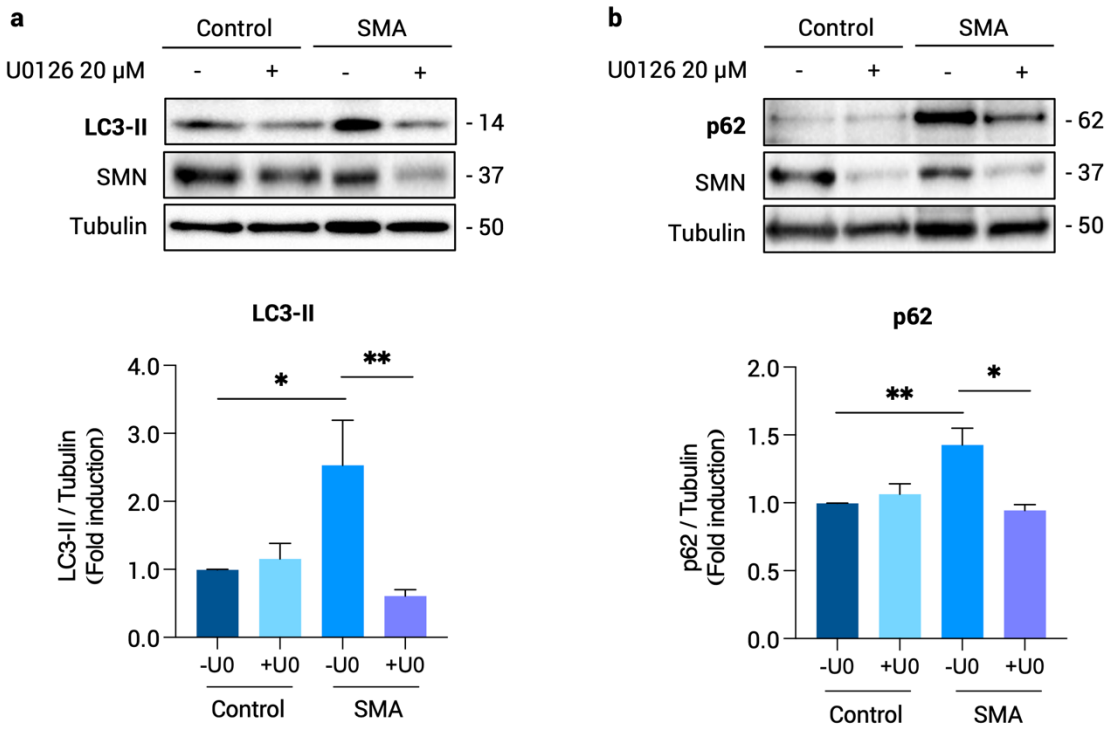

Figure 90 | ERK MAPK inhibition with U0126 regulates autophagy markers in SMA human MNs. Seven-day differentiated Control and SMA human MNs were treated with 20µM U0126 (U0) during 24 h or left untreated. Cell lysates were then obtained and submitted to western blot analysis. The antibodies anti-p62, anti-LC3-II and anti-SMN were probed in the blot membranes. Membranes were reprobed with an anti-α-tubulin antibody. Graphs represent the expression of (**a**) LC3-II vs α-tubulin, and of (**b**) p62 vs α-tubulin, and correspond to the quantification of at least 4 independent experiments ± SEM. Asterisks indicate differences using one-way Anova with Tukey's multiple comparisons post-test (*p<0.05; **p<0.01).

2. Intracellular calcium chelator BAPTA-AM prevents ERK hyper-phosphorylation in SMA human MNs

To elucidate the intracellular mechanisms involved in ERK phosphorylation increase observed in SMA MNs, we analyzed the effect of the intracellular calcium chelator BAPTA-AM on ERK phosphorylation in SMN-reduced cells. To this end, Control and SMA human iPSCs were differentiated to MNs. Seven-day cultures were treated with 10µM BAPTA-AM during 24 h and protein extracts were obtained and submitted to western blot using anti-SMN, anti-p-ERK and anti-pan-ERK antibodies. As expected, ERK phosphorylation was significantly increased in non-treated SMA MNs (SMA -BAPTA: 2.2±0.33, p=0.0019) compared to the non-treated Control (Control -BAPTA). Results showed that BAPTA-AM treatment reduced ERK phosphorylation in SMA (SMA +BAPTA: 0.84±0.12, p=0.0077) cells compared to its non-treated SMA control(SMA -BAPTA: 2.2±0.33), whereas no changes on ERK phosphorylation was observed in treated control human MNs (Control +BAPTA 1.08±0.12, p=0.99) compared to non-

treated Control cells (Control -BAPTA: 0.99 ± 0.001). Interestingly, SMN protein levels did not change in SMA (SMA +BAPTA: 0.44 ± 0.07, p>0.99) or in Control (Control +BAPTA: 0.99±0.00, p=0.99) treated cells, when compared to their respective non-treated conditions(SMA -BAPTA: 0.45±0.09; Control -BAPTA 0.98 ± 0.09)(**Figure 91**).

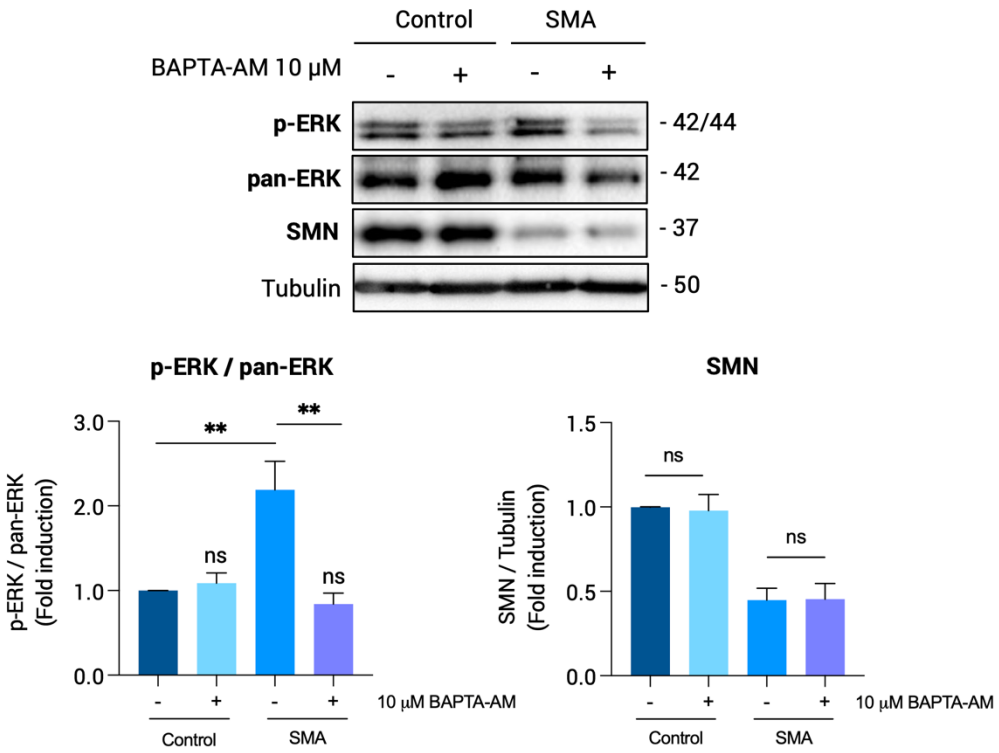

Figure 91 | Calcium chelator BAPTA-AM prevents ERK overactivation without modifying SMN levels. Seven-day differentiated Control and SMA human MNs were washed and treated with 10µM BAPTA-AM or left untreated. Twenty-four h later, protein extracts were obtained and submitted to western blot analysis using anti-p-ERK antibody and anti-SMN antibody. Membranes were stripped with an anti-pan-ERK antibody or reprobed with an anti-α-tubulin antibody. Graphs represent the expression of p-ERK vs pan-ERK, or SMN vs α-tubulin, corresponding to the quantification of 5 independent experiments ± SEM. Asterisks indicate differences using Student *t*-test or one-way Anova with Tukey's multiple comparisons post-test (*p<0.05; **p<0.01; no significant differences, ns, p>0.05).

To test the effectiveness of BAPTA-AM as a calcium chelator we evaluated the phosphorylation of CREB protein (p-CREB), a transcription factor activated by the calcium dependent Calmodulin Kinase II (CaMKII). Seven-day MNs were treated with 10µM BAPTA-AM and 24 h later protein extracts were obtained and submitted to western blot using anti-SMN, anti-p-CREB and anti-CREB antibodies. Results showed that CREB phosphorylation was reduced in non-treated SMA MNs (SMA -BAPTA: 0.54±0.11, p=0.0095) compared to the non-treated Control cells (Control -BAPTA). When treated with 10µM of BAPTA-AM, CREB phosphorylation was significantly reduced in both SMA (SMA +BAPTA: 0.18±0.08, p=0.04) and Control (Control +BAPTA: 0.44±0.04, p=0.0032) cells compared to their respective non-treated

control (Control -BAPTA: 1.03±0.008; SMA -BAPTA: 0.54±0.11). Total CREB protein levels did not change in SMA (SMA +BAPTA: 1.02±0.17, p=0.93) or in Control (Control +BAPTA: 1.13±0.36, p=0.97) treated cells, when compared to their respective non-treated conditions (SMA -BAPTA: 0.83±0.23; Control -BAPTA 1.03±0.008) (**Figure 92**). Together these results suggest that p-CREB is decreased in differentiated SMA human MNs, and that the calcium chelator BAPTA-AM prevents calcium-dependent CREB phosphorylation.

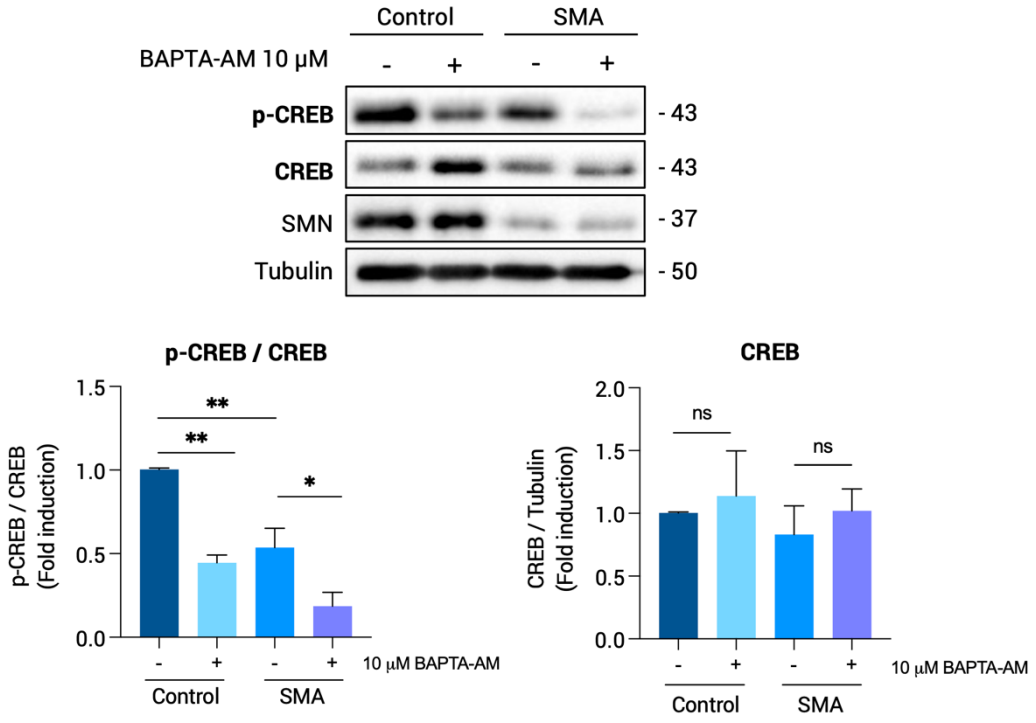

Figure 92 | Calcium chelator BAPTA-AM reduces CREB phosphorylation in both Control and SMA human MNs. Seven-day differentiated Control and SMA human MNs were washed and treated with 10µM BAPTA-AM or left untreated. Twenty-four h later, protein extracts were obtained and submitted to western blot using anti-p-CREB antibody and anti-SMN antibody. Membranes were stripped with an anti-CREB antibody or reprobed with an anti-α-tubulin antibody. Graphs represent the expression of p-CREB vs CREB, or CREB vs α-tubulin, corresponding to the quantification of 3 independent experiments ± SEM. Asterisks indicate differences using Student *t*-test or one-way Anova with Tukey's multiple comparisons post-test (*p<0.05; **p<0.01; no significant differences, ns, p>0.05).

3. ERK MAPK modulation with the calcium chelator BAPTA-AM prevents LC3-II increased levels in SMA human MNs

BAPTA-AM treatment reduced ERK hyperphosphorylation in differentiated SMA human MNs. To test the effect of the Ca^{2+} chelator on regulating the autophagy markers p62 and LC3-II, 7-day differentiated Control and SMA human MNs were treated with 10µM of BAPTA-AM

during 24h. Protein extracts were obtained and submitted to western blot analysis with anti-p62, anti-LC3, and anti-SMN antibodies (**Figure 93**). As expected, p62 and LC3-II levels were increased in non-treated SMA (p62: 1.35±0.09, p=0.0021; LC3-II: 1.92±0.25, p=0.0009) cells compared to the non-treated Control condition (Control -BAPTA).

BAPTA-AM treatment significantly reduced LC3-II in SMA (+BAPTA: 0.99±0.12, p=0.007) condition compared to non-treated SMA cells. No differences were observed on LC3-II protein level between treated and untreated treated Control (0.97±0.12, p=0.99) conditions (**Figure 93, right**). On the other hand, BAPTA-AM treatment did not significantly reduce p62 protein level in SMA (+BAPTA: 1.23±0.11, p=0.76) and Control (1.05±0.1, p=0.96) MNs compared to their respective non-treated controls (**Figure 93, left**). These observations suggested that BAPTA treatment reduced prevented ERK overactivation and restored LC3-II levels, but did not reduce p62 protein level.

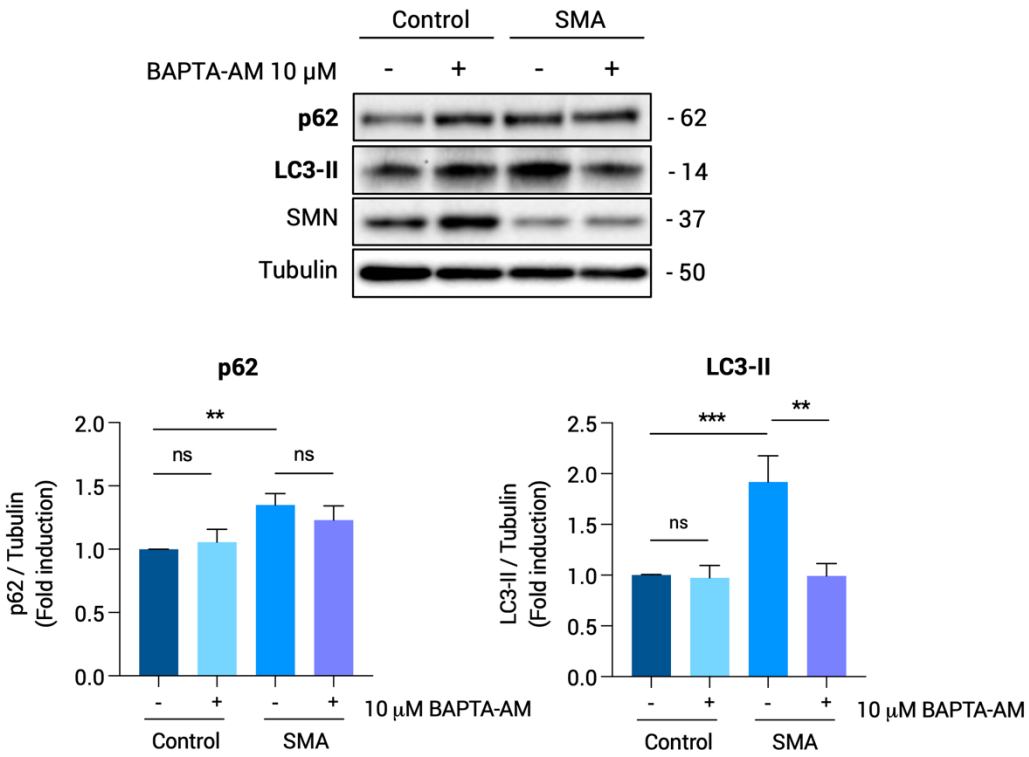

Figure 93 | Calcium chelator BAPTA-AM restores LC3-II autophagy marker through ERK MAPK regulation in SMA human MNs. Seven-day differentiated Control and SMA human MNs were washed and treated with 10µM BAPTA-AM or left untreated. Twenty-four h later, protein extracts were obtained and submitted to western blot analysis using anti-p62, anti-LC3 and anti-SMN antibodies. Membranes were reprobed with an anti-α-tubulin antibody. Graphs represent the expression of p62 (**left**) or LC3-II (**right**) vs α-tubulin, corresponding to the quantification of 6 independent experiments ± SEM. Asterisks indicate differences using Student *t*-test or one-way Anova with Tukey's multiple comparisons post-test (**p<0.01;***p<0.001; no significant differences, ns, p>0.05).

DISCUSSION

SMA pathological hallmarks include spinal MN loss and skeletal muscle atrophy, and can be manifested in severe, intermediate or mild forms depending on the amount of SMN protein that patients produce (Monani & De Vivo, 2014). The ubiquitous reduction of SMN levels can affect multiple tissues and organs, but MN degeneration and muscular atrophy remain the major alterations in SMA disease. Several hypotheses have arose regarding the affectation of spinal cord MNs in SMA disease. The characteristic morphology of these cells, consisting in a big soma and a single and very long axon, confer specific vulnerability to MNs. Most of the proteins in MNs are synthesized in the soma and transported along the axon to the synaptic terminals. Due to their morphology, these cells present high energy consumption and elevated number of mitochondria (Xu et al., 2016). Besides, intrinsic capability of Ca^{2+} buffering is low in MNs (Krieger et al., 1994). When a protein with essential roles such as SMN is lost, these MN features contribute to compromising cell integrity, favoring deregulation of survival signaling pathways, autophagy and apoptosis processes, and leading to neuronal degeneration and collapse. Moreover, MNs express lower levels of SMN from the *SMN2* gene relative to other spinal cells (Ruggiu et al., 2012), feature that could be contributing to the selective degeneration of these cells in SMA disease. Nevertheless, the cellular and molecular mechanisms leading to degeneration of SMA MNs are not completely understood. Hence, studying the causes underlying neuronal degeneration in SMA is still necessary to contribute to new therapeutic strategies development. To this end, we studied alterations undergoing in survival signaling pathways, autophagy and apoptosis in SMA disease models.

1. Increased neurite degeneration and apoptosis in SMA disease models

Apoptosis is a type of regulated cell death that under pathological conditions can contribute to the loss of neurons associated with numerous neurodegenerative disorders (reviewed in (Ghavami et al., 2014)). Previous results showed that neurite degeneration and cell survival were compromised in mouse Smn-reduced MNs (de la Fuente Ruiz, 2020; Garcera et al., 2011), and the overexpression of the antiapoptotic protein Bcl-XL prevented these alterations, suggesting apoptosis activation in SMN-reduced models (Garcera et al., 2011). These observations suggested a link between apoptosis activation and MN loss in SMA. Therefore, to evaluate members of the apoptotic pathway in the context of SMA disease, we used spinal cords and primary cultured MNs from two SMA mouse models, two human SMA fibroblast cell lines, and differentiated SMA MNs derived from human iPSCs.

Results revealed that mouse and human SMA MNs exhibited increased neurite degeneration, decreased cell survival, increased cleaved caspase-3 and higher presence of

nuclei with apoptotic morphology. Moreover, SMA human MNs exhibited reduced soma, nucleus, and cytoplasm size. Despite it is not clear whether apoptosis is the main cause of MN death in SMA disease, reduced cell survival, increased neurite degeneration, and the presence of apoptotic features suggest the involvement of this process in these cells' demise. Stereological counting of Nissl positive cells in lumbar sections of SMNdelta7 spinal cords showed reduced MN number in these mice (Piras et al., 2017). In accordance with this study, immunofluorescence analysis of thoracic and lumbar P11 SMNdelta7 spinal cords showed reduced MN count and size, and also NMJ denervation (Buettner et al., 2021). Similarly, another work described a selective loss of MNs innervating proximal and axial muscles, and reduced MN number over time, in postnatal SMNdelta7 mouse spinal cords (D'Errico et al., 2013). Additionally, the MNs of these mice exhibited smaller cell bodies (D'Errico et al., 2013). Another SMA mouse model (*Smn*$^{-/-}$;*SMN2*) showed facial and spinal MN decrease over time from P1 to P5 (Monani, Sendtner, et al., 2000). Together, these observations suggested that MN degeneration and survival are likely to be compromised in SMA disease models. Accordingly, our results revealed an increase in neurite degeneration prior to the reduction of cell survival in differentiated SMA human MNs. While neurite degeneration differences were evident at 7 DIV, the decrease in cell survival was significative at 14 DIV. Therefore, our observations and others suggest that neurite degeneration precedes MN collapse in SMA.

Several studies have described alterations in apoptosis-related proteins and increased cell death in different SMA models. For instance, increased apoptotic neuronal death was observed in 12-weeks SMA type I human fetuses with homozygous absence of *NAIP* gene (Soler-Botija et al., 2002). Moreover, the antiapoptotic proteins Bcl-2 and Bcl-XL were reduced in these patients MNs, suggesting a contribution of these proteins to the increased neuronal death (Soler-Botija et al., 2003). *NAIP* is part of a 500kb inverted duplication in the telomeric zone of chromosome 5q13, is located near *SMN1* gene, and is considered a SMA modifier. The protein encoded by *NAIP* is able to suppress apoptosis and was partially deleted in 67% of type I SMA, and in 42% of type II and III SMA patients (Roy et al., 1995). Furthermore, *NAIP* deletion was associated with an early onset, severe hypotonia, and worse outcome in Korean and Chinese patients (Ahn et al., 2017; Y. Zhang et al., 2020). Bcl-XL was also reduced in spinal cords from a SMA mouse model (*Smn*$^{+/-}$;*SMN2*$^{+/-}$), and Bcl-XL overexpression diminished muscle atrophy and MN degeneration, and increased 1.5 times their lifespan (L. K. Tsai et al., 2008). Activation of JNK pathway, involved in apoptosis-related gene expression, was observed in mouse and human SMA spinal cord extracts, suggesting its involvement in MN degeneration (Genabai et al., 2015). Moreover, pharmacological (Schellino et al., 2018) or

genetic (Genabai et al., 2015) inhibition of JNK pathway ameliorated motor functions and life expectancy in the SMNdelta7 mouse model (Genabai et al., 2015; Schellino et al., 2018), reduced MN loss to a 20%, and improved innervation and synapse formation at NMJs (Genabai et al., 2015). Decreased Bcl-2 and increased cleaved caspase-3 level were observed in spinal cord protein extracts of P9 SMNdelta7 mice (Piras et al., 2017). Notwithstanding, apoptosis has not always been observed in SMA disease models. For instance, apoptotic features were not observed in SMNdelta7 MNs with increased p53 phosphorylation (Simon et al., 2017). Increased S18 phosphorylation in p53 is associated with caspase-3 activation (Schuler et al., 2000), increased DNA damage, and cell death in mice (C. Chao et al., 2006; Hernández Borrero & El-Deiry, 2021; Sluss et al., 2004). Nevertheless, caspase-3 activation was not observed in these SMNdelta7 MNs *ex vivo* (Simon et al., 2017), suggesting a caspase-independent form of death occurring in these cells. On the other hand, several *in vitro* studies demonstrated apoptosis activation in SMA condition, suggesting a connection between SMN level and apoptosis activation. Depleting SMN in a drosophila cell line increased expression and activation of endogenous caspases (Ilangovan et al., 2003). Likewise, in the MN-like cell line NSC34, SMN reduction by RNA interference elevated caspase-3 activity, reduced cell viability, and increased the percentage of TUNEL-stained cells (Parker et al., 2008). Experiments using MNs from differentiated SMA-iPSC lines showed neurite outgrowth abnormalities and reduced capacity to form MNs (T. Chang et al., 2011; Sareen et al., 2012). These alterations were restored upon SMN re-expression in these cells (T. Chang et al., 2011). Additionally, differentiated SMA human MNs exhibited increased Fas ligand-mediated apoptosis with high levels of cleaved caspase-8 and caspase-3 (Sareen et al., 2012). This phenotype was counteracted using a caspase-3 inhibitor or blocking Fas receptor, rescuing the SMA cells from apoptosis (Sareen et al., 2012). According to these observations, our mouse and human SMA MNs showed high cleaved-caspase-3 levels and increased percentage of fragmented nuclei. Together, these observations suggest that apoptosis is active in SMA and that it may play an important role in the disease development.

2. Alterations of apoptosis-modulating proteins in SMA disease models

The analysis of the antiapoptotic proteins FAIM-L and XIAP in spinal cord extracts revealed a reduction of these markers at critical stages of SMA mouse embryonic development (E13 and E18), and at the disease end-stage (P5). Programmed cell death in the mouse spinal cord is produced between these two embryonic time points (Sun et al., 2005), and MN loss has been observed in the latest phases of SMA disease progression (Buettner et al., 2021; D'Errico

et al., 2013; Piras et al., 2017). Moreover, we detected increased cleaved-caspase-3 in MNs and in lumbar spinal cord extracts of the SMNdelta7 mouse model. FAIM-L is a cytosolic protein only present in neuronal cells (Segura et al., 2007), and regulates XIAP inhibiting its auto-ubiquitination by binding to XIAP BIR2 domain. FAIM-L binding prevents XIAP degradation, maintaining the protein stability and its antiapoptotic function as a caspase inhibitor (Moubarak et al., 2013). In addition, XIAP is a substrate of caspase-3, and its cleavage by the protease disabled the antiapoptotic effect of XIAP in endothelial cells (Levkau et al., 2001). Therefore, the reduction of FAIM-L and XIAP levels could correlate with increased cleaved-caspase-3 observed in SMA spinal cords. On the other hand, low XIAP levels may be related to NFkappaB signaling pathway dysregulations (Levkau et al., 2001). NFkappaB is one of the major regulators of *in vitro* MN survival, together with PI3K/Akt and ERK MAPK (Dolcet et al., 2001; Mincheva et al., 2011; Soler et al., 1999), and XIAP protein participates in regulating the NFkappaB signaling pathway (Dubrez-Daloz et al., 2008; Levkau et al., 2001; Saraei et al., 2018). RelA (p65) phosphorylation was reduced in cultured SMA MNs (Arumugam et al., 2018), and intrinsic NFkappaB pathway reduction increased nuclear fragmentation and reduced MN cell survival *in vitro* (Mincheva et al., 2011). Therefore, XIAP protein reduction could contribute to NFkappaB pathway alterations and to increased apoptosis in SMA disease. Nevertheless, further investigating NFkappaB members level in spinal cord extracts should be conducted to establish a connection between XIAP levels and the survival signaling pathway.

SMA human fibroblast cell lines western blot and immunofluorescence analyses revealed a reduction of XIAP levels in SMA patients. Since FAIM-L is only present in neurons (Segura et al., 2007), XIAP stability might be compromised in these fibroblasts and other non-neuronal SMA tissues. Although XIAP is degraded through the ubiquitin proteasome-system (UPS) (Moubarak et al., 2013), further investigation should be performed to elucidate whether XIAP proteasomal degradation is enhanced in these SMA human fibroblasts. For instance, blocking proteasome activity with bortezomib or MG132 could elucidate if proteasomal activity is enhanced in SMA fibroblasts. Nevertheless, XIAP degradation could also be mediated by autophagy (Wang et al., 2013), which is altered in several SMA disease models (Custer & Androphy, 2014; de la Fuente et al., 2020; Garcera et al., 2013; Periyakaruppiah et al., 2016; Piras et al., 2017; Rodriguez-Muela et al., 2018). Hence, targeting the proteasome system or the autophagy pathway may elucidate whether these reduced XIAP levels are due to alterations in proteasomal or autophagy activities.

Conversely, FAIM-L and XIAP were increased in isolated and cultured mouse and human SMA MNs. These differential results observed between spinal cord tissue, human fibroblast, and isolated MNs could be due to specific FAIM-L and XIAP functions in MNs. Our observations suggest that increased FAIM-L in cultured SMA MNs regulates XIAP stability resulting in an elevation or preservation of XIAP protein level. For instance, FAIM-L maintained endogenous levels of XIAP in murine cortical neurons, thereby protecting these cells against FasL-induced apoptosis (Moubarak et al., 2013). Changes of FAIM-L and XIAP proteins have been described in several neurodegenerative diseases. Reduced IAP-1 and XIAP level was observed in brain-derived cell line models of HD expressing mutant Htt protein (Goffredo et al., 2005). Moreover, these cells displayed increased cytochrome *C* release, and activation of caspase-9 and caspase-3 upon exposure to toxic stimuli, suggesting IAPs implication in HD cell death (Goffredo et al., 2005). On the other hand, ALS SOD1 mouse model exhibited increased XIAP and caspase-7 cleavage in spinal cord extracts at the disease end-stage (Guégan et al., 2001), indicating apoptosis activation and suggesting its contribution to MN death. XIAP protein expression was increased in human entorhinal cortex in 50% of AD patients analyzed, and was associated to a compensatory mechanism to suppress caspase activation in AD brains (Christie et al., 2007). On the other hand, FAIM-L expression reduction in hippocampal samples was associated with AD progression (Carriba et al., 2015). FAIM-L was also reduced in the entorhinal cortex and the hippocampus of the AD transgenic mouse model PS1xAPP, and the addition of their brain soluble fraction in cultured neurons decreased FAIM-L expression (Carriba et al., 2015), suggesting that FAIM-L decline was associated to Aß accumulation. These observations associate XIAP and FAIM-L expression with cell death in several neurodegenerative diseases.

Our observations and others suggest that decreased FAIM-L and XIAP in SMA spinal cords may be involved in SMA pathology progression and increased apoptosis. In cultured mouse and human SMA MNs, FAIM-L and XIAP increase may reflect a cellular reaction to prevent or slow down apoptosis induced by SMN reduction. Nevertheless, these cells exhibited apoptotic features, increased neurite degeneration and decreased cell survival, indicating that FAIM-L and XIAP expression are not sufficient for preventing MN degeneration and apoptosis activation in SMA models (**Figure 94**).

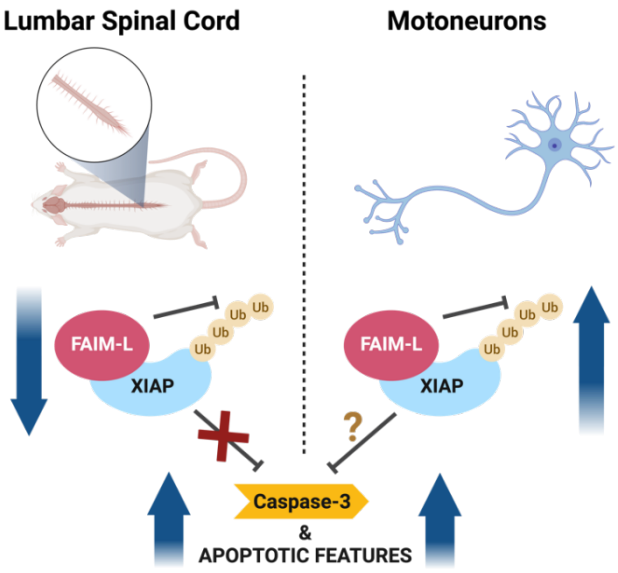

Figure 94 | Apoptosis markers dysregulation in SMA models.

FAIM-L and XIAP are decreased in spinal cord but increased in cultured MNs of SMA models. Notwithstanding, the antiapoptotic protein increase is not sufficient to counteract apoptosis in SMA cells. Created with BioRender.com.

3. Survival signaling pathway alterations in SMA disease models

Further alterations in survival signaling pathways may take place in SMA disease, contributing to decreasing antiapoptotic protein levels and increasing apoptotic features in SMA MNs. The activation of PI3K/Akt and ERK MAPK signaling pathways is essential for the survival and maintenance of several neuronal types during development (Frebel & Wiese, 2006). PI3K/Akt signaling pathway regulates the expression of antiapoptotic proteins such as Bcl-2, which was reduced in several SMA models (Anderson et al., 2003; Piras et al., 2017; Soler-Botija et al., 2003). Moreover, Akt inhibition caused apoptotic cell death in MNs (Dolcet et al., 2001). These observations suggest PI3K/Akt as one of the principal regulators of the apoptosis process in MNs. ERK MAPK signaling pathway is involved in promoting antiapoptotic proteins expression, such as Bcl-2 and Bcl-XL (K. Du & Montminy, 1998). Previous results suggested that ERK and Akt signaling pathways were dysregulated in SMN-reduced MNs (Biondi et al., 2010, 2015; Hensel et al., 2017). Akt phosphorylation was reduced whereas ERK phosphorylation was increased in SMA lumbar spinal cord and tibialis muscle protein extracts (Biondi et al., 2015; T. L. Lin et al., 2016), in SMN-reduced MN-like NSC34 cells (Hensel et al., 2012, 2014), and in iPSC derived SMA astrocytes (Mcgivern et al., 2013). Moreover, ERK phosphorylation increase was also observed in SMA human spinal cord extracts (Genabai et al., 2015). Hence, survival signaling pathway alterations occur in SMA disease models alongside or in addition to SMN reduction, and these changes may contribute to increase MN vulnerability to cell death.

Given the implication of PI3K/Akt and ERK MAPK signaling pathways in MN survival and in SMA disease, and since we observed apoptotic features in these cells, we explored

whether they were modified in SMN-reduced MNs. According to previous observations in other SMA models (Biondi et al., 2010, 2015; Hensel et al., 2017), our results revealed reduced Akt phosphorylation and increased ERK phosphorylation in cultured SMA mouse and human MNs. These changes of Akt and ERK phosphorylation profile in MNs may be contributing to exacerbate SMA disease progression. PI3K/Akt and ERK/MEK pathways have been linked to the positive regulation of SMN transcription through the Akt/CREB and the ERK/Elk-1 pathways, respectively (Biondi et al., 2015; Branchu et al., 2013; Demir et al., 2011). Therefore, we studied SMN regulation by using PI3K/Akt or ERK MAPK inhibitors, LY294002 and U0126, respectively. In agreement with previous studies, the pharmacological inhibition of either PI3K/Akt or ERK MAPK pathways reduced SMN protein and mRNA levels in cultured control and SMA mouse and human MNs.

Since PI3K/Akt inhibition was capable of modulating *SMN* at transcriptional level, we analyzed the regulation of *Gemin2* upon PI3K inhibition with LY294002. *Gemin2* expression and SMN protein level are directly linked (W. Feng et al., 2005; C. Y. Wu et al., 2011). Gemin2 is a protein that in the axonal compartment is associated in a complex with SMN, Gemin3, and hnRNPs (Talbot & Davies, 2008), localized in granules and transported through the neuronal processes and growth cones (R. Zhang et al., 2011). Our results revealed that LY294002 addition reduced *Gemin2* mRNA in mouse cultured MNs. Thereby, we postulate that reduced PI3K/Akt pathway activation in SMA MNs may contribute to SMN and Gemin2 reduction in the axonal compartments, and to altering their specific function in these cells. Nevertheless, no changes on *GEMIN2* mRNA were observed in differentiated SMA human MNs at basal level or when treated with LY294002. These controversial results could be due to a differential effect of the inhibitor on the cells. In mouse MNs *Smn* reduction was around a 40% while in human MNs *SMN* reduction was only around a 20%. Hence, we hypothesize that a greater reduction of SMN protein may influence on GEMIN2 levels, although further investigations should be conducted to corroborate this statement. Based on the literature, PI3K/Akt signaling pathway is likely to be modulating SMN transcription (Ahmad et al., 2016; Branchu et al., 2013). Accordingly, our results suggested that PI3K/Akt pathway regulates *SMN* at transcriptional level, and that Akt phosphorylation reduction may contribute to SMN protein level decrease in SMA MNs. Thereby, regulating PI3K/Akt pathway activity may increase SMN level. For instance, activation of the PI3K/Akt signaling pathway using NMDA raised SMN protein level in spinal cord explants of the SMNdelta7 mouse model (Biondi et al., 2010). Furthermore, NMDA treatment significantly reduced caspase-3 cleavage in P12 ventral lumbar spinal cord extracts, prevented MN loss, and significantly increased the lifespan of these mice (Biondi et

al., 2010). Therefore, increasing PI3K/Akt signaling activity should be considered for designing new therapeutic approaches since it may contribute to restore SMN protein levels and to prevent apoptosis in SMA MNs.

Regarding the ERK MAPK signaling pathway, ERK overactivation contribution to SMA disease is still unclear. The effects of ERK inhibition on SMA disease models and tissues are controversial. Previous studies demonstrated a beneficial effect of ERK inhibition, enhancing SMN protein level in SMA spinal cord and muscle by promoting *SMN2* transcription through the CaMKII/AKT/CREB signaling pathway (K. Du & Montminy, 1998; Li et al., 2011). Besides, ERK inhibition improved survival and motor functions on severe SMA mice models (Biondi et al., 2015; Bowerman, Murray, et al., 2012; Branchu et al., 2013). It is important to note that these discoveries regarding SMN transcription upregulation were observed mainly in SMA muscle and total spinal cord samples (Biondi et al., 2015; Bowerman, Murray, et al., 2012; Branchu et al., 2013) whereas our findings were described in isolated SMA MNs, which are diversely affected in SMA disease. In agreement with our results, another report showed that ERK phosphorylation inhibition was protective in total primary spinal cord cultures, but it aggravated the SMA phenotype and induced MN-specific cell death in the Taiwanese SMA mouse model (Hensel et al., 2017). These observations point out the differential outcomes of regulating survival signaling pathways in SMA disease depending on the affected tissue. Additionally, a transcriptional study on muscle tissue from SMA type I and III patients revealed distinct expression of proteins involved in cell survival and autophagy like PI3K/Akt, ERK MAPK or mTOR pathways between the two disease phenotypes (Millino et al., 2009). Therefore, according to the literature and our results, ERK phosphorylation increase in SMA disease may be playing a distinct role in modulating SMN levels and other molecular processes based on the specific cell type and SMN protein level dependency. These differences between tissue and MNs should be taken into account when designing therapies for treating SMA. On the other hand, ERK activation by NTFs increased FAIM-L expression in neuronal PC12 cells, protecting them from Fas-induced apoptosis by regulating XIAP (Moubarak et al., 2013; Segura et al., 2007). As observed in Chapter 1, FAIM-L protein levels were increased in cultured mouse and human SMA MNs. Therefore, increased ERK phosphorylation may promote FAIM-L expression in SMA MNs. To this end, we analyzed *FAIM-L* mRNA levels when ERK phosphorylation was reduced in mouse MNs. Results showed that ERK pharmacological inhibition reduced *FAIM-L* mRNA transcript levels, suggesting that the observed increase of FAIM-L in SMA MNs may be the consequence of ERK over-activation in these cells. Nevertheless, ERK overactivation and increased FAIM-L and XIAP protein levels

cannot fully counteract the initiation of the apoptotic process produced in SMA MNs. Therefore, it seems that other survival pathway alterations such as reduced RelA levels (Arumugam et al., 2018), JNK pathway activation (Genabai et al., 2015; Schellino et al., 2018), or decreased Akt phosphorylation may greatly contribute to promote apoptosis in these cells.

The changes observed in intracellular survival pathways led us hypothesize that reduced SMN protein is involved in this process, as SMN reduction contributes to MN survival and degeneration (Garcera et al., 2011), and these pathways are altered in other SMA mouse models (Biondi et al., 2015; Branchu et al., 2013; Hensel et al., 2017). Therefore, we explored Akt and ERK phosphorylation upon SMN protein increase or decrease with lentiviral approaches. Nevertheless, SMN protein modulation did not affect Akt or ERK phosphorylation status, either in mouse cultured MNs or in differentiated Control and SMA human MNs. These results suggested that SMN is not directly regulating the modifications of intracellular survival signaling pathways. Notwithstanding, these observations could be due to a short time period modulation of SMN protein. Hence, a sustained downregulation or upregulation of SMN protein over time may exert changes in the activity of these survival signaling pathways.

Overall, present results show reduction of Akt phosphorylation and increase of ERK phosphorylation in SMN-reduced mouse and human MNs. Moreover, pharmacologically inhibition of PI3K/Akt and ERK MAPK signaling pathways reduces SMN at protein and transcriptional level (**Figure 95)**.

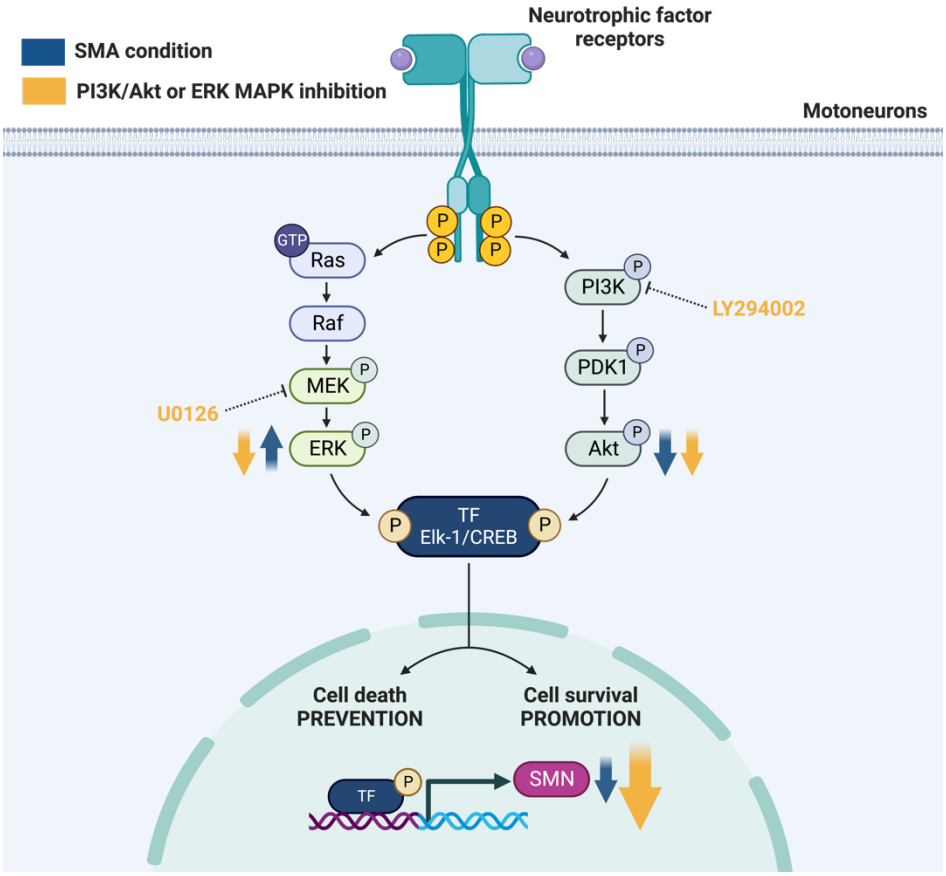

Figure 95 | PI3K/Akt and ERK MAPK signaling pathways are altered in SMA MNs and their regulation modulates SMN levels in MNs. In SMA condition, PI3K/Akt and ERK MAPK signaling pathway alterations may lead to decreased SMN levels. Inhibition of PI3K/Akt or ERK MAPK pathways reduces SMN at protein and at transcriptional level in healthy and SMA condition. Created with BioRender.com.

Reduced Akt phosphorylation and increased ERK phosphorylation could contribute to autophagy alterations in SMA cells. PI3K/Akt signaling pathway regulates the expression of Bcl-2, which was reduced in several SMA models (Anderson et al., 2003; Piras et al., 2017; Soler-Botija et al., 2003), and inhibits the nucleation phase of the autophagy process (Pattingre et al., 2005), where the Beclin 1 protein plays an important role (Pattingre et al., 2005; Yang & Klionsky, 2009). Moreover, elevated Beclin 1 was observed in SMN-reduced cells and SMA spinal cords (Garcera et al., 2013; Piras et al., 2017), whereas Bcl-2 level was decreased (Piras et al., 2017). Besides, Akt and ERK are upstream activators of mTOR protein (Melick & Jewell, 2020), which is implicated in autophagy inhibition. Together, these observations suggest reduced PI3K/Akt pathway activation, decreased Bcl-2 expression and increased ERK phosphorylation may contribute to autophagy alterations in SMA disease.

4. Autophagy alterations in SMA disease models

Autophagy dysregulation has been described in several neurodegenerative disorders such as HD (Fox et al., 2010; Ravikumar et al., 2004), AD (Boland et al., 2008), PD (Cooper et al., 2006; Winslow et al., 2010) and ALS (Farg et al., 2014), (reviewed in (Menzies et al., 2015; Rubinsztein et al., 2007; Williams et al., 2006)). ALS is a neurodegenerative disease that affects MNs in the brain, brainstem and spinal cord, resulting in progressive weakness and atrophy of voluntary skeletal muscles (Zufiría et al., 2016). ALS MN lines with C9ORF72 hexanucleotide-repeat expansions revealed increased colocalization of C9ORF72 with proteins from the endocytic and exocytic pathway (C. C. Yap & Winckler, 2009), suggesting dysregulation of endosomal trafficking in ALS patients with this expansion (Farg et al., 2014). Participation of autophagy during muscle (Dobrowolny et al., 2008) and MN atrophy (Custer & Androphy, 2014; Garcera et al., 2013) has been described in several experimental models and autophagy changes have been related to SMA disease (Custer & Androphy, 2014; de la Fuente et al., 2020; Garcera et al., 2013; Piras et al., 2017; Rodriguez-Muela et al., 2018).

Degeneration and loss of function of spinal cord MNs and muscle denervation are two of the major hallmarks of SMA, and skeletal muscle alterations play an important role in the pathophysiology of the disease (Hamilton & Gillingwater, 2013; J. K. Kim et al., 2020). The mechanism by which SMN reduction leads to MN degeneration and muscle atrophy remains a subject of intense research within the field. Muscular atrophy is triggered by several pathways among which autophagy deregulation has a major role (Castets et al., 2013). In muscle tissue, detrimental changes have been described in SMA models preceding the degeneration of MNs (Mutsaers et al., 2011). Furthermore, the selective reduction of SMN in muscle has been described to result in the development of a MN-independent disease (J. K. Kim et al., 2020). In SMA MNs, previous results have shown that LC3-II and p62 autophagy markers are increased in SMA mouse MNs (Garcera et al., 2013; Periyakaruppiah et al., 2016; Rodriguez-Muela et al., 2018). Moreover, the modulation of this process can increase or decrease SMN protein levels (de la Fuente et al., 2018, 2020; Periyakaruppiah et al., 2016), indicating the participation of autophagy in SMN protein regulation. Therefore, autophagy impairment in MNs may contribute to SMA disease progression.

The alterations of autophagy markers among diverse SMA tissues have not been fully described yet. Consequently, the analysis of autophagy contribution to muscle atrophy and neurodegeneration has become increasingly important. To this end, we studied the expression

of the following autophagy markers involved in the autophagy process in several SMA-affected tissues and cell types; mTOR, Beclin 1, LC3-II, p62/SQSTM1 (p62), and LAMP-1. These proteins have key roles in different phases of autophagy, and their analysis can provide information of alterations in the process. mTOR protein is responsible for allowing the initiation of the phagophore formation, and its phosphorylation blocks this first step (Klionsky, Petroni, et al., 2021). Therefore, increased mTOR phosphorylation indicates autophagy inhibition. Beclin 1 is part of the PI3KC3 complex, and takes part in the nucleation phase (Dikic & Elazar, 2018). Lipidated LC3 (LC3-II) associates to the autophagosome membrane until the fusion with the lysosome. Measuring LC3-II level gives information of the autophagosome amount in the cells (Klionsky, Abdel-Aziz, et al., 2021). p62 is a cargo protein degraded through autophagy. It accumulates when autophagy is inhibited, and reduced protein level can be observed when autophagy is induced (Bjørkøy et al., 2009). Therefore, high p62 levels indicate decreased autophagy flux, and low levels increased flux. LAMP-1 is found in the lysosomal membrane (Eskelinen et al., 2003), and gives information of the lysosome amount since it is the most abundant lysosomal membrane protein (Saftig & Klumperman, 2009).

Two main findings emerged from our study: the autophagy process was significantly altered in SMA muscle and MN cells; and mTOR and autophagy pathways alterations had different profiles in SMA muscle, spinal cord, fibroblasts, and MNs (**Figure 96**). All the changes observed in this work and in the literature of the studied proteins are collected in **Table 29**.

Table 29 | Autophagy markers protein level in human and mouse SMA models.

	Autophagy marker	Protein level	SMA cell type and tissue	References
Initiation	mTOR	No change	**Human:** Differentiated MNs **Mouse:** Muscle, Spinal cord, Isolated MNs	Present work
		Decreased	**Human:** Fibroblasts	Present work
Initiation	p-mTOR (Ser2448)	Decreased	**Human:** Fibroblasts **Mouse:** Muscle, Spinal cord	Present work, Yu-Ting Seng et al. 2016
		Increased	**Human:** Differentiated MNs **Mouse:** Isolated MNs	Present work
Nucleation	Beclin 1	Decreased	**Mouse:** Muscle	Present work
		Increased	**Human:** Differentiated MNs **Mouse:** Spinal cord, Isolated MNs	Present work, Garcera et al, 2013, Piras et al, 2017
Elongation	LC3-II	Decreased	**Human:** Muscle, Lymphocytes, Fibroblasts **Mouse:** Muscle	Present work
		Increased	**Human:** Differentiated MNs **Mouse:** Spinal cord, Isolated MNs	Present work, Piras et al, 2017, Garcera et al, 2013, de la Fuente et al, 2020
Elongation	p62/SQSTM1	No change	**Mouse:** Spinal cord	Piras et al, 2017
		Increased	**Human:** MNs, Fibroblasts **Mouse:** Isolated MNs	Present work, Custer et al. 2014, Periyakaruppiah et al, 2016, Rodriguez-Muela et al. 2018
		Decreased	**Mouse:** Muscle	Present work
Lysosomal fusion and degradation	LAMP-1	No change	**Mouse:** Muscle	Present work
		Decreased	**Human:** Differentiated MNs	Present work
		Increased	**Human:** Fibroblasts	Present work

4.1. Analysis of LC3, Beclin 1, p62 and LAMP-1 in SMA disease models

The analysis of LC3-II in SMA muscle, lymphocytes and fibroblasts revealed reduced protein level, indicating decreased autophagosome amount. In contrast, LC3-II was significantly elevated in the SMA condition at the disease endpoint (P5 gastrocnemius), indicating increased autophagosome formation or accumulation in muscle cells. These differential results could be due to systemic collapse at the final stage of the disease. The evaluation of other autophagy related proteins in SMA muscle showed reduced levels of Beclin 1 and p62, indicating a potential increase of the autophagy flux. Beclin 1 is the substrate of several proteases including caspases and calpain (R. Russo et al., 2011; Y. Zhu et al., 2010). Caspase-3, caspase-8 and calpain are activated in Smn-reduced cells in SMA pathology (de la Fuente et al., 2020; Sareen et al., 2012; Sheng et al., 2018); thereby, the activation of these proteases in muscle cells could be the basis for Beclin 1 reduction. These results suggested that Beclin 1 decline may contribute to the slowdown/decrease of autophagosome formation and lowering of LC3-II levels in muscle cells (Kang et al., 2011). Studies of muscle-specific SMN reduction may help to elucidate the contribution of autophagy, apoptosis, and calpain pathways on SMA muscle atrophy. Previous results suggested that skeletal muscle atrophy in severe SMA mice is manifested by increased proteasomal degradation but not by autophagosomal protein breakdown (Deguise et al., 2016). Conversely, our results indicated that autophagy markers, including LC3-II, Beclin 1 and p62, are deregulated in SMA muscle. When both pathways are affected, the atrophy process in muscle tissue may be accelerated (Taillandier & Polge, 2019), and muscle-specific regulatory mechanisms may exacerbate the situation (J. K. Kim et al., 2020; Woo Kim et al., 2020). In this context, some evidence indicates that proteasome and autophagy activities are altered in Smn-reduced MNs (Burnett et al., 2009; Garcera et al., 2013; Kwon et al., 2011; Periyakaruppiah et al., 2016). Moreover, treatment with the autophagy inhibitor Baphilomycin A1 reduced Smn protein level in MNs and the inhibition of the proteasome activity reverted this effect (Periyakaruppiah et al., 2016). These results indicate that both autophagy and proteasome regulate Smn protein level in SMA neurons, suggesting that similar regulation may occur in SMA muscle.

Autophagy markers analysis in human SMA fibroblast cell lines revealed p62 accumulation and decreased LC3-II and LAMP-1 levels. No changes were observed in Beclin 1 levels. Together with reduced LC3-II, autophagy markers levels in human SMA fibroblasts suggested a reduction of the autophagy flux in these cells, a decrease in the autophagosome number and less autophagolysosome formation.

Beclin 1, LC3-II, and p62 levels are increased in mouse SMA spinal cord (Piras et al., 2017) and MNs (Garcera et al., 2013; Periyakaruppiah et al., 2016). To validate these alterations in human SMA models, we analyzed these proteins and LAMP-1 in differentiated SMA human MNs. Western blot and immunofluorescence analysis revealed accumulation of LC3-II. Protein immunoblot experiments also revealed increased Beclin 1 and p62 level, and reduced LAMP-1 in differentiated SMA human MNs. Accumulation of LC3-II and p62 together with reduced LAMP-1 indicated a reduction in the autophagy flux and decreased autophagolysosome formation in SMA MNs. Together, these observations indicated that autophagy dysregulation in SMA is subjected to the cell type.

4.2. Analysis of mTOR protein level and phosphorylation ad Ser2448 in SMA disease models

To elucidate whether autophagy initiation was affected, we analyzed mTOR protein level and phosphorylation at Ser2448 (p-mTOR) in SMA tissues and cell types. mTOR is a Serine/Threonine protein kinase that senses multiple upstream stimuli thereby controlling cell growth and differentiation, metabolism, and autophagy (Switon et al., 2017). As mentioned, increased mTOR phosphorylation indicates autophagy inhibition, whereas reduced mTOR phosphorylation shows autophagy induction.

Our results revealed reduced p-mTOR in SMA mouse gastrocnemius protein extracts with no modifications of mTOR protein level. These results, together with decreased Beclin 1, LC3-II, and p62 suggested decreased autophagosome formation and increased autophagic flux in SMA muscle. mTOR pathway is upregulated during muscle hypertrophy and downregulated during muscle atrophy (Bodine et al., 2001). Atrophy and hypertrophy of skeletal muscle are associated with decreased mTOR and increased phosphorylation in Ser2448, suggesting that modulation of this site may have a significant role in protein synthesis control (Reynolds IV et al., 2002). However, chronic mTORC1 activation in the muscle results in severe muscle atrophy, principally due to an inability to induce autophagy in this tissue (Castets et al., 2013; Saxton & Sabatini, 2017). The activation of mTOR is also necessary for neuromuscular junction (NMJ) maintenance, and its inhibition causes NMJ loss and triggers a dying-back process producing MN injury (Castets et al., 2020). For instance, SMA muscle regulates mTOR-dependent axonal local translation via the secreted molecule CTRP3, compromising axonal outgrowth and protein synthesis in SMA neurons (Rehorst et al., 2019). Considering that turnover of old or damaged tissue plays a critical role in muscle

growth, these observations suggest that alternating periods of high and low mTORC1 activity are essential for maintaining optimal muscle health and function (Saxton & Sabatini, 2017).

In SMA fibroblasts, Ser2448 mTOR phosphorylation and basal levels were also decreased. These results, together with increased p62 and decreased LC3-II and LAMP-1 levels suggested decreased autophagosome formation and reduced autophagic flux. Thereby, mTOR reduction in these cells could contribute to the autophagic flux modulation due to a lack of autophagy inhibition.

Regarding spinal cord tissue, our results revealed reduced p-mTOR in SMA mouse spinal cord protein extracts with no modifications of mTOR protein level. These results, together with increased Beclin 1 (Piras et al., 2017) and LC3-II (de la Fuente et al., 2020) levels, and no changes on p62 (Piras et al., 2017), suggested increased autophagosome formation in the spinal cord tissue.

Since spinal cord lysates include MNs and their surrounding cells, we analyzed isolated SMA mouse and human MNs. Results revealed that p-mTOR was significantly increased in these cells, indicating that the initiation phase of the autophagy process was inhibited. Elevated p-mTOR, increased Beclin 1 (Figure 80 and Garcera et al., 2013), LC3-II, and p62, and reduced LAMP-1 protein levels, indicated autophagosome accumulation and reduced autophagic flux with decreased autophagolysosomal formation in SMN-reduced MNs.

Our observations suggest that mTOR and autophagy modulation may have a differential outcome in muscle and MNs in SMA. These discrepancies may influence in the effects of systemically targeting autophagy in SMA. In HD, where autophagy dysregulation has been observed, (reviewed in Menzies et al., 2015; Rubinsztein et al., 2007), different responses to autophagy induction have been described in muscle and in nervous system of a HD mouse model treated with everolimus (Fox et al., 2010). Everolimus is a rapamycin homolog that inhibits mTOR complex (Guertin & Sabatini, 2009). In this study, transgenic HD mice exhibited increased LC3-II and reduced LAMP-1 in muscle and reduced Htt accumulation upon everolimus treatment. However, no autophagy induction or Htt protein reduction were observed in striatum or cortex tissues of these mice (Fox et al., 2010). Therefore, autophagy regulation may have differential outcomes between muscle and nervous system. Nevertheless, whether autophagy inhibition or activation is beneficial in SMA and other MN diseases is still unclear. For instance, rapamycin treatment, which causes mTOR inhibition and promotes autophagy, is deleterious for severe SMA (Piras et al., 2017) and SOD1 (G93A) ALS

(X. Zhang et al., 2011) mice models. However, pharmacological (Barmada et al., 2014) or genetic (Hetz et al., 2009) autophagy induction had beneficial effects in ALS cellular models. Furthermore, autophagy induction with calpeptin, a calpain protease inhibitor, improved the lifespan and motor function of severe SMA mice and raised SMN levels (de la Fuente et al., 2018). On the other hand, the autophagy inhibitor 3-MA improved motor performance, extended the lifespan, and delayed MN death in lumbar spinal cord of a severe SMA mouse model (Piras et al., 2017). These differences may be due to additional effects of the compounds used, or to alterations of other cellular processes. For instance, mTOR is involved in regulating multiple cellular events including protein translation, autophagy, lysosome biogenesis, lipid synthesis, and growth factor signaling (Saxton & Sabatini, 2017). Hence, enhancing autophagy by systemic mTOR inhibition may be harmful due to its implication in multiple processes. On the other hand, calpain inhibition with calpeptin raised SMN protein level (de la Fuente et al., 2018, 2020). Calpain protease participates in SMN protein cleavage in muscle (Fuentes et al., 2010) and MNs (de la Fuente et al., 2018). Therefore, the beneficial effects observed in SMA mice are likely due to increased SMN level. SMA muscle shows increased autophagy flux. Thus, the use of 3-MA to systemically inhibit the autophagy process could improve motor function due to specific changes in SMA muscle. To study the specific modifications on autophagy of these treatments, autophagy markers' analysis should be conducted after treatment in muscle tissue and MNs.

The differences observed among several tissues and cell types reinforced the hypothesis indicating differences in the autophagy process between muscle, other tissues, and MNs in SMA disease (**Figure 96**). These divergences suggest the need to consider them when designing or using treatments like autophagy modulators as complementary strategies for SMA disease, as they might be modifying the tissue-specific autophagy response. Further exploration of these effects could provide novel insights into the SMA therapy field.

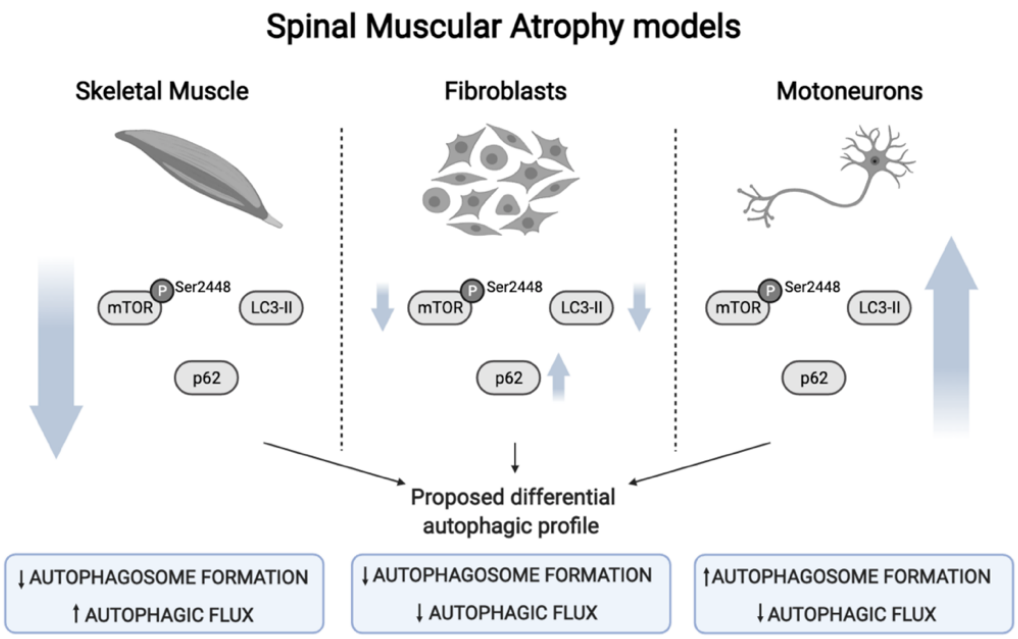

Figure 96 | Representation of the differences in autophagy-related proteins expression occurring in SMA disease models. Created with BioRender.com. (Sansa et al., 2021).

5. Autophagy regulation by mTOR and ERK hyperphosphorylation in SMA MNs

The exact mechanism by which ERK and mTOR are overactivated in SMA MNs remained unclear. Interestingly, participates in mTOR activation (Melick & Jewell, 2020; Saxton & Sabatini, 2017) which in turn, takes part in autophagy inhibition when phosphorylated (Jung et al., 2009). Moreover, previous and present results showed a reduced autophagic flux and increased autophagosome formation in SMA MNs. Thereby, we hypothesized that the alterations observed in SMA MNs regarding mTOR activity and autophagy markers levels could be due to further alteration of the ERK MAPK signaling pathway.

Results revealed that ERK MAPK inhibition reduced mTOR Ser2448 phosphorylation and level, and prevented p62 and LC3-II increase in human SMA MNs. Conversely, no changes on mTOR phosphorylation or in the autophagy markers were observed in Control cells. These results suggested that mTOR hyperphosphorylation and autophagy dysregulation in SMA MNs was produced as a consequence of ERK overactivation. Other studies have described autophagy and ERK MAPK pathway alterations in neurodegenerative diseases. For instance, autophagosome accumulation and increased ERK phosphorylation was found forming aggregates in the substantia nigra of PD patients (J. H. Zhu et al., 2002), in hippocampus of an AD mouse model (Dineley et al., 2001; X. Zhu et al., 2002), and in AD patients brain extracts (C. Russo et al., 2002). ERKs regulate diverse functions including cell growth and proliferation,

differentiation and survival or apoptosis (L. Chang & Karin, 2001). Some of these studies linked ERK MAPK pathway overactivation with an attempt of post-mitotic neurons to reenter the cell cycle, thus contributing to cell death (reviewed in X. Zhu et al., 2002). There is evidence of multiple interactions between ERK and other MAPKs with PD and AD-related proteins including, α-synuclein (J. H. Zhu et al., 2002), τ, AßPP, PS, and229 ApoE (reviewed in X. Zhu et al., 2002). Therefore, it is likely that ERK sustained overactivity could contribute to alter these proteins as well as to mTOR hyperphosphorylation and autophagy dysregulation in PD and AD, as observed in SMA. Nevertheless, the mechanism/s that led to ERK hyperactivation in these diseases and in SMA MNs were still unclear.

5.1. Intracellular Ca^{2+} alterations are responsible for ERK overactivation and autophagy dysregulation in SMA MNs

Activity-dependent changes in neurons are predominantly mediated by elevation in intracellular Ca^{2+} levels, which in turn have been reported to be upstream regulators of the ERK MAPK signaling pathway (Chuderland & Seger, 2008; Farnsworth et al., 1995; Finkbeiner & Greenberg, 1996). Neuronal capability to buffer Ca^{2+} in pathological conditions and during aging can be compromised (Zündorf & Reiser, 2011). Indeed, both high and low intracellular calcium concentrations have been associated to neuronal cell death (Franklin & Johnson, 1992). Evidences suggest that intracellular free Ca^{2+} could be increased in neurons of patients who develop MN diseases such as in ALS (Choi, 1988; Regan & Choi, 1991). In SMA, SMN-reduced MNs are electrically hyperexcitable and exhibit enhanced Na^{+} channels activity (Arumugam et al., 2017; H. Liu et al., 2015; Mentis et al., 2011). Experiments involving SMNdelta7 mutant mice revealed an abnormal amount of Ca^{+2}-dependent asynchronous release in the neuromuscular synaptic transmission during prolonged *ex vivo* stimulations with a suction electrode, suggesting an alteration in Ca^{2+} concentration in SMA synapses (Ruiz et al., 2010). Another study showed reduced Ca^{2+} incorporation capacity in presynaptic mitochondria during neural activity at motor nerve terminals of the Taiwanese SMA mouse model (Lopez-Manzaneda et al., 2021). Additionally, SMN-deficient MNs exhibited a reduction of spontaneous Ca^{2+} transients and severe deficits in clustering $Ca_v2.2$ channels in distal axons and growth cones, suggesting impaired Ca^{2+} signaling (Jablonka et al., 2007). SMA iPSC-derived astrocytes presented disrupted Ca^{2+} signaling. These cells had increased basal Ca^{2+} and enhanced ERK activation, although they were less able to incorporate Ca^{2+} after being stimulated with ATP (Mcgivern et al., 2013). Moreover, there is evidence that Ca^{2+} levels can control ERK subcellular localization; for instance, high intracellular Ca^{2+} concentrations promote cytoplasmic ERK localization (Chuderland & Seger, 2008). According to these

observations, we hypothesized that ERK hyperphosphorylation may be the consequence of intracellular Ca^{2+} dysregulations in SMA MNs, contributing to increase p-mTOR and to the accumulation of LC3-II and p62 proteins. To validate the hypothesis of Ca^{2+} being responsible for ERK overactivation, we treated these cells with the intracellular Ca^{2+} chelator BAPTA-AM. The treatment prevented ERK hyperphosphorylation in SMA MNs, whereas no changes on ERK phosphorylation were observed in Control cells. These results suggest a Ca^{2+} dysregulation in SMN-reduced MNs, but not in healthy MNs.

The effectiveness of BAPTA-AM as an intracellular Ca^{2+} chelator was verified by analyzing phosphorylated CREB levels. CREB is a transcription factor phosphorylated at Ser133 by PI3K/Akt and ERK MAPK signaling pathways (Bonni et al., 1999; Pugazhenthit et al., 2000), but also by CAMKII, which activity depends directly on Ca^{2+} levels (Mantamadiotis et al., 2012). Phospho-CREB levels were reduced in both Control and SMA conditions when compared to their respective untreated controls, showing that BAPTA-AM prevented calcium-dependent CREB phosphorylation. Furthermore, basal CREB phosphorylation was significantly reduced in SMA condition. Accordingly, other studies have observed reduced CREB phosphorylation in mouse SMA spinal cords (Biondi et al., 2010). CREB phosphorylation reduction could be related to decreased PI3K/Akt activity observed in SMA (Chapter 2), since the signaling pathway is an upstream CREB modulator (K. Du & Montminy, 1998; Li et al., 2011).

Based on previous studies, ERK MAPK inhibition and/or Akt phosphorylation induction should rise SMN protein levels (Biondi et al., 2010; Branchu et al., 2013). Our results and others agree that PI3K/Akt and ERK MAPK signaling pathways actively participate in SMN transcription in MNs (Branchu et al., 2013; Demir et al., 2011). Akt phosphorylation induction through NMDA receptor activation enhances *SMN2* transcription in spinal cords from a SMA mouse model (Branchu et al., 2013). ERK phosphorylation inhibition may lead to SMN protein increase in spinal cords and myotubes by promoting Akt phosphorylation through an upstream mechanism involving Ca^{2+} and CaMKII activation (Branchu et al., 2013). Conversely, our results show that ERK inhibition produced a reduction in *SMN* transcripts and SMN protein levels (Chapter 2). On the other hand, intracellular Ca^{2+} chelation prevented ERK phosphorylation in SMA cells, without reducing SMN protein level in Control or SMA MNs. These observations may indicate specific particularities of MNs in SMA disease, since we have observed diverse tissue and cell specific molecular changes, affecting processes such as autophagy (Chapter 3). Therefore, systemic reduction of ERK phosphorylation in SMA could be beneficial for the whole organism since it would rise SMN levels in spinal cord and muscle tissue. However, ERK

protein complete reduction could be deleterious for MNs, producing SMN protein level depletion.

LC3-II and p62 protein levels were analyzed in differentiated Control and SMA human MNs after BAPTA-AM treatment to elucidate whether intracellular Ca^{2+} could modulate autophagy markers level. LC3-II protein level, but not p62, was reduced in SMA-treated MNs. These outcomes showed that Ca^{2+} chelation prevented LC3-II increase in SMA MNs, indicating reduced autophagosome amount. However, sustained p62 levels after BAPTA treatment suggested no modification of the autophagy flux. These results could be related to dysregulations in autophagolysosome formation, since we have observed LAMP-1 protein level reduction in SMA MNs (Chapter 3). As mentioned, p62 is a cargo protein for ubiquitinated molecules and is eliminated through autophagy (Bjørkøy et al., 2009). Therefore, p62 protein may not be properly degraded in these cells. Further analysis by LC3 and p62 immunostaining of the autophagosome amount, and western blot analysis of LAMP-1 should be conducted to elucidate the autophagy flux status in these cells. Furthermore, blocking autophagy with Bafilomycin A1 the BAPTA-treated SMN-reduced MNs could provide insights of the autophagy flux status in these cells after Ca^{2+} chelation.

Taken together, all these observations point out to the link between Ca^{2+} levels and ERK signaling pathway activity, which in turn could be regulating autophagy and SMN levels in SMA MNs (**Figure 97**). Nonetheless, whether ERK overactivation is beneficial or deleterious in SMA disease is yet to be determined and may have divergent outcomes depending on the tissue-specific demand of SMN levels. Besides, in SMA MNS calpain activation due to Ca^{2+} dysregulation is also enhancing autophagosome accumulation and SMN protein reduction, and its inhibition restores LC3-II and SMN levels (de la Fuente et al., 2018, 2020). Hence, regulating Ca^{2+} and calpain activity in SMA cells could provide new SMN-independent approaches for SMA therapy.

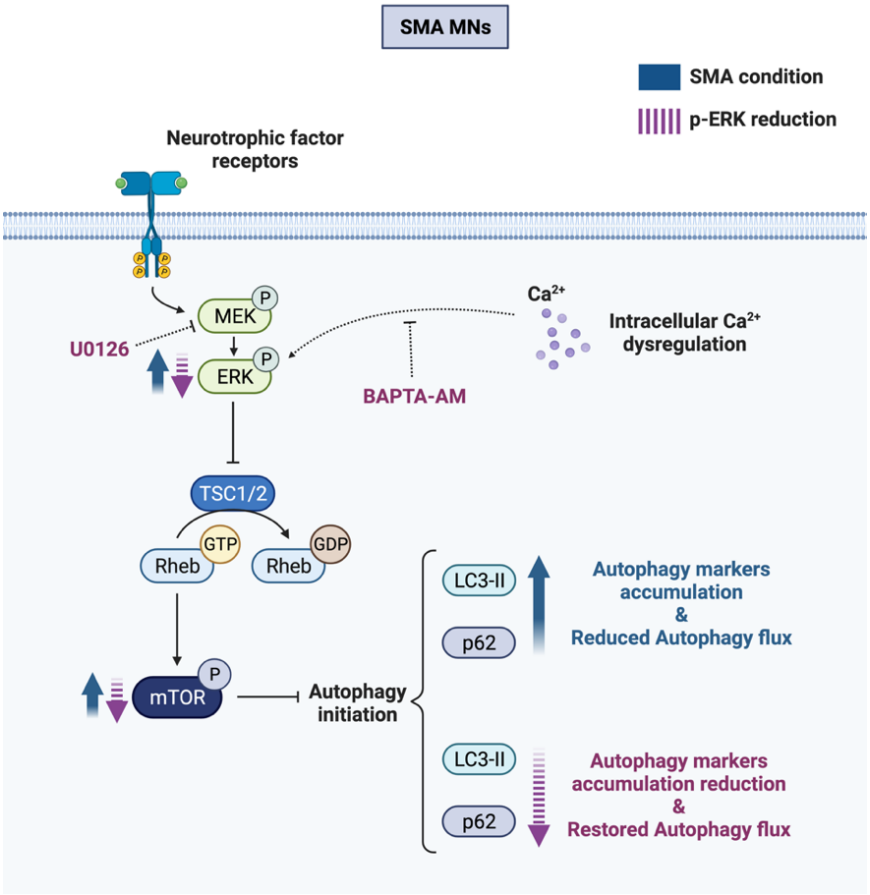

Figure 97 | Proposed mechanisms involved in ERK and autophagy pathways regulation in SMN-reduced MNs. ERK MAPK pharmacological inhibition or reduction of intracellular Ca^{2+} levels prevents ERK phosphorylation, reduces mTOR phosphorylation and restores markers to a level comparable to non-SMA MNs. Created with BioRender.com.

In summary, the present study shows alterations in survival signaling pathways, apoptosis, autophagy, and Ca^{2+} signaling in SMA disease, which may be contributing to increase cell degeneration, specifically affecting SMA MNs. SMA MNs exhibited higher percentage of neurite degeneration, decreased cell survival, increased caspase-3 cleavage and presence of nuclei with apoptotic morphology. The antiapoptotic proteins FAIM and XIAP were diminished in SMA spinal cord extracts. Conversely, these proteins were increased in MNs. However, the presence of active caspase-3 and fragmented nuclei indicated that FAIM-L and XIAP expression may not be sufficient to counteract apoptosis activation in MNs. These features may be due to coexisting alterations in survival signaling pathways. We described a decrease in Akt phosphorylation and an increase in ERK phosphorylation in SMA MNs. The inhibition of these pathways in MNs demonstrated their involvement in the transcriptional regulation of SMN protein. However, SMN endogenous regulation did not alter the phosphorylation of Akt and ERK. In addition, we described a differential regulation of

autophagy between SMA muscle, fibroblasts, spinal cord, and MNs. These outcomes reinforce the importance of designing targeted treatments for SMA disease based on the intrinsic cellular and molecular alterations besides focusing only on regulating SMN protein levels. Our results suggest a possible link between Ca^{2+} levels and disruption of ERK MAPK and autophagy pathways in SMA MNs, since these cells are more sensitive to Ca^{2+} homeostasis alterations. By inhibiting the ERK MAPK pathway or chelating intracellular free Ca^{2+} it is possible to regulate autophagy flux. Notwithstanding, complete ERK inhibition can be detrimental for MNs since SMN transcripts and protein level may decrease. Therefore, combinatorial regulation of ERK MAPK and intracellular Ca^{2+} in these cells could modulate autophagy and increase SMN protein level, thus providing novel SMN-independent targets to design combined therapies with the existing SMN-dependent treatments.

CONCLUSIONS

I. Differentiated Control and SMA human MNs exhibit the MN markers Islet1/2, HB9 and ChAT. SMN is reduced at transcriptional and protein level in differentiated SMA human MNs. These cells show reduced soma, cytoplasm and nucleus size compared to control MNs.

II. Cultured SMA MNs show reduced percentage of survival and increased neurite degeneration compared to control cells. Neurite degeneration precedes cell survival reduction.

III. Human and mouse SMA MNs show increased percentage of nuclei with apoptotic features and cleaved-caspase-3 protein level.

IV. The antiapoptotic proteins FAIM-L and XIAP are reduced in SMA mouse spinal cord extracts and increased in cultured SMA mouse and human MNs. However, XIAP protein level is reduced in SMA human fibroblasts.

V. The survival signaling pathways PI3K/Akt and ERK MAPK are altered in SMA MNs. Akt phosphorylation in Thr308 is significantly reduced in cultured SMA mouse and human MNs. ERK phosphorylation in Thr202/Tyr204 is significantly increased in cultured SMA mouse and human MNs.

VI. PI3K/Akt signaling pathway inhibition with LY294002 reduces SMN at transcriptional and protein level in cultured mouse and human MNs.

VII. ERK MAPK pathway inhibition with U0126 reduces SMN at transcriptional and protein level in cultured mouse and human MNs. The antiapoptotic protein FAIM-L is reduced at transcriptional level in cultured CD1 mouse MNs upon ERK MAKP signaling pathway inhibition.

VIII. Akt and ERK phosphorylation are not modified by SMN overexpression in cultured mouse and human MNs.

IX. The level of autophagy markers are different in SMA cellular tissues and models, suggesting a differential and tissue-dependent regulation of autophagy in SMA disease.

X. SMA mouse and human muscle exhibits decreased mTOR phosphorylation, Beclin 1, LC3-II and p62 level, suggesting reduced autophagosome formation and increased autophagy flux.

XI. SMA human fibroblasts show reduced mTOR phosphorylation and protein level, LC3-II, and LAMP-1; and increased p62 suggesting reduced autophagosome formation and flux.

XII. SMA human MNs exhibit increased Beclin 1, mTOR phosphorylation, LC3-II, and p62, and decreased LAMP-1 indicating autophagosome accumulation, reduced flux, and reduced autophagolysosome formation.

XIII. ERK MAPK pathway pharmacological inhibition with U0126 prevents mTOR phosphorylation increase and changes in LC3-II and p62 autophagy markers in SMA human MNs, suggesting that ERK overactivation is responsible for autophagy alterations in SMA MNs.

XIV. Intracellular Ca^{2+} chelation with BAPTA-AM prevents ERK hyperphosphorylation and LC3-II protein level increase in SMA but not in control human MNs. Intracellular free Ca^{2+} is likely to be dysregulated in SMA human MNs.

.

REFERENCES

A. Nash, L., K. Burns, J., Warman Chardon, J., Kothary, R., & J. Parks, R. (2017). Spinal Muscular Atrophy: More than a Disease of Motor Neurons? *Current Molecular Medicine*, *16*(9), 779–792. https://doi.org/10.2174/1566524016666161128113338

Ahmad, S., Bhatia, K., Kannan, A., & Gangwani, L. (2016). Molecular Mechanisms of Neurodegeneration in Spinal Muscular Atrophy. *Journal of Experimental Neuroscience*, *10*, 39–49. https://doi.org/10.4137/JEN.S33122

Ahn, E. J., Yum, M. S., Kim, E. H., Yoo, H. W., Lee, B. H., Kim, G. H., & Ko, T. S. (2017). Genotype-Phenotype Correlation of SMN1 and NAIP Deletions in Korean Patients with Spinal Muscular Atrophy. *Journal of Clinical Neurology (Seoul, Korea)*, *13*(1), 27. https://doi.org/10.3988/JCN.2017.13.1.27

Airaksinen, M. S., & Saarma, M. (2002). The GDNF family: Signalling, biological functions and therapeutic value. *Nature Reviews Neuroscience 2002 3:5*, *3*(5), 383–394. https://doi.org/10.1038/nrn812

Alves, C., Garner, R., & Nery, F. (2019). *Contribution of cardiac defects to spinal muscular atrophy pathology: a human tissue study*. Journal of Neuromuscular Disorders. https://www.scopus.com/record/display.uri?eid=2-s2.0-85084477427&origin=inward&featureToggles=FEATURE_NEW_DOC_DETAILS_EXPORT:1

Anderson, K., Potter, A., Baban, D., & Davies, K. E. (2003). Protein expression changes in spinal muscular atrophy revealed with a novel antibody array technology. *Brain : A Journal of Neurology*, *126*(Pt 9), 2052–2064. https://doi.org/10.1093/BRAIN/AWG208

Arakawa, Y., Sendtner, M., & Thoenen, H. (1990). Survival effect of ciliary neurotrophic factor (CNTF) on chick embryonic motoneurons in culture: comparison with other neurotrophic factors and cytokines. *The Journal of Neuroscience : The Official Journal of the Society for Neuroscience*, *10*(11), 3507–3515. https://doi.org/10.1523/JNEUROSCI.10-11-03507.1990

Araujo, A. prufer de Q. C., Araujo, M., & Swoboda, K. J. (2009). Vascular Perfusion Abnormalities in Infants with Spinal Muscular Atrophy. *The Journal of Pediatrics*, *155*(2), 292–294. https://doi.org/10.1016/J.JPEDS.2009.01.071

Arnold, A. S., Gueye, M., Guettier-Sigrist, S., Courdier-Fruh, I., Coupin, G., Poindron, P., & Gies, J. P. (2004). Reduced expression of nicotinic AChRs in myotubes from spinal muscular atrophy I patients. *Laboratory Investigation*, *84*(10), 1271–1278. https://www.nature.com/articles/3700163

Arumugam, S., Garcera, A., Soler, R. M., & Tabares, L. (2017). Smn-Deficiency Increases the Intrinsic Excitability of Motoneurons. *Frontiers in Cellular Neuroscience*, *11*. https://doi.org/10.3389/FNCEL.2017.00269

Arumugam, S., Mincheva-tasheva, S., Periyakaruppiah, A., de la Fuente, S., Soler, R. M., & Garcera, A. (2018). Regulation of Survival Motor Neuron Protein by the Nuclear Factor-Kappa B Pathway in Mouse Spinal Cord Motoneurons. *Molecular Neurobiology*, *55*(6), 5019–5030. https://doi.org/10.1007/s12035-017-0710-4

Bach, J. R., Saltstein, K., Sinquee, D., Weaver, B., & Komaroff, E. (2007). Long-term survival in Werdnig-Hoffmann disease. *American Journal of Physical Medicine and Rehabilitation*, *86*(5), 339–345. https://doi.org/10.1097/PHM.0B013E31804A8505

Badadani, M. (2012). Autophagy Mechanism, Regulation, Functions, and Disorders. *ISRN Cell Biology*, *2012*, 1–11. https://doi.org/10.5402/2012/927064

Balabanian, S., Gendron, N. H., & MacKenzie, A. E. (2007). Histologic and transcriptional assessment of a mild SMA model. *Neurological Research*, *29*(5), 413–424. https://doi.org/10.1179/016164107X159243

Baloh, R. H., Tansey, M. G., Lampe, P. A., Fahrner, T. J., Enomoto, H., Simburger, K. S., Leitner, M. L., Araki, T., Johnson, E. M., & Milbrandt, J. (1998). Artemin, a novel member of the GDNF ligand family, supports peripheral and central neurons and signals through the GFRalpha3-RET receptor complex. *Neuron*, *21*(6), 1291–1302. https://doi.org/10.1016/S0896-6273(00)80649-2

Baranello, G., Darras, B. T., Day, J. W., Deconinck, N., Klein, A., Masson, R., Mercuri, E., Rose, K., El-Khairi, M., Gerber, M., Gorni, K., Khwaja, O., Kletzl, H., Scalco, R. S., Seabrook, T., Fontoura, P., & Servais, L. (2021). Risdiplam in Type 1 Spinal Muscular Atrophy. *The New England Journal of Medicine*, *384*(10), 915–923. https://doi.org/10.1056/NEJMOA2009965

Barde, Y. A., Edgar, D., & Thoenen, H. (1982). Purification of a new neurotrophic factor from mammalian brain. *The EMBO Journal*, *1*(5), 549–553. https://doi.org/10.1002/J.1460-2075.1982.TB01207.X

Barmada, S. J., Serio, A., Arjun, A., Bilican, B., Daub, A., Ando, D. M., Tsvetkov, A., Pleiss, M., Li, X., Peisach, D., Shaw, C., Chandran, S., & Finkbeiner, S. (2014). Autophagy induction enhances TDP43 turnover and survival in neuronal ALS models. *Nature Chemical Biology*, *10*(8), 677–685. https://doi.org/10.1038/NCHEMBIO.1563

Bartley, M. G., Marquardt, K., Kirchhof, D., Wilkins, H. M., Patterson, D., & Linseman, D. A. (2012). Overexpression of amyloid-β protein precursor induces mitochondrial oxidative stress and activates the intrinsic apoptotic cascade. *Journal of Alzheimer's Disease*, *28*(4), 855–868. https://doi.org/10.3233/JAD-2011-111172

Bäumer, D., Lee, S., Nicholson, G., Davies, J. L., Parkinson, N. J., Murray, L. M., Gillingwater, T. H., Ansorge, O., Davies, K. E., & Talbot, K. (2009). Alternative Splicing Events Are a Late Feature of Pathology in a Mouse Model of Spinal Muscular Atrophy. *PLoS Genetics*, *5*(12), e1000773. https://doi.org/10.1371/journal.pgen.1000773

Berdyński, M., Miszta, P., Safranow, K., Andersen, P. M., Morita, M., Filipek, S., Żekanowski, C., & Kuźma-Kozakiewicz, M. (2022). SOD1 mutations associated with amyotrophic lateral sclerosis analysis of variant severity. *Scientific Reports 2022 12:1*, *12*(1), 1–11.

https://doi.org/10.1038/s41598-021-03891-8

Bergin, A., Kim, G., Price, D. L., Sisodia, S. S., Lee, M. K., & Rabin, B. A. (1997). Identification and characterization of a mouse homologue of the spinal muscular atrophy-determining gene, survival motor neuron. *Gene*, *204*(1–2), 47–53. https://doi.org/10.1016/S0378-1119(97)00510-6

Berkemeier, L. R., Winslow, J. W., Kaplan, D. R., Nikolics, K., Goeddel, D. V., & Rosenthal, A. (1991). Neurotrophin-5: A novel neurotrophic factor that activates trk and trkB. *Neuron*, *7*(5), 857–866. https://doi.org/10.1016/0896-6273(91)90287-A

Bertini, E., Dessaud, E., Mercuri, E., Muntoni, F., Kirschner, J., Reid, C., Lusakowska, A., Comi, G. P., Cuisset, J. M., Abitbol, J. L., Scherrer, B., Ducray, P. S., Buchbjerg, J., Vianna, E., van der Pol, W. L., Vuillerot, C., Blaettler, T., Fontoura, P., André, C., … Walter, M. C. (2017). Safety and efficacy of olesoxime in patients with type 2 or non-ambulatory type 3 spinal muscular atrophy: a randomised, double-blind, placebo-controlled phase 2 trial. *The Lancet. Neurology*, *16*(7), 513–522. https://doi.org/10.1016/S1474-4422(17)30085-6

Bertrandy, S., Burlet, P., Clermont, O., Huber, C., Fondrat, C., Thierry-Mieg, D., Munnich, A., & Lefebvre, S. (1999). The RNA-Binding Properties of SMN: Deletion Analysis of the Zebrafish Orthologue Defines Domains Conserved in Evolution. *Human Molecular Genetics*, *8*(5), 775–782. https://doi.org/10.1093/HMG/8.5.775

Bessou, P., Emonet-Dénand, F., & Laporte, Y. (1965). Motor fibres innervating extrafusal and intrafusal muscle fibres in the cat. *The Journal of Physiology*, *180*(3), 649–672. https://doi.org/10.1113/JPHYSIOL.1965.SP007722

Bezier, C., Hashemi, P. N., Cottin, S., Lafont, R., Veillet, S., Charbonnier, F., Dilda, P., Latil, M., & Biondi, O. (2022). FP.10 Combination of BIO101 with antisense oligonucleotide therapy demonstrates synergistic beneficial effects in severe SMA-like mice. *Neuromuscular Disorders*, *32*, S58. https://doi.org/10.1016/J.NMD.2022.07.071

Bianco, F., Pane, M., D'Amico, A., Messina, S., Delogu, A. B., Soraru, G., Pera, M. C., Mongini, T., Politano, L., Baranello, G., Vita, G., Tiziano, F. D., Morandi, L., Bertini, E., & Mercuri, E. (2015). Cardiac function in types II and III spinal muscular atrophy: Should we change standards of care? *Neuropediatrics*, *46*(1), 33–36. https://doi.org/10.1055/S-0034-1395348/ID/JR141155OA-21

Biondi, O., Branchu, J., Salah, A. Ben, Houdebine, L., Bertin, L., Chali, F., Desseille, C., Weill, L., Sanchez, G., Lancelin, C., Aïd, S., Lopes, P., Pariset, C., Lécolle, S., Côté, J., Holzenberger, M., Chanoine, C., Massaad, C., & Charbonnier, F. (2015). IGF-1R Reduction Triggers Neuroprotective Signaling Pathways in Spinal Muscular Atrophy Mice. *The Journal of Neuroscience : The Official Journal of the Society for Neuroscience*, *35*(34), 12063–12079. https://doi.org/10.1523/JNEUROSCI.0608-15.2015

Biondi, O., Branchu, J., Sanchez, G., Lancelin, C., Deforges, S., Lopes, P., Pariset, C., Lécolle, S., Côté, J., Chanoine, C., & Charbonnier, F. (2010). In vivo NMDA receptor activation accelerates motor unit maturation, protects spinal motor neurons, and enhances SMN2 gene expression in severe spinal muscular atrophy mice. *The Journal of Neuroscience : The Official Journal of the Society for Neuroscience*, *30*(34), 11288–11299. https://doi.org/10.1523/JNEUROSCI.1764-10.2010

Bjørkøy, G., Lamark, T., Pankiv, S., Øvervatn, A., Brech, A., & Johansen, T. (2009). Chapter 12 Monitoring Autophagic Degradation of p62/SQSTM1. *Methods in Enzymology*, *452*(C), 181–197. https://doi.org/10.1016/S0076-6879(08)03612-4

Blaschke, A. J., Weiner, J. A., & Chun, J. (1998). Programmed cell death is a universal feature of embryonic and postnatal neuroproliferative regions throughout the central nervous system. *The Journal of Comparative Neurology*, *396*(1), 39–50. https://doi.org/10.1002/(sici)1096-9861(19980622)396:1<39::aid-cne4>3.0.co;2-j

Bodart, J. F. L. (2010). Extracellular-regulated kinase - Mitogen-activated protein kinase cascade: Unsolved issues. In *Journal of Cellular Biochemistry* (Vol. 109, Issue 5, pp. 850–857). https://doi.org/10.1002/jcb.22477

Bodine, S. C., Stitt, T. N., Gonzalez, M., Kline, W. O., Stover, G. L., Bauerlein, R., Zlotchenko, E., Scrimgeour, A., Lawrence, J. C., Glass, D. J., & Yancopoulos, G. D. (2001). Akt/mTOR pathway is a crucial regulator of skeletal muscle hypertrophy and can prevent muscle atrophy in vivo. *Nature Cell Biology*, *3*(11), 1014–1019. https://doi.org/10.1038/NCB1101-1014

Boido, M., de Amicis, E., Valsecchi, V., Trevisan, M., Ala, U., Ruegg, M. A., Hettwer, S., & Vercelli, A. (2018). Increasing Agrin Function Antagonizes Muscle Atrophy and Motor Impairment in Spinal Muscular Atrophy. *Frontiers in Cellular Neuroscience*, *12*. https://doi.org/10.3389/FNCEL.2018.00017

Boido, M., & Vercelli, A. (2016). Neuromuscular Junctions as Key Contributors and Therapeutic Targets in Spinal Muscular Atrophy. *Frontiers in Neuroanatomy*, *10*(FEB). https://doi.org/10.3389/FNANA.2016.00006

Boland, B., Kumar, A., Lee, S., Platt, F. M., Wegiel, J., Yu, W. H., & Nixon, R. A. (2008). Autophagy induction and autophagosome clearance in neurons: relationship to autophagic pathology in Alzheimer's disease. *The Journal of Neuroscience : The Official Journal of the Society for Neuroscience*, *28*(27), 6926–6937. https://doi.org/10.1523/JNEUROSCI.0800-08.2008

Bonanno, S., Giossi, R., Zanin, R., Porcelli, V., Iannacone, C., Baranello, G., Ingenito, G., Iyadurai, S., Stevic, Z., Peric, S., & Maggi, L. (2022). Amifampridine safety and efficacy in spinal muscular atrophy ambulatory patients: a randomized, placebo-controlled, crossover phase 2 trial. *Journal of Neurology*, *269*(11), 5858. https://doi.org/10.1007/S00415-022-11231-7

Bonni, A., Brunet, A., West, A. E., Datta, S. R., Takasu, M. A., & Greenberg, M. E. (1999). Cell survival promoted by the Ras-MAPK signaling pathway by

transcription-dependent and -independent mechanisms. *Science (New York, N.Y.)*, *286*(5443), 1358–1362. https://doi.org/10.1126/SCIENCE.286.5443.1358

Boon, K. L., Xiao, S., McWhorter, M. L., Donn, T., Wolf-Saxon, E., Bohnsack, M. T., Moens, C. B., & Beattie, C. E. (2009). Zebrafish survival motor neuron mutants exhibit presynaptic neuromuscular junction defects. *Human Molecular Genetics*, *18*(19), 3615–3625. https://doi.org/10.1093/HMG/DDP310

Bordet, T., Berna, P., Abitbol, J. L., & Pruss, R. M. (2010). Olesoxime (TRO19622): A Novel Mitochondrial-Targeted Neuroprotective Compound. *Pharmaceuticals*, *3*(2), 345. https://doi.org/10.3390/PH3020345

Borgia, D., Malena, A., Spinazzi, M., Desbats, M. A., Salviati, L., Russell, A. P., Miotto, G., Tosatto, L., Pegoraro, E., Gianni Sorarú, Pennuto, M., & Vergani, L. (2017). Increased mitophagy in the skeletal muscle of spinal and bulbar muscular atrophy patients. *Human Molecular Genetics*, *26*(6), 1087–1103. https://doi.org/10.1093/HMG/DDX019

Bowerman, M., Anderson, C. L., Beauvais, A., Boyl, P. P., Witke, W., & Kothary, R. (2009). SMN, profilin IIa and plastin 3: a link between the deregulation of actin dynamics and SMA pathogenesis. *Molecular and Cellular Neurosciences*, *42*(1), 66–74. https://doi.org/10.1016/J.MCN.2009.05.009

Bowerman, M., Beauvais, A., Anderson, C. L., & Kothary, R. (2010). Rho-kinase inactivation prolongs survival of an intermediate SMA mouse model. *Human Molecular Genetics*, *19*(8), 1468–1478. https://doi.org/10.1093/HMG/DDQ021

Bowerman, M., Becker, C. G., Yán, R. J.˜ Ez-Muñ Oz, Y., Ning, K., Wood, M. J. A. A., Gillingwater, T. H., Talbot, K., Yáñez-Muñoz, R. J., Ning, K., Wood, M. J. A. A., Gillingwater, T. H., & Talbot, K. (2017). Therapeutic strategies for spinal muscular atrophy: SMN and beyond. *DMM Disease Models and Mechanisms*, *10*(8), 943–954. https://doi.org/10.1242/dmm.030148

Bowerman, M., Murray, L. M., Boyer, J. G., Anderson, C. L., & Kothary, R. (2012). Fasudil improves survival and promotes skeletal muscle development in a mouse model of spinal muscular atrophy. *BMC Medicine*, *10*, 24. https://doi.org/10.1186/1741-7015-10-24

Bowerman, M., Swoboda, K. J., Michalski, J. P., Wang, G. S., Reeks, C., Beauvais, A., Murphy, K., Woulfe, J., Screaton, R. A., Scott, F. W., & Kothary, R. (2012). Glucose metabolism and pancreatic defects in spinal muscular atrophy. *Annals of Neurology*, *72*(2), 256–268. https://doi.org/10.1002/ANA.23582

Boya, P., Codogno, P., & Rodriguez-Muela, N. (2018). Autophagy in stem cells: repair, remodelling and metabolic reprogramming. *Development (Cambridge, England)*, *145*(4). https://journals.biologists.com/dev/article/145/4/dev146506/48580/Autophagy-in-stem-cells-repair-remodelling-and

Boyer, J. G., Murray, L. M., Scott, K., De Repentigny, Y., Renaud, J. M., & Kothary, R. (2013). Early onset muscle weakness and disruption of muscle proteins in mouse models of spinal muscular atrophy. *Skeletal Muscle*, *3*(1). https://doi.org/10.1186/2044-5040-3-24

Boza-Morán, M. G., Martínez-Hernández, R., Bernal, S., Wanisch, K., Also-Rallo, E., Le Heron, A., Alías, L., Denis, C., Girard, M., Yee, J. K., Tizzano, E. F., & Yáñez-Muñoz, R. J. (2015). Decay in survival motor neuron and plastin 3 levels during differentiation of iPSC-derived human motor neurons. *Scientific Reports*, *5*. https://doi.org/10.1038/SREP11696

Branchu, J., Biondi, O., Chali, F., Collin, T., Leroy, F., Mamchaoui, K., Makoukji, J., Pariset, C., Lopes, P., Massaad, C., Chanoine, C., & Charbonnier, F. (2013). Shift from Extracellular Signal-Regulated Kinase to AKT/ cAMP Response Element-Binding Protein Pathway Increases Survival-Motor-Neuron Expression in Spinal-Muscular-Atrophy-Like Mice and Patient Cells. *Neurobiology of Disease*. https://doi.org/10.1523/JNEUROSCI.2728-12.2013

Bredesen, D. E., Rao, R. V., & Mehlen, P. (2006). Cell death in the nervous system. *Nature*, *443*(7113), 796. https://doi.org/10.1038/NATURE05293

Bricceno, K. V., Martinez, T., Leikina, E., Duguez, S., Partridge, T. A., Chernomordik, L. V., Fischbeck, K. H., Sumner, C. J., & Burnett, B. G. (2014). Survival motor neuron protein deficiency impairs myotube formation by altering myogenic gene expression and focal adhesion dynamics. *Human Molecular Genetics*, *23*(18), 4745–4757. https://doi.org/10.1093/HMG/DDU189

Briese, M., Esmaeili, B., Fraboulet, S., Burt, E. C., Christodoulou, S., Towers, P. R., Davies, K. E., & Sattelle, D. B. (2009). Deletion of smn-1, the Caenorhabditis elegans ortholog of the spinal muscular atrophy gene, results in locomotor dysfunction and reduced lifespan. *Human Molecular Genetics*, *18*(1), 97–104. https://doi.org/10.1093/hmg/ddn320

Brini, M., Calì, T., Ottolini, D., & Carafoli, E. (2014). Neuronal calcium signaling: Function and dysfunction. *Cellular and Molecular Life Sciences*, *71*(15), 2787–2814. https://doi.org/10.1007/S00018-013-1550-7/FIGURES/3

Buettner, J. M., Sime Longang, J. K., Gerstner, F., Apel, K. S., Blanco-Redondo, B., Sowoidnich, L., Janzen, E., Langenhan, T., Wirth, B., & Simon, C. M. (2021). Central synaptopathy is the most conserved feature of motor circuit pathology across spinal muscular atrophy mouse models. *IScience*, *24*(11), 103376. https://doi.org/10.1016/J.ISCI.2021.103376

Bühler, D., Raker, V., Lührmann, R., & Fischer, U. (1999). Essential role for the tudor domain of SMN in spliceosomal U snRNP assembly: implications for spinal muscular atrophy. *Human Molecular Genetics*, *8*(13), 2351–2357. https://doi.org/10.1093/HMG/8.13.2351

Burghes, A. H. M., & Beattie, C. E. (2009). *Splicing Missense mutation Spinal muscular atrophy: why do low levels of survival motor neuron protein make motor neurons sick?*

https://doi.org/10.1038/nrn2670

Burnett, B. G., Muñoz, E., Tandon, A., Kwon, D. Y., Sumner, C. J., & Fischbeck, K. H. (2009). Regulation of SMN Protein Stability. *Molecular and Cellular Biology*, *29*(5), 1107–1115. https://journals.asm.org/doi/full/10.1128/MCB.01262-08

Calucho, M., Bernal, S., Alías, L., March, F., Venceslá, A., Rodríguez-Álvarez, F. J., Aller, E., Fernández, R. M., Borrego, S., Millán, J. M., Hernández-Chico, C., Cuscó, I., Fuentes-Prior, P., & Tizzano, E. F. (2018). Correlation between SMA type and SMN2 copy number revisited: An analysis of 625 unrelated Spanish patients and a compilation of 2834 reported cases. *Neuromuscular Disorders*, *28*(3), 208–215. https://doi.org/10.1016/j.nmd.2018.01.003

Cantrell, D. A. (2001). Phosphoinositide 3-kinase signalling pathways. *Journal of Cell Science*, *114*(8), 1439–1445. https://doi.org/10.1242/JCS.114.8.1439

Cardone, M. H., Roy, N., Stennicke, H. R., Salvesen, G. S., Franke, T. F., Stanbridge, E., Frisch, S., & Reed, J. C. (1998). Regulation of Cell Death Protease Caspase-9 by Phosphorylation. *Science*, *282*(5392), 1318–1321. https://doi.org/10.1126/SCIENCE.282.5392.1318

Carriba, P., & Comella, J. X. (2014). *Amyloid beta , TNF α and FAIM-L ; approaching new therapeutic strategies for AD*. *5*(December), 1–3. https://doi.org/10.1038/nm1782

Carriba, P., & Comella, J. X. (2015). Neurodegeneration and neuroinflammation : two processes , one target. *Neural Regeneration Research*, *10*(10), 2015–2017. https://doi.org/10.4103/1673-5374.165269

Carriba, P., Jimenez, S., Navarro, V., Moreno-Gonzalez, I., Barneda-Zahonero, B., Moubarak, R. S., Lopez-Soriano, J., Gutierrez, A., Vitorica, J., & Comella, J. X. (2015). *Amyloid- β reduces the expression of neuronal FAIM-L , thereby shifting the inflammatory response mediated by TNF α from neuronal protection to death*. *6*(2), e1639-13. https://doi.org/10.1038/cddis.2015.6

Cartegni, L., & Krainer, A. R. (2002). Disruption of an SF2/ASF-dependent exonic splicing enhancer in SMN2 causes spinal muscular atrophy in the absence of SMN1. *Nature Genetics*, *30*(4), 377–384. https://doi.org/10.1038/ng854

Cashman, N. R., Durham, H. D., Blusztajn, J. K., Oda, K., Tabira, T., Shaw, I. T., Dahrouge, S., & Antel, J. P. (1992). Neuroblastoma x spinal cord (NSC) hybrid cell lines resemble developing motor neurons. *Developmental Dynamics : An Official Publication of the American Association of Anatomists*, *194*(3), 209–221. https://doi.org/10.1002/aja.1001940306

Castets, P., Ham, D. J., & Rüegg, M. A. (2020). The TOR Pathway at the Neuromuscular Junction: More Than a Metabolic Player? *Frontiers in Molecular Neuroscience*, *13*. https://doi.org/10.3389/FNMOL.2020.00162

Castets, P., Lin, S., Rion, N., Di Fulvio, S., Romanino, K., Guridi, M., Frank, S., Tintignac, L. A., Sinnreich, M., & Rüegg, M. A. (2013). Sustained activation of mTORC1 in skeletal muscle inhibits constitutive and starvation-induced autophagy and causes a severe, late-onset myopathy. *Cell Metabolism*, *17*(5), 731–744. https://doi.org/10.1016/J.CMET.2013.03.015

Cha, M. Y., Han, S. H., Son, S. M., Hong, H. S., Choi, Y. J., Byun, J., & Mook-Jung, I. (2012). Mitochondria-Specific Accumulation of Amyloid β Induces Mitochondrial Dysfunction Leading to Apoptotic Cell Death. *PLOS ONE*, *7*(4), e34929. https://doi.org/10.1371/JOURNAL.PONE.0034929

Chadwick, B. P., Helbling, L. A., Angrist, M., Chakravarti, A., Gusella, J. F., & Slaugenhaupt, S. A. (1998). Assignment of persephin (PSPN), a human neurotrophic factor, to chromosome 19p13.3 by radiation hybrid mapping and somatic cell hybrid PCR. *Cytogenetics and Cell Genetics*, *83*(3–4), 236–237. https://doi.org/10.1159/000015189

Chan, Y. B., Miguel-Aliaga, I., Franks, C., Thomas, N., Trülzsch, B., Sattelle, D. B., Davies, K. E., & van den Heuvel, M. (2003). Neuromuscular defects in a Drosophila survival motor neuron gene mutant. *Human Molecular Genetics*, *12*(12), 1367–1376. https://doi.org/10.1093/HMG/DDG157

Chandrasekhar, A. (2004). Turning heads: Development of vertebrate branchiomotor neurons. *Developmental Dynamics*, *229*(1), 143–161. https://doi.org/10.1002/DVDY.10444

Chang, L., & Karin, M. (2001). Mammalian MAP kinase signalling cascades. *Nature*, *410*(6824), 37–40. https://doi.org/10.1038/35065000

Chang, T., Zheng, W., Tsark, W., Bates, S., Huang, H., Lin, R. J., & Yee, J. K. (2011). Brief Report: Phenotypic Rescue of Induced Pluripotent Stem Cell-Derived Motoneurons of a Spinal Muscular Atrophy Patient. *Stem Cells*, *29*(12), 2090–2093. https://doi.org/10.1002/STEM.749

Chao, C., Herr, D., Chun, J., & Xu, Y. (2006). Ser18 and 23 phosphorylation is required for p53-dependent apoptosis and tumor suppression. *EMBO Journal*, *25*(11), 2615–2622. https://doi.org/10.1038/SJ.EMBOJ.7601167

Chao, M. V. (2003). Neurotrophins and their receptors: A convergence point for many signalling pathways. *Nature Reviews Neuroscience 2003 4:4*, *4*(4), 299–309. https://doi.org/10.1038/nrn1078

Charroux, B., Pellizzoni, L., Perkinson, R. A., Shevchenko, A., Mann, M., & Dreyfuss, G. (1999). Gemin3: A novel DEAD box protein that interacts with SMN, the spinal muscular atrophy gene product, and is a component of gems. *The Journal of Cell Biology*, *147*(6), 1181–1193. https://doi.org/10.1083/JCB.147.6.1181

Chaytow, H., Huang, Y. T., Gillingwater, T. H., & Faller, K. M. E. (2018). The role of survival motor neuron protein (SMN) in protein homeostasis. *Cellular and Molecular Life Sciences*, *75*(21), 3877–3894. https://doi.org/10.1007/S00018-018-2849-1/FIGURES/2

Chen, X., He, Y., & Lu, F. (2018). Autophagy in Stem Cell Biology: A perspective on Stem Cell Self-renewal and differentiation. *Stem Cells International*, *2018*, 12. https://doi.org/10.1155/2018/9131397

Chiriboga, C. A. (2022). Pharmacotherapy for Spinal

Muscular Atrophy in Babies and Children: A Review of Approved and Experimental Therapies. *Pediatric Drugs 2022 24:6*, *24*(6), 585–602. https://doi.org/10.1007/S40272-022-00529-8

Chiriboga, C. A., Bruno, C., Duong, T., Fischer, D., Kirschner, J., Mercuri, E., Gerber, M., Gorni, K., Kletzl, H., Carruthers, I., Martin, C., Warren, F., & Scoto, M. (2022). JEWELFISH: Safety, Pharmacodynamic and Exploratory Efficacy Data in Non-Naïve Patients with Spinal Muscular Atrophy (SMA) Receiving Treatment with Risdiplam (P15-5.004). *Neurology*, *98*(18 Supplement).

Choi, D. W. (1988). Glutamate neurotoxicity and diseases of the nervous system. *Neuron*, *1*(8), 623–634. https://doi.org/10.1016/0896-6273(88)90162-6

Christie, L. A., Su, J. H., Tu, C. H., Dick, M. C., Zhou, J., & Cotman, C. W. (2007). Differential regulation of inhibitors of apoptosis proteins in Alzheimer's disease brains. *Neurobiology of Disease*, *26*(1), 165–173. https://doi.org/10.1016/J.NBD.2006.12.017

Chuderland, D., Marmor, G., Shainskaya, A., & Seger, R. (2020). Calcium-mediated interactions regulate the subcellular localization of extracellular signal-regulated kinases (ERKs). *Cellular Physiology and Biochemistry*, *54*(3), 474–492. https://doi.org/10.33594/000000231

Chuderland, D., & Seger, R. (2008). Calcium regulates ERK signaling by modulating its protein-protein interactions. *Communicative & Integrative Biology*, *1*(1), 4. https://doi.org/10.4161/CIB.1.1.6107

Cifuentes-Diaz, C., Frugier, T., Tiziano, F. D., Lacène, E., Roblot, N., Joshi, V., Moreau, M. H., & Melki, J. (2001). Deletion of murine SMN exon 7 directed to skeletal muscle leads to severe muscular dystrophy. *Journal of Cell Biology*, *152*(5), 1107–1114. https://doi.org/10.1083/JCB.152.5.1107

Cifuentes-Diaz, C., Nicole, S., Velasco, E, M., Borra-Cebrian, C., Panozzo, C., Frugier, T., Millet, G., Roblot, N., Joshi, V., & Melki, J. (2002). Neurofilament accumulation at the motor endplate and lack of axonal sprouting in a spinal muscular atrophy mouse model. *Human Molecular Genetics*, *11*(12), 1439–1447. https://doi.org/10.1093/hmg/11.12.1439

Clapham, D. E. (2007). Calcium Signaling. *Cell*, *131*(6), 1047–1058. https://doi.org/10.1016/j.cell.2007.11.028

Clarke, A. J., & Simon, A. K. (2019). Autophagy in the renewal, differentiation and homeostasis of immune cells. *Nature Reviews. Immunology*, *19*(3), 170–183. https://doi.org/10.1038/S41577-018-0095-2

Collibee, S. E., Bergnes, G., Chuang, C., Ashcraft, L., Gardina, J., Garard, M., Jamison, C. R., Lu, K., Lu, P. P., Muci, A., Romero, A., Valkevich, E., Wang, W., Warrington, J., Yao, B., Durham, N., Hartman, J., Marquez, A., Hinken, A., … Morgan, B. P. (2021). Discovery of Reldesemtiv, a Fast Skeletal Muscle Troponin Activator for the Treatment of Impaired Muscle Function. *Journal of Medicinal Chemistry*, *64*(20), 14930–14941. https://doi.org/10.1021/ACS.JMEDCHEM.1C01067

Cooper, A. A., Gitler, A. D., Cashikar, A., Haynes, C. M., Hill, K. J., Bhullar, B., Liu, K., Xu, K., Strathearn, K. E., Liu, F., Cao, S., Caldwell, K. A., Caldwell, G. A., Marsischky, G., Kolodner, R. D., LaBaer, J., Rochet, J. C., Bonini, N. M., & Lindquist, S. (2006). Alpha-synuclein blocks ER-Golgi traffic and Rab1 rescues neuron loss in Parkinson's models. *Science (New York, N.Y.)*, *313*(5785), 324–328. https://doi.org/10.1126/SCIENCE.1129462

Coovert, D. D., Le, T. T., McAndrew, P. E., Strasswimmer, J., Crawford, T. O., Mendell, J. R., Coulson, S. E., Androphy, E. J., Prior, T. W., & Burghes, A. H. M. (1997). The survival motor neuron protein in spinal muscular atrophy. *Human Molecular Genetics*, *6*(8), 1205–1214. https://doi.org/10.1093/HMG/6.8.1205

Crawford, T. O., & Pardo, C. A. (1996). The neurobiology of childhood spinal muscular atrophy. *Neurobiology of Disease*, *3*(2), 97–110. https://doi.org/10.1006/nbdi.1996.0010

Crawford, T. O., Sladky, J. T., Hurko, O., Besner-Johnston, A., & Kelley, R. I. (1999). Abnormal Fatty Acid Metabolism in Childhood Spinal Muscular Atrophy. *Annals of Neurology*. https://doi.org/10.1002/1531-8249

Creedon, D. J., Tansey, M. G., Baloh, R. H., Osborne, P. A., Lampe, P. A., Fahrner, T. J., Heuckeroth, R. O., Milbrandt, J., & Johnson, E. M. (1997). Neurturin shares receptors and signal transduction pathways with glial cell line-derived neurotrophic factor in sympathetic neurons. *Proceedings of the National Academy of Sciences of the United States of America*, *94*(13), 7018–7023. https://doi.org/10.1073/PNAS.94.13.7018

Cullheim, S., Fleshman, J. W., Glenn, L. L., & Burke, R. E. (1987). Membrane area and dendritic structure in type-identified triceps surae alpha motoneurons. *Journal of Comparative Neurology*, *255*(1), 68–81. https://doi.org/10.1002/CNE.902550106

Curmi, F., & Cauchi, R. J. (2018). The multiple lives of DEAD-box RNA helicase DP103/DDX20/Gemin3. *Biochemical Society Transactions*, *46*(2), 329–341. https://doi.org/10.1042/BST20180016

Custer, S. K., & Androphy, E. J. (2014). Autophagy dysregulation in cell culture and animals models of spinal muscular atrophy. *Molecular and Cellular Neuroscience*, *61*, 133–140. https://doi.org/10.1016/J.MCN.2014.06.006

D'Errico, P., Boido, M., Piras, A., Valsecchi, V., De Amicis, E., Locatelli, D., Capra, S., Vagni, F., Vercelli, A., & Battaglia, G. (2013). Selective Vulnerability of Spinal and Cortical Motor Neuron Subpopulations in delta7 SMA Mice. *PLOS ONE*, *8*(12), e82654. https://doi.org/10.1371/JOURNAL.PONE.0082654

Dachs, E., Hereu, M., Piedrafita, L., Casanovas, A., Calderó, J., & Esquerda, J. E. (2011). Defective Neuromuscular Junction Organization and Postnatal Myogenesis in Mice With Severe Spinal Muscular Atrophy. *Journal of Neuropathology & Experimental Neurology*, *70*(6), 444–461. https://doi.org/10.1097/NEN.0B013E31821CBD8B

Darras, B. T., Crawford, T. O., Finkel, R. S., Mercuri, E., De Vivo, D. C., Oskoui, M., Tizzano, E. F., Ryan, M. M.,

Muntoni, F., Zhao, G., Staropoli, J., McCampbell, A., Petrillo, M., Stebbins, C., Fradette, S., Farwell, W., & Sumner, C. J. (2019). Neurofilament as a potential biomarker for spinal muscular atrophy. *Annals of Clinical and Translational Neurology*, *6*(5), 932. https://doi.org/10.1002/ACN3.779

Datta, S. R., Katsov, A., Hu, L., Petros, A., Fesik, S. W., Yaffe, M. B., & Greenberg, M. E. (2000). 14-3-3 Proteins and Survival Kinases Cooperate to Inactivate BAD by BH3 Domain Phosphorylation. *Molecular Cell*, *6*(1), 41–51. https://doi.org/10.1016/S1097-2765(05)00012-2

Daugas, E., Susin, S. A., Zamzami, N., Ferri, K. F., Irinopoulou, T., Larochette, N., Prévost, M., Leber, B., Andrews, D., Penninger, J., & Kroemer, G. (2000). Mitochondrio-nuclear translocation of AIF in apoptosis and necrosis. *FASEB Journal : Official Publication of the Federation of American Societies for Experimental Biology*, *14*(5), 729–739. https://doi.org/10.1096/fasebj.14.5.729

Davis, R. H., Godshall, B. J., Seffrood, E., Marcus, M., Lasalle, B. A., Wong, B., Schroth, M. K., & Swoboda, K. J. (2014). Nutritional practices at a glance: Spinal muscular atrophy type i nutrition survey findings. *Journal of Child Neurology*, *29*(11), 1467–1472. https://doi.org/10.1177/0883073813503988

Day, J. W., Finkel, R. S., Chiriboga, C. A., Connolly, A. M., Crawford, T. O., Darras, B. T., Iannaccone, S. T., Kuntz, N. L., Peña, L. D. M., Shieh, P. B., Smith, E. C., Kwon, J. M., Zaidman, C. M., Schultz, M., Feltner, D. E., Tauscher-Wisniewski, S., Ouyang, H., Chand, D. H., Sproule, D. M., … Mendell, J. R. (2021). Onasemnogene abeparvovec gene therapy for symptomatic infantile-onset spinal muscular atrophy in patients with two copies of SMN2 (STR1VE): an open-label, single-arm, multicentre, phase 3 trial. *The Lancet. Neurology*, *20*(4), 284–293. https://doi.org/10.1016/S1474-4422(21)00001-6

Day, J. W., Mendell, J. R., Al-Zaidy, S. A., Lehman, K. J., Mccolly, M., Lowes, L. P., Alfano, L. N., Reash, N. F., Iammarino, M. A., Church, K. R., Kleyn, A., Meriggioli, M. N., & Shell, ; Richard. (2021). Five-Year Extension Results of the Phase 1 START Trial of Onasemnogene Abeparvovec in Spinal Muscular Atrophy. *JAMA Neurology*. https://doi.org/10.1001/jamaneurol.2021.1272

Day, J. W., Mendell, J. R., Mercuri, E., Finkel, R. S., Strauss, K. A., Kleyn, A., Tauscher-Wisniewski, S., Tukov, F. F., Reyna, S. P., & Chand, D. H. (2021). Clinical Trial and Postmarketing Safety of Onasemnogene Abeparvovec Therapy. *Drug Safety*, *44*(10), 1109. https://doi.org/10.1007/S40264-021-01107-6

De Bernardi, M. A., Rabin, S. J., Colangelo, A. M., Brooker, G., & Mocchetti, I. (1996). trkA Mediates the Nerve Growth Factor-induced Intracellular Calcium Accumulation (∗). *Journal of Biological Chemistry*, *271*(11), 6092–6098. https://doi.org/10.1074/JBC.271.11.6092

de la Fuente Ruiz, S. (2020). Development of new therapeutic strategies for Spinal Muscular Atrophy. In *TDX (Tesis Doctorals en Xarxa)*. http://www.tesisenred.net/handle/10803/669753

de la Fuente, S., Sansa, A., Hidalgo, I., Vivancos, N., Romero-Guevara, R., Garcera, A., & Soler, R. M. (2020). Calpain system is altered in survival motor neuron-reduced cells from in vitro and in vivo spinal muscular atrophy models. *Cell Death and Disease*, *11*(6). https://doi.org/10.1038/s41419-020-2688-5

de la Fuente, S., Sansa, A., Periyakaruppiah, A., Garcera, A., & Soler, R. M. (2018). Calpain Inhibition Increases SMN Protein in Spinal Cord Motoneurons and Ameliorates the Spinal Muscular Atrophy Phenotype in Mice. *Molecular Neurobiology*, *calpain 1*. https://doi.org/10.1007/s12035-018-1379-z

De Vivo, D. C., Bertini, E., Swoboda, K. J., Hwu, W. L., Crawford, T. O., Finkel, R. S., Kirschner, J., Kuntz, N. L., Parsons, J. A., Ryan, M. M., Butterfield, R. J., Topaloglu, H., Ben-Omran, T., Sansone, V. A., Jong, Y. J., Shu, F., Staropoli, J. F., Kerr, D., Sandrock, A. W., … Farwell, W. (2019). Nusinersen initiated in infants during the presymptomatic stage of spinal muscular atrophy: Interim efficacy and safety results from the Phase 2 NURTURE study. *Neuromuscular Disorders : NMD*, *29*(11), 842–856. https://doi.org/10.1016/J.NMD.2019.09.007

De Vos, J., Bouckenheimer, J., Sansac, C., Lemaître, J. M., & Assou, S. (2016). Human induced pluripotent stem cells: A disruptive innovation. *Current Research in Translational Medicine*, *64*(2), 91–96. https://doi.org/10.1016/J.RETRAM.2016.04.001

Deguise, M. O., Baranello, G., Mastella, C., Beauvais, A., Michaud, J., Leone, A., De Amicis, R., Battezzati, A., Dunham, C., Selby, K., Warman Chardon, J., McMillan, H. J., Huang, Y. T., Courtney, N. L., Mole, A. J., Kubinski, S., Claus, P., Murray, L. M., Bowerman, M., … Kothary, R. (2019). Abnormal fatty acid metabolism is a core component of spinal muscular atrophy. *Annals of Clinical and Translational Neurology*, *6*(8), 1519–1532. https://doi.org/10.1002/ACN3.50855

Deguise, M. O., Boyer, J. G., McFall, E. R., Yazdani, A., De Repentigny, Y., & Kothary, R. (2016). Differential induction of muscle atrophy pathways in two mouse models of spinal muscular atrophy. *Scientific Reports*, *6*. https://doi.org/10.1038/SREP28846

Demir, O., Aysit, N., Onder, Z., Turkel, N., Ozturk, G., Sharrocks, A. D., & Kurnaz, I. A. (2011). ETS-domain transcription factor Elk-1 mediates neuronal survival: SMN as a potential target. *Biochimica et Biophysica Acta - Molecular Basis of Disease*, *1812*(6), 652–662. https://doi.org/10.1016/j.bbadis.2011.02.012

Derouet, D., Rousseau, F., Alfonsi, F., Froger, J., Hermann, J., Barbier, F., Perret, D., Diveu, C., Guillet, C., Preisser, L., Dumont, A., Barbado, M., Morel, A., DeLapeyrière, O., Gascan, H., & Chevalier, S. (2004). Neuropoietin, a new IL-6-related cytokine signaling through the ciliary neurotrophic factor receptor. *Proceedings of the National Academy of Sciences of the United States of America*, *101*(14), 4827–4832. https://doi.org/10.1073/pnas.0306178101

Deter, R. L., & De Duve, C. (1967). INFLUENCE OF GLUCAGON, AN INDUCER OF CELLULAR AUTOPHAGY, ON SOME PHYSICAL PROPERTIES

OF RAT LIVER LYSOSOMES. *Journal of Cell Biology*, *33*(2), 437–449. https://doi.org/10.1083/JCB.33.2.437

DiDonato, C. J., Chen, X. N., Noya, D., Korenberg, J. R., Nadeau, J. H., & Simard, L. R. (1997). Cloning, Characterization, and Copy Number of the Murine Survival Motor Neuron Gene: Homolog of the Spinal Muscular Atrophy-Determining Gene. *Genome Research*, *7*(4), 339–352. https://doi.org/10.1101/GR.7.4.339

Dijkhuizen, P. A., & Ghosh, A. (2005). BDNF regulates primary dendrite formation in cortical neurons via the PI3-kinase and MAP kinase signaling pathways. *Journal of Neurobiology*, *62*(2), 278–288. https://doi.org/10.1002/NEU.20100

Dikic, I., & Elazar, Z. (2018). Mechanism and medical implications of mammalian autophagy. In *Nature Reviews Molecular Cell Biology* (Vol. 19, Issue 6, pp. 349–364). https://doi.org/10.1038/s41580-018-0003-4

Dimitriadi, M., Derdowski, A., Kalloo, G., Maginnis, M. S., O'hern, P., Bliska, B., Sorkaç, A., Nguyen, K. C. Q., Cook, S. J., Poulogiannis, G., Atwood, W. J., Hall, D. H., & Hart, A. C. (2016). Decreased function of survival motor neuron protein impairs endocytic pathways. *Proceedings of the National Academy of Sciences of the United States of America*, *113*(30), E4377-4386. https://doi.org/10.1073/PNAS.1600015113/SUPPL_FILE/PNAS.1600015113.SD01.XLSX

Dimitriadi, M., Sleigh, J. N., Walker, A., Chang, H. C., Sen, A., Kalloo, G., Harris, J., Barsby, T., Walsh, M. B., Satterlee, J. S., Li, C., van Vactor, D., Artavanis-Tsakonas, S., & Hart, A. C. (2010). Conserved Genes Act as Modifiers of Invertebrate SMN Loss of Function Defects. *PLOS Genetics*, *6*(10), e1001172. https://doi.org/10.1371/JOURNAL.PGEN.1001172

Dineley, K. T., Westerman, M., Bui, D., Bell, K., Ashe, K. H., & Sweatt, J. D. (2001). Beta-amyloid activates the mitogen-activated protein kinase cascade via hippocampal alpha7 nicotinic acetylcholine receptors: In vitro and in vivo mechanisms related to Alzheimer's disease. *The Journal of Neuroscience : The Official Journal of the Society for Neuroscience*, *21*(12), 4125–4133. https://doi.org/10.1523/JNEUROSCI.21-12-04125.2001

Dobrowolny, G., Aucello, M., Rizzuto, E., Beccafico, S., Mammucari, C., Boncompagni, S., Belia, S., Wannenes, F., Nicoletti, C., Del Prete, Z., Rosenthal, N., Molinaro, M., Protasi, F., Fanò, G., Sandri, M., & Musarò, A. (2008). Skeletal muscle is a primary target of SOD1G93A-mediated toxicity. *Cell Metabolism*, *8*(5), 425–436. https://doi.org/10.1016/J.CMET.2008.09.002

Dolcet, X., Egea, J., Soler, R. M., Martin-Zanca, D., & Comella, J. X. (1999). Activation of phosphatidylinositol 3-kinase, but not extracellular-regulated kinases, is necessary to mediate brain-derived neurotrophic factor-induced motoneuron survival. *Journal of Neurochemistry*, *73*(2), 521–531. https://doi.org/10.1046/J.1471-4159.1999.0730521.X

Dolcet, X., Soler, R. M., Gould, T. W., Egea, J., Oppenheim, R. W., & Comella, J. X. (2001). Cytokines promote motoneuron survival through the janus kinase-dependent activation of the phosphatidylinositol 3-kinase pathway. *Molecular and Cellular Neuroscience*, *18*(6), 619–631. https://doi.org/10.1006/mcne.2001.1058

Dong, S., Wang, Q., Kao, Y. R., Diaz, A., Tasset, I., Kaushik, S., Thiruthuvanathan, V., Zintiridou, A., Nieves, E., Dzieciatkowska, M., Reisz, J. A., Gavathiotis, E., D'Alessandro, A., Will, B., & Cuervo, A. M. (2021). Chaperone-mediated autophagy sustains haematopoietic stem-cell function. *Nature*, *591*(7848), 117–123. https://www.nature.com/articles/s41586-020-03129-z

Du, K., & Montminy, M. (1998). CREB is a regulatory target for the protein kinase Akt/PKB. *The Journal of Biological Chemistry*, *273*(49), 32377–32379. https://doi.org/10.1074/JBC.273.49.32377

Du, S.-H., Tay, J. C.-K., Chen, C., Tay, F.-C., Tan, W.-K., Li, Z.-D., & Wang, S. (2015). Human iPS cell-derived fibroblast-like cells as feeder layers for iPS cell derivation and expansion. *Journal of Bioscience and Bioengineering*, *120*(2), 210–217. https://doi.org/10.1016/J.JBIOSC.2014.12.009

Dubowitz, V. (1999). Very severe spinal muscular atrophy (SMA type 0): An expanding clinical phenotype. *European Journal of Paediatric Neurology*, *3*(2), 49–51. https://doi.org/10.1016/S1090-3798(99)80012-9

Dubrez-Daloz, L., Dupoux, A., & Cartier, J. (2008). IAPs: More than just inhibitors of apoptosis proteins. *Cell Cycle*, *7*(8), 1036–1046. https://doi.org/10.4161/CC.7.8.5783

Duque, S. I., Arnold, W. D., Odermatt, P., Li, X., Porensky, P. N., Schmelzer, L., Meyer, K., Kolb, S. J., Schümperli, D., Kaspar, B. K., & Burghes, A. H. M. M. (2015). A large animal model of spinal muscular atrophy and correction of phenotype. *Annals of Neurology*, *77*(3), 399–414. https://doi.org/10.1002/ANA.24332

Durmus, H., Yilmaz, R., Gulsen-Parman, Y., Oflazer-Serdaroglu, P., Cuttini, M., Dursun, M. M. uh, & Deymeer, F. (2017). Muscle magnetic resonance imaging in spinal muscular atrophy type 3: Selective and progressive involvement. *Muscle & Nerve*, *55*(5), 651–656. https://doi.org/10.1002/MUS.25385

Ebert, A. D., & Svendsen, C. N. (2010). Human stem cells and drug screening: opportunities and challenges. *Nat Rev Drug Discov*. https://doi.org/10.1038/nrd3000

Stem cell model of spinal muscular atrophy, 67 Archives of neurology 665 (2010). https://doi.org/10.1001/ARCHNEUROL.2010.89

Ebert, A. D., Yu, J., Rose, F. F., Mattis, V. B., Lorson, C. L., Thomson, J. A., & Svendsen, C. N. (2009). Induced pluripotent stem cells from a spinal muscular atrophy patient. In *Nature* (Vol. 457, Issue 7227, pp. 277–280). https://doi.org/10.1038/nature07677

Edinger, A. L., & Thompson, C. B. (2004). Death by design: Apoptosis, necrosis and autophagy. *Current Opinion in Cell Biology*, *16*(6), 663–669.

https://doi.org/10.1016/j.ceb.2004.09.011

Eggert, C., Chari, A., Laggerbauer, B., & Fischer, U. (2006). Spinal muscular atrophy: The RNP connection. *Trends in Molecular Medicine*, *12*(3), 113–121. https://doi.org/10.1016/j.molmed.2006.01.005

Ekestern, E. (2004). Neurotrophic factors and amyotrophic lateral sclerosis. *Neuro-Degenerative Diseases*, *1*(2–3), 88–100. https://doi.org/10.1159/000080049

Enari, M., Sakahira, H., Yokoyama, H., Okawa, K., Iwamatsu, A., & Nagata, S. (1998). A caspase-activated DNase that degrades DNA during apoptosis, and its inhibitor ICAD. *Nature*, *391*(6662), 43–50. https://doi.org/10.1038/34112

Eskelinen, E. L. (2004). Maturation of Autophagic Vacuoles in Mammalian Cells. *Http://Dx.Doi.Org/10.4161/Auto.1.1.1270*, *1*(1), 1–10. https://doi.org/10.4161/AUTO.1.1.1270

Eskelinen, E. L., Tanaka, Y., & Saftig, P. (2003). At the acidic edge: emerging functions for lysosomal membrane proteins. *Trends in Cell Biology*, *13*(3), 137–145. https://doi.org/10.1016/S0962-8924(03)00005-9

Fallini, C., Bassell, G. J., & Rossoll, W. (2012). Spinal muscular atrophy: The role of SMN in axonal mRNA regulation. *Brain Research*, *1462*, 81–92. https://doi.org/10.1016/j.brainres.2012.01.044

Fallini, C., Donlin-Asp, P. G., Rouanet, J. P., Bassell, G. J., & Rossoll, W. (2016). Deficiency of the Survival of Motor Neuron Protein Impairs mRNA Localization and Local Translation in the Growth Cone of Motor Neurons. *The Journal of Neuroscience : The Official Journal of the Society for Neuroscience*, *36*(13), 3811–3820. https://doi.org/10.1523/JNEUROSCI.2396-15.2016

Farg, M. A., Sundaramoorthy, V., Sultana, J. M., Yang, S., Atkinson, R. A. K., Levina, V., Halloran, M. A., Gleeson, P. A., Blair, I. P., Soo, K. Y., King, A. E., & Atkin, J. D. (2014). C9ORF72, implicated in amytrophic lateral sclerosis and frontotemporal dementia, regulates endosomal trafficking. *Human Molecular Genetics*, *23*(13), 3579–3595. https://doi.org/10.1093/HMG/DDU068

Farnsworth, C. L., Freshney, N. W., Rosen, L. B., Ghosh, A., Greenberg, M. E., & Feig, L. A. (1995). Calcium activation of Ras mediated by neuronal exchange factor Ras-GRF. *Nature*, *376*(6540), 524–527. https://doi.org/10.1038/376524A0

Farooq, F., Balabanian, S., Liu, X., Holcik, M., & MacKenzie, A. (2009). p38 Mitogen-activated protein kinase stabilizes SMN mRNA through RNA binding protein HuR. *Human Molecular Genetics*, *18*(21), 4035–4045. https://doi.org/10.1093/hmg/ddp352

Farooq, F., Molina, F. A., Hadwen, J., MacKenzie, D., Witherspoon, L., Osmond, M., Holcik, M., & MacKenzie, A. (2011). Prolactin increases SMN expression and survival in a mouse model of severe spinal muscular atrophy via the STAT5 pathway. *The Journal of Clinical Investigation*, *121*(8), 3042–3050. https://doi.org/10.1172/JCI46276

Farooq, F. T., Holcik, M., & MacKenzie, A. (2013). Spinal Muscular Atrophy: Classification, Diagnosis, Background, Molecular Mechanism and Development of Therapeutics. *Neurodegenerative Diseases*. https://doi.org/10.5772/53800

Federici, T., Taub, J. S., Baum, G. R., Gray, S. J., Grieger, J. C., Matthews, K. A., Handy, C. R., Passini, M. A., Samulski, R. J., & Boulis, N. M. (2011). Robust spinal motor neuron transduction following intrathecal delivery of AAV9 in pigs. *Gene Therapy 2012 19:8*, *19*(8), 852–859. https://doi.org/10.1038/gt.2011.130

Feng, W., Gubitz, A. K., Wan, L., Battle, D. J., Dostie, J., Golembe, T. J., & Dreyfuss, G. (2005). Gemins modulate the expression and activity of the SMN complex. *Human Molecular Genetics*, *14*(12), 1605–1611. https://doi.org/10.1093/HMG/DDI168

Feng, Z., Ling, K. K. Y., Zhao, X., Zhou, C., Karp, G., Welch, E. M., Naryshkin, N., Ratni, H., Chen, K. S., Metzger, F., Paushkin, S., Weetall, M., & Ko, C. P. (2016). Pharmacologically induced mouse model of adult spinal muscular atrophy to evaluate effectiveness of therapeutics after disease onset. *Human Molecular Genetics*, *25*(5), 964–975. https://doi.org/10.1093/HMG/DDV629

Ferrara, N., & Adamis, A. P. (2016). Ten years of anti-vascular endothelial growth factor therapy. *Nature Reviews Drug Discovery 2016 15:6*, *15*(6), 385–403. https://doi.org/10.1038/nrd.2015.17

Ferri, A., Melki, J., & Kato, A. C. (2004). Progressive and selective degeneration of motoneurons in a mouse model of SMA. *Neuroreport*, *15*(2), 275–280. https://doi.org/10.1097/00001756-200402090-00013

Finkbeiner, S., & Greenberg, M. E. (1996). Ca2+-Dependent Routes to Ras: Mechanisms for Neuronal Survival, Differentiation, and Plasticity? *Neuron*, *16*(2), 233–236. https://doi.org/10.1016/S0896-6273(00)80040-9

Finkel, R. S., McDermott, M. P., Kaufmann, P., Darras, B. T., Chung, W. K., Sproule, D. M., Kang, P. B., Reghan Foley, A., Yang, M. L., Martens, W. B., Oskoui, M., Glanzman, A. M., Flickinger, J., Montes, J., Dunaway, S., O'Hagen, J., Quigley, J., Riley, S., Benton, M., … De Vivo, D. C. (2014). Observational study of spinal muscular atrophy type I and implications for clinical trials. *Neurology*, *83*(9), 810. https://doi.org/10.1212/WNL.0000000000000741

Finkel, R. S., Mercuri, E., Meyer, O. H., Simonds, A. K., Schroth, M. K., Graham, R. J., Kirschner, J., Iannaccone, S. T., Crawford, T. O., Woods, S., Muntoni, F., Wirth, B., Montes, J., Main, M., Mazzone, E. S., Vitale, M., Snyder, B., Quijano-Roy, S., Bertini, E., … Sejersen, T. (2018). Diagnosis and management of spinal muscular atrophy: Part 2: Pulmonary and acute care; medications, supplements and immunizations; other organ systems; and ethics. *Neuromuscular Disorders*, *28*(3), 197–207. https://doi.org/10.1016/j.nmd.2017.11.004

Fischer, U., Jänicke, R. U., & Schulze-Osthoff, K. (2003). Many cuts to ruin: a comprehensive update of caspase substrates. *Cell Death and Differentiation*, *10*(1), 76. https://doi.org/10.1038/SJ.CDD.4401160

Fischer, U., Liu, Q., & Dreyfuss, G. (1997). The SMN–SIP1 Complex Has an Essential Role in Spliceosomal snRNP Biogenesis. *Cell*, *90*(6), 1023–1029. https://doi.org/10.1016/S0092-8674(00)80368-2

Fletcher, E. V., Simon, C. M., Pagiazitis, J. G., Chalif, J. I., Vukojicic, A., Drobac, E., Wang, X., & Mentis, G. Z. (2017). Reduced sensory synaptic excitation impairs motor neuron function via Kv2.1 in spinal muscular atrophy. *Nature Neuroscience 2017 20:7*, *20*(7), 905–916. https://doi.org/10.1038/nn.4561

Fox, J. H., Connor, T., Chopra, V., Dorsey, K., Kama, J. A., Bleckmann, D., Betschart, C., Hoyer, D., Frentzel, S., Difiglia, M., Paganetti, P., & Hersch, S. M. (2010). The mTOR kinase inhibitor Everolimus decreases S6 kinase phosphorylation but fails to reduce mutant huntingtin levels in brain and is not neuroprotective in the R6/2 mouse model of Huntington's disease. *Molecular Neurodegeneration*, *5*(1). https://doi.org/10.1186/1750-1326-5-26

Franklin, J. L., & Johnson, E. M. (1992). Suppression of programmed neuronal death by sustained elevation of cytoplasmic calcium. *Trends in Neurosciences*, *15*(12), 501–508. https://doi.org/10.1016/0166-2236(92)90103-F

Frebel, K., & Wiese, S. (2006). Signalling molecules essential for neuronal survival and differentiation. *Biochemical Society Transactions*, *34*(6), 1287–1290. https://doi.org/10.1042/BST0341287

Frugier, T., Tiziano, F. D., Cifuentes-Diaz, C., Miniou, P., Roblot, N., Dierich, A., Le Meur, M., & Melki, J. (2000). Nuclear targeting defect of SMN lacking the C-terminus in a mouse model of spinal muscular atrophy. *Human Molecular Genetics*, *9*(5), 849–858. https://doi.org/10.1093/HMG/9.5.849

Fuentes, J. L., Strayer, M. S., & Matera, A. G. (2010). Molecular Determinants of Survival Motor Neuron (SMN) Protein Cleavage by the Calcium-Activated Protease, Calpain. *PLOS ONE*, *5*(12), e15769. https://doi.org/10.1371/journal.pone.0015769

Fukuda, T., Roberts, A., Ahearn, M., Zaal, K., Ralston, E., Plotz, P. H., & Raben, N. (2006). Autophagy and lysosomes in Pompe disease. *Autophagy*, *2*(4), 318–320. https://doi.org/10.4161/AUTO.2984

Gabanella, F., Butchbach, M. E. R. R., Saieva, L., Carissimi, C., Burghes, A. H. M. M., & Pellizzoni, L. (2007). Ribonucleoprotein Assembly Defects Correlate with Spinal Muscular Atrophy Severity and Preferentially Affect a Subset of Spliceosomal snRNPs. *PLoS ONE*, *2*(9), e921. https://doi.org/doi:10.1371/journal.pone.0000921.s002

Galluzzi, L., Bravo-San Pedro, J. M., Vitale, I., Aaronson, S. A., Abrams, J. M., Adam, D., Alnemri, E. S., Altucci, L., Andrews, D., Annicchiarico-Petruzzelli, M., Baehrecke, E. H., Bazan, N. G., Bertrand, M. J., Bianchi, K., Blagosklonny, M. V., Blomgren, K., Borner, C., Bredesen, D. E., Brenner, C., … Kroemer, G. (2015). Essential versus accessory aspects of cell death: Recommendations of the NCCD 2015. *Cell Death and Differentiation*, *22*(1), 58–73. https://doi.org/10.1038/cdd.2014.137

Galluzzi, L., Vitale, I., Aaronson, S. A., Abrams, J. M., Adam, D., Agostinis, P., Alnemri, E. S., Altucci, L., Amelio, I., Andrews, D. W., Annicchiarico-Petruzzelli, M., Antonov, A. V., Arama, E., Baehrecke, E. H., Barlev, N. A., Bazan, N. G., Bernassola, F., Bertrand, M. J. M., Bianchi, K., … Kroemer, G. (2018). Molecular mechanisms of cell death: Recommendations of the Nomenclature Committee on Cell Death 2018. *Cell Death and Differentiation*, *25*(3), 486–541. https://doi.org/10.1038/s41418-017-0012-4

Galluzzi, L., Vitale, I., Abrams, J. M., Alnemri, E. S., Baehrecke, E. H., Blagosklonny, M. V., Dawson, T. M., Dawson, V. L., El-Deiry, W. S., Fulda, S., Gottlieb, E., Green, D. R., Hengartner, M. O., Kepp, O., Knight, R. A., Kumar, S., Lipton, S. A., Lu, X., Madeo, F., … Kroemer, G. (2011). Molecular definitions of cell death subroutines: recommendations of the Nomenclature Committee on Cell Death 2012. *Cell Death & Differentiation 2012 19:1*, *19*(1), 107–120. https://doi.org/10.1038/cdd.2011.96

Ganley, I. G., Lam, D. H., Wang, J., Ding, X., Chen, S., & Jiang, X. (2009). ULK1·ATG13·FIP200 complex mediates mTOR signaling and is essential for autophagy. *Journal of Biological Chemistry*, *284*(18), 12297–12305. https://doi.org/10.1074/JBC.M900573200/ATTACHMENT/55F5A1E4-344E-41E8-AB54-8B442A4E401E/MMC1.PDF

Garbes, L., Heesen, L., Hölker, I., Bauer, T., Schreml, J., Zimmermann, K., Thoenes, M., Walter, M., Dimos, J., Peitz, M., Brüstle, O., Heller, R., & Wirth, B. (2013). VPA response in SMA is suppressed by the fatty acid translocase CD36. *Human Molecular Genetics*, *22*(2), 398–407. https://doi.org/10.1093/HMG/DDS437

Garcera, A., Bahi, N., Periyakaruppiah, A., Arumugam, S., & Soler, R. M. (2013). *Survival motor neuron protein reduction deregulates autophagy in spinal cord motoneurons in vitro*. *4*(6), e686-8. https://doi.org/10.1038/cddis.2013.209

Garcera, A., Mincheva, S., Gou-Fabregas, M., Caraballo-Miralles, V., Lladó, J., Comella, J. X., & Soler, R. M. (2011). A new model to study spinal muscular atrophy: Neurite degeneration and cell death is counteracted by BCL-XL Overexpression in motoneurons. *Neurobiology of Disease*, *42*(3), 415–426. https://doi.org/10.1016/j.nbd.2011.02.003

Gavet, O., & Pines, J. (2010). Progressive activation of CyclinB1-Cdk1 coordinates entry to mitosis. *Developmental Cell*, *18*(4), 533–543. https://doi.org/10.1016/J.DEVCEL.2010.02.013

Gavrilina, T. O., McGovern, V. L., Workman, E., Crawford, T. O., Gogliotti, R. G., Didonato, C. J., Monani, U. R., Morris, G. E., & Burghes, A. H. M. (2008). Neuronal SMN expression corrects spinal muscular atrophy in severe SMA mice while muscle-specific SMN expression has no phenotypic effect. *Human Molecular Genetics*, *17*(8), 1063. https://doi.org/10.1093/HMG/DDM379

Genabai, N. K., Ahmad, S., Zhang, Z., Jiang, X., Gabaldon, C. A., & Gangwani, L. (2015). Genetic inhibition of JNK3 ameliorates spinal muscular atrophy. *Human Mol*, *24*(24), 6986–7004. https://doi.org/10.1093/hmg/ddv401

Gerfen, C. R., Miyachi, S., Paletzki, R., & Brown, P. (2002). D1 dopamine receptor supersensitivity in the dopamine-depleted striatum results from a switch

in the regulation of ERK1/2/MAP kinase. *The Journal of Neuroscience : The Official Journal of the Society for Neuroscience*, *22*(12), 5042–5054. https://doi.org/10.1523/JNEUROSCI.22-12-05042.2002

Ghavami, S., Shojaei, S., Yeganeh, B., Ande, S. R., Jangamreddy, J. R., Mehrpour, M., Christoffersson, J., Chaabane, W., Moghadam, A. R., Kashani, H. H., Hashemi, M., Owji, A. A., & Łos, M. J. (2014). Autophagy and apoptosis dysfunction in neurodegenerative disorders. *Progress in Neurobiology*, *112*, 24–49. https://doi.org/10.1016/J.PNEUROBIO.2013.10.004

Giesemann, T., Rathke-Hartlieb, S., Rothkegel, M., Bartsch, J. W., Buchmeier, S., Jockusch, B. M., & Jockusch, H. (1999). A role for polyproline motifs in the spinal muscular atrophy protein SMN. Profilins bind to and colocalize with smn in nuclear gems. *The Journal of Biological Chemistry*, *274*(53), 37908–37914. https://doi.org/10.1074/JBC.274.53.37908

Giménez-Cassina, A., & Danial, N. N. (2015). Regulation of mitochondrial nutrient and energy metabolism by BCL-2 family proteins. *Trends in Endocrinology and Metabolism*, *26*(4), 165–175. https://doi.org/10.1016/j.tem.2015.02.004

Glascock, J., Sampson, J., Connolly, A. M., Darras, B. T., Day, J. W., Finkel, R., Howell, R. R., Klinger, K. W., Kuntz, N., Prior, T., Shieh, P. B., Crawford, T. O., Kerr, D., Jarecki, J., J, G., Glascock, J., Sampson, J., Connolly, A. M., Darras, B. T., … Jarecki, J. (2020). Revised Recommendations for the Treatment of Infants Diagnosed with Spinal Muscular Atrophy Via Newborn Screening Who Have 4 Copies of SMN2. *Journal of Neuromuscular Diseases*, *7*(2), 97–100. https://doi.org/10.3233/JND-190468

Glascock, J., Sampson, J., Haidet-Phillips, A., Connolly, A., Darras, B., Day, J., Finkel, R., Howell, R. R., Klinger, K., Kuntz, N., Prior, T., Crawford, T. O., Kerr, D., & Jarecki, J. (2018). Treatment Algorithm for Infants Diagnosed with Spinal Muscular Atrophy through Newborn Screening. *Journal of Neuromuscular Diseases*, *5*, 1. https://doi.org/10.3233/JND-180304

Glick, D., Barth, S., & Macleod, K. F. (2010). Autophagy: cellular and molecular mechanisms. *Journal of Pathology*, *221*(1), 3–12. https://doi.org/10.1002/path.2697

Glock, C., Heumüller, M., & Schuman, E. M. (2017). mRNA transport & local translation in neurons. *Current Opinion in Neurobiology*, *45*, 169–177. https://doi.org/10.1016/J.CONB.2017.05.005

Goffredo, D., Rigamonti, D., Zuccato, C., Tartari, M., Valenza, M., & Cattaneo, E. (2005). Prevention of cytosolic IAPs degradation: a potential pharmacological target in Huntington's Disease. *Pharmacological Research*, *52*(2), 140–150. https://doi.org/10.1016/J.PHRS.2005.01.006

Gou-Fabregas, M., Garcera, A., Mincheva, S., Perez-Garcia, M. J., Comella, J. X., & Soler, R. M. (2009). Specific vulnerability of mouse spinal cord motoneurons to membrane depolarization. *Journal of Neurochemistry*, *110*(6), 1842–1854. https://doi.org/10.1111/j.1471-4159.2009.06278.x

Gould, T. W., Yonemura, S., Oppenheim, R. W., Ohmori, S., & Enomoto, H. (2008). The neurotrophic effects of glial cell line-derived neurotrophic factor on spinal motoneurons are restricted to fusimotor subtypes. *The Journal of Neuroscience : The Official Journal of the Society for Neuroscience*, *28*(9), 2131–2146. https://doi.org/10.1523/JNEUROSCI.5185-07.2008

Grzeschik, S. M., Ganta, M., Prior, T. W., Heavlin, W. D., & Wang, C. H. (2005). Hydroxyurea enhances SMN2 gene expression in spinal muscular atrophy cells. *Annals of Neurology*, *58*(2), 194–202. https://doi.org/10.1002/ana.20548

Guégan, C., Vila, M., Rosoklija, G., Hays, A. P., & Przedborski, S. (2001). Recruitment of the mitochondrial-dependent apoptotic pathway in amyotrophic lateral sclerosis. *The Journal of Neuroscience : The Official Journal of the Society for Neuroscience*, *21*(17), 6569–6576. http://www.ncbi.nlm.nih.gov/pubmed/11517246

Guertin, D. A., & Sabatini, D. M. (2009). The pharmacology of mTOR inhibition. *Science Signaling*, *2*(67). https://doi.org/10.1126/SCISIGNAL.267PE24

Gutierrez, H., Hale, V. A., Dolcet, X., & Davies, A. (2005). NF-kappaB signalling regulates the growth of neural processes in the developing PNS and CNS. *Development (Cambridge, England)*, *132*(7), 1713–1726. https://doi.org/10.1242/DEV.01702

Hachiya, Y., Arai, H., Hayashi, M., Kumada, S., Furushima, W., Ohtsuka, E., Ito, Y., Uchiyama, A., & Kurata, K. (2005). Autonomic dysfunction in cases of spinal muscular atrophy type 1 with long survival. *Brain & Development*, *27*(8), 574–578. https://doi.org/10.1016/J.BRAINDEV.2005.02.009

Hamilton, G., & Gillingwater, T. H. (2013). Spinal muscular atrophy: Going beyond the motor neuron. *Trends in Molecular Medicine*, *19*(1), 40–50. https://doi.org/10.1016/j.molmed.2012.11.002

Hammond, S. M., Gogliotti, R. G., Rao, V., Beauvais, A., Kothary, R., & DiDonato, C. J. (2010). Mouse survival motor neuron alleles that mimic SMN2 splicing and are inducible rescue embryonic lethality early in development but not late. *PloS One*, *5*(12). https://doi.org/10.1371/JOURNAL.PONE.0015887

Hannon, G. J., & Rossi, J. J. (2004). Unlocking the potential of the human genome with RNA interference. *Nature 2004 431:7006*, *431*(7006), 371–378. https://doi.org/10.1038/nature02870

Hao, L. T., Burghes, A. H. M., & Beattie, C. E. (2011). Generation and Characterization of a genetic zebrafish model of SMA carrying the human SMN2 gene. *Molecular Neurodegeneration*, *6*(1), 1–9. https://doi.org/10.1186/1750-1326-6-24/COMMENTS

Hara, T., Nakamura, K., Matsui, M., Yamamoto, A., Nakahara, Y., Suzuki-Migishima, R., Yokoyama, M., Mishima, K., Saito, I., Okano, H., & Mizushima, N. (2006). Suppression of basal autophagy in neural cells causes neurodegenerative disease in mice. *Nature 2006 441:7095*, *441*(7095), 885–889.

https://doi.org/10.1038/nature04724

Hayashi-Nishino, M., Fujita, N., Noda, T., Yamaguchi, A., Yoshimori, T., & Yamamoto, A. (2009). A subdomain of the endoplasmic reticulum forms a cradle for autophagosome formation. *Nature Cell Biology 2009 11:12*, *11*(12), 1433–1437. https://doi.org/10.1038/ncb1991

Hayhurst, M., Wagner, A. K., Cerletti, M., Wagers, A. J., & Rubin, L. L. (2012). A cell-autonomous defect in skeletal muscle satellite cells expressing low levels of survival of motor neuron protein. *Developmental Biology*, *368*(2), 323–334. https://doi.org/10.1016/J.YDBIO.2012.05.037

Heath-Engel, H. M., Chang, N. C., & Shore, G. C. (2008). The endoplasmic reticulum in apoptosis and autophagy: role of the BCL-2 protein family. *Oncogene 2008 27:50*, *27*(50), 6419–6433. https://doi.org/10.1038/onc.2008.309

Heesen, L., Peitz, M., Torres-Benito, L., Hölker, I., Hupperich, K., Dobrindt, K., Jungverdorben, J., Ritzenhofen, S., Weykopf, B., Eckert, D., Hosseini-Barkooie, S. M., Storbeck, M., Fusaki, N., Lonigro, R., Heller, R., Kye, M. J., Brüstle, O., & Wirth, B. (2016). Plastin 3 is upregulated in iPSC-derived motoneurons from asymptomatic SMN1-deleted individuals. *Cellular and Molecular Life Sciences*, *73*(10), 2089–2104. https://doi.org/10.1007/s00018-015-2084-y

Heier, C. R., Satta, R., Lutz, C., & Didonato, C. J. (2010). Arrhythmia and cardiac defects are a feature of spinal muscular atrophy model mice. *Human Molecular Genetics*, *19*(20), 3906. https://doi.org/10.1093/HMG/DDQ330

Hensel, N., Baskal, S., Walter, L. M., Brinkmann, H., Gernert, M., & Claus, P. (2017). ERK and ROCK functionally interact in a signaling network that is compensationally upregulated in Spinal Muscular Atrophy. In *Neurobiology of Disease* (Vol. 108, pp. 352–361). https://doi.org/10.1016/j.nbd.2017.09.005

Hensel, N., & Claus, P. (2018). The Actin Cytoskeleton in SMA and ALS: How Does It Contribute to Motoneuron Degeneration? *The Neuroscientist*, *24(I)*, 54–72. https://doi.org/10.1177/1073858417705059

Hensel, N., Ratzka, A., Brinkmann, H., Klimaschewski, L., Grothe, C., & Claus, P. (2012). Analysis of the Fibroblast Growth Factor System Reveals Alterations in a Mouse Model of Spinal Muscular Atrophy. *PLoS ONE*, *7*(2), 31202. https://doi.org/10.1371/JOURNAL.PONE.0031202

Hensel, N., Stockbrügger, I., Rademacher, S., Broughton, N., Brinkmann, H., Grothe, C., & Claus, P. (2014). Bilateral crosstalk of rho- and extracellular-signal-regulated-kinase (ERK) pathways is confined to an unidirectional mode in spinal muscular atrophy (SMA). *Cellular Signalling*, *26*(3), 540–548. https://doi.org/10.1016/J.CELLSIG.2013.11.027

Hernández Borrero, L. J., & El-Deiry, W. S. (2021). Tumor suppressor p53: Biology, signaling pathways, and therapeutic targeting. *Biochimica et Biophysica Acta (BBA) - Reviews on Cancer*, *1876*(1), 188556. https://doi.org/10.1016/J.BBCAN.2021.188556

Hetman, M., Kanning, K., Cavanaugh, J. E., & Xia, Z. (1999). Neuroprotection by brain-derived neurotrophic factor is mediated by extracellular signal-regulated kinase and phosphatidylinositol 3-kinase. *The Journal of Biological Chemistry*, *274*(32), 22569–22580. https://doi.org/10.1074/JBC.274.32.22569

Hetz, C., Thielen, P., Matus, S., Nassif, M., Court, F., Kiffin, R., Martinez, G., Cuervo, A. M., Brown, R. H., & Glimcher, L. H. (2009). XBP-1 deficiency in the nervous system protects against amyotrophic lateral sclerosis by increasing autophagy. *Genes & Development*, *23*(19), 2294–2306. https://doi.org/10.1101/GAD.1830709

Ho, M., Patel, A., Hanley, C., Murphy, A., McSweeney, T., Zhang, L., McCann, A., O'Gorman, P., & Bianchi, G. (2019). Exploiting autophagy in multiple myeloma. *Journal of Cancer Metastasis and Treatment*, *5*, 70. https://doi.org/10.20517/2394-4722.2019.25

Holgado-Madruga, M., Moscatello, D. K., Emlet, D. R., Dieterich, R., & Wong, A. J. (1997). Grb2-associated binder-1 mediates phosphatidylinositol 3-kinase activation and the promotion of cell survival by nerve growth factor. *Proceedings of the National Academy of Sciences of the United States of America*, *94*(23), 12419–12424. https://doi.org/10.1073/PNAS.94.23.12419

Hosokawa, N., Hara, T., Kaizuka, T., Kishi, C., Takamura, A., Miura, Y., Iemura, S. I., Natsume, T., Takehana, K., Yamada, N., Guan, J. L., Oshiro, N., & Mizushima, N. (2009). Nutrient-dependent mTORC1 association with the ULK1-Atg13-FIP200 complex required for autophagy. *Molecular Biology of the Cell*, *20*(7), 1981–1991. https://doi.org/10.1091/MBC.E08-12-1248/ASSET/IMAGES/LARGE/ZMK0070990130007.JPEG

Hsieh-Li, H. M., Chang, J. G., Jong, Y. J., Wu, M. H., Wang, N. M., Tsai, C. H., & Li, H. (2000a). A mouse model for spinal muscular atrophy. *Nature Genetics 2000 24:1*, *24*(1), 66–70. https://doi.org/10.1038/71709

Hsieh-Li, H. M., Chang, J. G., Jong, Y. J., Wu, M. H., Wang, N. M., Tsai, C. H., & Li, H. (2000b). A mouse model for spinal muscular atrophy. *Nature Genetics*, *24*(1), 66–70. https://doi.org/10.1038/71709

Hua, Y., Vickers, T. A., Okunola, H. L., Bennett, C. F., Krainer, A. R., Yimin, H., Vickers, T. A., Okunola, H. L., Bennett, C. F., & Krainer, A. R. (2008). Antisense Masking of an hnRNP A1/A2 Intronic Splicing Silencer Corrects SMN2 Splicing in Transgenic Mice. *American Journal of Human Genetics*, *82*(4), 834–848. https://doi.org/10.1016/j.ajhg.2008.01.014

Humbert, S., Bryson, E. A., Cordelières, F. P., Connors, N. C., Datta, S. R., Finkbeiner, S., Greenberg, M. E., & Saudou, F. (2002). The IGF-1/Akt pathway is neuroprotective in Huntington's disease and involves Huntingtin phosphorylation by Akt. *Developmental Cell*, *2*(6), 831–837. https://doi.org/10.1016/S1534-5807(02)00188-0

Hurley, J. H., & Young, L. N. (2017). Mechanisms of Autophagy Initiation. *Https://Doi.Org/10.1146/Annurev-Biochem-061516-044820*, *86*, 225–244. https://doi.org/10.1146/ANNUREV-BIOCHEM-

061516-044820

Ichim, G., G Tait, S. W., & Tait, S. W. G. (2016). A fate worse than death: apoptosis as an oncogenic process. *Nature Publishing Group*, *16*(8), 539–548. https://doi.org/10.1038/nrc.2016.58

Ilangovan, R., Marshall, W. L., Hua, Y., & Zhou, J. (2003). Inhibition of apoptosis by Z-VAD-fmk in SMN-depleted S2 cells. *The Journal of Biological Chemistry*, *278*(33), 30993–30999. https://doi.org/10.1074/JBC.M303763200

Ip, N. Y., Ibanez, C. F., Nye, S. H., McClain, J., Jones, P. F., Gies, D. R., Belluscio, L., Le Beau, M. M., Espinosa, R., Squinto, S. P., Persson, H., & Yancopoulos, G. D. (1992). Mammalian neurotrophin-4: structure, chromosomal localization, tissue distribution, and receptor specificity. *Proceedings of the National Academy of Sciences of the United States of America*, *89*(7), 3060–3064. https://doi.org/10.1073/PNAS.89.7.3060

Itakura, E., & Mizushima, N. (2010). Characterization of autophagosome formation site by a hierarchical analysis of mammalian Atg proteins. *Autophagy*, *6*(6), 764–776. https://doi.org/10.4161/AUTO.6.6.12709

Jablonka, S., Beck, M., Lechner, B. D., Mayer, C., & Sendtner, M. (2007). Defective Ca2+ channel clustering in axon terminals disturbs excitability in motoneurons in spinal muscular atrophy. *Journal of Cell Biology*, *179*(1), 139–149. https://doi.org/10.1083/jcb.200703187

Jablonka, S., Holtmann, B., Meister, G., Bandilla, M., Rossoll, W., Fischer, U., & Sendtner, M. (2002). Gene targeting of Gemin2 in mice reveals a correlation between defects in the biogenesis of U snRNPs and motoneuron cell death. *Proceedings of the National Academy of Sciences of the United States of America*, *99*(15), 10126–10131. https://doi.org/10.1073/PNAS.152318699

Jablonka, S., Schrank, B., Kralewski, M., Rossoll, W., & Sendtner, M. (2000). Reduced survival motor neuron (Smn) gene dose in mice leads to motor neuron degeneration: an animal model for spinal muscular atrophy type III. *Human Molecular Genetics*, *9*(3), 341–346. https://doi.org/10.1093/HMG/9.3.341

Jin, H., Kanthasamy, A., Ghosh, A., Yang, Y., Anantharam, V., & Kanthasamy, A. G. (2011). α-synuclein negatively regulates protein kinase Cδ expression to suppress apoptosis in dopaminergic neurons by reducing p300 histone acetyltransferase activity. *Journal of Neuroscience*, *31*(6), 2035–2051. https://doi.org/10.1523/JNEUROSCI.5634-10.2011

Jing, C., Yeo, J., & Darras, B. T. (2020). Overturning the Paradigm of Spinal Muscular Atrophy as just a Motor Neuron Disease. *Pediatric Neurology*. https://doi.org/https://doi.org/10.1016/j.pediatrneurol.2020.01.003. This

Jung, C. H., Jun, C. B., Ro, S. H., Kim, Y. M., Otto, N. M., Cao, J., Kundu, M., & Kim, D. H. (2009). ULK-Atg13-FIP200 complexes mediate mTOR signaling to the autophagy machinery. *Molecular Biology of the Cell*, *20*(7), 1992–2003. https://doi.org/10.1091/MBC.E08-12-1249/ASSET/IMAGES/LARGE/ZMK00709901500 07.JPEG

Kang, R., Zeh, H. J., Lotze, M. T., & Tang, D. (2011). The Beclin 1 network regulates autophagy and apoptosis. *Cell Death and Differentiation*, *18*(4), 571–580. https://doi.org/10.1038/CDD.2010.191

Kannan, A., Jiang, X., He, L., Ahmad, S., & Gangwani, L. (2020). ZPR1 prevents R-loop accumulation, upregulates SMN2 expression and rescues spinal muscular atrophy. *Brain*, *143*(1), 69–93. https://doi.org/10.1093/brain/awz373

Kanning, K. C., Kaplan, A., & Henderson, C. E. (2010). Motor Neuron Diversity in Development and Disease. *Annual Review of Neuroscience*, *33*, 409–440. https://doi.org/10.1146/annurev.neuro.051508.135722

Kaplan, D. R., & Miller, F. D. (2000). Neurotrophin signal transduction in the nervous system. *Current Opinion in Neurobiology*, *10*(3), 381–391. https://doi.org/10.1016/S0959-4388(00)00092-1

Kariya, S., Park, G.-H. H., Maeno-Hikichi, Y., Leykekhman, O., Lutz, C., Arkovitz, M. S., Landmesser, L. T., & Monani, U. R. (2008). Reduced SMN protein impairs maturation of the neuromuscular junctions in mouse models of spinal muscular atrophy. *Human Molecular Genetics*, *17*(16). http://www.ncbi.nlm.nih.gov/pubmed/18492800

Kerr, D. A., Nery, J. P., Traystman, R. J., Chau, B. N., & Hardwick, J. M. (2000). Survival motor neuron protein modulates neuron-specific apoptosis. *Proceedings of the National Academy of Sciences of the United States of America*, *97*(24), 13312–13317. https://doi.org/10.1073/PNAS.230364197

Kerr, J. F. R., Wyllie, A. H. H., & Currie, A. R. (1972). Apoptosis: A Basic Biological Phenomenon With Wide-Ranging Implications in Tissue Kinetics. *Br. J. Cancer*, *26*, 239–257. https://doi.org/10.1038/bjc.1972.33

Khairallah, M. T., Astroski, J., Custer, S. K., Androphy, E. J., Franklin, C. L., & Lorson, C. L. (2017). SMN deficiency negatively impacts red pulp macrophages and spleen development in mouse models of spinal muscular atrophy. *Human Molecular Genetics*, *26*(5), 932–941. https://doi.org/10.1093/HMG/DDX008

Khatri, I. A., Chaudhry, U. S., Seikaly, M. G., Browne, R. H., & Iannaccone, S. T. (2008). Low bone mineral density in spinal muscular atrophy. *Journal of Clinical Neuromuscular Disease*, *10*(1), 11–17. https://doi.org/10.1097/CND.0B013E318183E0FA

Kieran, D., Sebastia, J., Greenway, M. J., King, M. A., Connaughton, D., Concannon, C. G., Fenner, B., Hardiman, O., & Prehn, J. H. M. (2008). Control of motoneuron survival by angiogenin. *The Journal of Neuroscience : The Official Journal of the Society for Neuroscience*, *28*(52), 14056–14061. https://doi.org/10.1523/JNEUROSCI.3399-08.2008

Kim, J. K., Jha, N. N., Feng, Z., Faleiro, M. R., Chiriboga, C. A., Wei-Lapierre, L., Dirksen, R. T., Ko, C. P., & Monani, U. R. (2020). Muscle-specific SMN reduction reveals motor neuron-independent disease in spinal muscular atrophy models. *The Journal of Clinical Investigation*, *130*(3), 1271–

1287. https://doi.org/10.1172/JCI131989

Kim, S. G., Buel, G. R., & Blenis, J. (2013). Nutrient regulation of the mTOR complex 1 signaling pathway. *Molecules and Cells*, *35*(6), 463–473. https://doi.org/10.1007/S10059-013-0138-2

Kim, Y. J., Yi, Y., Sapp, E., Wang, Y., Cuiffo, B., Kegel, K. B., Qin, Z. H., Aronin, N., & DiFiglia, M. (2001). Caspase 3-cleaved N-terminal fragments of wild-type and mutant huntingtin are present in normal and Huntington's disease brains, associate with membranes, and undergo calpaindependent proteolysis. *Proceedings of the National Academy of Sciences of the United States of America*, *98*(22), 12784–12789. https://doi.org/10.1073/PNAS.221451398

Kirkin, V., McEwan, D. G., Novak, I., & Dikic, I. (2009). A Role for Ubiquitin in Selective Autophagy. *Molecular Cell*, *34*(3), 259–269. https://doi.org/10.1016/J.MOLCEL.2009.04.026

Kissel, J. T., Scott, C. B., Reyna, S. P., Crawford, T. O., Simard, L. R., Krosschell, K. J., Acsadi, G., Elsheik, B., Schroth, M. K., Anjou, G. D. ', Lasalle, B., Prior, T. W., Sorenson, S., Maczulski, J. A., Bromberg, M. B., Chan, G. M., & Swoboda, K. J. (2011). SMA CARNIVAL TRIAL PART II: A Prospective, Single-Armed Trial of L-Carnitine and Valproic Acid in Ambulatory Children with Spinal Muscular Atrophy. *PLoS ONE*. https://doi.org/10.1371/journal.pone.0021296

Klionsky, D. J., Abdel-Aziz, A. K., Abdelfatah, S., Abdellatif, M., Abdoli, A., Abel, S., Abeliovich, H., Abildgaard, M. H., Abudu, Y. P., Acevedo-Arozena, A., Adamopoulos, I. E., Adeli, K., Adolph, T. E., Adornetto, A., Aflaki, E., Agam, G., Agarwal, A., Aggarwal, B. B., Agnello, M., … Tong, C. K. (2021). Guidelines for the use and interpretation of assays for monitoring autophagy (4th edition)1. *Autophagy*, *17*(1), 1–382. https://doi.org/10.1080/15548627.2020.1797280

Klionsky, D. J., Petroni, G., Amaravadi, R. K., Baehrecke, E. H., Ballabio, A., Boya, P., Bravo-San Pedro, J. M., Cadwell, K., Cecconi, F., Choi, A. M. K., Choi, M. E., Chu, C. T., Codogno, P., Colombo, M. I., Cuervo, A. M., Deretic, V., Dikic, I., Elazar, Z., Eskelinen, E., … Pietrocola, F. (2021). Autophagy in major human diseases. *The EMBO Journal*, *40*(19), 1–64. https://doi.org/10.15252/embj.2021108863

Koike, M., Shibata, M., Waguri, S., Yoshimura, K., Tanida, I., Kominami, E., Gotow, T., Peters, C., Von Figura, K., Mizushima, N., Saftig, P., & Uchiyama, Y. (2005). Participation of autophagy in storage of lysosomes in neurons from mouse models of neuronal ceroid-lipofuscinoses (Batten disease). *American Journal of Pathology*, *167*(6), 1713–1728. https://doi.org/10.1016/S0002-9440(10)61253-9/ATTACHMENT/4E7076AD-932D-42C2-B202-CE560FC72A57/MMC1.PDF

Kolb, S. J., & Kissel, J. T. (2015). Spinal Muscular Atrophy. *Neurologic Clinics*, *33*(4), 831–846. https://doi.org/10.1016/j.ncl.2015.07.004

Komatsu, M., Waguri, S., Chiba, T., Murata, S., Iwata, J. I., Tanida, I., Ueno, T., Koike, M., Uchiyama, Y., Kominami, E., & Tanaka, K. (2006). Loss of autophagy in the central nervous system causes neurodegeneration in mice. *Nature 2006 441:7095*, *441*(7095), 880–884. https://doi.org/10.1038/nature04723

Kong, L., Wang, X., Choe, D. W., Polley, M., Burnett, B. G., Bosch-Marcé, M., Griffin, J. W., Rich, M. M., & Sumner, C. J. (2009). Impaired synaptic vesicle release and immaturity of neuromuscular junctions in spinal muscular atrophy mice. *The Journal of Neuroscience : The Official Journal of the Society for Neuroscience*, *29*(3), 842–851. https://doi.org/10.1523/JNEUROSCI.4434-08.2009

Korsching, S. (1993). The neurotrophic factor concept: A reexamination. *Journal of Neuroscience*, *13*(7), 2739–2748. https://doi.org/10.1523/jneurosci.13-07-02739.1993

Kotzbauer, P. T., Lampe, P. A., Heuckeroth, R. O., Golden, J. P., Creedon, D. J., Johnson, E. M., & Milbrandt, J. (1996). Neurturin, a relative of glial-cell-line-derived neurotrophic factor. *Nature*, *384*(6608), 467–470. https://doi.org/10.1038/384467A0

Krieger, C., Jones, K., Kim, S. U., & Eisen, A. A. (1994). The role of intracellular free calcium in motor neuron disease. *Journal of the Neurological Sciences*, *124*(SUPPL.), 27–32. https://doi.org/10.1016/0022-510X(94)90173-2

Kroemer, G., Galluzzi, L., Vandenabeele, P., Abrams, J., Alnemri, E. S., Baehrecke, E. H., Blagosklonny, M. V, & El-deiry, W. S. (2009). *Classification of cell death : recommendations of the Nomenclature Committee on Cell Death 2009*. 3–11. https://doi.org/10.1038/cdd.2008.150

Kügler, S., Straten, G., Kreppel, F., Isenmann, S., Liston, P., & Bähr, M. (2000). The X-linked inhibitor of apoptosis (XIAP) prevents cell death in axotomized CNS neurons in vivo. *Cell Death and Differentiation*, *7*(9), 815–824. https://doi.org/10.1038/SJ.CDD.4400712

Kulich, S. M., & Chu, C. T. (2001). Sustained extracellular signal-regulated kinase activation by 6-hydroxydopamine: implications for Parkinson's disease. *Journal of Neurochemistry*, *77*(4), 1058. https://doi.org/10.1046/J.1471-4159.2001.00304.X

Kumagai, T., & Hashizume, Y. (1982). Morphological and morphometric studies on the spinal cord lesion in Werdnig-Hoffmann disease. *Brain and Development*, *4*(2), 87–96. https://doi.org/10.1016/S0387-7604(82)80002-8

Kwon, D. Y., Motley, W. W., Fischbeck, K. H., & Burnett, B. G. (2011). Increasing expression and decreasing degradation of SMN ameliorate the spinal muscular atrophy phenotype in mice. *Human Molecular Genetics*, *20*(18), 3667–3677. https://doi.org/10.1093/HMG/DDR288

Lambrechts, D., Robberecht, W., & Carmeliet, P. (2007). Heterogeneity in motoneuron disease. *Trends in Neurosciences*, *30*(10), 536–544. https://doi.org/10.1016/j.tins.2007.07.002

Laron, Z. (2001). Insulin-like growth factor 1 (IGF-1): a growth hormone. *J Clin Pathol: Mol Pathol*, *54*, 311–316. https://doi.org/10.1136/mp.54.5.311

Latchman, D. S. (1999). Cardiotrophin-1 (CT-1): a novel hypertrophic and cardioprotective agent. In *Int. J.*

Exp. Path (Vol. 80).

Latil, M., Bézier, C., Cottin, S., Lafont, R., Veillet, S., Dilda, P., Charbonnier, F., & Biondi, O. (2019). P.370BIO101 demonstrates combined beneficial effects on muscle and motor neurons in a mouse model of severe spinal muscular atrophy. *Neuromuscular Disorders*, *29*, S189. https://doi.org/10.1016/j.nmd.2019.06.532

Lawton, L. N., Bonaldo, M. D. F., Jelenc, P. C., Qiu, L., Baumes, S. A., Marcelino, R. A., De Jesus, G. M., Wellington, S., Knowles, J. A., Warburton, D., Brown, S., & Soares, M. B. (1997). Identification of a novel member of the TGF-beta superfamily highly expressed in human placenta. *Gene*, *203*(1), 17–26. https://doi.org/10.1016/S0378-1119(97)00485-X

Le, T. T., Pham, L. T., Butchbach, M. E. R., Zhang, H. L., Monani, U. R., Coovert, D. D., Gavrilina, T. O., Xing, L., Bassell, G. J., & Burghes, A. H. M. (2005). SMNDelta7, the major product of the centromeric survival motor neuron (SMN2) gene, extends survival in mice with spinal muscular atrophy and associates with full-length SMN. *Human Molecular Genetics*, *14*(6), 845–857. https://doi.org/10.1093/HMG/DDI078

Lee, D. F., Kuo, H. P., Chen, C. Te, Hsu, J. M., Chou, C. K., Wei, Y., Sun, H. L., Li, L. Y., Ping, B., Huang, W. C., He, X., Hung, J. Y., Lai, C. C., Ding, Q., Su, J. L., Yang, J. Y., Sahin, A. A., Hortobagyi, G. N., Tsai, F. J., … Hung, M. C. (2007). IKKβ Suppression of TSC1 Links Inflammation and Tumor Angiogenesis via the mTOR Pathway. *Cell*, *130*(3), 440–455. https://doi.org/10.1016/J.CELL.2007.05.058

Lee, H. K., Kumar, P., Fu, Q., Rosen, K. M., & Querfurth, H. W. (2009). The Insulin/Akt Signaling Pathway Is Targeted by Intracellular β-Amyloid. *Molecular Biology of the Cell*, *20*(5), 1533. https://doi.org/10.1091/MBC.E08-07-0777

Lee, R. H., & Heckman, C. J. (1998). Bistability in spinal motoneurons in vivo: Systematic variations in persistent inward currents. *Journal of Neurophysiology*, *80*(2), 583–593. https://doi.org/10.1152/JN.1998.80.2.583/ASSET/IMAGES/LARGE/JNP.AU24F8.JPEG

Lefebvre, S., Burglen, L., Reboullet, S., Clermont, O., Burlet, P., Viollet, L., Benichou, B., Cruaud, C., Millasseau, P., Zeviani, M., & Et Al. (1995). Identification and characterization of a spinal muscular atrophy-determining gene [see comments]. *Cell*, *80*(1), 155–165. http://www.ncbi.nlm.nih.gov/cgi-bin/Entrez/referer?http://www.ncbi.nlm.nih.gov/htbin-post/Omim/getmim?field=medline_uid&search=7813012

Lefebvre, S., Burlet, P., Liu, Q., Bertrandy, S., Clermont, O., Munnich, A., Dreyfuss, G., & Melki, J. (1997). Correlation between severity and SMN protein level in spinal muscular atrophy. *Nature Genetics*, *16*(3), 265–269. https://doi.org/10.1038/ng0797-265

Lesbordes, J. C., Cifuentes-Diaz, C., Miroglio, A., Joshi, V., Bordet, T., Kahn, A., & Milki, J. (2003). Therapeutic benefits of cardiotrophin-1 gene transfer in a mouse model of spinal muscular atrophy. *Human Molecular Genetics*, *12*(11), 1233–1239. https://doi.org/10.1093/HMG/DDG143

Levi-Montalcini, R. (1987). The nerve growth factor 35 years later. *Science*, *237*(4819), 1154–1162. https://doi.org/10.1126/SCIENCE.3306916/ASSET/97C94B0E-A746-4E59-8A69-DE363EDF81A9/ASSETS/SCIENCE.3306916.FP.PNG

Levkau, B., Garton, K. J., Ferri, N., Kloke, K., Nofer, J. R., Baba, H. A., Raines, E. W., & Breithardt, G. (2001). xIAP induces cell-cycle arrest and activates nuclear factor-kappaB : new survival pathways disabled by caspase-mediated cleavage during apoptosis of human endothelial cells. *Circulation Research*, *88*(3), 282–290. https://doi.org/10.1161/01.RES.88.3.282

Lewelt, A., Newcomb, T. M., & Swoboda, K. J. (2012). New Therapeutic Approaches to Spinal Muscular Atrophy. *Current Neurology and Neuroscience Reports*, 42–53. https://doi.org/10.1007/s11910-011-0240-9

Li, X. Y., Zhan, X. R., Liu, X. M., & Wang, X. C. (2011). CREB is a regulatory target for the protein kinase Akt/PKB in the differentiation of pancreatic ductal cells into islet β-cells mediated by hepatocyte growth factor. *Biochemical and Biophysical Research Communications*, *404*(2), 711–716. https://doi.org/10.1016/J.BBRC.2010.12.048

Liang, W. C., Yuo, C. Y., Chang, J. G., Chen, Y. C., Chang, Y. F., Wang, H. Y., Ju, Y. H., Chiou, S. S., & Jong, Y. J. (2008). The effect of hydroxyurea in spinal muscular atrophy cells and patients. *Journal of the Neurological Sciences*, *268*(1–2), 87–94. https://doi.org/10.1016/j.jns.2007.11.012

Lin, L. F. H., Doherty, D. H., Lile, J. D., Bektesh, S., & Collins, F. (1993). GDNF: a glial cell line-derived neurotrophic factor for midbrain dopaminergic neurons. *Science (New York, N.Y.)*, *260*(5111), 1130–1132. https://doi.org/10.1126/SCIENCE.8493557

Lin, T. L., Chen, T. H., Hsu, Y. Y., Cheng, Y. H., Juang, B. T., & Jong, Y. J. (2016). Selective Neuromuscular Denervation in Taiwanese Severe SMA Mouse Can Be Reversed by Morpholino Antisense Oligonucleotides. *PLOS ONE*, *11*(4), e0154723. https://doi.org/10.1371/JOURNAL.PONE.0154723

Lipnick, S. L., Agniel, D. M., Aggarwal, R., Makhortova, N. R., Finlayson, S. G., Brocato, A., Palmer, N., Darras, B. T., Kohane, I., & Rubin, L. L. (2019). Systemic nature of spinal muscular atrophy revealed by studying insurance claims. *PLOS ONE*, *14*(3), e0213680. https://doi.org/10.1371/JOURNAL.PONE.0213680

Lippmann, E. S., Al-Ahmad, A., Azarin, S. M., Palecek, S. P., & Shusta, E. V. (2014). A retinoic acid-enhanced, multicellular human blood-brain barrier model derived from stem cell sources. *Scientific Reports 2014 4:1*, *4*(1), 1–10. https://doi.org/10.1038/srep04160

Liu, F., Yang, X., Geng, M., & Huang, M. (2018). Targeting ERK, an Achilles' Heel of the MAPK pathway, in cancer therapy. *Acta Pharmaceutica Sinica B*, *8*(4), 552–562. https://doi.org/10.1016/J.APSB.2018.01.008

Liu, H., Lu, J., Chen, H., Du, Z., Li, X. J., & Zhang, S. C. (2015). Spinal muscular atrophy patient-derived motor neurons exhibit hyperexcitability. *Scientific Reports 2015 5:1*, *5*(1), 1–13. https://doi.org/10.1038/srep12189

Liu, X., Zou, H., Slaughter, C., & Wang, X. (1997). DFF, a heterodimeric protein that functions downstream of caspase-3 to trigger DNA fragmentation during apoptosis. *Cell*, *89*(2), 175–184. https://doi.org/10.1016/S0092-8674(00)80197-X

Locatelli, D., Terao, M., Fratelli, M., Zanetti, A., Kurosaki, M., Lupi, M., Barzago, M. M., Uggetti, A., Capra, S., D'Errico, P., Battaglia, G. S., & Garattini, E. (2012). Human axonal Survival of Motor Neuron (a-SMN) protein stimulates axon growth, cell motility, C-C motif ligand 2 (CCL2),andinsulin-like growth factor-1 (IGF1) production. In *Journal of Biological Chemistry* (Vol. 287, Issue 31, pp. 25782–25794). https://doi.org/10.1074/jbc.M112.362830

Lockshin, R. A., & Williams, C. M. (1965). PROGRAMMED CELL DEATH--I. CYTOLOGY OF DEGENERATION IN THE INTERSEGMENTAL MUSCLES OF THE PERNYI SILKMOTH. *Journal of Insect Physiology*, *11*(2). https://doi.org/10.1016/0022-1910(65)90099-5

Long, K. K., O'shea, K. M., Khairallah, R. J., Howell, K., Paushkin, S., Chen, K. S., Cote, S. M., Webster, M. T., Stains, J. P., Treece, E., Buckler, A., & Donovan, A. (2019). Specific inhibition of myostatin activation is beneficial in mouse models of SMA therapy. *Human Molecular Genetics*, *28*(7), 1076–1089. https://doi.org/10.1093/hmg/ddy382

Lopez-Manzaneda, M., Franco-Espin, J., Tejero, R., Cano, R., & Tabares, L. (2021). Calcium is reduced in presynaptic mitochondria of motor nerve terminals during neurotransmission in SMA mice. *Human Molecular Genetics*, *30*(8), 629–643. https://doi.org/10.1093/hmg/ddab065

LoPiccolo, J., Blumenthal, G. M., Bernstein, W. B., & Dennis, P. A. (2008). Targeting the PI3K/Akt/mTOR pathway: effective combinations and clinical considerations. *Drug Resistance Updates : Reviews and Commentaries in Antimicrobial and Anticancer Chemotherapy*, *11*(1–2), 32. https://doi.org/10.1016/J.DRUP.2007.11.003

Lorson, C. L., Hahnen, E., Androphy, E. J., & Wirth, B. (1999). A single nucleotide in the SMN gene regulates splicing and is responsible for spinal muscular atrophy. *Proceedings of the National Academy of Sciences of the United States of America*, *96*(11), 6307–6311. http://www.ncbi.nlm.nih.gov/pubmed/10339583

Lorson, C. L., Strasswimmer, J., Yao, J.-M., D.Baleja, J., Hahnen, E., Wirth, B., Le, T., Burghes, A. H. M., & Androphy, E. J. (1998). SMN oligomerization defect correlates with spinal muscular atrophy severity. *Nature Genetics*, *18*(3), 231–236. https://doi.org/10.1038/ng0598-63

Lustbader, J. W., Cirilli, M., Lin, C., Xu, H. W., Takuma, K., Wang, N., Caspersen, C., Chen, X., Pollak, S., Chaney, M., Trinchese, F., Liu, S., Gunn-Moore, F., Lue, L. F., Walker, D. G., Kappasamy, P., Zewier, Z. L., Arancio, O., Stern, D., … Wu, H. (2004). ABAD Directly Links Aβ to Mitochondrial Toxicity in Alzheimer's Disease. *Science*, *304*(5669), 448–452. https://doi.org/10.1126/SCIENCE.1091230

Ma, L., Chen, Z., Erdjument-Bromage, H., Tempst, P., & Pandolfi, P. P. (2005). Phosphorylation and Functional Inactivation of TSC2 by Erk: Implications for Tuberous Sclerosisand Cancer Pathogenesis. *Cell*, *121*(2), 179–193. https://doi.org/10.1016/J.CELL.2005.02.031

Madrid, L. V., Wang, C.-Y., Guttridge, D. C., Schottelius, A. J. G., Baldwin, A. S., & Mayo, M. W. (2000). Akt suppresses apoptosis by stimulating the transactivation potential of the RelA/p65 subunit of NF-kappaB. *Molecular and Cellular Biology*, *20*(5), 1626–1638. https://doi.org/10.1128/MCB.20.5.1626-1638.2000

Maggi, L., & Mantegazza, R. (2011). Treatment of myasthenia gravis: Focus on pyridostigmine. *Clinical Drug Investigation*, *31*(10), 691–701. https://doi.org/10.2165/11593300-000000000-00000/FIGURES/TAB1

Mailman, M. D., Heinz, J. W., Papp, A. C., Snyder, P. J., Sedra, M. S., Wirth, B., Burghes, A. H. M., & Prior, T. W. (2002). Molecular analysis of spinal muscular atrophy and modification of the phenotype by SMN2. *Genetics in Medicine*, *4*(1), 20–26. https://doi.org/10.1097/00125817-200201000-00004

Manczak, M., Anekonda, T. S., Henson, E., Park, B. S., Quinn, J., & Reddy, P. H. (2006). Mitochondria are a direct site of Aβ accumulation in Alzheimer's disease neurons: implications for free radical generation and oxidative damage in disease progression. *Human Molecular Genetics*, *15*(9), 1437–1449. https://doi.org/10.1093/HMG/DDL066

Mantamadiotis, T., Papalexis, N., & Dworkin, S. (2012). CREB signalling in neural stem/progenitor cells: Recent developments and the implications for brain tumour biology. *BioEssays*, *34*(4), 293–300. https://doi.org/10.1002/BIES.201100133

Marasco, L. E., Dujardin, G., Sousa-Luís, R., Liu, Y. H., Stigliano, J. N., Nomakuchi, T., Proudfoot, N. J., Krainer, A. R., & Kornblihtt, A. R. (2022). Counteracting chromatin effects of a splicing-correcting antisense oligonucleotide improves its therapeutic efficacy in spinal muscular atrophy. *Cell*, *185*(12), 2057-2070.e15. https://doi.org/10.1016/J.CELL.2022.04.031

Maretina, M. A., Zheleznyakova, G. Y., Lanko, K. M., Egorova, A. A., Baranov, V. S., & Kiselev, A. V. (2018). Molecular Factors Involved in Spinal Muscular Atrophy Pathways as Possible Disease-modifying Candidates. *Current Genomics*, *19*(5), 339–355. https://doi.org/10.2174/1389202919666180101154916

Markus, A., Patel, T. D., & Snider, W. D. (2002). Neurotrophic factors and axonal growth. *Current Opinion in Neurobiology*, *12*(5), 523–531. https://doi.org/10.1016/S0959-4388(02)00372-0

Marshall, C. J. (1995). Specificity of receptor tyrosine kinase signaling: transient versus sustained extracellular signal-regulated kinase activation. *Cell*, *80*(2), 179–185.

https://doi.org/10.1016/0092-8674(95)90401-8

Martínez-Hernández, R., Soler-Botija, C., Also, E., Alias, L., Caselles, L., Gich, I., Bernal, S., & Tizzano, E. F. (2009). The developmental pattern of myotubes in spinal muscular atrophy indicates prenatal delay of muscle maturation. *Journal of Neuropathology and Experimental Neurology*, *68*(5), 474–481. https://doi.org/10.1097/NEN.0B013E3181A10EA1

Matera, A. G., & Wang, Z. (2014). A day in the life of the spliceosome. *Nature Reviews. Molecular Cell Biology*, *15*(2), 108–121. https://doi.org/10.1038/NRM3742

Mcgivern, J. V., Patitucci, T. N., Nord, J. A., Barabas, M. E. A., Stucky, C. L., & Ebert, A. D. (2013). Spinal muscular atrophy astrocytes exhibit abnormal calcium regulation and reduced growth factor production. *Glia*, *61*(9), 1418–1428. https://doi.org/10.1002/GLIA.22522

Mcgovern, V. L., Gavrilina, T. O., Beattie, C. E., & Burghes, A. H. M. (2008). Embryonic motor axon development in the severe SMA mouse. *Human Molecular Genetics*, *17*(18), 2900–2909. https://doi.org/10.1093/HMG/DDN189

McWhorter, M. L., Monani, U. R., Burghes, A. H. M. M., & Beattie, C. E. (2003). Knockdown of the survival motor neuron (Smn) protein in zebrafish causes defects in motor axon outgrowth and pathfinding. *Journal of Cell Biology*, *162*(5), 919–931. https://doi.org/10.1083/jcb.200303168

Melick, C. H., & Jewell, J. L. (2020). Regulation of mTORC1 by Upstream Stimuli. *Genes*, *11*(9), 1–28. https://doi.org/10.3390/genes11090989

Melki, J., Lefebvre, S., Burglen, L., Burlet, P., Clermont, O., Millasseau, P., Reboullet, S., Bénichou, B., Zeviani, M., Le Paslier, D., Cohen, D., Weissenbach, J., & Munnich, A. (1994). De novo and inherited deletions of the 5q13 region in spinal muscular atrophies. *Science*, *264*(5164), 1474–1477. https://doi.org/10.1126/science.7910982

Melki, J., Sheth, P., Abdelhak, S., Burlet, P., Bachelot, M. F., Frézal, J., Munnich, A., & Lathrop, M. G. (1990). Mapping of acute (type I) spinal muscular atrophy to chromosome 5q12-q14. *The Lancet*, *336*(8710), 271–273. https://doi.org/10.1016/0140-6736(90)91803-I

Mentis, G. Z., Blivis, D., Liu, W., Drobac, E., Crowder, M. E., Kong, L., Alvarez, F. J., Sumner, C. J., & O'Donovan, M. J. (2011). Early functional impairment of sensory-motor connectivity in a mouse model of spinal muscular atrophy. *Neuron*, *69*(3), 453–467. https://doi.org/10.1016/J.NEURON.2010.12.032

Menzies, F. M., Fleming, A., & Rubinsztein, D. C. (2015). Compromised autophagy and neurodegenerative diseases. *Nature Reviews Neuroscience 2015 16:6*, *16*(6), 345–357. https://doi.org/10.1038/nrn3961

Mercuri, E., Deconinck, N., Mazzone, E. S., Nascimento, A., Oskoui, M., Saito, K., Vuillerot, C., Baranello, G., Boespflug-Tanguy, O., Goemans, N., Kirschner, J., Kostera-Pruszczyk, A., Servais, L., Gerber, M., Gorni, K., Khwaja, O., Kletzl, H., Scalco, R. S., Staunton, H., … Dunaway Young, S. (2022). Safety and efficacy of once-daily risdiplam in type 2 and non-ambulant type 3 spinal muscular atrophy (SUNFISH part 2): a phase 3, double-blind, randomised, placebo-controlled trial. *The Lancet. Neurology*, *21*(1), 42–52. https://doi.org/10.1016/S1474-4422(21)00367-7

Mercuri, E., Finkel, R., Montes, J., Mazzone, E. S., Sormani, M. P., Main, M., Ramsey, D., Mayhew, A., Glanzman, A. M., Dunaway, S., Salazar, R., Pasternak, A., Quigley, J., Pane, M., Pera, M. C., Scoto, M., Messina, S., Sframeli, M., Vita, G. L., … de Vivo, D. C. (2016). Patterns of disease progression in type 2 and 3 SMA: Implications for clinical trials. In *Neuromuscular Disorders* (Vol. 26, Issue 2, pp. 126–131). https://doi.org/10.1016/j.nmd.2015.10.006

Mercuri, E., Finkel, R. S., Muntoni, F., Wirth, B., Montes, J., Main, M., Mazzone, E., Vitale, M., Snyder, B., Quijano-Roy, S., Bertini, E., Davis, R. H., Meyer, O. H., Simonds, A. K., Schroth, M. K., Graham, R. J., Kirschner, J., Iannaccone, S. T., Crawford, T., … Szlagatys-Sidorkiewicz, A. (2018). Diagnosis and management of spinal muscular atrophy: Part 1: Recommendations for diagnosis, rehabilitation, orthopedic and nutritional care. *Neuromuscular Disorders*, *28*(2), 103–115. https://doi.org/10.1016/j.nmd.2017.11.005

Merenmies, J., & Rauvala, H. (1990). Molecular cloning of the 18-kDa growth-associated protein of developing brain. *Journal of Biological Chemistry*, *265*(28), 16721–16724. https://doi.org/10.1016/S0021-9258(17)44817-4

Messina, S., & Sframeli, M. (2020). New treatments in spinal muscular atrophy: Positive results and new challenges. *Journal of Clinical Medicine*, *9*(7), 1–16. https://doi.org/10.3390/jcm9072222

Messina, S., Sframeli, M., Maggi, L., D'Amico, A., Bruno, C., Comi, G., & Mercuri, E. (2021). Spinal muscular atrophy: state of the art and new therapeutic strategies. *Neurological Sciences*. https://doi.org/10.1007/s10072-021-05258-3

Meyer, K., Ferraiuolo, L., Schmelzer, L., Braun, L., McGovern, V., Likhite, S., Michels, O., Govoni, A., Fitzgerald, J., Morales, P., Foust, K. D., Mendell, J. R., Burghes, A. H. M., & Kaspar, B. K. (2015). Improving single injection CSF delivery of AAV9-mediated gene therapy for SMA: a dose-response study in mice and nonhuman primates. *Molecular Therapy : The Journal of the American Society of Gene Therapy*, *23*(3), 477–487. https://doi.org/10.1038/MT.2014.210

Michaud, M., Arnoux, T., Bielli, S., Durand, E., Rotrou, Y., Jablonka, S., Robert, F., Giraudon-Paoli, M., Riessland, M., Mattei, M. G., Andriambeloson, E., Wirth, B., Sendtner, M., Gallego, J., Pruss, R. M., & Bordet, T. (2010). Neuromuscular defects and breathing disorders in a new mouse model of spinal muscular atrophy. *Neurobiology of Disease*, *38*(1), 125–135. https://doi.org/10.1016/J.NBD.2010.01.006

Micheau, O., Boveresses, C., & Epalinges, C.-. (2003). *Induction of TNF Receptor I-Mediated Apoptosis via Two Sequential Signaling Complexes*. *114*, 181–190.

Middleton, G., Hamanoue, M., Enokido, Y., Wyatt, S., Pennica, D., Jaffray, E., Hay, R. T., & Davies, A. M. (2000). Cytokine-induced nuclear factor kappa B activation promotes the survival of developing neurons. *The Journal of Cell Biology*, *148*(2), 325–

332. https://doi.org/10.1083/JCB.148.2.325

Miguel-Aliaga, I., Chan, Y. B., Davies, K. E., & Van Den Heuvel, M. (2000). Disruption of SMN function by ectopic expression of the human SMN gene in Drosophila. *FEBS Letters*, *486*(2), 99–102. https://doi.org/10.1016/S0014-5793(00)02243-2

Milbrandt, J., De Sauvage, F. J., Fahrner, T. J., Baloh, R. H., Leitner, M. L., Tansey, M. G., Lampe, P. A., Heuckeroth, R. O., Kotzbauer, P. T., Simburger, K. S., Golden, J. P., Davies, J. A., Vejsada, R., Kato, A. C., Hynes, M., Sherman, D., Nishimura, M., Wang, L. C., Vandlen, R., … Johnson, E. M. (1998). Persephin, a novel neurotrophic factor related to GDNF and neurturin. *Neuron*, *20*(2), 245–253. https://doi.org/10.1016/S0896-6273(00)80453-5

Millino, C., Fanin, M., Vettori, A., Laveder, P., Mostacciuolo, M., Angelini, C., & Lanfranchi, G. (2009). Different atrophy-hypertrophy transcription pathways in muscles affected by severe and mild spinal muscular atrophy. *BMC Medicine*, *7*. https://doi.org/10.1186/1741-7015-7-14

Milnerwood, A. J., Gladding, C. M., Pouladi, M. A., Kaufman, A. M., Hines, R. M., Boyd, J. D., Ko, R. W. Y., Vasuta, O. C., Graham, R. K., Hayden, M. R., Murphy, T. H., & Raymond, L. A. (2010). Early Increase in Extrasynaptic NMDA Receptor Signaling and Expression Contributes to Phenotype Onset in Huntington's Disease Mice. *Neuron*, *65*(2), 178–190. https://doi.org/10.1016/J.NEURON.2010.01.008

Mincheva, S., Garcera, A., Gou-Fabregas, M., Encinas, M., Dolcet, X., & Soler, R. M. (2011). The canonical nuclear factor-κB pathway regulates cell survival in a developmental model of spinal cord motoneurons. *Journal of Neuroscience*, *31*(17), 6493–6503. https://doi.org/10.1523/JNEUROSCI.0206-11.2011

Mizushima, N., Levine, B., Cuervo, A. M., & Klionsky, D. J. (2008). Autophagy fights disease through cellular self-digestion. *Nature 2008 451:7182*, *451*(7182), 1069–1075. https://doi.org/10.1038/nature06639

Mohseni, R., Ali Hamidieh, A., Shoae-Hassani, A., Ghahvechi-Akbari, M., Majma, A., Mohammadi, M., Nikougoftar, M., Shervin-Badv, R., Ai, J., Montazerlotfelahi, H., Reza Ashrafi, M., Ali Hamidieh aahamidieh, A., & Reza Ashrafi ashrafim, M. (2022). An open-label phase 1 clinical trial of the allogeneic side population adipose-derived mesenchymal stem cells in SMA type 1 patients. *Neurological Sciences*. https://doi.org/10.1007/s10072-021-05291-2/Published

Monani, U. R. (2005). Spinal muscular atrophy: A deficiency in a ubiquitous protein; a motor neuron-specific disease. *Neuron*, *48*(6), 885–896. https://doi.org/10.1016/j.neuron.2005.12.001

Monani, U. R., Coovert, D. D., & Burghes, a H. (2000). Animal models of spinal muscular atrophy. *Human Molecular Genetics*, *9*(16), 2451–2457. https://doi.org/10.1177/0883073807305667

Monani, U. R., & De Vivo, D. C. (2014). Neurodegeneration in spinal muscular atrophy: From disease phenotype and animal models to therapeutic strategies and beyond. *Future Neurology*, *9*(1), 49–65. https://www.futuremedicine.com/doi/full/10.2217/fnl.13.58

Monani, U. R., Sendtner, M., Coovert, D. D., Parsons, D. W., Andreassi, C., Le, T. T., Jablonka, S., Schrank, B., Rossoll, W., Prior, T. W., Morris, G. E., & Burghes, a H. (2000). The human centromeric survival motor neuron gene (SMN2) rescues embryonic lethality in Smn(-/-) mice and results in a mouse with spinal muscular atrophy. *Human Molecular Genetics*, *9*(3), 333–339. https://doi.org/10.1093/hmg/ddm236

Montague, K., Malik, B., Gray, A. L., La Spada, A. R., Hanna, M. G., Szabadkai, G., & Greensmith, L. (2014). Endoplasmic reticulum stress in spinal and bulbar muscular atrophy: a potential target for therapy. *Brain : A Journal of Neurology*, *137*(Pt 7), 1894–1906. https://doi.org/10.1093/BRAIN/AWU114

Moubarak, R. S., Planells-Ferrer, L., Urresti, J., Reix, S., Segura, M. F., Carriba, P., Marqués-Fernàndez, F., Sole, C., Llecha-Cano, N., Lopez-Soriano, J., Sanchis, D., Yuste, V. J., & Comella, J. X. (2013). FAIM-L Is an IAP-Binding Protein That Inhibits XIAP Ubiquitinylation and Protects from Fas-Induced Apoptosis. *Journal of Neuroscience*, *33*(49), 19262–19275. https://doi.org/10.1523/JNEUROSCI.2479-13.2013

Müller, L. U., Daley, G. Q., & Williams, D. A. (2009). Upping the Ante: Recent Advances in Direct Reprogramming. *The American Society of Gene Therapy*. https://doi.org/10.1038/mt.2009.72

Murray, B., Alessandrini, A., Cole, A. J., Yee, A. G., & Furshpan, E. J. (1998). Inhibition of the p44/42 MAP kinase pathway protectshippocampal neurons in a cell-culture model of seizure activity. *Proceedings of the National Academy of Sciences of the United States of America*, *95*(20), 11975. https://doi.org/10.1073/PNAS.95.20.11975

Murray, L. M., Comley, L. H., Thomson, D., Parkinson, N., Talbot, K., & Gillingwater, T. H. (2008). Selective vulnerability of motor neurons and dissociation of pre- and post-synaptic pathology at the neuromuscular junction in mouse models of spinal muscular atrophy. *Human Molecular Genetics*, *17*(7), 949–962. https://doi.org/10.1093/hmg/ddm367

Mutsaers, C. A., Wishart, T. M., Lamont, D. J., Riessland, M., Schreml, J., Comley, L. H., Murray, L. M., Parson, S. H., Lochmüller, H., Wirth, B., Talbot, K., & Gillingwater, T. H. (2011). Reversible molecular pathology of skeletal muscle in spinal muscular atrophy. *Human Molecular Genetics*, *20*(22), 4334–4344. https://doi.org/10.1093/HMG/DDR360

Nakamura, T., & Mizuno, S. (2010). The discovery of hepatocyte growth factor (HGF) and its significance for cell biology, life sciences and clinical medicine. *Proceedings of the Japan Academy. Series B, Physical and Biological Sciences*, *86*(6), 588–610. https://doi.org/10.2183/PJAB.86.588

Nakamura, T., Nawa, K., & Ichihara, A. (1984). Partial purification and characterization of hepatocyte growth factor from serum of hepatectomized rats.

Biochemical and Biophysical Research Communications, *122*(3), 1450–1459. https://doi.org/10.1016/0006-291X(84)91253-1

Nand Rai, S., Dilnashin, H., Birla, H., Sen Singh, S., Zahra, W., Singh Rathore, A., Kumar Singh, B., & Pratap Singh, S. (2019). The Role of PI3K/Akt and ERK in Neurodegenerative Disorders. *Neurotoxicity Research*. https://doi.org/10.1007/s12640-019-0003-y

Nascimbeni, A. C., Codogno, P., & Morel, E. (2017). Phosphatidylinositol-3-phosphate in the regulation of autophagy membrane dynamics. *The FEBS Journal*, *284*(9), 1267–1278. https://doi.org/10.1111/FEBS.13987

Nguyen, N., Lee, S. B., Lee, Y. S., Lee, K. H., & Ahn, J. Y. (2009). Neuroprotection by NGF and BDNF against neurotoxin-exerted apoptotic death in neural stem cells are mediated through TRK receptors, activating PI3-kinase and MAPK pathways. *Neurochemical Research*, *34*(5), 942–951. https://doi.org/10.1007/S11064-008-9848-9/FIGURES/4

Nichterwitz, S., Nijssen, J., Storvall, H., Schweingruber, C., Comley, L. H., Allodi, I., Van Der Lee, M., Deng, Q., Sandberg, R., & Hedlund, E. (2020). LCM-seq reveals unique transcriptional adaptation mechanisms of resistant neurons and identifies protective pathways in spinal muscular atrophy. *Genome Research*, *30*(8), 1083–1096. https://doi.org/10.1101/GR.265017.120/-/DC1

Nishimura, A. L., Mitne-Neto, M., Silva, H. C. A., Richieri-Costa, A., Middleton, S., Cascio, D., Kok, F., Oliveira, J. R. M., Gillingwater, T., Webb, J., Skehel, P., & Zatz, M. (2004). A mutation in the vesicle-trafficking protein VAPB causes late-onset spinal muscular atrophy and amyotrophic lateral sclerosis. *American Journal of Human Genetics*, *75*(5), 822–831. https://doi.org/10.1086/425287

Noda, T., & Ohsumi, Y. (1998). Tor, a Phosphatidylinositol Kinase Homologue, Controls Autophagy in Yeast *. *Journal of Biological Chemistry*, *273*(7), 3963–3966. https://doi.org/10.1074/JBC.273.7.3963

Nölle, A., Zeug, A., Van bergeijk, J., Tönges, L., Gerhard, R., Brinkmann, H., Al rayes, S., Hensel, N., Schill, Y., Apkhazava, D., Jablonka, S., O'mer, J., Kumar srivastav, R., Baasner, A., Lingor, P., Wirth, B., Ponimaskin, E., Niedenthal, R., Grothe, C., & Claus, P. (2011). The spinal muscular atrophy disease protein SMN is linked to the rho-kinase pathway via profilin. *Human Molecular Genetics*, *20*(24), 4865–4878. https://doi.org/10.1093/HMG/DDR425

Obexer, P., Ausserlechner, M. J., & Suzuki-Karasaki, Y. (2014). X-linked inhibitor of apoptosis protein – a critical death resistance regulator and therapeutic target for personalized cancer therapy. *Frontiers in Oncology*. https://doi.org/10.3389/fonc.2014.00197

Oliván, S., Calvo, A. C., Rando, A., Herrando-Grabulosa, M., Manzano, R., Zaragoza, P., Tizzano, E. F., Aquilera, J., & Osta, R. (2016). Neuroprotective Effect of Non-viral Gene Therapy Treatment Based on Tetanus Toxin C-fragment in a Severe Mouse Model of Spinal Muscular Atrophy. *Frontiers in Molecular Neuroscience*, *9*(AUG). https://doi.org/10.3389/FNMOL.2016.00076

Oppenheim, R. W. (1989). The neurotrophic theory and naturally occurring motoneuron death. *Trends in Neurosciences*, *12*(7), 252–255. https://doi.org/10.1016/0166-2236(89)90021-0

Oppenheim, R. W., Prevette, D., Qin-Wei, Y., Collins, F., & MacDonald, J. (1991). Control of embryonic motoneuron survival in vivo by ciliary neurotrophic factor. *Science*, *251*(5001), 1616–1618. https://doi.org/10.1126/science.2011743

Oprea, G. E., Kröber, S., McWhorter, M. L., Rossoll, W., Müller, S., Krawczak, M., Bassell, G. J., Beattie, C. E., & Wirth, B. (2008). Plastin 3 Is a Protective Modifier of Autosomal Recessive Spinal Muscular Atrophy. *Science (New York, N.Y.)*, *320*(5875), 524. https://doi.org/10.1126/SCIENCE.1155085

Otomo, C., Metlagel, Z., Takaesu, G., & Otomo, T. (2012). Structure of the human ATG12~ATG5 conjugate required for LC3 lipidation in autophagy. *Nature Structural & Molecular Biology 2012 20:1*, *20*(1), 59–66. https://doi.org/10.1038/nsmb.2431

Ottesen, E. W., Howell, M. D., Singh, N. N., Seo, J., Whitley, E. M., & Singh, R. N. (2016). Severe impairment of male reproductive organ development in a low SMN expressing mouse model of spinal muscular atrophy. *Scientific Reports 2016 6:1*, *6*(1), 1–17. https://doi.org/10.1038/srep20193

Owen, N., Doe, C. L., Mellor, J., & Davies, K. E. (2000). Characterization of the Schizosaccharomyces pombe orthologue of the human survival motor neuron (SMN) protein. *Human Molecular Genetics*, *9*(5), 675–684. https://doi.org/10.1093/HMG/9.5.675

Ozes, O. N., Mayo, L. D., Gustin, J. A., Pfeffer, S. R., Pfeffer, L. M., & Donner, D. B. (1999). NF-kappaB activation by tumour necrosis factor requires the Akt serine-threonine kinase. *Nature*, *401*(6748), 82–85. https://doi.org/10.1038/43466

Pagliardini, S., Giavazzi, A., Setola, V., Lizier, C., Di Luca, M., DeBiasi, S., & Battaglia, G. (2000). Subcellular localization and axonal transport of the survival motor neuron (SMN) protein in the developing rat spinal cord. *Human Molecular Genetics*, *9*(1), 47–56. https://doi.org/10.1093/HMG/9.1.47

Palacino, J., Swalley, S. E., Song, C., Cheung, A. K., Shu, L., Zhang, X., Van Hoosear, M., Shin, Y., Chin, D. N., Keller, C. G., Beibel, M., Renaud, N. A., Smith, T. M., Salcius, M., Shi, X., Hild, M., Servais, R., Jain, M., Deng, L., … Sivasankaran, R. (2015). SMN2 splice modulators enhance U1-pre-mRNA association and rescue SMA mice. *Nature Chemical Biology*, *11*(7), 511–517. https://doi.org/10.1038/nchembio.1837

Papadimitriou, D., Le Verche, V., Jacquier, A., Ikiz, B., Przedborski, S., & Re, D. B. (2010). Inflammation in ALS and SMA: sorting out the good from the evil. *Neurobiology of Disease*. https://doi.org/10.1016/j.nbd.2009.10.005

Parente, V., & Corti, S. (2018). Advances in spinal muscular atrophy therapeutics. *Therapeutic Advances in Neurological Disorders*, *11*. https://doi.org/10.1177/1756285618754501

Park, G. H., Kariya, S., & Monani, U. R. (2010). Spinal Muscular Atrophy: New and Emerging Insights from Model Mice. *Current Neurology and*

Neuroscience Reports, *10*(2), 108. https://doi.org/10.1007/S11910-010-0095-5

Parker, G. C., Li, X., Anguelov, R. A., Toth, G., Cristescu, A., & Acsadi, G. (2008). Survival motor Neuron protein regulates apoptosis in anin vitro model of Spinal muscular atrophy. *Neurotoxicity Research*, *13*(1), 39–48. https://doi.org/10.1007/BF03033366

Parzych, K. R., & Klionsky, D. J. (2014). An Overview of Autophagy: Morphology, Mechanism, and Regulation. *Antioxidants & Redox Signaling*. https://doi.org/10.1089/ars.2013.5371

Passini, M. A., Bu, J., Richards, A. M., Treleaven, C. M., Sullivan, J. A., O'Riordan, C. R., Scaria, A., Kells, A. P., Samaranch, L., San Sebastian, W., Federici, T., Fiandaca, M. S., Boulis, N. M., Bankiewicz, K. S., Shihabuddin, L. S., & Cheng, S. H. (2015). Translational fidelity of intrathecal delivery of self-complementary AAV9-survival motor neuron 1 for spinal muscular atrophy. *Human Gene Therapy*, *113178*(303), 1–48. https://doi.org/10.1089/HUM.2014.011

Patapoutian, A., & Reichardt, L. F. (2001). Trk receptors: mediators of neurotrophin action. *Current Opinion in Neurobiology*, *11*(3), 272–280. https://doi.org/10.1016/S0959-4388(00)00208-7

Pattingre, S., Tassa, A., Qu, X., Garuti, R., Xiao, H. L., Mizushima, N., Packer, M., Schneider, M. D., & Levine, B. (2005). Bcl-2 Antiapoptotic Proteins Inhibit Beclin 1-Dependent Autophagy. *Cell*, *122*(6), 927–939. https://doi.org/10.1016/J.CELL.2005.07.002

Paushkin, S., Charroux, B., Abel, L., Perkinson, R. A., Pellizzoni, L., & Dreyfuss, G. (2000). The Survival Motor Neuron Protein of Schizosacharomyces pombe: CONSERVATION OF SURVIVAL MOTOR NEURON INTERACTION DOMAINS IN DIVERGENT ORGANISMS. *Journal of Biological Chemistry*, *275*(31), 23841–23846. https://doi.org/10.1074/JBC.M001441200

Pellizzoni, L., Baccon, J., Charroux, B., & Dreyfuss, G. (2001). The survival of motor neurons (SMN) protein interacts with the snoRNP proteins fibrillarin and GAR1. *Current Biology : CB*, *11*(14), 1079–1088. https://doi.org/10.1016/S0960-9822(01)00316-5

Pellizzoni, L., Charroux, B., & Dreyfuss, G. (1999). SMN mutants of spinal muscular atrophy patients are defective in binding to snRNP proteins. *Proceedings of the National Academy of Sciences of the United States of America*, *96*(20), 11167–11172. https://doi.org/10.1073/PNAS.96.20.11167

Pellizzoni, L., Charroux, B., Rappsilber, J., Mann, M., & Dreyfuss, G. (2001). A functional interaction between the survival motor neuron complex and RNA polymerase II. *J Cell Biol*, *152*(1), 75–85. https://doi.org/10.1083/jcb.152.1.75

Pérez-García, M. J., Ceña, V., De Pablo, Y., Llovera, M., Comella, J. X., & Soler, R. M. (2004). Glial Cell Line-derived Neurotrophic Factor Increases Intracellular Calcium Concentration: ROLE OF CALCIUM/CALMODULIN IN THE ACTIVATION OF THE PHOSPHATIDYLINOSITOL 3-KINASE PATHWAY *. *Journal of Biological Chemistry*, *279*(7), 6132–6142. https://doi.org/10.1074/JBC.M308367200

Pérez-García, M. J., Gou-Fabregas, M., De Pablo, Y., Llovera, M., Comella, J. X., & Soler, R. M. (2008). Neuroprotection by neurotrophic factors and membrane depolarization is regulated by calmodulin kinase IV. *The Journal of Biological Chemistry*, *283*(7), 4133–4144. https://doi.org/10.1074/JBC.M705477200

Periyakaruppiah, A. (2015). *Study of Survival Motor Neuron protein regulation and the role of autophagy in Spinal Muscular Atrophy* [Universitat de Lleida]. http://hdl.handle.net/10803/296677

Periyakaruppiah, A., de la Fuente, S., Arumugam, S., Bahí, N., Garcera, A., & Soler, R. M. (2016). Autophagy modulators regulate survival motor neuron protein stability in motoneurons. *Experimental Neurology*, *283*, 287–297. https://doi.org/10.1016/j.expneurol.2016.06.032

Peter, C. J., Evans, M., Thayanithy, V., Taniguchi-Ishigaki, N., Bach, I., Kolpak, A., Bassell, G. J., Rossoll, W., Lorson, C. L., Bao, Z. Z., & Androphy, E. J. (2011). The COPI vesicle complex binds and moves with survival motor neuron within axons. *Human Molecular Genetics*, *20*(9), 1701–1711. https://doi.org/10.1093/HMG/DDR046

Piepers, S., Van Den Berg, L. H., Brugman, F., Scheffer, H., Ruiterkamp-Versteeg, M., Van Engelen, B. G., Faber, C. G., De Visser, M., Van Der Pol, W. L., & Wokke, J. H. J. (2008). A natural history study of late onset spinal muscular atrophy types 3b and 4. *Journal of Neurology*, *255*(9), 1400–1404. https://doi.org/10.1007/s00415-008-0929-0

Piras, A., Schiaffino, L., Boido, M., Valsecchi, V., Guglielmotto, M., De Amicis, E., Puyal, J., Garcera, A., Tamagno, E., Soler, R. M., & Vercelli, A. (2017). Inhibition of autophagy delays motoneuron degeneration and extends lifespan in a mouse model of spinal muscular atrophy. *Cell Death and Disease*, *8*(12). https://doi.org/10.1038/s41419-017-0086-4

Planells-Ferrer, L., Urresti, J., Coccia, E., Galenkamp, K. M. O., Calleja-Yagüe, I., López-Soriano, J., Carriba, P., Barneda-Zahonero, B., Segura, M. F., & Comella, J. X. (2016). Fas apoptosis inhibitory molecules: more than death-receptor antagonists in the nervous system. *Journal of Neurochemistry*, *139*(1), 11–21. https://doi.org/10.1111/JNC.13729

Poruk, K. E., Davis, R. H., Smart, A. L., Chisum, B. S., LaSalle, B. A., Chan, G. M., Gill, G., Reyna, S. P., & Swoboda, K. J. (2012). Observational study of caloric and nutrient intake, bone density, and body composition in infants and children with Spinal Muscular Atrophy type I. *Neuromuscular Disorders : NMD*, *22*(11), 966. https://doi.org/10.1016/J.NMD.2012.04.008

Powe, C. E., Allen, M., Puopolo, K. M., Merewood, A., Worden, S., Johnson, L. C., Fleischman, A., & Welt, C. K. (2010). Recombinant human prolactin for the treatment of lactation insufficiency. *Clinical Endocrinology*, *73*(5), 645–653. https://doi.org/10.1111/J.1365-2265.2010.03850.X

Press, C., & Milbrandt, J. (2008). Nmnat delays axonal degeneration caused by mitochondrial and oxidative stress. *Journal of Neuroscience*, *28*(19), 4861–4871.

https://doi.org/10.1523/JNEUROSCI.0525-08.2008

Price, J. M., Donahoe, P. K., Ito, Y., & Hendren, W. H. (1977). Programmed cell death in the Müllerian duct induced by Müllerian inhibiting substance. *The American Journal of Anatomy*, *149*(3), 353–375. https://doi.org/10.1002/AJA.1001490304

Prior, T. W., Krainer, A. R., Hua, Y., Swoboda, K. J., Snyder, P. C., Bridgeman, S. J., Burghes, A. H. M., & Kissel, J. T. (2009). A Positive Modifier of Spinal Muscular Atrophy in the SMN2 Gene. In *American Journal of Human Genetics* (Vol. 85, Issue 3, pp. 408–413). https://doi.org/10.1016/j.ajhg.2009.08.002

Pugazhenthit, S., Nesterova, A., Sable, C., Heidenreich, K. A., Boxer, L. M., Heasley, L. E., & Reusch, J. E. B. (2000). Akt/protein kinase B up-regulates Bcl-2 expression through cAMP-response element-binding protein. *The Journal of Biological Chemistry*, *275*(15), 10761–10766. https://doi.org/10.1074/JBC.275.15.10761

Purves, D., Augustine, G. ., Fitzpatrick, D., Katz, L. C., Anthony-Samuel, L., McNamara, J. O., & Williams, S. M. (2003). *Neurosciences*. Sinauer Associates Oxford University Press.

Qin, S., Yang, C., Zhang, B., Li, X., Sun, X. I. N., & Li, G. (2016). *XIAP inhibits mature Smac-induced apoptosis by degrading it through ubiquitination in NSCLC*. 1289–1296. https://doi.org/10.3892/ijo.2016.3634

Ragagnin, A. M. G., Shadfar, S., Vidal, M., Jamali, M. S., & Atkin, J. D. (2019). Motor neuron susceptibility in ALS/FTD. *Frontiers in Neuroscience*, *13*(JUN). https://doi.org/10.3389/FNINS.2019.00532/FULL

Rage, F., Boulisfane, N., Rihan, K., Neel, H., Gostan, T., Bertrand, E., Bordonné, R., & Soret, A. (2013). Genome-wide identification of mRNAs associated with the protein SMN whose depletion decreases their axonal localization. *Rna*, *19*(12), 1755–1766. https://doi.org/10.1261/rna.040204.113

Rajendra, T. K., Gonsalvez, G. B., Walker, M. P., Shpargel, K. B., Salz, H. K., & Matera, A. G. (2007). A Drosophila melanogaster model of spinal muscular atrophy reveals a function for SMN in striated muscle. *Journal of Cell Biology*, *176*(6), 831–841. https://doi.org/10.1083/jcb.200610053

Rao, V. K., Kapp, D., & Schroth, M. (2018). Gene therapy for spinal muscular atrophy: An emerging treatment option for a devastating disease. *Journal of Managed Care and Specialty Pharmacy*, *24*, S3–S16. https://doi.org/10.18553/JMCP.2018.24.12-A.S3/ASSET/IMAGES/SMALL/FIG4.GIF

Rashnonejad, A., Gündüz, C., Süslüer, S. Y., Onay, H., Durmaz, B., Bandehpour, M., & Özkinay, F. (2016). In vitro gene manipulation of spinal muscular atrophy fibroblast cell line using gene-targeting fragment for restoration of SMN protein expression. *Gene Therapy*, *23*(1), 10–17. https://doi.org/10.1038/gt.2015.92

Ratni, H., Ebeling, M., Baird, J., Bendels, S., Bylund, J., Chen, K. S., Denk, N., Feng, Z., Green, L., Guerard, M., Jablonski, P., Jacobsen, B., Khwaja, O., Kletzl, H., Ko, C. P., Kustermann, S., Marquet, A., Metzger, F., Mueller, B., … Mueller, L. (2018). Discovery of Risdiplam, a Selective Survival of Motor Neuron-2 (SMN2) Gene Splicing Modifier for the Treatment of Spinal Muscular Atrophy (SMA). *Journal of Medicinal Chemistry*, *61*(15), 6501–6517. https://doi.org/10.1021/acs.jmedchem.8b00741

Ratovitski, T., Nakamura, M., D'Ambola, J., Chighladze, E., Liang, Y., Wang, W., Graham, R., Hayden, M. R., Borchelt, D. R., Hirschhorn, R. R., & Ross, C. A. (2007). N-Terminal Proteolysis of Full-Length Mutant Huntingtin in an Inducible PC12 Cell Model of Huntington's Disease. *Http://Dx.Doi.Org/10.4161/Cc.6.23.4992*, *6*(23), 2970–2981. https://doi.org/10.4161/CC.6.23.4992

Ravanan, P., Srikumar, I. F., & Talwar, P. (2017). Autophagy: The spotlight for cellular stress responses. *Life Sciences*, *188*, 53–67. https://doi.org/10.1016/J.LFS.2017.08.029

Ravikumar, B., Duden, R., & Rubinsztein, D. C. (2002). Aggregate-prone proteins with polyglutamine and polyalanine expansions are degraded by autophagy. *Human Molecular Genetics*, *11*(9), 1107–1117. https://doi.org/10.1093/HMG/11.9.1107

Ravikumar, B., Vacher, C., Berger, Z., Davies, J. E., Luo, S., Oroz, L. G., Scaravilli, F., Easton, D. F., Duden, R., O'Kane, C. J., & Rubinsztein, D. C. (2004). Inhibition of mTOR induces autophagy and reduces toxicity of polyglutamine expansions in fly and mouse models of Huntington disease. *Nature Genetics 2004 36:6*, *36*(6), 585–595. https://doi.org/10.1038/ng1362

Regan, R. F., & Choi, D. W. (1991). Glutamate neurotoxicity in spinal cord cell culture. *Neuroscience*, *43*(2–3), 585–591. https://doi.org/10.1016/0306-4522(91)90317-H

Rehorst, W. A., Thelen, M. P., Nolte, H., Türk, C., Cirak, S., Peterson, J. M., Wong, G. W., Wirth, B., Krüger, M., Winter, D., & Kye, M. J. (2019). Muscle regulates mTOR dependent axonal local translation in motor neurons via CTRP3 secretion: implications for a neuromuscular disorder, spinal muscular atrophy. *Acta Neuropathologica Communications*, *7*(1). https://doi.org/10.1186/S40478-019-0806-3

Reiner, A., Medina, L., Figueredo-Cardenas, G., & Anfinson, S. (1995). Brainstem motoneuron pools that are selectively resistant in amyotrophic lateral sclerosis are preferentially enriched in parvalbumin: evidence from monkey brainstem for a calcium-mediated mechanism in sporadic ALS. *Experimental Neurology*, *131*(2), 239–250. https://doi.org/10.1016/0014-4886(95)90046-2

Reynolds IV, T. H., Bodine, S. C., & Lawrence, J. C. (2002). Control of Ser2448 phosphorylation in the mammalian target of rapamycin by insulin and skeletal muscle load. *The Journal of Biological Chemistry*, *277*(20), 17657–17662. https://doi.org/10.1074/JBC.M201142200

Riessland, M., Kaczmarek, A., Schneider, S., Swoboda, K. J., Löhr, H., Bradler, C., Grysko, V., Dimitriadi, M., Hosseinibarkooie, S., Torres-Benito, L., Peters, M., Upadhyay, A., Biglari, N., Kröber, S., Hölker, I., Garbes, L., Gilissen, C., Hoischen, A., Nürnberg, G.,

… Wirth, B. (2017). Neurocalcin Delta Suppression Protects against Spinal Muscular Atrophy in Humans and across Species by Restoring Impaired Endocytosis. In *American Journal of Human Genetics* (Vol. 100, Issue 2, pp. 297–315). https://doi.org/10.1016/j.ajhg.2017.01.005

Righi, M., Tongiorgi, E., & Cattaneo, A. (2000). Brain-derived neurotrophic factor (BDNF) induces dendritic targeting of BDNF and tyrosine kinase B mRNAs in hippocampal neurons through a phosphatidylinositol-3 kinase-dependent pathway. *The Journal of Neuroscience : The Official Journal of the Society for Neuroscience*, *20*(9), 3165–3174. https://doi.org/10.1523/JNEUROSCI.20-09-03165.2000

Rindt, H., Feng, Z., Mazzasette, C., Glascock, J. J., Valdivia, D., Pyles, N., Crawford, T. O., Swoboda, K. J., Patitucci, T. N., Ebert, A. D., Sumner, C. J., Ko, C. P., & Lorson, C. L. (2015). Astrocytes influence the severity of spinal muscular atrophy. *Human Molecular Genetics*, *24*(14), 4094–4102. https://doi.org/10.1093/HMG/DDV148

Ripolone, M., Ronchi, D., Violano, R., Vallejo, D., Fagiolari, G., Barca, E., Lucchini, V., Colombo, I., Villa, L., Berardinelli, A., Balottin, U., Morandi, L., Mora, M., Bordoni, A., Fortunato, F., Corti, S., Parisi, D., Toscano, A., Sciacco, M., … Moggio, M. (2015). Impaired Muscle Mitochondrial Biogenesis and Myogenesis in Spinal Muscular Atrophy. *JAMA Neurology*, *72*(6), 666–675. https://doi.org/10.1001/JAMANEUROL.2015.0178

Risson, V., Mazelin, L., Roceri, M., Sanchez, H., Moncollin, V., Corneloup, C., Richard-Bulteau, H., Vignaud, A., Baas, D., Defour, A., Freyssenet, D., Tanti, J. F., Le-Marchand-Brustel, Y., Ferrier, B., Conjard-Duplany, A., Romanino, K., Bauché, S., Hantaï, D., Mueller, M., … Gangloff, Y. G. (2009). Muscle inactivation of mTOR causes metabolic and dystrophin defects leading to severe myopathy. *The Journal of Cell Biology*, *187*(6), 859. https://doi.org/10.1083/JCB.200903131

Rochette, C. F., Gilbert, N., & Simard, L. R. (2001). SMN gene duplication and the emergence of the SMN2 gene occurred in distinct hominids: SMN2 is unique to Homo sapiens. *Human Genetics*, *108*(3), 255–266. https://doi.org/10.1007/s004390100473

Rodriguez-Muela, N., Parkhitko, A., Grass, T., Gibbs, R. M., Norabuena, E. M., Perrimon, N., Singh, R., & Rubin, L. L. (2018). Blocking p62-dependent SMN degradation ameliorates spinal muscular atrophy disease phenotypes. *The Journal of Clinical Investigation*, *128*(7), 3008–3023. https://doi.org/10.1172/JCI95231

Rosenthal, A., Goeddel, D. V., Nguyen, T., Lewis, M., Shih, A., Laramee, G. R., Nikolics, K., & Winslow, J. W. (1990). Primary structure and biological activity of a novel human neurotrophic factor. *Neuron*, *4*(5), 767–773. https://doi.org/10.1016/0896-6273(90)90203-R

Rossoll, W., Jablonka, S., Andreassi, C., Kröning, A.-K. K., Karle, K., Monani, U. R., & Sendtner, M. (2003). Smn, the spinal muscular atrophy-determining gene product, modulates axon growth and localization of β-actin mRNA in growth cones of motoneurons. *Journal of Cell Biology*, *163*(4), 801–812. https://doi.org/10.1083/jcb.200304128

Roux, P. P., Ballif, B. A., Anjum, R., Gygi, S. P., & Blenis, J. (2004). Tumor-promoting phorbol esters and activated Ras inactivate the tuberous sclerosis tumor suppressor complex via p90 ribosomal S6 kinase. *Proceedings of the National Academy of Sciences of the United States of America*, *101*(37), 13489–13494. https://doi.org/10.1073/PNAS.0405659101/ASSET/6FD259C3-D3B9-40B1-B9B2-984DDB95C335/ASSETS/GRAPHIC/ZPQ0380460150006.JPEG

Roy, N., Mahadevan, M. S., McLean, M., Shutter, G., Yaraghi, Z., Farahani, R., Baird, S., Besner-Johnston, A., Lefebvre, C., Kang, X., Salih, M., Aubry, H., Tamai, K., Guan, X., Ioannou, P., Crawford, T. O., de Jong, P. J., Surh, L., Ikeda, J. E., … MacKenzie, A. (1995). The gene for neuronal apoptosis inhibitory protein is partially deleted in individuals with spinal muscular atrophy. *Cell*, *80*(1), 167–178. https://doi.org/10.1016/0092-8674(95)90461-1

Rubinsztein, D. C., Gestwicki, J. E., Murphy, L. O., & Klionsky, D. J. (2007). Potential therapeutic applications of autophagy. *Nature Reviews Drug Discovery 2007 6:4*, *6*(4), 304–312. https://doi.org/10.1038/nrd2272

Rudnicki, S. A., Andrews, J. A., Duong, T., Cockroft, B. M., Malik, F. I., Meng, L., Wei, J., Wolff, A. A., Genge, A., Johnson, N. E., Tesi-Rocha, C., Connolly, A. M., Darras, B. T., Felice, K., Shieh, P. B., Mah, J. K., Statland, J., Campbell, C., Habib, A. A., … Day, J. W. (2021). Reldesemtiv in Patients with Spinal Muscular Atrophy: a Phase 2 Hypothesis-Generating Study. *Neurotherapeutics : The Journal of the American Society for Experimental NeuroTherapeutics*, *18*(2), 1127–1136. https://doi.org/10.1007/S13311-020-01004-3

Rudnik-Schöneborn, S., Heller, R., Berg, C., Betzler, C., Grimm, T., Eggermann, T., Eggermann, K., Wirth, R., Wirth, B., & Zerres, K. (2008). Congenital heart disease is a feature of severe infantile spinal muscular atrophy. *Journal of Medical Genetics*, *45*(10), 635–638. https://doi.org/10.1136/JMG.2008.057950

Ruggiu, M., McGovern, V. L., Lotti, F., Saieva, L., Li, D. K., Kariya, S., Monani, U. R., Burghes, A. H. M., & Pellizzoni, L. (2012). A Role for SMN Exon 7 Splicing in the Selective Vulnerability of Motor Neurons in Spinal Muscular Atrophy. *Molecular and Cellular Biology*, *32*(1), 126–138. https://doi.org/10.1128/MCB.06077-11/SUPPL_FILE/MCB6077-11_SUP_LEGS.DOC

Ruiz, R., Casañas, J. J., Torres-Benito, L., Cano, R., & Tabares, L. (2010). Altered intracellular Ca2+ homeostasis in nerve terminals of severe spinal muscular atrophy mice. *The Journal of Neuroscience : The Official Journal of the Society for Neuroscience*, *30*(3), 849–857. https://doi.org/10.1523/JNEUROSCI.4496-09.2010

Russman, B. S. (2007). Spinal muscular atrophy: clinical classification and disease heterogeneity. *Journal of Child Neurology*, *22*(8), 946–951.

https://doi.org/10.1177/0883073807305673

Russo, C., Dolcini, V., Salis, S., Venezia, V., Violani, E., Carlo, P., Zambrano, N., Russo, T., & Schettini, G. (2002). Signal Transduction through Tyrosine-Phosphorylated Carboxy-Terminal Fragments of APP via an Enhanced Interaction with Shc/Grb2 Adaptor Proteins in Reactive Astrocytes of Alzheimer's Disease Brain. *Annals of the New York Academy of Sciences*, *973*(1), 323–333. https://doi.org/10.1111/J.1749-6632.2002.TB04660.X

Russo, R., Berliocchi, L., Adornetto, A., Varano, G. P., Cavaliere, F., Nucci, C., Rotiroti, D., Morrone, L. A., Bagetta, G., & Corasaniti, M. T. (2011). Calpain-mediated cleavage of Beclin-1 and autophagy deregulation following retinal ischemic injury in vivo. *Cell Death & Disease*, *2*(4). https://doi.org/10.1038/CDDIS.2011.29

Saftig, P., & Klumperman, J. (2009). Lysosome biogenesis and lysosomal membrane proteins: trafficking meets function. *Nature Reviews. Molecular Cell Biology*, *10*(9), 623–635. https://doi.org/10.1038/NRM2745

Sakurai, M., Hayashi, T., Abe, K., Itoyuama, Y., & Tabayashi, K. (2001). Induction of phosphatidylinositol 3-kinase and serine-threonine kinase-like immunoreactivity in rabbit spinal cord after transient ischemia. *Neuroscience Letters*, *302*(1), 17–20. https://doi.org/10.1016/S0304-3940(01)01609-3

Sánchez-Alegría, K., Flores-León, M., Avila-Muñoz, E., Rodríguez-Corona, N., & Arias, C. (2018). PI3K Signaling in Neurons: A Central Node for the Control of Multiple Functions. *International Journal of Molecular Sciences*. https://doi.org/10.3390/ijms19123725

Sanchez, G., Dury, A. Y., Murray, L. M., Biondi, O., Tadesse, H., El fatimy, R., Kothary, R., Charbonnier, F., Khandjian, E. W., & Côté, J. (2013). A novel function for the survival motoneuron protein as a translational regulator. *Human Molecular Genetics*, *22*(4), 668–684. https://doi.org/10.1093/HMG/DDS474

Sansa, A., Hidalgo, I., Miralles, M. P., de la Fuente, S., Perez-Garcia, M. J., Munell, F., Soler, R. M., & Garcera, A. (2021). Spinal Muscular Atrophy autophagy profile is tissue-dependent: differential regulation between muscle and motoneurons. *Acta Neuropathologica Communications*, *9*(1), 1–15. https://doi.org/10.1186/S40478-021-01223-5/TABLES/1

Saraei, R., Soleimani, M., Movassaghpour Akbari, A. A., Farshdousti Hagh, M., Hassanzadeh, A., & Solali, S. (2018). The role of XIAP in resistance to TNF-related apoptosis-inducing ligand (TRAIL) in Leukemia. *Biomedicine & Pharmacotherapy*, *107*, 1010–1019. https://doi.org/10.1016/J.BIOPHA.2018.08.065

Sareen, D., Ebert, A. D., Heins, B. M., McGivern, J. V., Ornelas, L., & Svendsen, C. N. (2012). Inhibition of apoptosis blocks human motor neuron cell death in a stem cell model of spinal muscular atrophy. *PLoS ONE*, *7*(6). https://doi.org/10.1371/journal.pone.0039113

Sarkar, S. (2013). Regulation of autophagy by mTOR-dependent and mTOR-independent pathways: autophagy dysfunction in neurodegenerative diseases and therapeutic application of autophagy enhancers. *Biochemical Society Transactions*, *41*(5), 1103–1130. https://doi.org/10.1042/BST20130134

Sarkar, S., Floto, R. A., Berger, Z., Imarisio, S., Cordenier, A., Pasco, M., Cook, L. J., & Rubinsztein, D. C. (2005). Lithium induces autophagy by inhibiting inositol monophosphatase. *Journal of Cell Biology*, *170*(7), 1101–1111. https://doi.org/10.1083/JCB.200504035

Saxton, R. A., & Sabatini, D. M. (2017). mTOR Signaling in Growth, Metabolism, and Disease. *Cell*, *169*(2), 361–371. https://doi.org/10.1016/J.CELL.2017.03.035

Schaller, S., Buttigieg, D., Alory, A., Jacquier, A., Barad, M., Merchant, M., Gentien, D., De La Grange, P., & Haase, G. (2017). Novel combinatorial screening identifies neurotrophic factors for selective classes of motor neurons. *Proceedings of the National Academy of Sciences of the United States of America*, *114*(12), E2486–E2493. https://doi.org/10.1073/PNAS.1615372114/-/DCSUPPLEMENTAL

Schellino, R., Boido, M., Borsello, T., & Vercelli, A. (2018). Pharmacological c-Jun NH2-Terminal Kinase (JNK) Pathway Inhibition Reduces Severity of Spinal Muscular Atrophy Disease in Mice. *Frontiers in Molecular Neuroscience*, *11*, 308. https://doi.org/10.3389/FNMOL.2018.00308/BIBTEX

Schindelin, J., Arganda-Carreras, I., Frise, E., Kaynig, V., Longair, M., Pietzsch, T., Preibisch, S., Rueden, C., Saalfeld, S., Schmid, B., Tinevez, J. Y., White, D. J., Hartenstein, V., Eliceiri, K., Tomancak, P., & Cardona, A. (2012). Fiji: an open-source platform for biological-image analysis. *Nature Methods*, *9*(7), 676–682. https://doi.org/10.1038/NMETH.2019

Scholar Rock. (2021). *Scholar Rock Announces Positive 12-Month Top-Line Results From the TOPAZ Phase 2 Clinical Trial Evaluating Apitegromab in Patients With Type 2 and Type 3 Spinal Muscular Atrophy (SMA) - Scholar Rock, Inc.*

Schrank, B., Götz, R., Gunnersen, J. M., Ure, J. M., Toyka, K. V, Smith, A. G., & Sendtner, M. (1997). Inactivation of the survival motor neuron gene, a candidate gene for human spinal muscular atrophy, leads to massive cell death in early mouse embryos. *Proceedings of the National Academy of Sciences of the United States of America*, *94*(18), 9920–9925. https://doi.org/10.1073/pnas.94.18.9920

Schuler, M., Bossy-Wetzel, E., Goldstein, J. C., Fitzgerald, P., & Green, D. R. (2000). p53 Induces Apoptosis by Caspase Activation through Mitochondrial Cytochrome c Release. *Journal of Biological Chemistry*, *275*(10), 7337–7342. https://doi.org/10.1074/JBC.275.10.7337

Schweingruber, C., & Hedlund, E. (2022). The Cell Autonomous and Non-Cell Autonomous Aspects of Neuronal Vulnerability and Resilience in Amyotrophic Lateral Sclerosis. *Biology*, *11*(8). https://doi.org/10.3390/BIOLOGY11081191

Scott, F. L., Denault, J., Riedl, S. J., Shin, H., Renatus, M., & Salvesen, G. S. (2005). XIAP inhibits caspase-3 and -7 using two binding sites : evolutionarily conserved mechanism of IAPs. *The EMBO Journal*, *24*(3), 645–655. https://doi.org/10.1038/sj.emboj.7600544

Segura, M. F., Sole, C., Pascual, M., Moubarak, R. S., Perez-garcia, M. J., Gozzelino, R., Iglesias, V., Badiola, N., Bayascas, J. R., Llecha, N., Rodriguez-alvarez, J., Soriano, E., Yuste, V. J., & Comella, J. X. (2007). *The Long Form of Fas Apoptotic Inhibitory Molecule Is Expressed Specifically in Neurons and Protects Them against Death Receptor-Triggered Apoptosis*. *27*(42), 11228–11241. https://doi.org/10.1523/JNEUROSCI.3462-07.2007

Selenko, P., Sprangers, R., Stier, G., Bühler, D., Fischer, U., & Sattler, M. (2001). SMN tudor domain structure and its interaction with the Sm proteins. *Nature Structural Biology*, *8*(1), 27–31. https://doi.org/10.1038/83014

Sendtner, M., Arakawa, Y., Stockli, K. A., Kreutzberg, G. W., & Thoenen, H. (1991). Effect of ciliary neurotrophic factor (CNTF) on motoneuron survival. *Journal of Cell Science*, *100*(SUPPL. 15), 103–109. https://doi.org/10.1242/jcs.1991.supplement_15.14

Sendtner, M., Kreutzberg, G. W., & Thoenen, H. (1990). Ciliary neurotrophic factor prevents the degeneration of motor neurons after axotomy. *Nature 1990 345:6274*, *345*(6274), 440–441. https://doi.org/10.1038/345440a0

Sendtner, M., Pei, G., Beck, M., Schweizer, U., & Wiese, S. (2000). Developmental motoneuron cell death and neurotrophic factors. *Cell and Tissue Research*, *301*(1), 71–84. https://doi.org/10.1007/S004410000217

Shafey, D., Boyer, J. G., Bhanot, K., & Kothary, R. (2010). Identification of novel interacting protein partners of SMN using tandem affinity purification. *Journal of Proteome Research*, *9*(4), 1659–1669. https://doi.org/10.1021/PR9006987

Shafey, D., Côté, P. D., & Kothary, R. (2005). Hypomorphic Smn knockdown C2C12 myoblasts reveal intrinsic defects in myoblast fusion and myotube morphology. *Experimental Cell Research*, *311*(1), 49–61. https://doi.org/10.1016/J.YEXCR.2005.08.019

Shamas-Din, A., Kale, J., Leber, B., & Andrews, D. W. (2013). Mechanisms of action of Bcl-2 family proteins. *Cold Spring Harbor Perspectives in Biology*, *5*(4), 1–21. https://doi.org/10.1101/cshperspect.a008714

Shanmugarajan, S., Tsuruga, E., Swoboda, K. J., Maria, B. L., Ries, W. L., & Reddy, S. V. (2009). Bone loss in survival motor neuron (Smn−/−SMN2) genetic mouse model of spinal muscular atrophy. *The Journal of Pathology*, *219*(1), 52. https://doi.org/10.1002/PATH.2566

Sharma, A., Lambrechts, A., Le, T. H. T. T., Le, T. H. T. T., Sewry, C. A., Ampe, C., Burghes, A. H. M., & Morris, G. E. (2005). A role for complexes of survival of motor neurons (SMN) protein with gemins and profilin in neurite-like cytoplasmic extensions of cultured nerve cells. *Experimental Cell Research*, *309*(1), 185–197. https://doi.org/10.1016/J.YEXCR.2005.05.014

Sheng, L., Wan, B., Feng, P., Sun, J., Rigo, F., Frank Bennett, C., Akerman, M., Krainer, A. R., & Hua, Y. (2018). Downregulation of Survivin contributes to cell-cycle arrest during postnatal cardiac development in a severe spinal muscular atrophy mouse model. *Human Molecular Genetics*, *27*(3), 486–498. https://doi.org/10.1093/HMG/DDX418

Shin, E. M., Hay, H. S., Lee, M. H., Goh, J. N., Tan, T. Z., Sen, Y. P., Lim, S. W., Yousef, E. M., Ong, H. T., Thike, A. A., Kong, X., Wu, Z., Mendoz, E., Sun, W., Salto-Tellez, M., Lim, C. T., Lobie, P. E., Lim, Y. P., Yap, C. T., … Tergaonkar, V. (2014). DEAD-box helicase DP103 defines metastatic potential of human breast cancers. *The Journal of Clinical Investigation*, *124*(9), 3807–3824. https://doi.org/10.1172/JCI73451

Shpargel, K. B., & Matera, A. G. (2005). Gemin proteins are required for efficient assembly of Sm-class ribonucleoproteins. *Proceedings of the National Academy of Sciences of the United States of America*, *102*(48), 17372–17377. https://doi.org/10.1073/PNAS.0508947102

Silke, J., & Meier, P. (2013). Inhibitor of apoptosis (IAP) proteins-modulators of cell death and inflammation. *Cold Spring Harbor Perspectives in Biology*, *5*(2), 1–19. https://doi.org/10.1101/cshperspect.a008730

Simic, G., Mladinov, M., Simic, D. S., Milosevic, N. J., Islam, A., Pajtak, A., Barisic, N., Sertic, J., Lucassen, P. J., Hof, P. R., & Kruslin, B. (2008). Abnormal motoneuron migration, differentiation, and axon outgrowth in spinal muscular atrophy. *Acta Neuropathologica*, *115*(3), 313–326. https://doi.org/10.1007/S00401-007-0327-1/FIGURES/11

Simon, C. M., Dai, Y., Van Alstyne, M., Koutsioumpa, C., Pagiazitis, J. G., Chalif, J. I., Wang, X., Rabinowitz, J. E., Henderson, C. E., Pellizzoni, L., & Mentis, G. Z. (2017). Converging Mechanisms of p53 Activation Drive Motor Neuron Degeneration in Spinal Muscular Atrophy. *Cell Reports*, *21*(13), 3767–3780. https://doi.org/10.1016/J.CELREP.2017.12.003

Simon, C. M., Jablonka, S., Ruiz, R., Tabares, L., & Sendtner, M. (2010). Ciliary neurotrophic factor-induced sprouting preserves motor function in a mouse model of mild spinal muscular atrophy. *Human Molecular Genetics*, *19*(6), 973–986. https://doi.org/10.1093/HMG/DDP562

Singh, J., Salcius, M., Liu, S. W., Staker, B. L., Mishra, R., Thurmond, J., Michaud, G., Mattoon, D. R., Printen, J., Christensen, J., Bjornsson, J. M., Pollok, B. A., Kiledjian, M., Stewart, L., Jarecki, J., & Gurney, M. E. (2008). DcpS as a therapeutic target for spinal muscular atrophy. *ACS Chemical Biology*, *3*(11), 711–722. https://doi.org/10.1021/CB800120T/SUPPL_FILE/CB800120T_SI_002.PDF

Singh, R. N., Howell, M. D., Ottesen, E. W., & Singh, N. N. (2017). Diverse role of survival motor neuron protein. *Biochimica et Biophysica Acta - Gene Regulatory Mechanisms*, *1860*(3), 299–315. https://doi.org/10.1016/j.bbagrm.2016.12.008

Sintusek, P., Catapano, F., Angkathunkayul, N., Marrosu, E., Parson, S. H., Morgan, J. E., Muntoni, F., & Zhou, H. (2016). Histopathological Defects in Intestine in Severe Spinal Muscular Atrophy Mice Are Improved by Systemic Antisense Oligonucleotide Treatment. *PLOS ONE*, *11*(5), e0155032. https://doi.org/10.1371/JOURNAL.PONE.0155032

Sleigh, J. N., Buckingham, S. D., Esmaeili, B., Viswanathan, M., Cuppen, E., Westlund, B. M., & Sattelle, D. B. (2011). A novel Caenorhabditis elegans allele, smn-1(cb131), mimicking a mild form of spinal muscular atrophy, provides a convenient drug screening platform highlighting new and pre-approved compounds. *Human Molecular Genetics*, *20*(2), 245–260. https://doi.org/10.1093/HMG/DDQ459

Sleigh, J. N., Gillingwater, T. H., & Talbot, K. (2011). The contribution of mouse models to understanding the pathogenesis of spinal muscular atrophy. *DMM Disease Models and Mechanisms*, *4*(4), 457–467. https://doi.org/10.1242/dmm.007245

Sluss, H. K., Armata, H., Gallant, J., & Jones, S. N. (2004). Phosphorylation of Serine 18 Regulates Distinct p53 Functions in Mice. *Molecular and Cellular Biology*, *24*(3), 976–984. https://doi.org/10.1128/MCB.24.3.976-984.2004

Snyder, B. R., Gray, S. J., Quach, E. T., Huang, J. W., Leung, C. H., Samulski, R. J., Boulis, N. M., & Federici, T. (2011). Comparison of Adeno-Associated Viral Vector Serotypes for Spinal Cord and Motor Neuron Gene Delivery. *Https://Home.Liebertpub.Com/Hum*, *22*(9), 1129–1135. https://doi.org/10.1089/HUM.2011.008

Sole, C., Dolcet, X., Segura, M. F., Gutierrez, H., Gozzelino, R., Sanchis, D., Bayascas, J. R., Gallego, C., Moscat, J., Davies, A. M., & Comella, J. X. (2004). *The death receptor antagonist FAIM promotes neurite outgrowth by a mechanism that depends on ERK and NF- B signaling*. *167*(3), 479–492. https://doi.org/10.1083/jcb.200403093

Soler-Botija, C., Ferrer, I., Alvarez, J. L., Baiget, M., & Tizzano, E. F. (2003). Downregulation of Bcl-2 proteins in type I spinal muscular atrophy motor neurons during fetal development. *Journal of Neuropathology and Experimental Neurology*, *62*(4), 420–426. https://doi.org/10.1093/JNEN/62.4.420

Soler-Botija, C., Ferrer, I., Gich, I., Baiget, M., & Tizzano, E. F. (2002). Neuronal death is enhanced and begins during foetal development in type I spinal muscular atrophy spinal cord. *Brain*, *125*(7), 1624–1634. https://doi.org/10.1093/BRAIN/AWF155

Soler, R. M., Dolcet, X., Encinas, M., Egea, J., Bayascas, J. R., & Comella, J. X. (1999). Receptors of the glial cell line-derived neurotrophic factor family of neurotrophic factors signal cell survival through the phosphatidylinositol 3- kinase pathway in spinal cord motoneurons. In *Journal of Neuroscience* (Vol. 19, Issue 21, pp. 9160–9169). https://doi.org/10.1523/jneurosci.19-21-09160.1999

Somers, E., Lees, R. D., Hoban, K., Sleigh, J. N., Zhou, H., Muntoni, F., Talbot, K., Gillingwater, T. H., & Parson, S. H. (2016). Vascular Defects and Spinal Cord Hypoxia in Spinal Muscular Atrophy. *Annals of Neurology*, *79*(2), 217–230. https://doi.org/10.1002/ANA.24549

Spillantini, M. G., Crowther, R. A., Jakes, R., Hasegawa, M., & Goedert, M. (1998). alpha-Synuclein in filamentous inclusions of Lewy bodies from Parkinson's disease and dementia with lewy bodies. *Proceedings of the National Academy of Sciences of the United States of America*, *95*(11), 6469–6473. https://doi.org/10.1073/PNAS.95.11.6469

Stam, M., Wadman, R. I., Wijngaarde, C. A., Bartels, B., Asselman, F. L., Otto, L. A. M., Goedee, H. S., Habets, L. E., De Groot, J. F., Schoenmakers, M. A. G. C., Cuppen, I., Van Den Berg, L. H., & Van Der Pol, W. L. (2018). Protocol for a phase II, monocentre, double-blind, placebo-controlled, cross-over trial to assess efficacy of pyridostigmine in patients with spinal muscular atrophy types 2-4 (SPACE trial). *BMJ Open*, *8*(7). https://doi.org/10.1136/BMJOPEN-2017-019932

Stanga, S., Caretto, A., Boido, M., & Vercelli, A. (2020). Mitochondrial dysfunctions: A red thread across neurodegenerative diseases. *International Journal of Molecular Sciences*, *21*(10). https://doi.org/10.3390/ijms21103719

Stevens, D., Claborn, M. K., Gildon, B. L., Kessler, T. L., & Walker, C. (2020). Onasemnogene Abeparvovec-xioi: Gene Therapy for Spinal Muscular Atrophy. *Annals of Pharmacotherapy*, *54*(10), 1001–1009. https://doi.org/10.1177/1060028020914274

Stifani, N. (2014). Motor neurons and the generation of spinal motor neuron diversity. *Frontiers in Cellular Neuroscience*, *8*(OCT), 293. https://doi.org/10.3389/FNCEL.2014.00293/BIBTEX

Sugarman, E. A., Nagan, N., Zhu, H., Akmaev, V. R., Zhou, Z., Rohlfs, E. M., Flynn, K., Hendrickson, B. C., Scholl, T., Sirko-Osadsa, D. A., & Allitto, B. A. (2012). Pan-ethnic carrier screening and prenatal diagnosis for spinal muscular atrophy: Clinical laboratory analysis of >72 400 specimens. *European Journal of Human Genetics*, *20*(1), 27–32. https://doi.org/10.1038/ejhg.2011.134

Sugino, T., Nozaki, K., Takagi, Y., Hattori, I., Hashimoto, N., Moriguchi, T., & Nishida, E. (2000). Activation of Mitogen-Activated Protein Kinases after Transient Forebrain Ischemia in Gerbil Hippocampus. *The Journal of Neuroscience*, *20*(12), 4506. https://doi.org/10.1523/JNEUROSCI.20-12-04506.2000

Sun, W., Gould, T. W., Newbern, J., Milligan, C., Yoen Choi, S., Kim, H., & Oppenheim, R. W. (2005). Phosphorylation of c-Jun in avian and mammalian motoneurons in vivo during programmed cell death: an early reversible event in the apoptotic cascade. *The Journal of Neuroscience : The Official Journal of the Society for Neuroscience*, *25*(23), 5595–5603. https://doi.org/10.1523/JNEUROSCI.4970-04.2005

Switon, K., Kotulska, K., Janusz-Kaminska, A., Zmorzynska, J., & Jaworski, J. (2017). Molecular neurobiology of mTOR. *Neuroscience*, *341*, 112–153.

https://doi.org/10.1016/J.NEUROSCIENCE.2016.11.017

Swoboda, K. J., Scott, C. B., Crawford, T. O., Simard, L. R., Reyna, S. P., Krosschell, K. J., Acsadi, G., Elsheik, B., Schroth, M. K., Anjou, G. D. ', Lasalle, B., Prior, T. W., Sorenson, S. L., Maczulski, J. A., Bromberg, M. B., Chan, G. M., & Kissel, J. T. (2010). SMA CARNIVAL Trial Part I: Double-Blind, Randomized, Placebo-Controlled Trial of L-Carnitine and Valproic Acid in Spinal Muscular Atrophy. *PLoS ONE*. https://doi.org/10.1371/journal.pone.0012140

Taillandier, D., & Polge, C. (2019). Skeletal muscle atrogenes: From rodent models to human pathologies. *Biochimie*, *166*, 251–269. https://doi.org/10.1016/J.BIOCHI.2019.07.014

Talbot, K., & Davies, K. E. (2008). Is Good Housekeeping the Key to Motor Neuron Survival? *Cell*, *133*(4), 572–574. https://doi.org/10.1016/J.CELL.2008.05.002

Talbot, K., Ponting, C. P., Theodosiou, A. M., Rodrigues, N. R., Surtees, R., Mountford, R., & Davies, K. E. (1997). Missense mutation clustering in the survival motor neuron gene: a role for a conserved tyrosine and glycine rich region of the protein in RNA metabolism? *Human Molecular Genetics*, *6*(3), 497–500. https://doi.org/10.1093/HMG/6.3.497

Tanaka, Y., Guhde, G., Suter, A., Eskelinen, E. L., Hartmann, D., Lüllmann-Rauch, R., Janssen, P. M. L., Blanz, J., Von Figura, K., & Saftig, P. (2000). Accumulation of autophagic vacuoles and cardiomyopathy in LAMP-2-deficient mice. *Nature 2000 406:6798*, *406*(6798), 902–906. https://doi.org/10.1038/35022595

Tarabal, O., Caraballo-Miralles, V., Cardona-Rossinyol, A., Correa, F. J., Olmos, G., Lladó, J., Esquerda, J. E., & Calderó, J. (2014). Mechanisms involved in spinal cord central synapse loss in a mouse model of spinal muscular atrophy. *Journal of Neuropathology and Experimental Neurology*, *73*(6), 519–535. https://doi.org/10.1097/NEN.0000000000000074

Tchevkina, E., & Komelkov, A. (2012). Protein Phosphorylation as a Key Mechanism of mTORC1/2 Signaling Pathways. *Protein Phosphorylation in Human Health*. https://doi.org/10.5772/48274

Thomas, N. H., & Dubowitz, V. (1994). The natural history of type I (severe) spinal muscular atrophy. *Neuromuscular Disorders*, *4*(5–6), 497–502. https://doi.org/10.1016/0960-8966(94)90090-6

Thomson, A. K., Somers, E., Powis, R. A., Shorrock, H. K., Murphy, K., Swoboda, K. J., Gillingwater, T. H., & Parson, S. H. (2017). Survival of motor neurone protein is required for normal postnatal development of the spleen. *Journal of Anatomy*, *230*(2), 337–346. https://doi.org/10.1111/JOA.12546

Tisdale, S., & Pellizzoni, L. (2015). Disease Mechanisms and Therapeutic Approaches in Spinal Muscular Atrophy. *Journal of Neuroscience*, *35*(23), 8691–8700. https://doi.org/10.1523/JNEUROSCI.0417-15.2015

Tovar-y-Romo, L. B., Ramírez-Jarquín, U. N., Lazo-Gómez, R., & Tapia, R. (2014). Trophic factors as modulators of motor neuron physiology and survival: Implications for ALS therapy. *Frontiers in Cellular Neuroscience*, *8*(FEB), 61. https://doi.org/10.3389/FNCEL.2014.00061/BIBTEX

Tripathi, P., Guo, H., Dreser, A., Yamoah, A., Sechi, A., Jesse, C. M., Katona, I., Doukas, P., Nikolin, S., Ernst, S., Aronica, E., Glaß, H., Hermann, A., Steinbusch, H., Feller, A. C., Bergmann, M., Jaarsma, D., Weis, J., & Goswami, A. (2021). Pathomechanisms of ALS8: altered autophagy and defective RNA binding protein (RBP) homeostasis due to the VAPB P56S mutation. *Cell Death & Disease*, *12*(5). https://doi.org/10.1038/S41419-021-03710-Y

Tsai, L. K., Tsai, M. S., Ting, C. H., Wang, S. H., & Li, H. (2008). Restoring Bcl-xL levels benefits a mouse model of spinal muscular atrophy. *Neurobiology of Disease*, *31*(3), 361–367. https://doi.org/10.1016/J.NBD.2008.05.014

Tsai, M. S., Chiu, Y. T., Wang, S. H., Hsieh-Li, H. M., Lian, W. C., & Li, H. (2006). Abolishing Bax-Dependent Apoptosis Shows Beneficial Effects on Spinal Muscular Atrophy Model Mice. *Molecular Therapy*, *13*(6), 1149–1155. https://doi.org/10.1016/j.ymthe.2006.02.008

Tseng, Y. T., Chen, C. S., Jong, Y. J., Chang, F. R., & Lo, Y. C. (2016). Loganin possesses neuroprotective properties, restores SMN protein and activates protein synthesis positive regulator Akt/mTOR in experimental models of spinal muscular atrophy. *Pharmacol Res*, *111*, 58–75. https://doi.org/10.1016/j.phrs.2016.05.023

Tsukada, M., & Ohsumi, Y. (1993). Isolation and characterization of autophagy-defective mutants of Saccharomyces cerevisiae. *FEBS Letters*, *333*(1–2), 169–174. https://doi.org/10.1016/0014-5793(93)80398-E

Vai, S., Bianchi, M. L., Moroni, I., Mastella, C., Broggi, F., Morandi, L., Arnoldi, M. T., Bussolino, C., & Baranello, G. (2015). Bone and Spinal Muscular Atrophy. *Bone*, *79*, 116–120. https://doi.org/10.1016/J.BONE.2015.05.039

Van Damme, P., Van Hoecke, A., Lambrechts, D., Vanacker, P., Bogaert, E., Van Swieten, J., Carmeliet, P., Van Den Bosch, L., & Robberecht, W. (2008). Progranulin functions as a neurotrophic factor to regulate neurite outgrowth and enhance neuronal survival. *The Journal of Cell Biology*, *181*(1), 37–41. https://doi.org/10.1083/JCB.200712039

Van Meerbeke, J. P., Gibbs, R. M., Plasterer, H. L., Miao, W., Feng, Z., Lin, M. Y., Rucki, A. A., Wee, C. D., Xia, B., Sharma, S., Jacques, V., Li, D. K., Pellizzoni, L., Rusche, J. R., Ko, C. P., & Sumner, C. J. (2013). The DcpS inhibitor RG3039 improves motor function in SMA mice. *Human Molecular Genetics*, *22*(20), 4074–4083. https://doi.org/10.1093/HMG/DDT257

Varon, S., Manthorpe, M., & Adler, R. (1979). Cholinergic neuronotrophic factors: I. Survival, neurite outgrowth and choline acetyltransferase activity in monolayer cultures from chick embryo ciliary ganglia. *Brain Research*, *173*(1), 29–45.

https://doi.org/10.1016/0006-8993(79)91093-X

Vauzour, D., Vafeiadou, K., Rice-Evans, C., Williams, R. J., & Spencer, J. P. E. (2007). Activation of pro-survival Akt and ERK1/2 signalling pathways underlie the anti-apoptotic effects of flavanones in cortical neurons. *Journal of Neurochemistry*, *103*(4), 1355–1367. https://doi.org/10.1111/J.1471-4159.2007.04841.X

Vega, Q. C., Worby, C. A., Lechner, M. S., Dixon, J. E., & Dressler, G. R. (1996). Glial cell line-derived neurotrophic factor activates the receptor tyrosine kinase RET and promotes kidney morphogenesis. *Proceedings of the National Academy of Sciences of the United States of America*, *93*(20), 10657–10661. https://doi.org/10.1073/PNAS.93.20.10657

Verhaart, I. E. C. C., Robertson, A., Wilson, I. J., Aartsma-Rus, A., Cameron, S., Jones, C. C., Cook, S. F., & Lochmüller, H. (2017). Prevalence, incidence and carrier frequency of 5q-linked spinal muscular atrophy - A literature review. *Orphanet Journal of Rare Diseases*, *12*(1). https://doi.org/10.1186/s13023-017-0671-8

Vestergaard, P., Glerup, H., Steffensen, B. F., Rejnmark, L., Rahbek, J., & Mosekilde, L. (2001). Fracture risk in patients with muscular dystrophy and spinal muscular atrophy. *Journal of Rehabilitation Medicine*, *33*(4), 150–155. https://doi.org/10.1080/165019701750300609

Viollet, L., Bertrandy, S., Brunialti, A. L. B., Lefebvre, S., Burlet, P., Clermont, O., Cruaud, C., Guénet, J. L., Munnich, A., & Melki, J. (1997). cDNA isolation, expression, and chromosomal localization of the mouse survival motor neuron gene (Smn). *Genomics*, *40*(1), 185–188. https://doi.org/10.1006/GENO.1996.4551

Vitte, J. M., Davoult, B., Roblot, N., Mayer, M., Joshi, V., Courageot, S., Tronche, F., Vadrot, J., Moreau, M. H., Kemeny, F., & Melki, J. (2004). Deletion of murine Smn exon 7 directed to liver leads to severe defect of liver development associated with iron overload. *The American Journal of Pathology*, *165*(5), 1731–1741. https://doi.org/10.1016/S0002-9440(10)63428-1

Von Lewinski, F., & Keller, B. U. (2005). Ca2+, mitochondria and selective motoneuron vulnerability: Implications for ALS. *Trends in Neurosciences*, *28*(9), 494–500. https://doi.org/10.1016/j.tins.2005.07.001

Wadman, R. I., van der Pol, W. L., Bosboom, W. M. J., Asselman, F. L., van den Berg, L. H., Iannaccone, S. T., & Vrancken, A. F. J. E. (2019). Drug treatment for spinal muscular atrophy type I. *The Cochrane Database of Systematic Reviews*, *12*(12). https://doi.org/10.1002/14651858.CD006281.PUB5

Wagey, R., Pelech, S. L., Duronio, V., & Krieger, C. (1998). Phosphatidylinositol 3-Kinase: Increased Activity and Protein Level in Amyotrophic Lateral Sclerosis. *Journal of Neurochemistry*, *71*(2), 716–722. https://doi.org/10.1046/J.1471-4159.1998.71020716.X

Wan, L., Battle, D. J., Yong, J., Gubitz, A. K., Kolb, S. J., Wang, J., & Dreyfuss, G. (2005). The Survival of Motor Neurons Protein Determines the Capacity for snRNP Assembly: Biochemical Deficiency in Spinal Muscular Atrophy. *Molecular and Cellular Biology*, *25*(13), 5543–5551. https://doi.org/10.1128/MCB.25.13.5543-5551.2005/ASSET/2F42A487-0FC3-4A3A-9979-6824A6581CFF/ASSETS/GRAPHIC/ZMB0130551010006.JPEG

Wang, N., Feng, Y., Zhu, M., Siu, F. M., Ng, K. M., & Che, C. M. (2013). A novel mechanism of XIAP degradation induced by timosaponin AIII in hepatocellular carcinoma. *Biochimica et Biophysica Acta (BBA) - Molecular Cell Research*, *1833*(12), 2890–2899. https://doi.org/10.1016/J.BBAMCR.2013.07.018

Wei, Z., & Liu, H. T. (2002). MAPK signal pathways in the regulation of cell proliferation in mammalian cells. *Cell Research 2002 12:1*, *12*(1), 9–18. https://doi.org/10.1038/sj.cr.7290105

Williams, A., Jahreiss, L., Sarkar, S., Saiki, S., Menzies, F. M., Ravikumar, B., & Rubinsztein, D. C. (2006). Aggregate-Prone Proteins Are Cleared from the Cytosol by Autophagy: Therapeutic Implications. *Current Topics in Developmental Biology*, *76*, 89–101. https://doi.org/10.1016/S0070-2153(06)76003-3

Winslow, A. R., Chen, C. W., Corrochano, S., Acevedo-Arozena, A., Gordon, D. E., Peden, A. A., Lichtenberg, M., Menzies, F. M., Ravikumar, B., Imarisio, S., Brown, S., O'Kane, C. J., & Rubinsztein, D. C. (2010). α-Synuclein impairs macroautophagy: implications for Parkinson's disease. *The Journal of Cell Biology*, *190*(6), 1023–1037. https://doi.org/10.1083/JCB.201003122

Winter, J. N., Jefferson, L. S., & Kimball, S. R. (2011). ERK and Akt signaling pathways function through parallel mechanisms to promote mTORC1 signaling. *American Journal of Physiology - Cell Physiology*, *300*(5), C1172. https://doi.org/10.1152/AJPCELL.00504.2010

Wirth, B. (2000). An update of the mutation spectrum of the survival motor neuron gene (SMN1) in autosomal recessive spinal muscular atrophy (SMA). *Human Mutation*, *15*(3), 228–237. https://doi.org/10.1002/(SICI)1098-1004(200003)15:3<228::AID-HUMU3>3.0.CO;2-9

Wirth, B. (2021). Spinal Muscular Atrophy: In the Challenge Lies a Solution. *Trends in Neurosciences*, *44*(4), 306–322. https://doi.org/10.1016/j.tins.2020.11.009

Wirth, B., Karakaya, M., Kye, M. J., & Mendoza-Ferreira, N. (2020). Twenty-Five Years of Spinal Muscular Atrophy Research: From Phenotype to Genotype to Therapy, and What Comes Next. In *Annual Review of Genomics and Human Genetics* (Vol. 21, pp. 231–261). https://doi.org/10.1146/annurev-genom-102319-103602

Wirth, B., Mendoza-Ferreira, N., & Torres-Benito, L. (2017). Spinal Muscular Atrophy Disease Modifiers. *Spinal Muscular Atrophy: Disease Mechanisms and Therapy*, 191–210. https://doi.org/10.1016/B978-0-12-803685-3.00012-4

Wishart, T. M., Mutsaers, C. A., Riessland, M., Reimer, M. M., Hunter, G., Hannam, M. L., Eaton, S. L., Fuller, H. R., Roche, S. L., Somers, E., Morse, R., Young, P.

J., Lamont, D. J., Hammerschmidt, M., Joshi, A., Hohenstein, P., Morris, G. E., Parson, S. H., Skehel, P. A., … Gillingwater, T. H. (2014). Dysregulation of ubiquitin homeostasis and β-catenin signaling promote spinal muscular atrophy. *Journal of Clinical Investigation*, *124*(4), 1821–1834. https://doi.org/10.1172/JCI71318

Witzemann, V. (2006). Development of the neuromuscular junction. *Cell and Tissue Research*, *326*(2), 263–271. https://doi.org/10.1007/S00441-006-0237-X/FIGURES/2

Woo Kim, K., Cho, H. J., Abdul Khaliq, S., Hui Son, K., & Yoon, M. S. (2020). Comparative Analyses of mTOR/Akt and Muscle Atrophy-Related Signaling in Aged Respiratory and Gastrocnemius Muscles. *International Journal of Molecular Sciences*, *21*(8). https://doi.org/10.3390/IJMS21082862

Workman, E., Saieva, L., Carrel, T. L., Crawford, T. O., Liu, D., Lutz, C., Beattie, C. E., Pellizzoni, L., & Burghes, A. H. M. (2009). A SMN missense mutation complements SMN2 restoring snRNPs and rescuing SMA mice. *Human Molecular Genetics*, *18*(12), 2215–2229. https://doi.org/10.1093/HMG/DDP157

Wu, C. Y., Whye, D., Glazewski, L., Choe, L., Kerr, D., Lee, K. H., Mason, R. W., & Wang, W. (2011). Proteomic assessment of a cell model of spinal muscular atrophy. *BMC Neuroscience*, *12*(1), 1–13. https://doi.org/10.1186/1471-2202-12-25/FIGURES/10

Wu, G., Chai, J., Suber, T. L., Wu, J. W., Du, C., Wang, X., & Shi, Y. (2000). Structural basis of IAP recognition by Smac/DIABLO. *Nature*, *408*(6815), 1008–1012. https://doi.org/10.1038/35050012

Xu, C. C., Denton, K. R., Wang, Z. B., Zhang, X., & Li, X. J. (2016). Abnormal mitochondrial transport and morphology as early pathological changes in human models of spinal muscular atrophy. *Disease Models & Mechanisms*, *9*(1), 39–49. https://doi.org/10.1242/DMM.021766

Yamamoto, Y., & Henderson, C. E. (1999). Patterns of Programmed Cell Death in Populations of Developing Spinal Motoneurons in Chicken , Mouse , and Rat. *Developmental Biology*, *71*(1), 60–71. https://doi.org/10.1006/DBIO.1999.9413

Yang, Z., & Klionsky, D. J. (2009). An Overview of the Molecular Mechanisms of Autophagy. In *Current Top Microbiology Immunology* (Vol. 335). https://doi.org/10.1007/978-3-642-00302-8

Yap, C. C., & Winckler, B. (2009). Vesicular Sorting to Axons and Dendrites. *Encyclopedia of Neuroscience*, 115–120. https://doi.org/10.1016/B978-008045046-9.00743-9

Yap, T. A., Garrett, M. D., Walton, M. I., Raynaud, F., de Bono, J. S., & Workman, P. (2008). Targeting the PI3K–AKT–mTOR pathway: progress, pitfalls, and promises. *Current Opinion in Pharmacology*, *8*(4), 393–412. https://doi.org/10.1016/J.COPH.2008.08.004

Yeo, W., & Gautier, J. (2004). Early neural cell death: Dying to become neurons. *Developmental Biology*, *274*(2), 233–244. https://doi.org/10.1016/j.ydbio.2004.07.026

Ylä-Anttila, P., Vihinen, H., Jokitalo, E., & Eskelinen, E. L. (2009). 3D tomography reveals connections between the phagophore and endoplasmic reticulum. *Autophagy*, *5*(8), 1180–1185. https://doi.org/10.4161/AUTO.5.8.10274

Young, P. J., Man, N. T., Lorson, C. L., Le, T. T., Androphy, E. J., Burghes, A. H., & Morris, G. E. (2000). The exon 2b region of the spinal muscular atrophy protein, SMN, is involved in self-association and SIP1 binding. *Human Molecular Genetics*, *9*(19), 2869–2877. http://www.ncbi.nlm.nih.gov/pubmed/11092763

Yung, H. W., Charnock-Jones, D. S., & Burton, G. J. (2011). Regulation of AKT Phosphorylation at Ser473 and Thr308 by Endoplasmic Reticulum Stress Modulates Substrate Specificity in a Severity Dependent Manner. *PLoS ONE*, *6*(3), 17894. https://doi.org/10.1371/JOURNAL.PONE.0017894

Zhang, H. L., Pan, F., Hong, D., Shenoy, S. M., Singer, R. H., & Bassell, G. J. (2003). Active transport of the survival motor neuron protein and the role of exon-7 in cytoplasmic localization. *The Journal of Neuroscience : The Official Journal of the Society for Neuroscience*, *23*(16), 6627–6637. https://doi.org/10.1523/JNEUROSCI.23-16-06627.2003

Zhang, H., Xing, L., Rossoll, W., Wichterle, H., Singer, R. H., & Bassell, G. J. (2006). Multiprotein Complexes of the Survival of Motor Neuron Protein SMN with Gemins Traffic to Neuronal Processes and Growth Cones of Motor Neurons. *Journal of Neuroscience*, *26*(33), 8622–8632. https://doi.org/10.1523/JNEUROSCI.3967-05.2006

Zhang, R., So, B. R., Li, P., Yong, J., Glisovic, T., Wan, L., & Dreyfuss, G. (2011). Structure of a key intermediate of the SMN complex reveals Gemin2's crucial function in snRNP assembly. *Cell*, *146*(3), 384–395. https://doi.org/10.1016/J.CELL.2011.06.043

Zhang, X., Li, L., Chen, S., Yang, D., Wang, Y., Zhang, X., Wang, Z., & Le, W. (2011). Rapamycin treatment augments motor neuron degeneration in SOD1(G93A) mouse model of amyotrophic lateral sclerosis. *Autophagy*, *7*(4), 412–425. https://doi.org/10.4161/AUTO.7.4.14541

Zhang, Y., He, J., Zhang, Y., Li, L., Tang, X., Wang, L., Guo, J., Jin, C., Tighe, S., Zhang, Y., Zhu, Y., & Zhu, B. (2020). The analysis of the association between the copy numbers of survival motor neuron gene 2 and neuronal apoptosis inhibitory protein genes and the clinical phenotypes in 40 patients with spinal muscular atrophy: Observational study. *Medicine*, *99*(3). https://doi.org/10.1097/MD.0000000000018809

Zhang, Z., Lotti, F., Dittmar, K., Younis, I., Wan, L., Kasim, M., & Dreyfuss, G. (2008). SMN Deficiency Causes Tissue-Specific Perturbations in the Repertoire of snRNAs and Widespread Defects in Splicing. *Cell*, *133*(4), 585–600. https://doi.org/10.1016/j.cell.2008.03.031

Zhang, Z., Pinto, A. M., Wan, L., Wang, W., Berg, M. G., Oliva, I., Singh, L. N., Dengler, C., Wei, Z., & Dreyfuss, G. (2013). Dysregulation of

synaptogenesis genes antecedes motor neuron pathology in spinal muscular atrophy. *Proceedings of the National Academy of Sciences of the United States of America*, *110*(48), 19348–19353. https://doi.org/10.1073/PNAS.1319280110/SUPPL_FILE/SD06.XLSX

Zhu, J. H., Kulich, S. M., Oury, T. D., & Chu, C. T. (2002). Cytoplasmic aggregates of phosphorylated extracellular signal-regulated protein kinases in Lewy body diseases. *The American Journal of Pathology*, *161*(6), 2087–2098. https://doi.org/10.1016/S0002-9440(10)64487-2

Zhu, X., Lee, H. G., Raina, A. K., Perry, G., & Smith, M. A. (2002). The role of mitogen-activated protein kinase pathways in Alzheimer's disease. *Neuro-Signals*, *11*(5), 270–281. https://doi.org/10.1159/000067426

Zhu, Y., Zhao, L., Liu, L., Gao, P., Tian, W., Wang, X., Jin, H., Xu, H., & Chen, Q. (2010). Beclin 1 cleavage by caspase-3 inactivates autophagy and promotes apoptosis. *Protein & Cell*, *1*(5), 468–477. https://doi.org/10.1007/S13238-010-0048-4

Zimmermann, S., & Moelling, K. (1999). Phosphorylation and regulation of Raf by Akt (protein kinase B). *Science (New York, N.Y.)*, *286*(5445), 1741–1744. https://doi.org/10.1126/SCIENCE.286.5445.1741

Zucchi, E., Bonetto, V., Sorarù, G., Martinelli, I., Parchi, P., Liguori, R., & Mandrioli, J. (2020). Neurofilaments in motor neuron disorders: towards promising diagnostic and prognostic biomarkers. *Molecular Neurodegeneration 2020 15:1*, *15*(1), 1–20. https://doi.org/10.1186/S13024-020-00406-3

Zufiría, M., Gil-Bea, F. J., Fernández-Torrón, R., Poza, J. J., Muñoz-Blanco, J. L., Rojas-García, R., Riancho, J., & de Munain, A. L. (2016). ALS: A bucket of genes, environment, metabolism and unknown ingredients. *Progress in Neurobiology*, *142*, 104–129. https://doi.org/10.1016/J.PNEUROBIO.2016.05.004

Zündorf, G., & Reiser, G. (2011). Calcium dysregulation and homeostasis of neural calcium in the molecular mechanisms of neurodegenerative diseases provide multiple targets for neuroprotection. *Antioxidants & Redox Signaling*, *14*(7), 1275–1288. https://doi.org/10.1089/ars.2010.3359

PUBLICATIONS AND CONFERENCES

1. PUBLICATIONS

1. Sandra de la Fuente, **Alba Sansa**, Ambika Periyakaruppiah, Ana Garcera and Rosa M Soler. *Calpain Inhibition Increases SMN Protein in Spinal Cord Motoneurons and Ameliorates the Spinal Muscular Atrophy Phenotype in Mice*. Molecular Neurobiology. (2019) Jun;56(6):4414-4427. doi: 10.1007/s12035-018-1379-z.

2. Sandra de la Fuente, **Alba Sansa**, Iván Hidalgo, Nuria Vivancos, Ricardo Romero-Guevara, Ana Garcera and Rosa M Soler. *Calpain system is altered in Survival Motor Neuron-reduced cells from in vitro and in vivo Spinal Muscular Atrophy models.* Cell Death & Disease. (2020). Jun;11,487. doi: 10.1038/s41419-020-2688-5.

3. **Alba Sansa**, Sandra de la Fuente, Joan X Comella, Ana Garcera and Rosa M Soler. *Intracellular pathways involved in cell survival are deregulated in mouse and human spinal muscular atrophy motoneurons*. Neurobiology of Disease. (2021). Jul; 155:105366. doi:10.1016/j.nbd.2021.105366.

4. **Alba Sansa**, Maria P. Miralles, Ivan Hidalgo, Sandra de la Fuente, M. Jose Perez-Garcia, Francina Munell, Rosa M Soler and Ana Garcera. *Spinal Muscular Atrophy autophagy profile is tissue-dependent: differential regulation between muscle and motoneurons.* Acta Neuropathologica Communications. (2021). Jul 3;9(1):122. doi: 10.1186/s40478-021-01223-5.

5. Maria P. Miralles, **Alba Sansa,** Maria Beltran, Rosa M Soler and Ana Garcera. *Survival motor neuron protein and neurite degeneration are regulated by Gemin3 in Spinal Muscular Atrophy motoneurons.* Frontiers in Cellular Neuroscience (2022). Accepted 06 December 2022. doi: 10.3389/fncel.2022.1054270

6. **Alba Sansa**, Maria P. Miralles, Maria Beltran, Jordi Calderó, Ana Garcera and Rosa M Soler. *ERK MAPK signaling pathway inhibition as a potential target to prevent autophagy alterations in Spinal Muscular Atrophy motoneurons.* Submitted and sent for peer-review to Cell Death & Disease (2022).

2. NATIONAL AND INTERNATIONAL CONFERENCES

1. **X Simposi de Neurobiologia,** October 6-7th 2016; Barcelona, Spain; Abstract and Oral Presentation "*Calcium-dependent protease Calpain regulates Survival Motor Neuron Protein in cultured mouse motoneurons*". S. de la Fuente, **A. Sansa**, A. Garcerá and R.M.Soler.
2. **I Congreso Interdisciplinar de Neurología y Neurociencia,** March 10-11th 2017; Lleida, Spain; Abstract and Oral Presentation "*Study of the effects of membrane depolarization on Smn protein levels in the NSC-34 cell line*". **A. Sansa**, S. de la Fuente, A. Garcera and R.M.Soler.

3. **I Congreso Interdisciplinar de Neurología y Neurociencia,** March 10-11th 2017; Lleida, Spain; Abstract and Oral Presentation "*Calcium-dependent protease Calpain regulates Survival Motor Neuron Protein in cultured mouse motoneurons*". S. de la Fuente, **A. Sansa**, A. Garcera and R.M.Soler.
4. **11th FENS Forum of Neuroscience,** July 7-11th 2018; Berlin, Germany; Abstract and Poster Presentation "*Nuclear factor-Kappa B and apoptosis pathways are altered in cultured motoneurons of a spinal muscular atrophy mouse model"*. **A. Sansa**, S. Arumugam, S. De la Fuente, N.Vivancos, M.J.Perez-Garcia, J.X. Comella, A. Garcera and R.M. Soler.
5. **11th FENS Forum of Neuroscience,** July 7-11th 2018; Berlin, Germany; Abstract and Poster Presentation "*Calpain knockdown increases Survival Motor Neuron protein in spinal cord motor neurons"*. S. De la Fuente, **A. Sansa**, A. Garcera and R.M. Soler.
6. **11th FENS Forum of Neuroscience,** July 7-11th 2018; Berlin, Germany; Abstract and Poster Presentation "*Study of autophagy markers and NF-kappa pathway in muscle cells of a spinal muscular atrophy mouse model*". A. Garcera, S. Arumugam, **A. Sansa**, I. Hidalgo, S. De la Fuente and R.M. Soler.
7. **II Congreso Interdisciplinar de Neurología y Neurociencia,** March 8-9th 2019; Lleida, Spain; Abstract and Oral Presentation "*Alteration of Apoptotic markers in a Spinal Muscular Atrophy Mouse Model*". **A. Sansa**, S. de la Fuente, A. Garcera and R.M.Soler.
8. **II Congreso Interdisciplinar de Neurología y Neurociencia,** March 8-9th 2019; Lleida, Spain; Abstract and Oral Presentation "*Protective effects of Calpain inhibition on Spinal Muscular Atrophy mouse model*". S. de la Fuente, **A. Sansa**, A. Garcera and R.M.Soler.
9. **II Congreso Interdisciplinar de Neurología y Neurociencia,** March 8-9th 2019; Lleida, Spain; Abstract and Poster Presentation "*Study of the effect of neurotrophic factors treatment on motoneurons and its relationship with Spinal Muscular Atrophy*". N.Vivancos, **A. Sansa**, S. de la Fuente, I. Hidalgo, A. Garcera and R.M.Soler.
10. **II Congreso Interdisciplinar de Neurología y Neurociencia,** March 8-9th 2019; Lleida, Spain; Abstract and Poster Presentation "*Study of autophagy markers in spinal cord of Spinal Muscular Atrophy mild mouse model*". I. Hidalgo, A. Garcera, **A. Sansa**, N.Vivancos, S. de la Fuente, J. Calderó and R.M.Soler.
11. **Jornades de Doctorat 2019 Universitat de Lleida,** 2019; Lleida, Spain; Abstract and Poster Presentation: "*Alteration of Apoptotic markers in a Spinal Muscular Atrophy Mouse Model*". **A. Sansa**, S. de la Fuente, A. Garcera and R.M.Soler.
12. **2nd International Scientific Congress SMA Europe,** February 5-7th 2020; Evry, France; Abstract and Poster Presentation: "*Characterisation of survival signalling pathways in*

motoneurons from an in vitro model of human SMA iPS Cells". **A. Sansa**, N. Vivancos, S. de la Fuente, A. Garcera and R.M.Soler.

13. **2nd International Scientific Congress SMA Europe,** February 5-7th 2020; Evry, France; Abstract and Poster Presentation: "*Calpeptin Treatment Increases SMN protein in Spinal Cord Motoneurons and Ameliorates the SMA phenotype in Mice*". S. de la Fuente, **A. Sansa**, I. Hidalgo, A. Garcera and R.M.Soler.
14. **III Congreso Interdisciplinar de Neurología y Neurociencia,** October 15-16th 2021; Lleida, Spain; Abstract and Poster Presentation "*Characterisation of survival signaling pathways in motoneurons from an in vitro model of human SMA iPS cells*". **A. Sansa**, M.P. Miralles, A. Garcera and R.M.Soler.
15. **III Congreso Interdisciplinar de Neurología y Neurociencia,** October 15-16th 2021; Lleida, Spain; Abstract and Poster Presentation "*SMN or Bcl-XL protein overexpression rescues degeneration of Spinal Muscular Atrophy human motoneurons*". M.P. Miralles, **A. Sansa**, A. Garcera and R.M.Soler.
16. **1st Annual Scientific Symposium IRBLleida,** December 2nd 2021; Lleida, Spain; Abstract and Poster Presentation "*Differential regulation of autophagic markers between muscle and motoneurons in Spinal Muscular Atrophy models".* **A. Sansa**, M.P. Miralles, R.M.Soler and A. Garcerá.
17. **3rd International Scientific Congress SMA Europe,** October 21-23rd 2022; Barcelona, Spain; Abstract and Poster Presentation: "*Spinal Muscular Atrophy muscle and motoneurons exhibit a differential regulation of autophagic markers*". **A. Sansa**, M.P. Miralles, S. Gras, J. Calderó, R.M.Soler and A. Garcera.
18. **3rd International Scientific Congress SMA Europe,** October 21-23rd 2022; Barcelona, Spain; Abstract and Poster Presentation: "*Survival-related signaling pathways are altered in human differentiated Spinal Muscular Atrophy motoneurons*". M.P. Miralles, **A. Sansa**, A. Gatius, O. Tarabal, A. Garcera and R.M.Soler.
19. **II edition Motor Neuron Diseases: Understanding the pathogenetic mechanisms to develop therapies,** November 4-5th 2022; Turin, Italy; Abstract and Poster Presentation: "*Differential autophagic markers regulation between Spinal Muscular Atrophy muscle and motoneurons*". **A. Sansa**, R.M.Soler and A. Garcera.
20. **SEFAGIA 2022: Sociedad Española de Autofagia,** November 9-11th; Toledo, Spain; Abstract and Poster Presentation: "*Autophagy deregulation differs between muscle and motoneurons in Spinal Muscular Atrophy*". A. Garcera, **A. Sansa**, M.P. Miralles, Maria Beltran and R.M.Soler**.**